Towards an aminostratigraphy of foraminifera for Pleistocene sea-level records: testing the intra-crystalline approach to amino acid racemisation dating



Lucy Wheeler

PhD

University of York

Chemistry

July 2022

Abstract

Sea-level records of past interglacials are important archives for understanding long term mechanisms of sea-level change, and for informing predictions of future sea-level rise. Linking sea-level records to the global climate record is essential for assessing processes, leads and lags in the climate system. However, these fragmentary deposits are often challenging to date. Amino acid racemisation dating (AAR, also known as amino acid geochronology) is a technique commonly used to date Pleistocene deposits. Recently, improvements in AAR have been made by isolating an 'intra-crystalline' fraction of proteins, which in certain biominerals acts a closed system, reducing the variability of AAR results. This thesis aimed to assess whether the intra-crystalline approach improves the reliability of AAR in calcareous foraminifera, and whether this class of biomineral can be used to inform the chronology of Pleistocene sea-level deposits. A combination of oxidative pretreatment experiments and high-temperature decomposition experiments were therefore carried out on several species of foraminifera commonly preserved in Pleistocene sea-level records.

These experiments found that biomineral protein in the foraminifer species investigated undergoes predictable patterns of breakdown, making these species suitable substrates for AAR. Contrary to observations in several other calcareous biominerals, this work found no substantial differences in performance between the whole-shell and intra-crystalline approaches to AAR. A weak oxidation pre-treatment using H_2O_2 , common in the preparation of foraminifera for AAR, was therefore used in the development of a pilot aminostratigraphy of UK Pleistocene sea-level records. The majority of the AAR results from this pilot study were consistent with the known chronology of the sites, with the exception of samples which showed indications of contamination. These results demonstrate the importance of analysing a large number (\geq 10) of replicate samples where possible, to enable identification of outliers and estimation of reliable mean D/L values for foraminifera from Pleistocene sea-level records.

Table of Contents

Abstract	2
Table of Contents	3
List of Tables	9
List of Figures	11
Acknowledgements	21
Declaration	22
Chapter 1 – Introduction	23
. 1.1 Sea-level change in the Quaternary	
1.1.1 Introduction to the Quaternary	
1.1.2 Astronomical drivers of climate change	
1.1.3 Sea-level change	
1.1.3.1 Past sea-level change as an analogue for the future	
1.2 Dating Quaternary sea-level records	
1.2.1 Introduction to Quaternary geochronology	
1.2.2 Correlative dating methods	31
1.2.3 Radiometric dating methods	31
1.2.3.1 Principles of radiometric dating	31
1.2.3.2 Radiocarbon dating	
1.2.3.3 U-series dating	33
1.2.4 Trapped charge dating methods	34
1.2.5 Amino acid racemisation dating	36
1.3 Principles of amino acid racemisation dating	36
1.3.1.1 A note on naming conventions	37
1.3.2 Amino acids in biominerals	37
1.3.3 Amino acid racemisation	40
1.3.4 Amino acid racemisation as a dating method	42
1.3.4.1 Intra-crystalline protein diagenesis (IcPD)	43
1.3.4.2 Analytical methods for quantifying amino acid enantiomers	45
1.4 Mechanisms of protein decomposition	46
1.4.1 Free, terminal and in-chain amino acid racemisation	47

1.4.1.1 Free amino acids	47
1.4.1.2 Peptide-bound amino acids	49
1.4.2 Hydrolysis	51
1.4.3 Decomposition reactions	52
1.4.3.1 Deamination and decarboxylation	53
1.4.3.2 Condensation	54
1.4.3.3 R-group decomposition	54
1.4.4 Environmental influences on racemisation rates	56
1.4.4.1 Protein structure and matrix effects	56
1.4.4.2 External influences on racemisation rates	57
1.4.4.2.1 Temperature	57
1.4.4.2.2 pH	
1.4.4.2.3 Presence or absence of water	
1.4.4.2.4 Other external influences	
1.4.5 Summary	
1.5 Foraminifera	59
1.5.1 Foraminifera as a tool for palaeoenvironmental reconstruction	60
1.5.2 Foraminifer tests as a substrate for AAR	60
1.5.2.1 Biomineralisation in calcareous foraminifera	
1.5.2.2 Applications of AAR to foraminifera	62
1.5.2.3 Intra-crystalline approaches to AAR of foraminifera	
1.6 Project aims	64
Chapter 2 – Routine Experimental Procedures	65
2.1 Picking of foraminifera and species identification	65
2.2 Oxidative pre-treatments	65
2.3 Demineralisation and hydrolysis	66
2.4 Chiral separation of amino acids	66
2.4.1 RP-HPLC method	67
2.4.2 UHPLC method	68
2.5 Data analysis	69
Chapter 3 – Assessing the intra-crystalline approach to amino acid geochr	onology of
Neogloboquadrina pachyderma (sinistral)	70
Abstract	70
3.1 Introduction	71

3.2 Materials and Methods	73
3.2.1 Location	73
3.2.2 Age model	74
3.2.3 Preparation of foraminifera	75
3.2.3.1 Isolation of the intra-crystalline fraction	76
3.2.3.2 Analysis of racemisation trends in Nps	76
3.2.4 Amino acid analysis	76
3.2.4.1 Separation by ion exchange liquid chromatography (IEC)	77
3.2.4.2 Separation by reverse-phase high performance liquid chromatography (RP-HPLC)	77
3.2.4.3 Data screening	
3.2.5 IEC A/I to RP-HPLC D/L conversion	78
3.3 Results and discussion	80
3.3.1 Testing oxidation times	80
3.3.1.1 The effect of bleaching on amino acid concentration	80
3.3.1.2 The effect of bleaching on amino acid composition	81
3.3.1.3 The effect of bleaching on A/I values	82
3.3.2 Comparison of down-core diagenetic trends in racemisation between unbleached and bleached Nps	83
3.3.2.1 Trends in concentration and composition	84
3.3.2.2 Trends in racemisation	85
3.3.3 IEC A/I to RP-HPLC D/L conversions	91
3.4 Conclusions	93
Acknowledgements	94
Chapter 4 – Testing the effect of oxidising pre-treatments on amino acids in sub-moder	n-
and Pleistocene foraminifera	95
4.1 Introduction	95
4.2 Materials and Methods	96
4.2.1 Sample collection	96
4.2.2 Preparation and analysis	97
4.3 Results of sequential oxidation of sub-modern foraminifera	
4.3.1 Amino acid concentration	
4.3.2 Amino acid composition	
4.3.3 Effect of oxidation on D/L values	
4.3.3 Effect of oxidation on D/L values	102
4.5.4.108108100	[1.17]

4.4 Results of oxidation experiments carried out on mid-Pleistocene foraminifera	104
4.4.1 Amino acid concentration	105
4.4.2 Amino acid composition	106
4.4.3 Effect of oxidative pre-treatments on D/L values	108
4.4.4 Discussion	111
4.5 Conclusions	112
Chapter 5 – Patterns of decomposition in <i>Ammonia</i> spp. and <i>H. germanica</i> at high	
temperatures	114
5.1 Introduction	114
5.1.1 Assessing the integrity of a biomineral system using high-temperature experiments	115
5.1.2 Modelling amino acid racemisation	115
5.1.2.1 Reversible first order kinetics	116
5.1.2.2 Empirical non-linear functions	117
5.1.2.3 Application of kinetic parameters to naturally-aged samples	118
5.2 Materials and methods	120
5.2.1 Oxidation and heating experiments	120
5.2.2 Data screening.	122
5.2.3 Approach for modelling kinetic parameters	123
5.3 Results	123
5.3.1 Amino acid concentration	123
5.3.1.1 Contribution of laboratory contamination to amino acid concentration	123
5.3.1.2 Trends in amino acid concentration	126
5.3.1.3 Leaching of amino acids from the biomineral fraction	130
5.3.2 Amino acid composition	133
5.3.3 Peptide bond hydrolysis	135
5.3.4 Racemisation	137
5.3.4.1 General trends	137
5.3.4.2 D/L Covariance	142
5.3.4.3 Relative racemisation trends	146
5.3.4.4 Modelling racemisation	151
5.3.4.4.1 RFOK _a	151
5.3.4.4.2 SPK and CPK	154
5.4 Conclusions	158
5.4.1 Methodological issues: sample size and sources of contamination	158

5.4.2 Closed-system behaviour in the whole-shell and intra-crystalline fractions	159
5.4.3 Patterns of decomposition	159
5.4.4 Behaviour of kinetic models	160
5.4.5 Overall conclusions	161
Chapter 6 – Application of AAR to foraminifera from UK Pleistocene sea-level dep	oosits162
6.1 Introduction	162
6.2 Materials and Methods	163
6.2.1 Sample locations	163
6.2.2 Pre-treatment and analysis	165
6.3 Results and discussion	166
6.3.1 Data screening	166
6.3.2 AAR of foraminifera from UK Pleistocene sites – overview	168
6.3.3 West Sussex Coastal Plain	175
6.3.3.1 Earnley	177
6.3.3.2 Norton Farm	
6.3.3.3 Portfield Pit	178
6.3.3.4 West Street, Selsey	179
6.3.3.5 Discussion of West Sussex Coastal Plain results	180
6.3.4 Nar Valley Clays	181
6.3.4.1 Results	183
6.3.5 March Gravels	185
6.3.5.1 Northam Pit	189
6.3.5.2 Somersham Quarry, Section SBK	189
6.3.5.3 King's Dyke Quarry and West Face Quarry	190
6.3.6 Greylake 3, Burtle Beds	192
6.4 Conclusions	193
6.4.1 Preservation of foraminifer proteins in the Early Pleistocene - Strumpshaw Fen Sa	ndpit196
6.4.1.1 Results	197
Chapter 7 – Conclusions and future work	200
7.1 Isolation and behaviour of intra-crystalline proteins in foraminifera	200
7.2 Patterns of decomposition in foraminifera	201
7.3 The effect of oxidising pre-treatment on D/L variability in foraminifera	202
7.4 Use of AAR of foraminifera to provide chronological control in UK sea-level deposits.	202

7.5 Future work	203
7.5.1 Method development	203
7.5.2 Further development of foraminifer-based aminostratigraphy	203
7.5.2.1 Recommendations for analysing foraminifera from Pleistocene sea-level deposits	204
Appendices	206
Selected abbreviations	246
References	247

List of Tables

Table 1.1 – Summary of dating methods used for the Quaternary. 29
Table 1.2 – Naturally occurring amino acids and their quantification and chiral separation by ion exchange chromatography (IEC), high performance liquid chromatography (RP-HPLC) and ultra high performance liquid chromatography (UHPLC) (see Section 1.3.4.2)
Table 2.1 – Solvent gradient program for RP-HPLC (Penkman, 2005). 67
Table 2.2 – Solvent gradient program for UHPLC, adapted from Crisp (2013). 68
Table 3.1 – Screening criteria used to identify outliers and total number of samples excluded by each criterion for each analytical method. 78
Table 3.2 – Results of linear regressions using \log_2 transformed A/I and D/L values. PU refers to the prediction uncertainty calculated using the Nps data set for the pooled regression, and a 'dummy' data set for the Nps-specific regression (as used by Whitacre et al. (2017)). Success rate refers to the proportion of predicted ranges which included the D/L value measured by RP-HPLC93
Table 4.1 – Oxidising pre-treatments carried out on sub-modern and Pleistocene <i>Ammonia</i> spp., <i>H. germanica</i> and <i>E. williamsoni</i> . See Section 4.2.1 above for additional site information97
Table 4.2 – Results of two-way ANOVA for Pleistocene <i>Ammonia</i> spp. and <i>H. germanica</i> . A <i>p</i> -value of < 0.05 indicates a statistically significant result (highlighted in green). A statistically significant interaction (between pre-treatment and amino acid) shows that the effect of the pre-treatment differs between amino acids
Table 4.3 – Results of two-way Tukey post-hoc analysis for Pleistocene <i>Ammonia</i> spp. and <i>H. germanica</i> . An adjusted p -value of < 0.05 indicates a statistically significant difference between the two pre-treatments (highlighted in green). U: unbleached (sonication only); 3H: 3% H_2O_2 ; 30H: 30% H_2O_2 ; 12N: 12% NaOCl
Table 5.1 – High-temperature experiment time points for <i>Ammonia</i> spp. and <i>H. germanica</i> . Numbers in brackets refer to samples which dried out during heating; numbers in italics refer to samples which partially dried out. U = unbleached, B = 24 h 12% NaOCl
Table 5.2 – Subsamples from high-temperature experiments excluded according to screening criteria. 122
Table 5.3 – Number of samples from each fraction of the 110° C experiment with D/L values > 1, which have been excluded from the kinetic models. U = unbleached, B = 24 h 12% NaOCl123
Table 5.4 – Results of RFOK _a linear models for unbleached (whole-shell) and bleached (intracrystalline) <i>Ammonia</i> spp., heated to 110°C. k_1 is the rate of racemisation (slope / (1+K), where K = 1): c is the intercept: Adi. R^2 is the adjusted R^2 value, R^2 values < 0.6 are highlighted in red152

Table 5.5 – Results of RFOK _a linear models for unbleached (whole-shell) and bleached (intracrystalline) <i>H. germanica</i> , heated to 110°C. k_1 is the rate of racemisation (slope / (1+K), where K = 1); c is the intercept; Adj. R^2 is the adjusted R^2 value. R^2 values ≤ 0.6 are highlighted in red15	3
Table 5.6 – Results of SPK and CPK linear models for Asx in unbleached (whole-shell) and bleached (intra-crystalline) <i>H. germanica</i> and <i>Ammonia</i> spp., heated to 110° C. k_1 is the rate of racemisation (slope / (1+K), where K = 1); Adj. R^2 is the adjusted R^2 value. For clarity c (the intercept) has been omitted from this table; these values are given in Appendix A3.4 . R^2 values ≤ 0.6 are highlighted in red	
Table 6.1 – Foraminifera from UK Pleistocene sites analysed in this study. *Species abbreviations: Am: Ammonia spp. (not identified to species level), HG: Haynesina germanica, EW: Elphidium williamsoni; Elp: Elphidium spp. (not identified to species level); EF: Elphidium frigidum; EP: Elphidium pseudolessoni. All samples prepared with a 2 hour 3% H ₂ O ₂ pre-treatment and analysed using UHPLC according to Section 2.4.2.	
Table 6.2 – Foraminifera from UK sites analysed as part of the iGlass project presented in this chapter. *Species abbreviations: Am: <i>Ammonia</i> spp. (not identified to species level); HG: <i>Haynesin germanica</i> ; Elp: <i>Elphidium</i> spp. (not identified to species level). All samples prepared with a 48 hou 12% NaOCl pre-treatment and analysed using RP-HPLC according to Penkman et al. (2008)16	ır
Table 6.3 – Proportion of foraminifer samples with [L-Ser]/[L-Asx] above cut-off values of 0.8 and 1.2. 1.2.	7
Table 6.4 – Chronological evidence from West Sussex Coastal Plain sites. Laboratory codes for OSL dates are given in italics. IcPD: intra-crystalline protein diagenesis approach to AAR using a strong oxidative pre-treatment (H_2O_2) used; A/I: isoleucine epimerisation, whole-shell approach	6
Table 6.5 — Chronological evidence from Nar Valley Clay sites. IcPD: intra-crystalline proteindiagenesis approach to AAR using a strong oxidative pre-treatment (NaOCI); AAR: weak oxidativepre-treatment (H_2O_2) used.	2
Table 6.6 – Chronological evidence from March Gravel sites. Laboratory codes for OSL dates are given in italics. For King's Dyke Quarry and West Face Quarry, the original context information is given with the equivalent facies association in the revised nomenclature (Langford, in preparation) where possible (equivalence is denoted by \equiv). IcPD: intra-crystalline protein diagenesis approach to AAR using a strong oxidative pre-treatment (NaOCl); AAR: weak oxidative pre-treatment (H ₂ O ₂) used; A/I: isoleucine epimerisation, whole-shell approach	О

List of Figures

Fig. 1.1 – Section of the Cenozoic era, showing the Neogene and Quaternary periods (not to scale). Chronological boundaries taken from the International Commission on Stratigraphy (Cohen et al., 2013).
Fig. 1.2 – Pleistocene δ^{18} O (oxygen isotope) record, showing fluctuations between warm interglacial and cool glacial climates. Select marine isotope stages are labelled. Adapted from Lisiek and Raymo (2005) and Raymo <i>et al.</i> (2018)
Fig. 1.3 – A schematic representation of the three Milankovitch cycles – changes to the Earth's orbit around the sun over geological timescales (not to scale)25
Fig. 1.4 – Structure of a) an amino acid and b) a peptide formed from three amino acid residues. The peptide bonds are indicated by dotted rectangles
Fig. 1.5 – Chirality of amino acids: a) amino acids with one stereogenic centre at the α -carbon, forming two enantiomers (mirror images with identical physical properties); b) isoleucine, an amino acid with two stereogenic centres (at the α - and β -carbon positions), which has four stereoisomers
Fig. 1.6 – Schematic representation of inter- and intra-crystalline biomineral proteins (adapted from Sykes et al. (1995)
Fig. 1.7 – Derivatisation of an amino acid with <i>N</i> -isobutyryl-L-cysteine (IBLC, a chiral compound which converts the amino acid epimer into an enantiomer) and <i>o</i> -phthaldialdehyde (OPA, a fluorescent tag enabling detection), used by Kaufman and Manley (1998)
Fig. 1.8 – Different positions of amino acids in a peptide chain and as a free amino acid47
Fig. 1.9 – Racemisation of a free amino acid (zwitterionic form) via α -proton abstraction, forming a planar carbanion intermediate (adapted from Bada and Schroeder (1975))47
Fig. 1.10 – Ionic forms of an amino acid; in solution these forms are present in equilibrium, with the proportions of each form depending on the properties of the amino acid and the pH of the solution48
Fig. 1.11 – C-terminus carbanion intermediate stabilisation by formation of a five-membered ring (adapted from Smith and Evans (1980))49
Fig. 1.12 – Diketopiperazine formation and decomposition (adapted from Steinberg and Bada (1983))50
Fig. 1.13 – Succinimide formation and decomposition, where X is OH (aspartic acid) or NH ₂ (asparagine); a) reformation of the aspartyl residue, b) generation of an isoaspartyl residue50
Fig. 1.14 – Hydrolysis of a peptide bond to generate a C- and N-terminus51
Fig. 1.15 – Amino acid decomposition pathways: a) reductive deamination; b) decarboxylation; c) oxidative deamination: d) condensation.

Fig. 1.16 – Decarboxylation reactions of aspartic acid
Fig. 1.17 – Decomposition of glutamic acid via γ-lactam formation
Fig. 1.18 – Decomposition of the hydroxy amino acids serine and threonine by dehydration (top) and aldol cleavage (bottom) (from Bada et al. (1978))
Fig. 1.19 – Schematic representation of the pH dependence of amino acid racemisation in solution (adapted from Bada (1970))
Fig. 1.20 – Formation and structure of test chambers in calcareous foraminifera (adapted from Tyszka et al. (2019))
Fig. 2.1 – Typical RP-HPLC chromatogram of a 0.5 D/L standard amino acid solution with quantified amino acids labelled. L-hArg (L-homo-arginine) is the internal standard
Fig. 2.2 – Typical UHPLC chromatogram of a 0.5 D/L standard amino acid solution with quantified amino acids labelled. L-hArg (L-homo-arginine) is the internal standard
Fig. 3.1 – Location of MD99-2288 and MD99-2289 IMAGES cores in the Norwegian Sea. Isobath depths in metres; bathymetry data from NOAA.
Fig. 3.2 – Bayesian age depth model (Blaauw and Christeny, 2011) for 120-1863 cm of core MD99-2289. Radiocarbon ages are shown in blue; NGRIP tie points and tephra zones are shown in teal. The dark blue line shows the model's weighted mean age. Dashed lines represent the model's 95% probability intervals
Fig. 3.3 – Trends in concentration of total hydrolysable amino acids ([THAA]) with increasing bleach time for Nps at three core depths: a) 250 cm, b) 500 cm and c) 1450 cm. Dots show individual replicates; bars show means of all replicates at each time and depth point. Where data are absent, this is because experiments of this duration were not carried out
Fig. 3.4 – The effect of increasing exposure to bleach on total hydrolysable amino acid (THAA) composition of Nps tests at three core depths (analysed using IEC). While there is some variability in the THAA composition in the first 48 hours of bleach exposure, no clear compositional changes are caused by oxidation. Due to poor separation of Ser from Thr using IEC, these amino acids are reported together.
Fig. 3.5 – Trends in A/I value with increasing bleach time for Nps at a) 250 cm, b) 500 cm and c) 1450 cm. Dots show individual replicates; bars show means of all replicates at each time and depth point. Where data are absent, this is because experiments of this duration were not carried out, with the exception of 360 hours at 500 cm, where none of the samples had resolved A-Ile peaks. An increase in A/I is observed between 24-48 hours at 250 cm, while bleaching has no clear effect on A/I at 500 cm and 1450 cm.
Fig. 3.6 – Down core trends in total hydrolysable amino acid concentration of bleached and unbleached Nps tests (analysed using RP-HPLC).
Fig. 3.7 – Down-core compositions of unbleached and bleached (48 h) Nps tests analysed by IEC, showing a relatively stable composition of both the whole and intra-crystalline fractions of amino

acids. Due to poor separation of Ser from Thr using IEC, these amino acids are reported together.
85
Fig. 3.8 – Downcore trends in A/I for Nps analysed by IEC: a) A/I against depth showing samples taken between 10-2951.5 cm (corrected depth); b) A/I against age for samples taken between 120-1863 cm, the range of the age model for the core (see Fig. 3.2). Horizontal lines show 1σ age error from age model. Bleached samples were subjected to 48 h NaOCl exposure. A locally weighted smoothing (loess) function has been applied (solid line) to highlight the differences between the racemisation trends for bleached and unbleached Nps
Fig. 3.9 – Trends in racemisation for four amino acids (i) Asx, ii) Glx, iii) Ser, iv) Ile) analysed by RP-HPLC. a) D/L against depth showing samples taken between 10-2951.5 cm (corrected depth); b) D/L against age for samples taken between 120-1863 cm, the range of the age model for the core (see Fig. 3.2). Horizontal lines show 1σ age error from age model. All four amino acids have higher D/L values for bleached than unbleached Nps in older samples. Bleached samples were subjected to 48 h NaOCl exposure. A locally weighted smoothing (loess) function has been applied to highlight the differences between the racemisation trends for bleached and unbleached Nps88
Fig. 3.10 – Trends in racemisation for four amino acids (i) Asx, ii) Glx, iii) Ser, iv) Ile) analysed by RP-HPLC for the youngest part (10-60 ka, 10-1500 cm) of the core: a) D/L against depth; b) D/L against age. Horizontal lines show 1σ age error from age model. During this early stage of racemisation D/L values are similar between bleached and unbleached Nps for Asx, Glx and Ala. Bleached samples were subjected to 48 h bleach exposure. A locally weighted smoothing (loess) function has been applied to highlight the differences between the racemisation trends for bleached and unbleached Nps
Fig. 3.11 — Covariance of Asx and Glx D/L for bleached and unbleached Nps analysed by RP-HPLC, showing decreased variability of D/L values on bleaching for young material (Asx D/L < 0.2). A locally weighted smoothing (loess) function has been applied to show the general trends of the data90
Fig. 3.12 – Relationship between IEC Ile A/I and RP-HPLC amino acid D/L values, modelled by log_2 -transformed linear regressions. Lines represent the Nps-specific and pooled linear regressions; shaded envelopes are 2σ prediction uncertainties using a 'dummy' data set for the Nps-specific regressions (as used by Whitacre et al. (2017)) and the Nps data set for the pooled regressions92
Fig. 4.1 – Concentration of total hydrolysable amino acids ([THAA]) in unbleached (H_2O sonication only) and oxidized (H_2O_2 or NaOCl) samples of sub-modern <i>Ammonia</i> spp., <i>H. germanica</i> and <i>E. williamsoni</i> . Weak oxidation (H_2O_2) experiments were not carried out for <i>E. williamsoni</i> . Dots show individual replicates; bars show means of all replicates99
Fig. 4.2 – Relative proportion of well-resolved amino acids (% [THAA]) in sub-modern <i>Ammonia</i> spp., <i>H. germanica</i> and <i>E. williamsoni</i> over the course of extended exposure to 12% w/v NaOCl. Amino acids are shown in order of elution. The <i>E. williamsoni</i> samples were analysed using UHPLC, which resolves amino acids somewhat differently to RP-HPLC (see Section 2.4): therefore its

composition is not directly comparable to <i>Ammonia</i> spp. or <i>H. germanica</i> . Poorly resolved amino acids (Thr, His, Arg and Met) have been excluded
Fig. 4.3 – Proportion of Asx and Gly in unbleached (H_2O sonication only) and oxidized (H_2O_2 or NaOCl) samples of sub-modern <i>Ammonia</i> spp., <i>H. germanica</i> and <i>E. williamsoni</i> . Weak oxidation (H_2O_2) experiments were not carried out for <i>E. williamsoni</i> . Error bars show ± 1 standard deviation (σ). Dots show individual replicates; bars show means of all replicates. The corresponding proportion of Glx, Ser, Phe and Ile is given in Appendix 2
Fig. 4.4 – Relative proportion of amino acids (% [THAA]) in sub-modern $Ammonia$ spp. and H . $germanica$ treated with an oxidising agent for 4 hours. Four different pre-treatments were used: Sonication only (unbleached, U), 4 h 3% H_2O_2 (3H), 4 h 30% H_2O_2 (30H), and 4 h 12% NaOCl (12N).
Fig. 4.5 – Asx, Glx, Ser, Phe and Ile THAA D/L in <i>Ammonia</i> spp., <i>H. germanica</i> and <i>E. williamsoni</i> treated with various oxidising agents. Weak oxidation (H_2O_2) experiments were not carried out for <i>E. williamsoni</i> ; otherwise where bars are missing, it is because the respective D-amino acid was not detected in any of the samples at that time point. Dots show individual replicates; bars show means of all replicates
Fig. 4.6 – Effect of pre-treatment on total hydrolysable amino acid concentration ([THAA]) in Pleistocene <i>Ammonia</i> spp. and <i>H. germanica</i> ($n=10$ for each pre-treatment). Boxes show the median and the first and third quartiles; the whiskers extend to the minimum and maximum values, with samples beyond 1.5 times the interquartile range treated as outliers (points). U: unbleached (sonication only); $3H: 3\% H_2O_2$; $3OH: 30\% H_2O_2$; $12N: 12\% NaOCl.$ All oxidative pre-treatments had a duration of 2 hours
Fig. 4.7 – The effect of pre-treatment on the relative proportion of amino acids (% [THAA]) in Pleistocene <i>Ammonia s</i> pp. and <i>H. germanica</i> . U: unbleached (sonication only); 3H: 3% H ₂ O ₂ ; 30H: 30% H ₂ O ₂ ; 12N: 12% NaOCl. All oxidative pre-treatments had a duration of 2 hours
Fig. 4.8 – Variability of the relative proportion of amino acids (% [THAA]) for Asx, Glx, Ser, Gly, Phe and Ile with each pre-treatment for Pleistocene <i>Ammonia</i> spp. and <i>H. germanica</i> . Error bars represent \pm 1 σ around the average % composition. U: unbleached (sonication only); 3H: 3% H ₂ O ₂ ; 30H: 30% H ₂ O ₂ ; 12N: 12% NaOCl. All oxidative pre-treatments had a duration of 2 hours107
Fig. 4.9 – Effect of pre-treatment on Asx, Glx, Ser, Phe and Ile D/L of Pleistocene <i>H. germanica</i> and <i>Ammonia</i> spp. ($n=10$ for each pre-treatment). Boxes show the median and the first and third quartiles; the whiskers extend to the minimum and maximum values, with samples beyond 1.5 times the interquartile range treated as outliers (points). U: unbleached (sonication only); 3H: 3% H_2O_2 ; 30H: 30% H_2O_2 ; 12N: 12% NaOCl. All oxidative pre-treatments had a duration of 2 hours109
Fig. 4.10 – Coefficient of variance (standard deviation / mean) of the D/L values of Asx, Glx, Ser, Phe and Ile of mid-Pleistocene <i>Ammonia</i> spp. and <i>H. germanica</i> , subjected to a range of pre-treatments ($n = 10$ for each pre-treatment)
Fig. 5.1 – Relative concentrations (amino acid peak area divided by L-hArg peak area) of key amino

acids in blank set X (blanks analysed alongside 110°C suite of experiments) and blank set Y

(separate suite of 10 blanks heated to 110°C for 5 days). Boxes show the median and the first and
third quartiles; the whiskers extend to the minimum and maximum values, with samples beyond
1.5 times the interquartile range treated as outliers (points)

- Fig. 5.2 Concentration of key amino acids in unbleached (whole-shell) and bleached (intracrystalline) samples and analytical blank set Y (set of 10 blanks heated for 5 days). Samples from both species (*Ammonia* spp. and *H. germanica*), and across the full range of time points at 110°C, have been combined in this figure to show the range of amino acid concentrations detected in this suite of experiments. The concentration of amino acids in the blanks is calculated using an assumed 'sample size' of 60 tests. Boxes show the median and the first and third quartiles; the whiskers extend to the minimum and maximum values, with samples beyond 1.5 times the interquartile range treated as outliers (points). The upper Gly whisker on the THAAf graph has been truncated to allow easier comparison of the lower concentration amino acids. Left: free amino acids in foraminifer fraction (FAAf); right: total hydrolysable amino acids in foraminifer fraction (THAAf). 125

- **Fig. 5.5** Total concentration of amino acids in bleached (intra-crystalline) *Ammonia* spp. and *H. germanica* during 140°C heating experiment. The bars show the average concentration of each fraction over time; the points show individual replicates. The average total concentration of amino acids in blank set Y (see **Section 5.3.1.1**), given an assumed 'sample size' of 60 tests, is shown as a dark orange line; the pale orange lines are \pm 1 σ around the mean of the blank amino acid concentration. Upper: free amino acid (FAA) fraction; lower: total hydrolysable amino acid (THAA) fraction.
- Fig. 5.6 Concentration of Asx, Gly and Ser and total amino acids in supernatant waters from unbleached (whole-shell) and bleached (intra-crystalline) *Ammonia* spp. during 110°C heating experiment. The bars show the average concentration of each fraction over time; the points show individual replicates. The average total concentration of amino acids in blank set Y (see **Section 5.3.1.1**), given an assumed 'sample size' of 60 tests, is shown as a dark orange line; the pale orange lines are $\pm 1 \sigma$ around the mean of the blank amino acid concentration. Note the individual y-axis

(THAA) fraction
Fig. 5.7 – Concentration of Asx, Gly and Ser and total amino acids in supernatant waters from unbleached (whole-shell) and bleached (intra-crystalline) H . $germanica$ during $110^{\circ}C$ heating experiment. The bars show the average concentration of each fraction over time; the points show individual replicates. The average total concentration of amino acids in blank set Y (see Section 5.3.1.1), given an assumed 'sample size' of 60 tests, is shown as a dark orange line; the pale orange lines are \pm 1 σ around the mean of the blank amino acid concentration. Note the individual y-axis range for each plot. Upper: free amino acid (FAA) fraction; lower: total hydrolysable amino acid (THAA) fraction.
Fig. 5.8 – Concentrations of a) free (FAA) Asx and b) total hydrolysable (THAA) Asx in unbleached (whole-shell) and bleached (intra-crystalline) <i>Ammonia spp.</i> and <i>H. germanica</i> biomineral powders and the supernatant water in each vial during 110°C heating experiments. The shaded areas show the average concentration of each fraction over time; the points show individual replicates. Note the different y-axis ranges used for the unbleached and bleached graphs. Corresponding figures for Gly, Ser and all amino acids ('total') can be found in Appendix A3.1
Fig. 5.9 – Change in composition of free (FAA) and total hydrolysable (THAA) amino acids in unbleached (whole-shell) and bleached (intra-crystalline) <i>Ammonia</i> spp. and <i>H. germanica</i> during 110°C heating experiment. X-axis labels show the time points for which data were collected. Arg, Tyr, Met, His and Thr are poorly resolved using RP-HPLC, and have therefore been excluded134
Fig. 5.10 – Percentage of amino acids in free state (% FAA) for Asx, Glx, Gly, Ala, Leu and all amino acids ('total') in unbleached (whole-shell) and bleached (intra-crystalline) <i>Ammonia</i> spp., heated to 110°C.
Fig. 5.11 – Percentage of amino acids in free state (% FAA) for Asx, Glx, Gly, Ala, Leu and all amino acids ('total') in bleached (intra-crystalline) <i>Ammonia</i> spp., heated to 140°C. Leu was not detected in any FAA samples heated for less than 1 day
Fig. 5.12 – Percentage of amino acids in free state (% FAA) for Asx, Glx, Gly, Ala, Leu and all amino acids ('total') in unbleached (whole-shell) and bleached (intra-crystalline) <i>H. germanica</i> , heated to 110°C.
Fig. 5.13 – Percentage of amino acids in free state (% FAA) for Asx, Glx, Gly, Ala, Leu and all amino acids ('total') in bleached (intra-crystalline) <i>H. germanica</i> , heated to 140°C137
Fig. 5.14 – Racemisation of Asx, Glx, Ser, Ala, Val, Phe, Leu and Ile in the free amino acid (FAA) and total hydrolysable amino acid (THAA) fractions of unbleached (whole-shell) and bleached (intracrystalline) <i>Ammonia</i> spp. and <i>H. germanica</i> at 110° C. Samples with an amino acid concentration below the average + 1 σ of the blanks are highlighted in orange
Fig. 5.15 – Racemisation of Asx, Glx, Ser, Ala, Val, Phe, Leu and Ile in the free amino acid (FAA) and total hydrolysable amino acid (THAA) fractions of bleached (intra-crystalline) <i>Ammonia</i> spp. and <i>H. germanica</i> , heated to 140°C. Samples with an amino acid concentration below the average + 1 σ of the blanks are highlighted in orange.

Fig. 5.16 – Covariance between D/L values in the free amino acid (FAA) and total hydrolysable amino acid (THAA) fractions for various amino acids in unbleached (whole-shell) and bleached (intra-crystalline) <i>Ammonia</i> spp., heated to 110° C. Samples with either an FAA or THAA concentration below the average + 1 σ of the blank are highlighted in orange
Fig. 5.17 – Covariance between D/L values in the free amino acid (FAA) and total hydrolysable amino acid (THAA) fractions for various amino acids in unbleached (whole-shell) and bleached (intra-crystalline) H . $germanica$, heated to 110°C. Samples with either an FAA or THAA concentration below the average + 1 σ of the blank are highlighted in orange
Fig. 5.18 – Covariance between Asx D/L and other amino acids in unbleached (whole-shell) and bleached (intra-crystalline) <i>Ammonia</i> spp., heated to 110° C. Samples with either Asx or another amino acid concentration below the average + 1 σ of the blank are highlighted in orange. Upper: free amino acids (FAA); lower: total hydrolysable amino acids (THAA)
Fig. 5.19 – Covariance between Asx D/L and other amino acids in unbleached (whole-shell) and bleached (intra-crystalline) <i>H. germanica</i> , heated to 110° C. Samples with either Asx or another amino acid concentration below the average + 1 σ of the blank are highlighted in orange. Upper: free amino acids (FAA); lower: total hydrolysable amino acids (THAA)
Fig. 5.20 – Comparison between racemisation of Asx, Glx, Ala, Phe and Leu in unbleached (wholeshell) and bleached (intra-crystalline) <i>Ammonia</i> spp., heated to 110° C. The solid line shows the average D/L over time; the points are individual replicates. Samples with amino acid concentrations below the average + 1 σ of the blank are shown as open diamonds. Left: free amino acids (FAA); right: total hydrolysable amino acids (THAA).
Fig. 5.21 – Comparison between racemisation of Asx, Glx, Ala, Phe and Leu in unbleached (wholeshell) and bleached (intra-crystalline) H . $germanica$, heated to 110°C. The solid line shows the average D/L over time; the points are individual replicates. Samples where the amino acid concentration was below the average $+ 1 \sigma$ of the blank are shown as open diamonds. Left: free amino acids (FAA); right: total hydrolysable amino acids (THAA)
Fig. 5.22 – Comparison between racemisation of Asx, Glx, Ala, Phe and Leu in FAA and THAA unbleached (whole-shell) and bleached (intra-crystalline) <i>Ammonia</i> spp. and <i>H. germanica</i> , heated to 110° C. The solid (unbleached) and dashed (bleached) lines show the average D/L over time; the closed (unbleached) and open (bleached) circles are individual replicates. Note that samples with amino acid concentration below the average + 1 σ of the blank have not been highlighted in this graph.
Fig. 5.23 – Comparison between amino acids (Asx, Glx, Ala, Phe, Leu) in different fractions (FAA and THAA, unbleached (whole-shell) and bleached (intra-crystalline)) of <i>Ammonia</i> spp. and <i>H. germanica</i> , heated to 110° C. The solid (unbleached) and dashed (bleached) lines show the average D/L over time; the closed (unbleached) and open (bleached) circles are individual replicates. Note that samples with amino acid concentration below the average + 1 σ of the blank have not been highlighted in this graph.

Fig. 5.24 – RFOK _a of Asx, Glx, Ala, Phe and Leu for unbleached (whole-shell) and bleached (intracrystalline) <i>Ammonia</i> spp., heated to 110°C. The solid lines show the linear regression between time and -ln[(X_e -X)/ X_e]; the shaded regions show \pm 1 σ around the linear regression. FAA Phe and Leu have been excluded due to missing FAA D/L values at early time points (see Section 5.3.4.2).
Fig. 5.25 – RFOK _a of Asx, Glx, Ala, Phe and Leu for unbleached (whole-shell) and bleached (intracrystalline) H . $germanica$, heated to 110° C. The solid lines show the linear regression between time and $-\ln[(X_e-X)/X_e]$; the shaded regions show $\pm 1~\sigma$ around the linear regression. FAA Phe and Leu have been excluded due to missing FAA D/L values at early time points (see Section 5.3.4.2)153
Fig. 5.26 — Optimisation of n for SPK and CPK models applied to Asx in unbleached (whole-shell) and bleached (intra-crystalline) $Ammonia$ spp. and H . $germanica$, heated to 110° C. Orange diamonds show the value of n with the highest R^2 value. Optimisation was carried out with values of n between 0.1 and 10 , in increments of 0.1
Fig. 5.27 – SPK of Asx for unbleached (whole-shell) and bleached (intra-crystalline) <i>Ammonia</i> spp. and <i>H. germanica</i> , heated to 110°C. Lines show linear regression between time and D/L ⁿ , where the value of n is optimised to provide the highest value of R ² (see Fig. 5.26). The shaded region shows \pm 1 σ around the linear regression.
Fig. 5.28 – CPK of Asx for unbleached (whole-shell) and bleached (intra-crystalline) <i>Ammonia</i> spp. and <i>H. germanica</i> , heated to 110°C. Lines show linear regression between time and -ln([1+D/L]/[1-D/L]) ^{n} , where the value of n is optimised to provide the highest value of R^2 (see Fig. 5.26). The shaded region shows \pm 1 σ around the linear regression. Note that each plot has its own y-axis range, so the slope of each linear regression should not be directly compared
Fig. 5.29 – Comparison between k_1 of Asx, estimated by each of three models (reversible first order kinetics (RFOK _a), simple power law kinetics (SPK), and constrained power law kinetics (CPK)), for unbleached (whole-shell) and bleached (intra-crystalline) <i>Ammonia</i> spp. and <i>H. germanica</i> , heated to 110° C. Note the logarithmic y-axis scale.
Fig. 6.1 – Location of UK Pleistocene sea-level sites analysed in this study. Study regions inset: West Sussex Coastal Plain (Section 6.3.3), Nar Valley (Section 6.3.4), March Gravels (Section 6.3.5)163
Fig. 6.2 – [L-Ser]/[L-Asx] vs Asx, Glx and Ser D/L for all Pleistocene foraminifer samples. 'Elphidium spp.' includes both Elphidium spp. (not identified to species level) and E. williamsoni. The vertical lines show [L-Ser]/[L-Asx] values of 0.8 and 1.2.
Fig. 6.3 – Covariance of Asx with Glx, Phe, Leu and Ile D/L in THAA (total hydrolysable amino acid) fraction of Ammonia spp., Elphidium spp. (including E. williamsoni) and H. germanica from UK Pleistocene sea-level sites. Samples treated with H_2O_2 (dark blue) were analysed using UHPLC; samples treated with NaOCl (pale blue) were analysed using RP-HPLC. Samples with [L-Ser]/[L-Asx] > 0.8 are shown as open circles.
Fig. 6.4 – Asx vs Glx D/L covariance for THAA (total hydrolysable amino acid) fraction of <i>Ammonia</i> spp. samples from various UK Pleistocene sites. Samples with an [L-Ser]/[L-Asx] value > 0.8 are highlighted as open shapes. BB: Burtle Beds; BE: Blackborough End Quarry; BH: Bradmoor Hill; ELY:

Earnley; HF: Horse Fen; KD: King's Dyke Quarry; NP: Northam Pit; RC: Railway Cottage; SH: Somersham; WSS: West Street, Selsey; HE: Humber Estuary, 'sub-modern' material for comparison. See Table 6.1 and Table 6.2 for additional site details
Fig. 6.5 – Asx vs Glx D/L covariance for THAA (total hydrolysable amino acid) fraction of <i>H. germanica</i> samples from various UK Pleistocene sites. Samples with an [L-Ser]/[L-Asx] value > 0.8 are shown as open shapes. BB: Burtle Beds; ELY: Earnley; KD: King's Dyke Quarry; NF: Norton Farm; NP: Northam Pit; PP: Portfield Pit; RC: Railway Cottage; WF: West Face Quarry; WSS: West Street, Selsey; HE: Humber Estuary, 'sub-modern' material for comparison. See Table 6.1 and Table 6.2 for additional site details.
Fig. 6.6 – Asx vs Glx D/L covariance for THAA (total hydrolysable amino acid) fraction of <i>E. williamsoni</i> and <i>Elphidium</i> spp. (not identified to species level) samples from various UK Pleistocene sites. Samples with an [L-Ser]/[L-Asx] value > 0.8 are shown as open shapes. BB: Burtle Beds; BE: Blackborough End Quarry; BH: Bradmoor Hill; ELY: Earnley; HF: Horse Fen; KD: King's Dyke Quarry; NF: Norton Farm; PP: Portfield Pit; RC: Railway Cottage; WSS: West Street, Selsey. See Table 6.1 and Table 6.2 for additional site details
Fig. 6.7 – THAA Asx vs Glx D/L values for all foraminifer samples from UK Pleistocene sites (see Table 6.1 and Table 6.2), and <i>B. tentaculata</i> opercula samples (dark red) from Horse Fen (Barlow et al., 2017), Earnley (Penkman (unpublished data); see Table 6.4), King's Dyke Quarry (Presslee (unpublished data); see Table 6.6), and West Face Quarry and Somersham (Penkman et al. (2013), Presslee (unpublished data); see Table 6.6). Average <i>B. tentaculata</i> opercula D/L values for UK Pleistocene sites in Penkman et al. (2013) where Glx D/L < 0.5 are shown in pale red to demonstrate the different racemisation trajectories of the two biomineral classes. Foraminiferal samples with an [L-Ser]/[L-Asx] value > 0.8 are highlighted as open circles. The dashed line shows a 1:1 relationship between Asx and Glx D/L
Fig. 6.8 – Asx vs Glx and Ile D/L covariance for THAA (total hydrolysable amino acid) fraction of <i>Ammonia</i> spp., <i>H. germanica</i> and <i>E. williamsoni</i> from West Sussex Coastal Plain sites. ELY: Earnley; NF: Norton Farm; PP: Portfield Pit; WSS: West Street, Selsey. Samples with [L-Ser]/[L-Asx] > 0.8 are flagged as open circles. All foraminifer AAR results are shown in grey for comparison (see Section 6.3.2 for Asx vs Glx D/L plots of each species with all sites labelled)
Fig. 6.9 – Asx vs Glx and Ile D/L covariance for THAA (total hydrolysable amino acid) fraction of <i>Ammonia</i> spp., <i>H. germanica</i> and <i>Elphidium</i> spp. (not identified to species level) from Nar Valley Clay sites. BE: Blackborough End Quarry; BH: Bradmoor Hill; HF: Horse Fen; RC: Railway Cottage. Samples with [L-Ser]/[L-Asx] > 0.8 are flagged as open circles. All foraminifer AAR results are shown in grey for comparison (see Section 6.3.2 for Asx vs Glx D/L plots of each species with all sites labelled)
Fig. 6.10 – Asx D/L values for THAA (total hydrolysable amino acid) fraction of <i>Ammonia</i> spp., <i>H. germanica</i> and <i>Elphidium</i> spp. (not identified to species level) from Nar Valley cores. BE: Blackborough End Quarry; BH: Bradmoor Hill; HF4: Horse Fen Core 4; RC: Railway Cottage. Diamonds refer to samples treated with 2 h 3% H ₂ O ₂ ; circles refer to samples treated with 48h 12% NaOCl. Samples with [L-Ser]/[L-Asx] > 0.8 are flagged as open shapes. HF2 (Horse Fen Core 2) was

depth' refers only to the sampling location in each core, and does not correspond to m OD185
Fig. 6.11 – Asx vs Glx and Ile D/L covariance for THAA (total hydrolysable amino acid) fraction of Ammonia spp., H. germanica and E. williamsoni from March Gravel sites. KD: King's Dyke, NP: Northam Pit, SH: Somersham, WF: West Face Quarry. Samples with [L-Ser]/[L-Asx] > 0.8 are flagged as open shapes. All foraminifer AAR results are shown in grey for comparison (see Section 6.3.2 for Asx vs Glx D/L plots of each species with all sites labelled).
Fig. 6.12 – Simplified schematic of the aggradational sequence of a) King's Dyke Quarry and b) West ace Quarry (formerly Funtham's Lane), with relevant existing chronological information (top) and campling locations of foraminifera for this study (bottom). IcPD: intra-crystalline protein diagenesis approach to AAR using a strong oxidative pre-treatment (NaOCI); A/I: isoleucine epimerisation, whole-shell approach. Details of chronological work are given in Table 6.6 . Revised nomenclature aken from Langford (in preparation); for corresponding nomenclature from original publications, see Table 6.1 . Not to scale; locations of samples taken for AAR and OSL dating are approximate. 193
Fig. 6.13 —Asx vs Glx and Ile D/L covariance for THAA (total hydrolysable amino acid) fraction of Ammonia spp., H. germanica and Elphidium spp. (not identified to species level) from Burtle Beds Greylake 3. Samples with [L-Ser]/[L-Asx] > 0.8 are flagged as open shapes. All foraminifer AAR results are shown in grey for comparison (see Section 6.3.2 for Asx vs Glx D/L plots of each species with all sites labelled).
Fig. 6.14 – Asx vs Glx D/L covariance of THAA (total hydrolysable amino acid) fraction of <i>Ammonia</i> app., <i>H. germanica</i> and <i>Elphidium</i> spp. (including <i>E. williamsoni</i>) from UK Pleistocene sea-level ecords with five or more samples with [L-Ser]/[L-Asx] < 0.8 (ELY: Earnley; NP: Northam Pit; NV: Nar alley Clays (comprising Blackborough End Quarry, Bradmoor Hill, Horse Fen and Railway Cottage); PP: Portfield Pit; WSS: West Street, Selsey). Samples from these sites with [L-Ser]/[L-Asx] > 0.8 have been excluded from this figure.
Fig. 6.15 – a) 'normal' chromatogram of an <i>E. williamsoni</i> sample, with internal standard L-hArg beak height of ~100 LU (sample no: NF-EW71H*, NEaar no: 14258); b) chromatogram of 'stained' <i>E. frigidum</i> sample (SF-EF80H*, NEaar no: 14267) rehydrated with 64 μL L-hArg solution, showing strong 'peak suppression' (L-hArg peak ~20 LU); c) chromatogram of 'stained' SF-EF80H* rehydrated with 265 μL L-hArg solution, showing a normal L-hArg peak but peaks of other amino acids except L-Ser close to the limit of detection; d) chromatogram of 'stained' SF-EFx86H* (NEaar no: 14723) following SPE step, rehydrated with 64 μL L-hArg solution, showing little to no recovery of amino acids.
Fig. 6.16 – Foraminifera from sample SF-YK11 from Strumpshaw Fen Sandpit, showing orange- brown 'staining' from iron-containing compounds. Width of picture is approximately 1 cm. Inset: modern, 'pristine' foraminifera from the Humber Estuary with a pale, glassy appearance198

only sampled at one depth, so is not included. Note individual y-axis range for each plot; 'core

Acknowledgements

I owe a huge debt of gratitude to the many people who supported me through this project. Firstly my primary supervisor, Kirsty Penkman, for knowing when to push me and when to tell me not to push myself so hard — and for putting up with all the sarcastic colour-coded comments in my many drafts! Many thanks also to my secondary supervisors, Natasha Barlow and Roland Gehrels, for all your support, and to Jane Thomas-Oates who provided invaluable feedback in TAP meetings as my independent panel member. Thank you to Sheila Taylor, Maria Gehrels and Sam Presslee for both training and technical support, to the NEaar group for being a such wonderful research community, and to York's sea-level research group for accepting me as a willing interloper.

I am tremendously grateful to those who helped me obtain samples, without whom I would have had no foraminifera to study: Graham Rush, Harry Langford, Becky Briant, Martin Bates, Adrian Read and Alice Dowsett. I am also indebted to Jo Brendryen, Richard Preece and Becky Briant for the time they took to help a chemist muddle through unfamiliar geography, and to Matthew Kosnik for his programming assistance. Emily Millman has been a wonderful co-author to work with, as have Darrell Kaufman and Katherina Billups. I must also give a special mention to the approximately 32,990 foraminifera I picked over the course of this project – thank you for giving up your secrets, and sorry about the hydrochloric acid.

I could never have come this far without the emotional and practical support of my family. Particular thanks to Gemma for acting as my proof-reader – any remaining mistakes are my responsibility alone. Thank you also to Rhey for your unwavering support, and to Usama – for everything.

Declaration

I declare that this thesis is a presentation of original work and I am the sole author. This work has not previously been presented for an award at this, or any other, University. All sources are acknowledged as references.

The work carried out as part of this thesis and presented in **Chapter 3** has resulted in the following publication:

Wheeler, L. J., Penkman, K. E. H., & Sejrup, H. P. (2021). Assessing the intra-crystalline approach to amino acid geochronology of *Neogloboquadrina pachyderma* (sinistral). *Quaternary Geochronology*, **61**, 101131. https://doi.org/10.1016/j.quageo.2020.101131

A portion of the work carried out in **Chapter 4** forms part of the following publication, which is presented in full in **Appendix 1**:

Millman, E., Wheeler, L. J., Billups, K., Kaufman. D., Penkman, K. E. H. (2022). Testing the effect of oxidizing pre-treatments on amino acids in benthic and planktic foraminifera tests. *Quaternary Geochronology*, **73**, 101401. https://doi.org/10.1016/j.quageo.2022.101401

Lucy Wheeler

Chapter 1 – Introduction

1.1 Sea-level change in the Quaternary

Sea-level rise driven by anthropogenic climate change is a major challenge facing humanity in the 21st century; understanding the drivers of sea level are therefore critical to predicting future sealevel rise and mitigating its effects (Oppenheimer et al., 2019). The factors affecting sea level are complex and operate on a wide range of timescales from daily to multi-millennial. Instrumental measurements and historical records provide a detailed record of sea level as far back as the 18th century in some regions; however, to understand longer term drivers of global and regional sealevel change it is necessary to reconstruct past sea levels from the geological record. This is of particular interest to the current geological period, the Quaternary (Shennan et al., 2012; Horton et al., 2018; Fox-Kemper et al., 2021).

Interpreting Quaternary sea-level records is challenging, especially with respect to timing as geological records are often sparse and fragmentary. A wide range of dating techniques have been developed, and improving dating techniques is an area of active research. Amino acid racemisation dating (AAR, also known as amino acid geochronology, AAG) is one such technique, which uses the decomposition of amino acids trapped in biominerals to estimate age. This thesis focuses on the application of AAR to foraminifera, a class of microfossil found in many marine and estuarine deposits, and widely used in Quaternary sea-level reconstructions.

1.1.1 Introduction to the Quaternary

The Quaternary period is the most recent geological period in the Cenozoic era, comprising the Pleistocene (2.6 - 0.012 Ma) and Holocene (0.012 Ma to present) epochs (Gibbard et al., 2010) (**Fig. 1.1**). The Quaternary is characterised by repeated fluctuations in climate, with corresponding changes in the extent of global ice sheet coverage (Head et al., 2008). This results in significant changes in global sea level between lower sea level during cool glacial climates and higher sea level during warm interglacial climates.

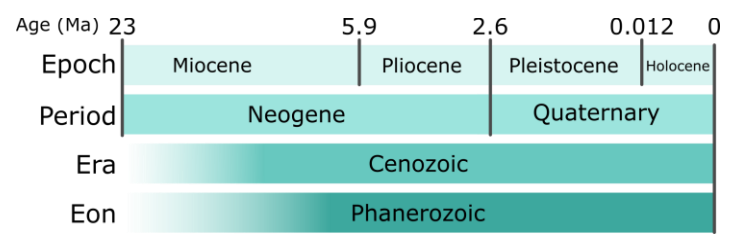


Fig. 1.1 – Section of the Cenozoic era, showing the Neogene and Quaternary periods (not to scale). Chronological boundaries taken from the International Commission on Stratigraphy (Cohen et al., 2013).

The study of former glacial climates reaches back to the early 19th century, with one or more 'ice ages' characterised from terrestrial geological records (Agassiz, 1840; Imbrie, 1982). However, it was not until global temperature reconstructions from deep-sea sediment cores were carried out in the early 1970s that the full scale of the Quaternary's fluctuating climate was truly appreciated (e.g. Shackleton and Opdyke, 1977). Over 100 glacial and interglacial stages have now been identified in the Quaternary through the marine oxygen isotope record (Lisiecki and Raymo, 2005) (Fig. 1.2). These are referred to as marine oxygen isotope stages (MIS) and are numbered from the current interglacial (MIS 1) back in time, with even MIS numbers representing glacials and odd MIS numbers representing interglacials. Substages within glacial or interglacial stages are denoted with letters (Aitken and Stokes, 1997).

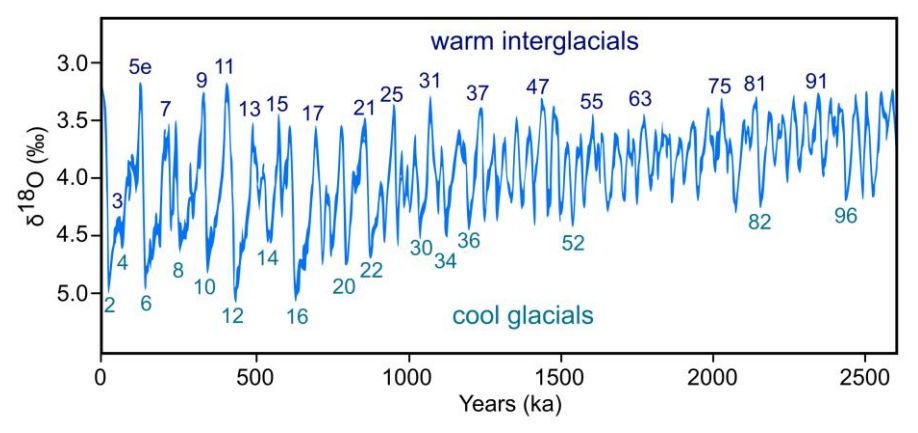


Fig. 1.2 – Pleistocene δ^{18} O (oxygen isotope) record, showing fluctuations between warm interglacial and cool glacial climates. Select marine isotope stages are labelled. Adapted from Lisieki and Raymo (2005) and Raymo *et al.* (2018).

Interstadials are periods which are too short or too cool to be considered 'true' interglacials, although the precise boundary between an interstadial and an interglacial is not well defined (Past Interglacials Working Group of PAGES, 2016). Due to its relatively cool climate in comparison to other numbered stages, MIS 3 is considered an interstadial rather than an interglacial (Fig. 1.2). Therefore MIS 5e is the Last Interglacial (LIG), the preceding substages MIS 5a-5d being interstadials.

1.1.2 Astronomical drivers of climate change

A key driver of climate change in the Quaternary and late Pliocene is changes in insolation (the amount and distribution of sunlight received by the Earth) due to long-scale variations in the Earth's orbit around the sun (Berger, 1988). The foundational mathematical model of insolation cycles was developed by the theoretician Milankovitch and published in 1941, based on theoretical and geological work carried out in the late 1800s, and later validated by the collection of continuous high-resolution records of the Earth's climate throughout the Quaternary (Imbrie, 1982).

Long-term changes in insolation are a combination of three periodic cycles, known as Milankovitch cycles (Fig. 1.3). The shortest of these is the 21 ka precession or 'wobble' of the Earth's axis of rotation, which causes shifts in the Earth's seasons over time (Berger, 1988). The cycle of obliquity takes place over 41 ka and causes changes in the severity of the Earth's seasons through changes to the angle of its axis relative to its plane of orbit around the sun, from 21.8° to 24.4° (Bradley, 1999). The eccentricity of the Earth's orbit is its deviation from a perfect circle, and varies over 100 and 400 ka cycles (Berger, 1988). The main impact of the eccentricity cycles is a modulation of the precession cycle.

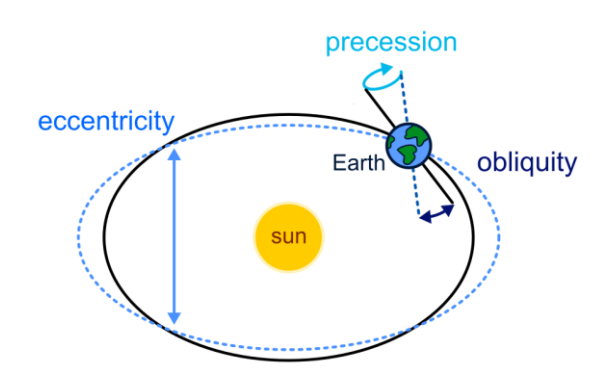


Fig. 1.3 – A schematic representation of the three Milankovitch cycles – changes to the Earth's orbit around the sun over geological timescales (not to scale).

The response of the Earth's climate to the Milankovitch cycles is thought to take place primarily through changes to seasons in the Northern Hemisphere. Short, mild summers allow for the accumulation of widespread continental ice sheets, while long, hot summers diminish them. The strength, timing and duration of interglacials depend on the particular patterns of insolation caused by combinations of the three Milankovitch cycles (Past Interglacials Working Group of

PAGES, 2016). However, the relationship between orbital forcing and glaciation is not linear, as the climatic response to orbital forcing is strongly influenced by interactions between the components of the Earth's climate system (Pillans et al., 1998; Tzedakis et al., 2012).

Much work remains on relating the complex response of global and regional climates to these and other forcing factors, including anthropogenic activities (Fox-Kemper et al., 2021). Understanding the complex influences governing the Quaternary's climate cycles is critical to understanding the ways in which anthropogenic forcing has and will continue to shape the climate of the Holocene.

1.1.3 Sea-level change

Sea level is driven by processes operating on a wide range of spatial and temporal scales; untangling this web of influences to understand past sea-level change and predict future changes therefore presents a major research challenge (Oppenheimer et al., 2019).

Relative sea level (RSL) is the level of the sea surface relative to a given point of the solid Earth at a given location (normally present day mean sea level), and is the quantity measured by a tide gauge (Shennan et al., 2015). Global mean sea level (GMSL) is the global average of relative sea levels. GMSL is also referred to as 'eustatic sea level' (Mitrovica and Milne, 2003); however, deprecation of this term has been advocated to avoid ambiguity (Gregory et al., 2019).

On glacial-interglacial timescales, GMSL is driven by exchange of water mass between the land and oceans, primarily due to the advance and retreat of terrestrial ice sheets (Milne, 2014). During glacial stages, ice sheets are extensive, and the GMSL is low. During the Last Glacial Maximum (LGM, ~21 ka BP), for example, global mean sea level is thought to have been approximately 120-135 m lower than today (Clark and Mix, 2002). Subsequent retreat of ice sheets during deglaciation causes GMSL rise. The contribution to GMSL change through changing water mass balance in the ocean is referred to as barystatic sea level rise. The term 'barystatic' has recently been proposed to replace the commonly used 'eustatic' in this context, to avoid conflation with GMSL (Gregory et al., 2019). Thermostatic sea-level change – that is, the thermal expansion or contraction of the ocean – also plays a significant role in GMSL change, and may be the dominant contribution to sea-level rise in the 21st century (Milne, 2014).

Barystatic sea-level change is not globally uniform, due to a process of glacial isostatic adjustment (GIA). Isostasy is the response of the Earth's surface to changes in mass load (in the form of water or ice). When an ice sheet advances, its weight depresses the landmass beneath it, causing a local

rise in RSL despite a falling GMSL. Subsequent retreat of the ice sheet during glacial termination causes the landmass to rebound over the course of tens of thousands of years – resulting in a falling RSL in regions close to the retreating ice sheet during a period of GMSL rise (Milne, 2014). Gravitational attraction of the ocean to ice sheets during glacial stages also causes local variations in the height of the sea surface, and therefore RSL (Farrell and Clark, 1976).

RSL is also influenced on local scales by short-term processes such as tides, storms, erosion and subsistence. On longer timescales, crustal motions such as lithosphere formation and subduction, continental collision, and convective flow within the Earth's mantle also influence RSLs (Geophysics Study Committee and National Research Council, 1991; Austermann et al., 2017). Understanding these processes is vital for both interpreting RSL records and using them to estimate GMSL changes during past glacial or interglacial periods; likewise, predicting future sea-level changes in particular regions requires an understanding of how global sea-level trends are altered by regional processes.

1.1.3.1 Past sea-level change as an analogue for the future

Since 1901, the mean rate of GMSL rise has been 0.8-1.9 mm a⁻¹, with the rate of GMSL rise accelerating to 3.2-4.2 mm a⁻¹ during the period 2006-2018 (Fox-Kemper et al., 2021). In some regions, RSLs are rising at a rate of up to 20 mm a⁻¹ (Nicholls and Cazenave, 2010). This change is predicted to have severe impacts on coastal regions due to increased submergence, erosion and flooding events, especially in developing countries with the fewest resources for risk mitigation and adaptation (Oppenheimer et al., 2019). With around 10% of the world's population living in low elevation (< 10 m) coastal zones as of 2007, and coastal urban areas experiencing the greatest population growth (McGranahan et al., 2007), sea-level rise will be one of the major challenges facing humanity in the 21st century.

Predictions about how sea levels will change in the future on a global and regional scale are based on models constrained by past changes in sea level. Reliable instrumental records of sea level, in the form of tide gauges, extend back as far as the 1700s in a few locations, with the majority of current tide gauge stations being established in the 1950s or later (Jevrejeva et al., 2006; Horton et al., 2018). High-resolution satellite altimetry data are available for most of the globe from the 1990s onwards (Horton et al., 2018). Using these records it is possible to elucidate short-term (annual to centennial) influences on global and regional sea level; however to understand long term sea-level patterns it is necessary to infer past sea levels from the complex, often fragmentary archaeological and geological records available (Shennan et al., 2015). While the uncertainties

involved in reconstructing past sea levels limit their application to quantitative predictions of future sea level (Fox-Kemper et al., 2021), these records are important for understanding long-term drivers of sea-level change, and to constrain and test models of the Earth's climate and its responses to anthropogenic forcing (e.g. Horton et al., 2018; Gilford et al., 2020). Particular attention has been paid to past interglacials as analogues of Holocene climate, to understand the millennial-scale sensitivity of the Earth's climate, in particular its ice sheets, to climate-forcing variables such as insolation, CO_2 concentration and changes to the Earth's atmospheric and ocean circulation systems (Rovere et al., 2016).

The Last Interglacial (LIG; MIS 5e, ~128 - 116 ka, (Stirling et al., 1998)) is perhaps the most studied of the Earth's past interglacial periods, due to the relatively widespread preservation of marine and terrestrial records compared to older interglacials, affording the greatest resolution of climate data from past interglacials (Pedoja et al., 2014). During this period global mean temperatures were slightly warmer (0.5-1°C) than pre-industrial conditions, with stronger warming in the Arctic (Oppenheimer et al., 2019; Otto-Bliesner et al., 2021), a trend which is also observed in post-industrial records due to anthropogenic warming. At the peak of the LIG at ~125 ka, GMSL was likely between 5-10 m above GMSL today, with the largest contribution to sea-level rise coming from polar ice sheets (Fox-Kemper et al., 2021).

The reliability of the LIG to act as an analogue for modern climate change is limited by its difference in orbital forcing compared to the Holocene (Yin and Berger, 2012). Greater summer insolation in the Northern Hemisphere during the early LIG (due to its higher orbital eccentricity than the Holocene) may have contributed to as much as 45% of ice sheet loss (Van De Berg et al., 2011). Nonetheless, the LIG provides a useful record of how ice sheets respond to a warming climate, which can be used as an analogue for anthropogenic climate forcing.

MIS 11 (~428 - 397 ka) is generally considered to be a better analogue for the effect of orbital forcing on the climate of the Holocene, as its orbital geometry is closer to Holocene orbital geometry than any other well-characterised interglacial in the last 500,000 years (Howard, 1997; Loutre and Berger, 2000; Candy et al., 2014). However, MIS 11 featured an unusual 'double peak' of insolation, leading to a brief lapse of interglacial climate between two insolation maxima. Having both low eccentricity and only one insolation peak, attention has also been given to MIS 19 (~740 ka) as a more appropriate analogue to current insolation conditions (e.g. Yin and Berger, 2012) — however records from this older interglacial are much more fragmentary, lower in resolution, and more difficult to obtain (Rohling et al., 2010).

Reconstructions of past climates are important for calibrating and validating climate models under climate regimes not represented by the historical record (e.g. Braconnot et al., 2012; Schmidt et al., 2014). Records of past sea-level change can be especially useful as an indirect proxy to estimate and model ice-sheet growth and retreat (e.g. Milne et al., 2002; Goelzer et al., 2016; Creveling et al., 2017). However, these records are often sparse and difficult to interpret, especially with respect to their timing, presenting a major challenge for past sea-level reconstruction (Schmidt et al., 2014; Marino et al., 2015). Improving chronological control of sea-level records is therefore an area of particular interest in Quaternary research.

1.2 Dating Quaternary sea-level records

1.2.1 Introduction to Quaternary geochronology

Geochronology is the determination of the age of rocks, sediments and fossils, either by correlation to other records or by measuring the material's absolute age. Developing chronologies for terrestrial sea-level records from past interglacials can be especially challenging due to their sparse, fragmentary nature. A range of techniques have been developed to tackle this challenge; as each method has its advantages and disadvantages, a variety of methods is typically used to constrain ages of past interglacial sea-level deposits (Lowe and Walker, 2014). The key dating techniques used in Quaternary geochronology are summarised below in **Table 1.1**; the principles and shortcomings of the techniques most commonly used in Quaternary sea-level reconstruction are discussed in further detail below.

Table 1.1 – Summary of dating methods used for the Quaternary.

Method	Substrate(s)	What is being measured?	Age range				
Correlative & relative techniques							
Stratigraphy	Any sedimentary sequence	Sequence of deposition	Entire geological record, depending on sequence				
Biostratigraphy	Fossil-bearing sediments	Changes in species distribution	Up to 3.5 Ga, depending on sequence				
Tephrochronology	Tephra	Volcanic eruptions	Distinct isochronic markers throughout the Quaternary and beyond				
Palaeomagnetism	Minerals with residual magnetism	Variations in the polarity of the Earth's magnetic field	Up to 50 ka for secular variation; several global polarity reversals during Quaternary ^a				

Method	Substrate(s)	What is being measured?	Age range				
Oxygen isotopes	Ocean sediments (foraminifera)	Ocean temperature and global ice coverage	Up to 5.3 Ma ^a				
Annual banding records	Wood, corals, speleothems, annually banded sediments, ice, etc.	Annual growth/deposition, typically forming 'floating chronologies' which can be cross-matched to form continuous chronologies	Continuous chronologies: Corals: 0.4 ka ^b Molluscs: 1.4 ka ^c Tree rings: 12 ka ^d Ice cores: 110 ka ^b				
Amino acid racemisation	Fossil biominerals	Time since cessation of tissue turnover	Up to 2.5 Ma depending on latitude, typically up to ~1 Ma ^e				
	Numerical radiometric techniques						
Radiocarbon	Organic material	Time since cessation of tissue turnover	Up to ~45 ka, ~60 ka in some cases ^d				
Uranium series	Carbonate materials (biominerals and speleothems)	Time since mineral formation or U uptake	²³⁰ Th/ ²³⁴ U 0.1 to 500 ka ^a ²³¹ Pa/ ²³⁵ U: 5-200 ka ^a ²³¹ Pa/ ²³⁰ Th: 5-250 ka ^a ⁴ He/U: 100 ka to 10 Ma ^a U-Pb: 1 Ma up to ~4 Ga ^f				
Potassium-argon dating	Volcanic rocks	Time since crystallisation	100 ka up to ~4 Gaª				
Cosmogenic nuclides	Rock surfaces	Duration of exposure to cosmic rays	Up to between 0.2 ka ^a and 10 Ma ^b depending on nuclide				
	Numerical	trapped charge techniques					
Thermoluminescence (TL)	Quartz- and feldspar-rich materials, biominerals	Time since exposure to heat (or biomineral formation)	0.1 to between 100-300 ka depending on material ^a				
Optically stimulated luminescence (OSL)	Quartz- and feldspar-rich materials	Time since exposure to light	0.2-0.3 to 100-150 ka ^d				
Electron spin resonance (ESR)	Biominerals, speleothem calcite	Time since exposure to heat or light	A few ka up to 2 Ma for certain materials ^d				
Fission track dating	Volcanic minerals	Number of damage trails caused by spontaneous fission reactions	0.1 ka up to > 2.5 Ma ^d				

^a Lowe and Walker (2014)

b Walker (2005)
c Butler et al. (2013)

d Walker and Lowe (2007)
Wehmiller and Miller (2000)

f Rasbury and Cole (2009)

1.2.2 Correlative dating methods

Correlative methods used in Quaternary geochronology include stratigraphy, biostratigraphy, tephrochronology, palaeomagnetism and stable isotopes (Table 1.1). The basic principle of time-stratigraphic correlation is that if a depositional event can be reliably identified in a range of locations, then a date range obtained for the event in one location applies to all locations (Walker, 2005). Tephrochronology, for example, is used throughout the Quaternary to correlate regional stratigraphic sequences, as volcanic eruptions provide an essentially instantaneous time marker in the stratigraphic record (e.g. Tzedakis et al., 2001). Biostratigraphy is the use of fossil assemblages to make stratigraphic correlations. In the Quaternary, this technique enables glacial and interglacial horizons to be distinguished through the different ecological makeup of warmer and cooler environments, although differentiating successive interglacials from each other can be a challenge (Schreve and Thomas, 2001; Thomas, 2001). Pollen, molluscs and mammals are the most commonly used fossils in Quaternary biostratigraphy (Schreve and Thomas, 2001). Oxygen isotope stratigraphy has a resolution of only a few thousand years, but enables deposits to be correlated to the global MIS framework (e.g. Bleil and Gard, 1989; Tzedakis et al., 2001).

The major challenge of correlative dating methods is determining the synchroneity of depositional events. This is especially important for terrestrial deposits, which are often dominated by local and regional patterns not present in global ice-core or marine records (Gibbard and Hughes, 2020). A range of correlative techniques is usually applied to a single site or region to reduce uncertainties arising from limitations of any single technique (Walker, 2005).

1.2.3 Radiometric dating methods

1.2.3.1 Principles of radiometric dating

Radiometric dating methods use the decay of radioisotopes as a 'clock' for measuring the passage of time. As radioactive decay is exponential, the age of a sample relates directly to its radioactivity or radioisotopic ratio through the half-life of the radioisotope under study.

Early emission-counting techniques measured the radioactivity of a sample by counting the alpha (He²⁺) or beta (e⁻ or e⁺) particle emissions of the sample over a given length of time. This method requires large sample sizes and long analysis times, especially in ancient samples where radioactivity is low (Smart and Frances, 1991). By contrast, the newer techniques of accelerator

mass spectrometry (AMS) and inductively coupled plasma mass spectrometry (ICPMS) measure the ratios of individual isotopes. AMS and ICPMS are quickly gaining dominance in the field of radioanalytics due to their smaller sample size requirements and shorter analytical times compared to emission-counting techniques (Povinec, 2018).

Depending on the radioisotopes used, the suite of radiometric dating methods covers almost the entire span of the Earth's history. ⁴⁰K has a half-life of 1.3 x 10⁹ years (Smart and Frances, 1991), so its decay series can be used to date igneous rocks as old as four billion years. On the other end of the scale, ¹³⁷Cs (half-life of 30 years) is routinely used to date samples from the last century (Shennan et al., 2015). The most commonly used radiometric dating methods for Quaternary sealevel studies are radiocarbon and U-series (Milne, 2014; Shennan et al., 2015); these are discussed in more detail below.

1.2.3.2 Radiocarbon dating

Radiocarbon dating relies on the decay of radiocarbon (14 C) in organic materials. 14 C is generated from 14 N in the atmosphere by cosmic radiation. It is incorporated into living material during growth, where it remains in equilibrium with atmospheric 14 C during the lifetime of the tissue. 14 C undergoes exponential radioactive decay with a half-life of 5,730 \pm 40 years (Godwin, 1962); once tissue turnover ceases and no additional 14 C is incorporated into the organic material, the concentration of 14 C in the material decreases at this rate of decay. Beyond $^{\sim}45$ ka, the concentration of 14 C in a sample is generally too low to be accurately determined, with even very small amounts of contamination leading to large age errors, although in a few limited cases the range of the technique has been extended to $^{\sim}60$ ka (Walker and Lowe, 2007).

Several factors complicate the derivation of numerical ages from radiocarbon measurements, including contamination, isotopic fractionation, variations over time in the generation of atmospheric ¹⁴C, and marine reservoir effects. Efforts to reduce the impact of contamination are largely focused on careful sampling and preparation techniques such as acid or alkaline pretreatments (Walker, 2005). Conversion of radiocarbon measurements into calendar ages requires the use of calibration curves which account for changes in atmospheric ¹⁴C over time. Calibration curves have been developed using materials dated by both radiocarbon dating and other methods, principally dendrochronology and U-series dating (Walker, 2005). The most widely used calibration curves are those developed by the IntCal Working Group (Lowe and Walker, 2014). The most

recent iterations of these curves are IntCal20 (for the Northern Hemisphere), SHCal20 (for the Southern Hemisphere) and Marine20 (for marine samples) (Reimer et al., 2020).

For marine samples, an additional complication is the residence time of carbon in the world's oceans. At the sea surface, dissolved carbon is in equilibrium with the atmosphere; however once this carbon is transported into intermediate and deep waters, it undergoes radioactive decay without immediate replenishment from the atmosphere. This results in a 'marine reservoir effect' which may vary from less than 30 years in shallow waters to thousands of years in the deep oceans (Walker, 2005). A database of marine reservoir ages can be found at calib.org/marine; new local reservoir ages are added to the database regularly (Reimer and Reimer, 2001).

The ~50 ka age limit of radiocarbon dating limits its application to sea-level records from the last deglaciation and younger. Radiocarbon dating is the primary technique used to date sea-level deposits during this period and is found extensively in Holocene (Hibbert et al., 2018) and post-LGM sea-level databases (Khan et al., 2019).

1.2.3.3 U-series dating

U-series dating encompasses a range of techniques, based on different parts of the ²³⁸U, ²³⁵U and ²³²Th decay chains (Lowe and Walker, 2014). The most commonly applied method of U-series dating to sea-level research is the daughter decay technique. Uranium is highly soluble, while several of its decay products, such as ²³⁰Th and ²³¹Pa, are insoluble. In the precipitation of certain minerals, U is taken up into the mineral matrix from the surrounding water, while its insoluble decay products are not. Following formation of the mineral, the decay of U leads to an accumulation of its daughter products within the mineral matrix, enabling a calculation of the time since its formation, usually by measuring the ratio of ²³⁰Th to ²³⁴U (Lowe and Walker, 2014). This technique is applicable to a range of materials including corals, mollusc shells, bone, speleothems, tufa and phosphates, and has an age range of 0.1 to 500 ka (Lowe and Walker, 2014).

As they can provide an indication of past sea levels and can be dated using U-series dating, corals are widely used in Quaternary sea-level reconstructions where they occur at tropical and subtropical latitudes (Hibbert et al., 2016). While it is theoretically possible to date corals up to ~500 ka using U-series dating, most reliably dated fossil corals are from the last glacial cycle due to a paucity of well-preserved specimens older than MIS 5 (Andersen et al., 2010). U-series dated speleothems have also been used to a lesser extent to reconstruct Quaternary sea levels (Dutton et al., 2009; Onac et al., 2012), through the identification of sea-level rise due to cessation of

speleothem growth, encrustation by aquatic organisms, or sub-aquatic overgrowths from mineralrich groundwaters.

Conventional U-series dating assumes that the sample has behaved throughout diagenesis as a closed system – that is, that there has been no loss or gain of parent or daughter isotopes. Therefore the major challenge of U-series dating is identifying open-system behaviour caused by geochemical alteration of the mineral. This is a particular problem in older samples, as the extent of open-system mobilisation increases with age (Stirling and Andersen, 2009). Two main approaches are used to address this issue: screening and open-system modelling (Hibbert et al., 2016). Screening aims to identify and remove samples which do not conform to closed-system behaviour; however, the choice of screening criteria may have a large effect on which samples are excluded (Hibbert et al., 2016), and with very old material it is often necessary to reject the majority of samples due to the mobilisation of isotopes (Stirling and Andersen, 2009).

In an alternative approach, various models of open-system redistribution of Th and U in corals have been developed (e.g. Gallup et al., 1994; Thompson et al., 2003; Villemant and Feuillet, 2003). The performance of these models is variable (Chutcharavan and Dutton, 2021), especially for samples older than ~200 ka (Frank et al., 2006). An additional complication is the challenge of verifying models without closed-system samples from the same coral or reef terrace, which become increasingly rare in older samples (Stirling and Andersen, 2009). Overall there is no community consensus about which screening criteria or open-system models are best for accommodating diagenetically altered coral U-series dates (Stirling and Andersen, 2009; Hibbert et al., 2018; Chutcharavan and Dutton, 2021).

U-series dating is widely used in the sea-level research community, especially beyond the limits of radiocarbon dating. In recent years, several databases of sea-level records dated using U-series and radiocarbon methods have been collated (e.g. Hibbert et al., 2018; Chutcharavan and Dutton, 2021), focusing mainly on material from the LIG and younger.

1.2.4 Trapped charge dating methods

Trapped charge methods – thermoluminescence (TL), optically stimulated luminescence (OSL) and electron spin resonance (ESR) – are a subset of radiometric techniques which measure the number of electrons accumulated in crystal defects by radiative exposure (Walker, 2005). The longer the mineral is subjected to radiation, the greater the number of trapped charges; thus the technique measures the time elapsed since some 'zeroing' event which frees the electrons from the crystal

defects (Walker, 2005). This zeroing event may be exposure to sunlight, heating, biomineralisation or recrystallisation – therefore, one major advantage of trapped charge techniques is that they can date erosional, depositional or reworking events for which radiometric dating would give erroneously old ages (Fuchs and Owen, 2008).

The techniques differ in the method used to detect the trapped electrons. In TL and OSL, heat and light respectively are used to liberate electrons, while ESR excites trapped electrons (which are paramagnetic) using a magnetic field. The age limit of luminescence dating depends on the saturation of the luminescence signal, which depends on the mineral studied and the environmental supply of radiation (Fuchs and Owen, 2008).

Measured luminescence signal intensity of a sample is converted into age using its environmental dose rate. This is the rate of radiation absorbed by the mineral both from its endogenous radioactive isotopes and from surrounding material. The dose rate is typically determined either by direct counting of emissions (*in* or *ex situ*) or measuring the concentration of radioactive elements (U, Th and K) in the surrounding sediment (Duller, 2008). Determination of the dose rate may be complicated by heterogeneity of the surrounding sediment, radioactive element concentrations which approach the limits of analytical detection, or changes in the dose rate over the sample's burial history (Duller, 2008).

Incomplete zeroing of the luminescence signal is another major challenge in determining reliable age estimates using luminescence dating, especially in fluvial and marine sediments (Preusser et al., 2008). Advances in the technique have enabled more rigorous identification of incomplete zeroing events, in particular the single aliquot regeneration (SAR) method which enables luminescence measurements of single mineral grains, which can then be checked against other grains in the sample for internal consistency (Rhodes, 2011).

One of the largest sources of uncertainty in OSL/TL dating is the water content of a sample and its surroundings (Duller, 2008). Water between mineral grains absorbs some of the radiation, so the higher the water content of a sample the less radiation is absorbed by the luminescent mineral. Typically a 1% increase in water content results in a 1% increase in calculated age (Duller, 2008). Modern-day water content is usually used as a guideline for the average water content during burial, but potential changes in hydrological conditions must also be taken into account (Preusser et al., 2008). Beyond ~300 ka, there are additional challenges validating OSL/TL ages due to a lack of independent dating (Wallinga, 2002).

Trapped charge dating methods are frequently used alongside other dating methods in late Quaternary sea-level reconstructions around the world (e.g. Britain (Briant et al., 2004, 2012), continental Europe (Marks et al., 2014), Russia (Gualtieri et al., 2003), Australia (Murray-Wallace et al., 2010) and North America (Owen et al., 2007)).

1.2.5 Amino acid racemisation dating

Amino acid racemisation dating (AAR) is a dating method based on the decomposition of proteins in biomineral sub-fossils, and is applicable to timescales spanning from 150 ka to 2.5 Ma depending on the diagenetic temperature and properties of the biomineral (Wehmiller and Miller, 2000). A key application of AAR is Quaternary sea-level records from temperate latitudes, which are critical for reconstructing ice-sheet contributions to past GMSL change (Dutton et al., 2015). Temperate latitude estuarine deposits have been widely used to reconstruct Holocene sea-levels (see Barlow et al., 2013); however, past interglacial estuarine deposits are more challenging to date as they fall beyond the limits of radiocarbon dating. U-series dating is less reliable for molluscs than for corals, which are not commonly found at high latitudes (Shennan et al., 2015), and incomplete bleaching or variable water contents often complicate trapped charge measurements, especially in estuarine and fluvial environments (Duller, 2008; Preusser et al., 2008). While biostratigraphy of pollen, molluscs and vertebrates can provide both palaeoenvironmental and chronological information, differentiating between successive interglacial periods can be challenging (e.g. Schreve and Thomas, 2001; Thomas, 2001). AAR of biomineral sub-fossils from these locations therefore provides additional chronological control for these challenging-to-date environments.

AAR has been used to date Quaternary sea-level deposits around the world, including in Britain (e.g. Bates *et al.*, 2010; Penkman *et al.*, 2013; Barlow *et al.*, 2017), Australia (e.g. Cann et al., 1988; Nash et al., 2018), North America (e.g. Wehmiller et al., 2010) and Europe (e.g. Pierini et al., 2016; Torres et al., 2016), typically focusing on differentiating between sea-level highstands from different interglacials. The principles of AAR are discussed in detail below.

1.3 Principles of amino acid racemisation dating

This section covers the principles of AAR and its history as a Quaternary dating technique. The mechanisms of protein decomposition are discussed in **Section 1.4**; an discussion of the application of AAR to foraminifera and sea-level reconstructions is in **Section 1.5.2**.

1.3.1.1 A note on naming conventions

The name 'amino acid racemisation dating' is not technically accurate, as a range of other reactions besides racemisation inform the estimation of age in this technique (see **Section 1.4**). Amino acid geochronology (AAG) has been proposed as a more accurate alternative, and has gained some use in recent years; however, as AAR remains the most widely used acronym in the wider Quaternary community, this thesis will use AAR to refer to this technique (with the exception of **Chapter 3** where 'AA geochronology' was chosen for editorial reasons).

1.3.2 Amino acids in biominerals

Amino acids are an important class of molecule ubiquitous in biology as the building blocks of proteins. Amino acids are comprised of an α -carbon bonded to an NH₂ (amino) group, a COOH (carboxylic acid) group, a hydrogen atom, and a fourth substituent R (**Fig. 1.4a**). There are twenty commonly occurring amino acids in nature (**Table 1.2**), each with a different R-group. Peptides are formed from chains of two or more amino acids linked by peptide bonds (**Fig. 1.4b**); amino acids in a peptide are referred to as residues. Large chains of amino acids are referred to as proteins; the division between a peptide and a protein is not strictly defined, but is typically considered to be around 50 amino acid residues (Gold, 2019). The sequence of amino acids in a protein determines its secondary structure and functionality.

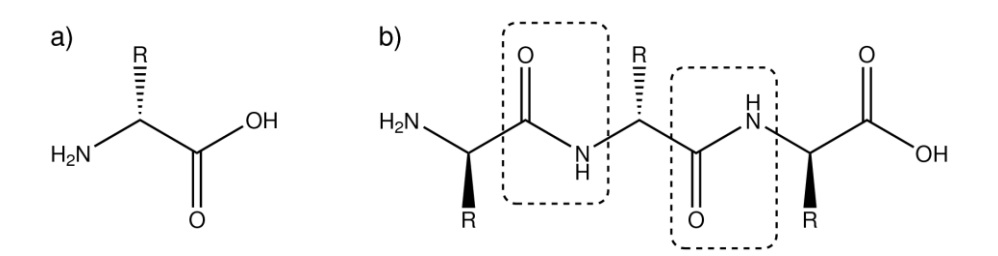


Fig. 1.4 – Structure of a) an amino acid and b) a peptide formed from three amino acid residues. The peptide bonds are indicated by dotted rectangles.

 $\textbf{Table 1.2} - \textbf{Naturally occurring amino acids and their quantification and chiral separation by ion exchange chromatography (IEC), high performance liquid chromatography (RP-HPLC) and ultra high$

performance liquid chromatography (UHPLC) (see Section 1.3.4.2).

Amino acid	R-group Structure (the far left carbon in each structure is the α -carbon)	1-	3- letter code	Quantification (✓); Chiral separation (★)		
		letter code		IEC	RP- HPLC	UHPLC
Aspartic acid	ОН	D	Asp ^a	✓	*	*
Asparagine	O NH ₂	N	Asn ^a			
Glutamic acid	ОН	Е	Glu ^b	✓	*	* *
Glutamine	O NH ₂	Q	Gln ^b	-		
Serine	ОН	S	Ser	√	*	*
Glycine	—-н	G	Gly	√	✓	✓
Arginine	H ₂ N NH	R	Arg		✓	*
Alanine	CH₃	А	Ala	✓	*	*
Histidine	N N N N N N N N N N N N N N N N N N N	Н	His		✓	*
Valine		V	Val	√	*	*
Phenylalanine		F	Phe		*	*
Isoleucine		I	Ile	*	*	*

Amino acid	R-group Structure	1- letter	3-	Quantification (✔); Chiral separation (★)		
	(the far left carbon in each structure is the α -carbon)	letter letter code code		IEC	RP- HPLC	UHPLC
Leucine		L	Leu	✓	*	*
Threonine	OH	Т	Thr	✓	✓	*
Methionine	\\\\\\\\\\\\\\\\\\\\\\\\\\\\\\\\\\\\\\	М	Met		*	*
Tyrosine	OH	Y	Tyr		*	*
Lysine	NH ₂	K	Lys			
Proline ^c	HO	Р	Pro			
Cysteine and Selenocysteine	SH SeH	C, U	Cys, Sec			
Tryptophan		W	Trp			

^a Asp and Asn are analytically indistinguishable (Section 1.3.4.2), so are referred to jointly as Asx.

Biomineral-secreting organisms use proteins to direct mineral precipitation and control both the shape (Albeck et al., 1993) and mechanical properties (Gries et al., 2012) of the biomineral. Biomineral proteins were first identified in fossil material in 1954 by Abelson et al., and their decomposition over geologic time was soon proposed as a potential dating method (Abelson, 1955).

^b Glu and Gln are analytically indistinguishable (**Section 1.3.4.2**), so are referred to jointly as Glx.

 $^{^{}c}$ The R-group of proline is bonded to both the α -carbon and the nitrogen of the amino group (shown in blue).

The preservation of proteins and amino acids in the fossil record is highly dependent on the biomineral structure and depositional environment. The limits of protein and amino acid preservation is a subject of intense interest and debate, with issues such as contamination presenting a significant challenge when identifying very small amounts of highly degraded proteins or amino acids in fossil material (e.g. Saitta et al., 2019; Liang et al., 2020). At present the oldest well-substantiated intact peptides come from ~3.8 Ma ostrich eggshell (equivalent to ~16 Ma at 10°C) (Demarchi et al., 2016); claims of surviving peptides from older material are controversial (e.g. Buckley et al., 2008, 2017).

Amino acids can persist for longer in the fossil record as products of peptide hydrolysis. The oldest well-substantiated amino acids have been found in ~80 Ma dinosaur eggshell (Saitta et al., 2020). There is some evidence that amino acids can be preserved over even longer timescales in amber, but more work is required (McCoy et al., 2019).

1.3.3 Amino acid racemisation

Of the twenty commonly occurring amino acids in nature, all except glycine (Gly) are chiral – that is, they are asymmetric and therefore non-superimposable on their mirror forms (Steiner, 1968). Most chiral amino acids have only one stereogenic centre, at the α -carbon, so exist as one of two enantiomers (**Fig. 1.5a**), mirrored forms with chemically identical properties (Schroeder and Bada, 1976). Isoleucine (Ile) and threonine (Thr) have two stereogenic centres, so have four stereoisomers (two enantiomers, and two epimers, which are not mirrored forms and therefore do not have identical chemical properties (**Fig. 1.5b**)).

In biology, the orientation of the α -carbon stereocentre is denoted by the prefix L- or D-, depending on its stereochemistry relative to glyceraldehyde. With the exception of some bacteria (Bhattacharyya and Banerjee, 1974), and rare cases of D-amino acids in some plant and animal proteins (see Miyamoto and Homma, 2018), all proteins in living cells are synthesised using L-amino acids.

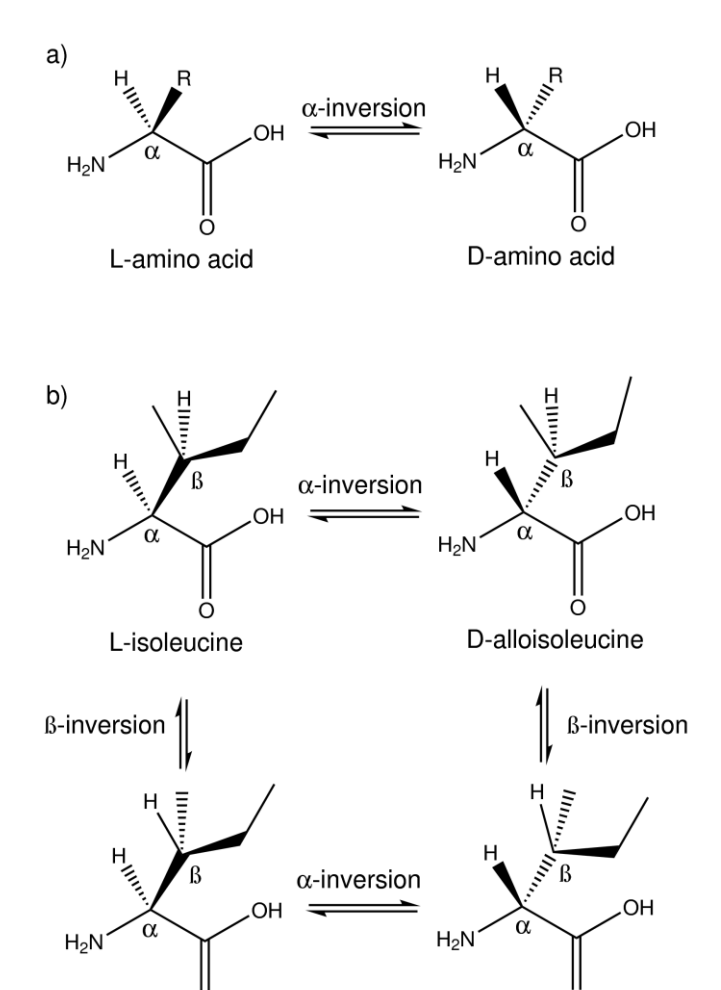


Fig. 1.5 – Chirality of amino acids: a) amino acids with one stereogenic centre at the α -carbon, forming two enantiomers (mirror images with identical physical properties); b) isoleucine, an amino acid with two stereogenic centres (at the α - and β -carbon positions), which has four stereoisomers.

D-isoleucine

L-alloisoleucine

The preference in biology for one stereoisomer over the other is thermodynamically unfavourable, and conversion from one stereoisomer to a mixture of isomers is spontaneous. This process is called racemisation and in amino acids can take place at the α -carbon stereocentre (α -inversion, **Fig. 1.5a**) or at the β -carbon stereocentre for amino acids with two stereocentres (β -inversion, **Fig. 1.5b**). In living tissue, enzymes preserve the enantiomeric excess of L- over D- amino acids; however once these functions cease (i.e. when tissue turnover stops, in most cases on death of the organism) the degree of racemisation increases until equilibrium is reached (Murray-Wallace, 1995).

For amino acids with more than one stereogenic centre, or amino acids within peptide chains, this process is technically called epimerisation as only one stereogenic centre is inverted; however, for simplicity 'racemisation' is frequently used to refer to both racemisation and epimerisation (Bada,

1972a). For epimerisation, as rates of conversion between epimers are different, the equilibrium mixture of epimers is not necessarily equal (Murray-Wallace, 1995).

1.3.4 Amino acid racemisation as a dating method

If the constituent amino acids of a protein are not lost from a system, then the ratio of L- to D-amino acids in a sample should, for a given temperature regime and set of environmental parameters, correspond to the amount of time that has passed since the cessation of tissue turnover (Hare and Mitterer, 1968).

In 1967 Hare and Abelson used enzyme digestion to quantify the D/L value of various amino acids in proteins from recent (Pleistocene) and ancient (Miocene) shells, finding that racemisation occurred "[on] the order of 10⁵ years". The first application of amino acid racemisation to geochronology was carried out by Hare and Mitterer (1968) to estimate the age of *Mercenaria* fossils. The field rapidly expanded in the following decades to include analyses of a range of other substrates, including other molluscs (Miller and Hare, 1975; Andrews et al., 1979; Wehmiller, 1980), marine sediments (e.g. Bada et al., 1970), foraminifera (e.g. King and Neville (1977), see also Section 1.5.2.2), wood (e.g. Lee et al., 1976), corals (e.g. Wehmiller et al., 1976), bones (e.g. Dungworth, 1976; Bada and Shou, 1980) and teeth (e.g. Bada, 1981).

The requirement for analysing a closed system of proteins to prevent external influences on the rate of racemisation was recognised early in the development of AAR as a dating technique (Schroeder and Bada, 1976). During early work, the physical integrity of samples, concordance of results with expected diagenetic trends, and agreement between AAR results and other dating methods were generally taken as sufficient evidence that these biomineral matrices were closed system with respect to amino acids (Miller and Hare, 1980; Towe, 1980). However, controversy surrounding spurious ages for North American human bones (Bada et al., 1974) drew attention to the importance of demonstrating closed-system behaviour in substrates dated by AAR (Bada, 1985). Recent work has focused on calcareous biominerals such as mollusc shells, eggshell, corals and foraminifera, with an increasing focus on the well-protected intra-crystalline fraction of proteins in these biominerals (Penkman, 2017).

1.3.4.1 Intra-crystalline protein diagenesis (IcPD)

The majority of proteins in a biomineral matrix form an inter-crystalline 'mesh' between crystallites (Towe, 1980), which may be susceptible to leaching, contamination or changes in chemical environment. This inter-crystalline fraction may therefore be an unreliable source of amino acids for dating (Sykes et al., 1995). However, in some species a small fraction of biomineral protein has been identified which is highly resistant to chemical oxidation (see discussion below). These proteins are thought to be *intra*-crystalline – that is, totally occluded by the biomineral structure (**Fig. 1.6**), although the exact relationship between the biomineral and so-called intra-crystalline protein has been a subject of debate (see Wehmiller and Miller, 2000).

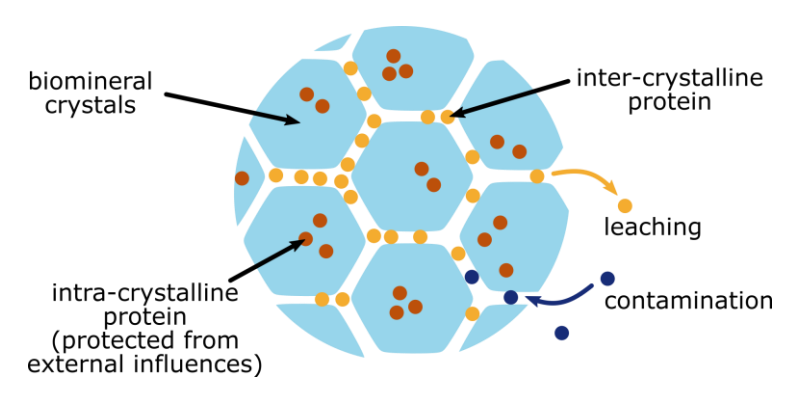


Fig. 1.6 – Schematic representation of inter- and intra-crystalline biomineral proteins (adapted from Sykes et al. (1995).

Organic material protected by an encapsulating crystal matrix was observed in biominerals using electron microscopy and diffraction as early as the 1970s (Towe and Thompson, 1972; Towe, 1980). The question of whether intra-crystalline proteins lie within single crystals or are simply 'sandwiched' between parallel crystal faces in a multi-crystal structure (or both) has been the subject of a large body of research, especially in the field of bioinspired material design (Li et al., 2011). Experiments where calcite precipitates in the presence of biomineral-directing macromolecules have found that single crystals can incorporate macromolecules during growth, without disrupting their long-range lattice structure (Li et al., 2009; Cho et al., 2016). Additionally, organic-rich voids in single crystals in nacre, an aragonitic biomineral, have been observed using electron microscopy (Gries et al., 2009; Li et al., 2011), which may be representative of a 'true' intra-crystalline protein. For the purposes of AAR, the intra-crystalline fraction of proteins can be operationally defined as 'the organic matter within biominerals which is resistant to strong chemical oxidation' (Sykes et al., 1995), which may also include well-protected inter-crystalline proteins (Bright and Kaufman, 2011a).

Due to their better-protected nature, it has been hypothesised that analysing only intra-crystalline proteins, by using a strong oxidising pre-treatment to remove inter-crystalline proteins, may improve the reliability of AAR by minimising the effects of leaching, contamination, and external influences on the rate of racemisation (Sykes et al., 1995). This is the intra-crystalline protein diagenesis, or intra-crystalline protein decomposition (IcPD) approach to AAR. Assessments of the IcPD approach have been carried out on a range of biominerals, including bivalves (e.g. Penkman et al., 2008; Demarchi et al., 2015; Pierini et al., 2016; Ortiz et al., 2017), gastropods (e.g. Penkman et al., 2008; Demarchi et al., 2013c; Ortiz et al., 2018), sand dollars (Kosnik et al., 2017), ostracodes (Bright and Kaufman, 2011a), avian eggshell (Crisp et al., 2013), coral (Ingalls et al., 2003; Hendy et al., 2012) and proboscidean tooth enamel (Dickinson et al., 2019). Sodium hypochlorite (NaOCl, bleach) is the standard oxidising agent used; weaker oxidising agents such as hydrogen peroxide (H₂O₂) were found to be less effective in mollusc shells (Penkman et al., 2008), while in ostracodes strong and weak oxidising pre-treatments had similar effects (Bright and Kaufman, 2011a). The effect of oxidation varies substantially between substrates – a plateau of total amino acid concentration, indicating that the intra-crystalline fraction has been isolated, may occur in as little as 18 (Penkman et al., 2008) or as much as 72 hours (Crisp et al., 2013). The isolated intracrystalline fraction typically comprises ~10% of the total amino acid content (Penkman et al., 2008; Demarchi et al., 2013c) but may be as much as 70% (Demarchi et al., 2015), with the proportion of intra-crystalline protein typically being higher in ancient material (e.g. Penkman et al., 2008; Bright and Kaufman, 2011a; Kosnik et al., 2017; Ortiz et al., 2017, 2018; Dickinson et al., 2019), presumably due to the loss of open system inter-crystalline protein during diagenesis.

Analysis of only the intra-crystalline protein fraction reduces leaching of endogenous amino acids during decomposition and between-sample D/L variability for various biominerals, for example some gastropods and bivalves (Penkman et al., 2008; Demarchi et al., 2013b; Pierini et al., 2016; Ortiz et al., 2018), coral (Hendy et al., 2012), ostrich eggshell (Crisp et al., 2013), and enamel (Dickinson et al., 2019). However, some biominerals do not show lower variability in the intracrystalline fraction compared to the whole-shell protein fraction. In ostracodes, this behaviour is thought to result from the presence of well-protected inter-crystalline proteins in the oxidation-resistant fraction (Bright and Kaufman, 2011a), while open-system behaviour in aragonitic biominerals such as *Margaritifera falcata* and *Glycymeris* spp. may arise from remineralisation to the more stable calcite structure of CaCO₃ (Orem and Kaufman, 2011; Demarchi et al., 2015; Ortiz et al., 2017). In the bivalve Corbicula fluminalis, the high variability of D/L values in the intracrystalline fraction is thought to be due to this species' complex biomineral structure rather than

open-system behaviour (Penkman et al., 2008). Finally, some biominerals have been found to have a closed-system intra-crystalline fraction with similar variability of D/L values to the whole-shell fraction, proposed to be due to the rapid loss of inter-crystalline proteins in the early stages of diagenesis (e.g. sand dollars (Kosnik et al., 2017), the marine gastropod *Phorcus lineatus* (Ortiz et al., 2018)).

1.3.4.2 Analytical methods for quantifying amino acid enantiomers

Early uses of amino acid racemisation as a geochronometer focused on the decomposition of L-isoleucine to its epimer D-alloisoleucine, as these two epimers could be separated using ion exchange chromatography (IEC) without requiring chiral derivatisation (Schroeder and Bada, 1976). However, the development of gas chromatography (GC) (Schroeder and Bada, 1976) and, more recently, reverse-phase high performance liquid chromatography (RP-HPLC) techniques (Kaufman and Manley, 1998; Kaufman, 2000) have allowed for the enantiomeric separation of a wider range of amino acids (**Table 1.2**) by conversion of enantiomeric amino acids into epimers using a chiral compound such as *N*-isobutyryl-L-cysteine (see **Fig. 1.7**). RP-HPLC is now the analytical method most commonly used for AAR (Bravenec et al., 2018), with ten or more amino acids routinely analysed (Powell et al., 2013). While a method of separating amino acids using ultra high performance liquid chromatography (UHPLC) has been developed which allows chiral separation of a higher number of amino acids in a shorter time than RP-HPLC (Crisp, 2013), it has yet to be fully published and is not used routinely.

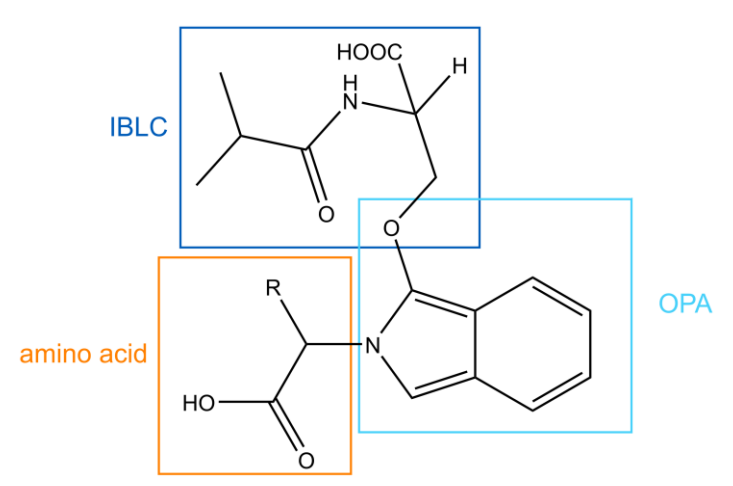


Fig. 1.7 – Derivatisation of an amino acid with N-isobutyryl-L-cysteine (IBLC, a chiral compound which converts the amino acid epimer into an enantiomer) and o-phthaldialdehyde (OPA, a fluorescent tag enabling detection), used by Kaufman and Manley (1998).

Which amino acid D/L values are reported depends on the substrate analysed and the laboratory carrying out the analysis. Isoleucine remains a key amino acid due to its historic use, but poor resolution using RP-HPLC has somewhat limited its application to AAR in recent years (Wehmiller, 2013a). Aspartic (Asp) and glutamic acid (Glu) are now the most widely reported amino acids due to their early elution and good chiral resolution using RP-HPLC, and differing racemisation rates providing coverage of a wide range of timescales (Kaufman, 2006). While some studies focus on aspartic and glutamic acid (e.g. Kaufman et al., 2013; Grimley and Oches, 2015; West et al., 2019; Ryan et al., 2020), other amino acids are often reported to provide complimentary chronological information — most frequently alanine (Ala), valine (Val), phenylalanine (Phe) and/or leucine (Leu) (e.g. Murray-Wallace et al., 2010; Penkman et al., 2013; Kosnik et al., 2017; Ortiz et al., 2018; Dickinson et al., 2019; Nicholas et al., 2019). While its complicated racemisation kinetics preclude its use as a chronometer, serine (Ser) D/L can be used to screen for compromised samples (Bright et al., 2010).

1.4 Mechanisms of protein decomposition

Protein decomposition takes places as a complex network of interrelated reactions. The peptide bonds that form proteins hydrolyse over time to generate peptides and eventually free amino acids; simultaneously, amino acids undergo decomposition through racemisation and other reactions, the kinetics of which are determined by the amino acid's position within a peptide chain, its neighbouring amino acid residues, and other external factors.

Due to the complexity of proteins, studying the kinetics of their decomposition is a major challenge. A combination of high-temperature decomposition experiments on modern material (e.g. Bada and Schroeder, 1972; Wehmiller, 1980; Mitterer and Kriausakul, 1989; Kaufman, 2000; Allen et al., 2013; Tomiak et al., 2013), analysis of naturally-aged material (e.g. Bada and Man, 1980; Goodfriend et al., 1992; Kaufman, 2003a; Ortiz et al., 2017), studies of free amino acids or model peptides (e.g. Bada, 1970; Hare, 1976; Kriausakul and Mitterer, 1978; Smith and Reddy, 1989; Kuge et al., 2004), and theoretical models (e.g. Takahashi et al., 2010; Nakayoshi et al., 2020) have been used to investigate the mechanisms of protein decomposition. For ease of reference, a detailed discussion of the mathematical approaches to modelling amino acid decomposition is presented in **Chapter 5** alongside the high-temperature kinetic experiments carried out in this thesis.

1.4.1 Free, terminal and in-chain amino acid racemisation

In aqueous solution, the racemisation of any given free (non-peptide bound) amino acid follows reversible first order kinetics (RFOK, see **Chapter 5** for further discussion) (Bada, 1970, 1984). However, in calcareous biominerals the racemisation of amino acids is up to an order of magnitude faster than in free solution, particularly during initial stages of racemisation (Wehmiller and Hare, 1971), and deviates from RFOK as racemisation proceeds to equilibrium (Bada and Schroeder, 1975). The principal explanation for this deviation is that in biominerals, amino acids exist in bound proteinaceous, peptide, terminal and free forms (**Fig. 1.8**), all with unique rates of racemisation (Bada and Man, 1980; Bada, 1982).

interior C-terminal
$$H_2N$$
 H_2N H_3 H_4N H_2N H_2N H_2N H_3 H_4N H_5 H

Fig. 1.8 – Different positions of amino acids in a peptide chain and as a free amino acid.

1.4.1.1 Free amino acids

In the free state, racemisation of amino acids takes place primarily via α -proton abstraction to form a planar carbanion; the carbanion subsequently receives a proton from a nearby water molecule, either regenerating the original amino acid or producing its enantiomer (Neuberger, 1948; Bada and Schroeder, 1975) (Fig. 1.9).

Fig. 1.9 – Racemisation of a free amino acid (zwitterionic form) via α -proton abstraction, forming a planar carbanion intermediate (adapted from Bada and Schroeder (1975)).

The rate of racemisation of an amino acid depends on the stability of its carbanion, which is strongly influenced by the ionic form of the amino acid (Bada, 1984) (**Fig. 1.10**). NH₃⁺ has a greater electron-withdrawing capacity (and therefore carbanion stabilisation effect) than the neutral NH₂, resulting in a faster rate of racemisation. Conversely, COO⁻ destabilises the carbanion relative to COOH, therefore reducing the rate of racemisation (Smith and Evans, 1980). At moderate pH, amino acids are predominantly present in their zwitterionic form (the amino group protonated and carboxylic acid deprotonated). Zwitterions have higher racemisation rates than neutral amino acids, as the stabilising effect of NH₃⁺ outweighs the destabilising effect of COO⁻. Different ionic species are present at high or low pH, altering the racemisation rate of an amino acid (see **Section 1.4.4.2.2**).

Fig. 1.10 – Ionic forms of an amino acid; in solution these forms are present in equilibrium, with the proportions of each form depending on the properties of the amino acid and the pH of the solution.

At a given pH, an amino acid's rate of racemisation depends on the nature of its R-group (Sato et al., 1970). The R-group influences racemisation firstly by direct stabilisation of the carbanion through the R-group's electron-withdrawing effects. Secondly, the R-group influences the pK_a of the amino and carboxylic acid groups, which determines which ionic species are present in solution. Therefore, amino acids with highly electron withdrawing R-groups, such as Ser and Asp, have the greatest rates of racemisation in the free form, while amino acids with electron-donating R-groups, such as Leu and Ile, racemise more slowly (Smith and Evans, 1980; Bada, 1984). Steric effects also play a role in determining racemisation rates, particularly for the aliphatic amino acids (Ala, Val, Leu and Ile) where electronic factors play a more minimal role (Smith and Evans, 1980).

In a peptide chain, the position of an amino acid and the nature of its neighbours dramatically influences its racemisation rate (Smith and Evans, 1980), complicating this relationship in biomineral proteins.

1.4.1.2 Peptide-bound amino acids

In general, when an amino acid residue is in an interior position, its racemisation rate is relatively slow – similar to or slightly faster than the racemisation rate of free amino acids (Smith and Evans, 1980; Mitterer and Kriausakul, 1984; Kimber and Griffin, 1987; Kaufman and Sejrup, 1995). However, when a residue is exposed by hydrolysis to a terminal position, the rate of racemisation rapidly increases. The relative rates of racemisation at the N- and C-termini depend on the nature of the amino acid R-group and, to a lesser extent, the R-groups of its interior neighbours (Moir and Crawford, 1988).

Electrostatic theory predicts that racemisation will be fastest in the presence of a positively charged amino group and slowest in the presence of a negatively charged carboxylate group. Thus when a peptide is in its zwitterionic form, N-terminus amino acid residues should racemise more quickly than C-terminus residues, and for small, non-sterically hindered amino acids (e.g. Ile, Val, Ser) this proves to be the case (Kriausakul and Mitterer, 1978; Smith and Evans, 1980; e.g. Bada, 1984). However, for bulky amino acids (e.g. Ala, Phe, Asp, methionine (Met)) the reverse is true: the rate of C-terminus racemisation is of similar magnitude or in some cases greater than N-terminus racemisation (Smith and Evans, 1980). This may in part be due to the intramolecular stabilisation of the carbanion at the C-terminus through the formation of a five-membered ring, which is disrupted by bulky R-groups (Fig. 1.11). The nature of neighbouring amino acids also influences the rate of racemisation through steric effects (Smith and Evans, 1980).

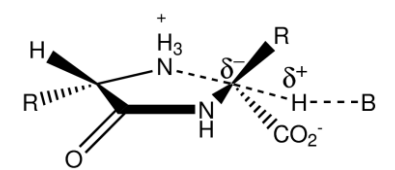


Fig. 1.11 – C-terminus carbanion intermediate stabilisation by formation of a five-membered ring (adapted from Smith and Evans (1980)).

Conversely, other research has suggested that the relative racemisation rates of the N- and C-termini depend primarily on the ability of a pair of terminal amino acids to form a diketopiperazine (DKPs) through internal aminolysis (loss of NH₃) at the N-terminus of a peptide, which generates a six-membered ring (Steinberg and Bada, 1983) (**Fig. 1.12**). At neutral pH, the rate of racemisation of residues in the DKP ring exceed both terminal and internal racemisation rates (Mitterer and Kriausakul, 1984; Gaines and Jeffrey, 1988). Therefore, the tendency of a pair of residues at the N-terminus to form a DKP strongly influences their racemisation rates. DKP formation also accelerates

hydrolysis of the pair of residues, forming a rapidly racemising dipeptide (Steinberg and Bada, 1981).

Fig. 1.12 – Diketopiperazine formation and decomposition (adapted from Steinberg and Bada (1983)).

While the majority of amino acids undergo very slow racemisation at internal positions, asparagine, aspartic acid and serine have been found to undergo rapid in-chain racemisation, which may explain their rapid racemisation rates, as amino acids spend most of their time as bound residues during early stages of diagenesis (Demarchi et al., 2013a). Asparagine and its hydroxy derivative aspartic acid can undergo in-chain formation of a five-membered succinimide via the loss of either ammonia or water (Fig. 1.13). Rehydration of the succinimide intermediate generates either an aspartyl residue (Fig. 1.13a) or an isoaspartyl residue (Fig. 1.13b); due to the relative abundance of water in the system compared to ammonia, asparagine is virtually never regenerated (Radkiewicz et al., 1996; Conrad et al., 2010).

$$\begin{array}{c|c} & & & & \\ & &$$

Fig. 1.13 – Succinimide formation and decomposition, where X is OH (aspartic acid) or NH_2 (asparagine); a) reformation of the aspartyl residue, b) generation of an isoaspartyl residue.

Racemisation at the α -carbon is highly accelerated in the succinimide due to the increased acidity of the α -proton (Conrad et al., 2010). This enables rapid racemisation of aspartic acid to take place in the bound state (Geiger and Clarke, 1987; Kuge et al., 2004). Indeed, racemisation at the succinimide could account for the bulk of total aspartic acid racemisation observed (Radkiewicz et al., 1996). A proposed mechanism of in-chain serine racemisation involves enolisation of carbonyl neighbouring the serine residue (Takahashi et al., 2010), but has yet to be experimentally verified. It is possible that threonine, the other proteinogenic hydroxy-amino acid, may undergo a similar inchain racemisation reaction (Demarchi et al., 2013a).

1.4.2 Hydrolysis

Hydrolysis is the cleavage of a C-N peptide bond to regenerate the C- and N-termini of the constituent amino acids by the addition of a water molecule (**Fig. 1.14**). Hydrolysis takes place throughout the diagenetic history of a fossil protein, and typically slows over time as weaker peptide bonds are preferentially cleaved (Miller et al., 1992). In dipeptides, hydrolysis follows irreversible first order kinetics (IFOK, **Equation 1.1**).

Fig. 1.14 – Hydrolysis of a peptide bond to generate a C- and N-terminus.

$$ln\left(\frac{[THAA] - [FAA]}{[THAA]}\right) = -kt$$

Equation 1.1 – Irreversible first order kinetics (IFOK)

Hydrolysis is an important factor in the rate of racemisation, as it provides the mechanism through which amino acids are exposed to faster-racemising terminal positions, before being released into the slower-racemising free state. Therefore, the overall racemisation rate of an amino acid in a biomineral depends not only on its racemisation rates in each state (interior, terminal and free), but also on the time it spends in the terminal positions – that is, the relative rates of hydrolysis of

its peptide bonds. For example, the rapid racemisation rate of aspartic acid during early stages of diagenesis is partially attributed to the relative weakness of Asp-X peptide bonds (Goodfriend et al., 1992; Goodfriend and Hare, 1995). The racemisation rate follows a parabolic curve as aspartic acid residues are first converted to rapidly-racemising terminal states, then the slowly-racemising free state.

Like racemisation through α -proton abstraction, hydrolysis requires available water molecules to proceed. Therefore, the availability of water will influence the rate and extent of hydrolysis during the latter stages of diagenesis. The observation that hydrolysis rarely proceeds to completion in fossil shells has been suggested to be due to limitations of water availability in the intra-crystalline environment (Walton, 1998). Stabilisation of peptides by mineral-peptide interaction, limiting the ability of water molecules to approach the peptide bond, may also contribute to the persistence of peptides over geological time (Demarchi et al., 2016).

1.4.3 Decomposition reactions

Decomposition of amino acids can take place while the amino acid is in the bound, terminal or free state, with characteristic rates of decomposition for each state. Due to the complexity of natural systems and the wide range of possible decomposition reactions and products, the majority of studies exploring amino acid decomposition have focused on model systems (Walton, 1998) such as aqueous free amino acids (e.g. Bada, 1972b; Smith et al., 1978) or short synthetic peptides (e.g. Kriausakul and Mitterer, 1978; Moir and Crawford, 1988; Demarchi et al., 2013a); the decomposition of amino acids within longer peptides or proteins is less well studied. The rate of amino acid decomposition may influence its observed racemisation rate, especially through decomposition of highly racemised free amino acids. Amino acids with especially high decomposition rates may exhibit steady state behaviour for part of their diagenesis, where continual loss of highly racemised free amino acids inhibits racemic equilibrium (Schroeder and Bada, 1977).

The key decomposition pathways of amino acids are deamination, decarboxylation and condensation (**Fig. 1.15**). The R-groups of amino acids can also undergo decomposition; a selection of key R-group decomposition reactions are discussed below.

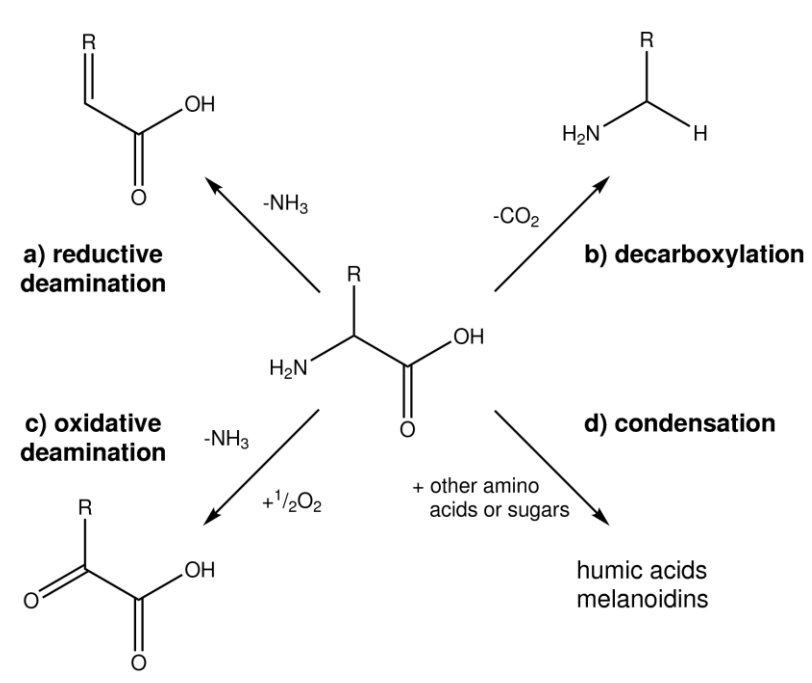


Fig. 1.15 – Amino acid decomposition pathways: a) reductive deamination; b) decarboxylation; c) oxidative deamination; d) condensation.

1.4.3.1 Deamination and decarboxylation

The two main pathways of decomposition for free amino acids are deamination and decarboxylation (Vallentyne, 1964; Bada et al., 1995; Sato et al., 2004). Deamination is the loss of ammonia from an amino acid. It may take place through a reductive pathway to produce an unsaturated carboxylic acid (**Fig. 1.15a**), or through an oxidative pathway to produce an α -keto acid (**Fig. 1.15c**). In aerobic aqueous solutions, oxidative deamination dominates (Bada and Miller, 1970), but in an oxygen-restricted intra-crystalline environment, reductive deamination may be the dominant deamination pathway. Deamination is catalysed by metal ions through chelation by the carbanion intermediate (Bada and Miller, 1970). The carboxylic acid product of deamination may subsequently undergo decarboxylation to generate an aldehyde (Bada and Miller, 1970).

Decarboxylation is the loss of carbon dioxide from an amino acid to produce an amine (Fig. 1.15b). Amine decomposition takes place at a slower rate than the parent amino acid decarboxylation (Bada et al., 1995), so it is probable that amines are a predominant decomposition product present in fossils.

As with racemisation, the susceptibility of an amino acid to deamination and decarboxylation at a given pH depends on the nature of the R-group of the amino acid (Sato et al., 2004). In peptides, decarboxylation may take place at the C-terminus and deamination at the N-terminus; in this case both the nature of the terminal amino acid and its neighbours influence the relative rate of

decomposition. In general, hydrophilic amino acids are more susceptible to decomposition than hydrophobic amino acids (Sato et al., 2004).

1.4.3.2 Condensation

Free amino acids may also undergo condensation reactions to form insoluble heterogeneous polymeric structures (Vallentyne, 1964; Bada et al., 1999) (Fig. 1.15). In the presence of other molecules such as sugars, melanoidins may be formed through condensation (Rafalska et al., 1991). Although this does not count for substantial losses of amino acids in aqueous solution, amino acid residues in condensed structures were found to have slower rates of racemisation than free amino acids, possibly due to steric hindrance (Rafalska et al., 1991). Therefore, condensation in the intra-crystalline environment may represent an additional 'sink' of highly racemised, but slowly racemising, amino acids.

1.4.3.3 R-group decomposition

Decomposition of amino acid R-groups may take place in both bound and free states, resulting in the formation of either other proteinogenic amino acids, or non-proteinogenic amino acids.

Asparagine (Asn) and glutamine (Gln) undergo deamination to produce aspartic acid and glutamic acid respectively (Hill, 1965); lysine (Lys) is also susceptible to deamination (Bada, 1970; Walton, 1998). The deamination reaction proceeds more quickly for asparagine than glutamine, due to its ability to generate succinimide intermediates with neighbouring residues (Geiger and Clarke, 1987) (Fig. 1.13). The deamination of asparagine to aspartic acid may be a significant contributing factor to the atypical pattern of racemisation observed for aspartic acid (Goodfriend et al., 1992, 1995; Brinton and Bada, 1995). Due to the rapid rate of deamination it is considered unlikely that either asparagine or glutamine persist in the fossil record (Walton, 1998); therefore the effect of the racemisation rate of asparagine on the observed kinetics of aspartic acid is likely to be limited to the early stages of diagenesis.

Aspartic acid may also undergo β -decarboxylation to produce alanine (**Fig. 1.16**). Both α - and β -decarboxylation of aspartic acid were found to take place at extremely slow rates in high temperature decomposition experiments (Bada and Miller, 1970). However, in a study of fossil molluscs, an increase in β -alanine over time was attributed to α -decarboxylation of aspartic acid;

the author reasoned that β -decarboxylation could also take place, and could in part explain and observed increase in alanine over the diagenetic sequence (Walton, 1998).

Fig. 1.16 – Decarboxylation reactions of aspartic acid.

The main decomposition pathway of glutamic acid is through the formation of a γ -lactam (**Fig. 1.17**). Glutamic acid undergoes dehydration to form pyroglutamic acid, which may then decarboxylate to generate pyrrolidone (Bada and Miller, 1970). The low proportion of free glutamic acid observed in fossil samples is attributed to this process (Walton, 1998). Glutamic acid may also undergo β -decarboxylation (decarboxylation of the R-group) to produce α -aminobutyric acid (Bada et al., 1978).

Fig. 1.17 – Decomposition of glutamic acid via γ -lactam formation.

The hydroxy amino acids serine and threonine can undergo dehydration of their hydroxy group to generate an unsaturated amino acid (Vallentyne, 1964; Bada and Man, 1980). Following this dehydration, serine can also decompose to generate alanine (Fig. 1.18). The conversion of serine to alanine is thought to be the main cause of the increase in alanine concentrations observed in diagenetic sequences; as such it has been proposed as a dating tool to complement AAR measurements (Westaway, 2009). In the free state, serine and threonine may also undergo aldol cleavage to generate glycine and formaldehyde or acetaldehyde, respectively.

dehydration
$$X = H$$
, Ser $X = CH_3$, Thr $X = H$, formaldehyde $X = CH_3$, acetaldehyde $X = CH_3$, acetaldehyde

Fig. 1.18 – Decomposition of the hydroxy amino acids serine and threonine by dehydration (top) and aldol cleavage (bottom) (from Bada et al. (1978)).

1.4.4 Environmental influences on racemisation rates

As racemisation is a chemical reaction, its rate is influenced by a range of environmental factors which complicate the relationship between a sample's age and its D/L values. The effect of some environmental factors, such as pH, water availability and contamination, can be minimised by analysing only a closed system of biominerals, while other factors such as temperature and the species effect must be controlled for by careful sample choice.

1.4.4.1 Protein structure and matrix effects

While the racemisation rate of an amino acid strongly depends on the nature of its R-group and that of its nearest neighbours, it may also be influenced by the secondary (local folding) and tertiary (overall three-dimensional) structure of the protein. Because an amino acid's racemisation rate via the carbanion mechanism is dependent on the approach of a base to abstract the α -proton, the molecular environment surrounding the amino acid can potentially radically influence the racemisation rate (Smith and Evans, 1980; Moir and Crawford, 1988). For example, aspartic acid racemises very slowly in collagen at diagenetic temperatures; this is thought to be due to the rigid helical structure of collagen, which prevents the aspartic acid from adopting the conformation necessary to generate a succinimide (Collins et al., 1999). Unfortunately, protein structures denature at the high temperatures required for kinetic experiments, making dedicated studies of the effect of protein structure on racemisation rates challenging (Smith and Evans, 1980; Collins et al., 1999).

The effect of protein structure on racemisation rate may be a driving factor of the widely observed 'species effect' on amino acid racemisation in biominerals. The species effect has been observed in a range of biomineral classes, including foraminifera (e.g. King and Hare, 1972a), ostracodes (e.g. Ortiz et al., 2013), and at the genus level in molluscs (e.g. Lajoie et al., 1980; Wehmiller, 1980). Differences in racemisation rates have also been observed between different biomineral structures within the same shell (Goodfriend and Hare, 1995). The biomineral itself may also influence the rate of amino acid racemisation, for example through conformational changes caused by bonding interactions between the biomineral and the protein (Weiner, 1979). The effect of protein and biomineral structure on amino acid racemisation rates can be controlled by analysing monospecific samples, or samples of the same genus where species-level identification is not possible.

1.4.4.2 External influences on racemisation rates

Besides the nature of the biomineral and the biomineral protein, amino acid racemisation rates are influenced by temperature, pH, and the presence of other compounds in the surrounding environment. The rate of racemisation in bound amino acids appears to be less influenced by environmental factors compared to free amino acids (Smith and Evans, 1980).

1.4.4.2.1 Temperature

As a chemical reaction, racemisation is strongly dependent on temperature; the rate of racemisation approximately doubles with every 5°C temperature increase (Schroeder and Bada, 1976). Some environments, such as caves and deep-sea sediments, have relatively stable temperature histories (e.g. Sejrup et al., 1984b); however in most cases potential fluctuations in burial temperature must be taken into account. For example, it is important to identify potentially spurious results arising from changes in either burial depth (Murray-Wallace et al., 1988) or artificial heating (Crisp, 2013; Ortiz et al., 2020). Latitude and glacial-interglacial climate cycles also impact racemisation rates; therefore AAR dates can only be calibrated across a region with a shared climate history (e.g. Miller and Mangerud, 1985; Penkman et al., 2013).

1.4.4.2.2 pH

The racemisation rate of a free amino acid depends on the distribution of the amino acid's ionic forms in solution, as each ionic form has its own distinct rate of racemisation. Therefore, the rate of racemisation for an amino acid is strongly pH dependent. At pH between 5-8, the pH has

relatively little effect on the racemisation rate of free amino acids (Bada, 1972b). At high pH (> 8) high concentrations of hydroxide ions increase the rate of carbanion formation, leading to an increase in racemisation rate; at lower pH (< 5), racemisation rates are faster due to the protonation of amino and carboxylic acid groups (Bada, 1970) (**Fig. 1.19**). However, at very low pH (< 2), low concentrations of hydroxide ions inhibit racemisation (Bada, 1972b).

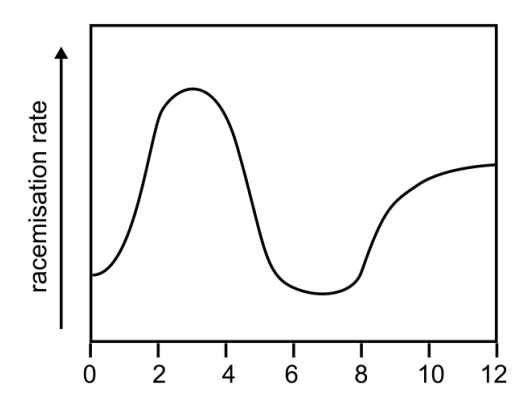


Fig. 1.19 – Schematic representation of the pH dependence of amino acid racemisation in solution (adapted from Bada (1970)).

While the biomineral matrix buffers pore waters to a pH of around 8 (Miller et al., 2013), the rate of amino acid racemisation has found to be pH dependent at high pH in some biominerals (Bright and Kaufman, 2011b; Orem and Kaufman, 2011). In the case of the bivalve *Margaritifera falcata*, even intra-crystalline amino acids racemised faster at high pH (Orem and Kaufman, 2011); conversely, the rate of racemisation of intra-crystalline amino acids in ostrich eggshell was found to be independent of pH (Crisp, 2013). pH dependence of racemisation in biominerals may therefore be indicative of open-system behaviour.

1.4.4.2.3 Presence or absence of water

For racemisation of the α -carbon to occur through the proton abstraction mechanism, water must be present. Total desiccation radically reduces racemisation rates (Hare and Mitterer, 1968), but this is virtually impossible to achieve in the natural environment (Bada and Schroeder, 1975; Hare, 1976; Bada, 1982). However, variations in the availability of water in the biomineral matrix may have a substantial impact on the rate of hydrolysis and racemisation (Wehmiller et al., 1976), which could contribute to observed species-specific variations in racemisation rates. The binding of both proteins and water molecules to the calcite surface has been suggested to further reduce the availability of water for hydrolysis and racemisation in biominerals (Demarchi et al., 2016).

1.4.4.2.4 Other external influences

The presence of exogenous compounds can influence the rate of amino acid racemisation in samples which do not behave as a closed system. For example, metal ions can catalyse racemisation by stabilising the intermediate carbanion (Gillard and Phipps, 1970; Smith and Evans, 1980), resulting in racemisation rates orders of magnitude faster for free amino acids in open-system biominerals in some cases (Bada and Schroeder, 1975). Microbial action can also increase the rates of racemisation in a biomineral via racemising enzymes, which have been found in open-system biominerals such as bone (Child et al., 1993).

1.4.5 Summary

The complexity of protein decomposition presents a major challenge to amino acid racemisation dating, as it is not possible to directly model the complex, interdependent reactions which contribute to an amino acid's overall racemisation rate in any given biomineral. While models based on the decomposition of different pools of amino acids within a protein have been developed (e.g. Collins and Riley, 2000), a 'black box' approach remains typical in AAR, with efforts made to limit internal and external influences on racemisation rates. Therefore it is important to assess each substrate to determine its suitability for AAR and the particular diagenetic behaviour of its biomineral protein.

1.5 Foraminifera

Foraminifera are a phylum of single-celled protists found in marine and estuarine ecosystems around the world. Foraminifera appear in the fossil record in the early Cambrian, but are thought to have first evolved during the Neoproterozoic era, between 900 and 650 million years ago (Pawlowski et al., 2003). The phylum Foraminifera is extremely diverse and abundant, comprising nearly 9,000 formally described extant species and over 30,000 fossil species (Boudagher-Fadel, 2015a). The majority of extant species of foraminifera are benthic (i.e. they live on, in or near sediments), although around 90 extant species are planktonic (i.e. they live in the water column) (Boudagher-Fadel, 2015b).

Foraminifera are characterised by chambered shells or 'tests' made of secreted calcium carbonate (calcareous), organic material, or scavenged mineral particles (agglutinated), which protect the cell. Surrounding the test is a layer of protoplasm from which extends a variety of appendages used for

anchorage, movement, predation, scavenging and waste disposal (Brasier and Armstrong, 1980). Foraminifer tests are usually less than 0.5 mm wide, although the largest known tests can grow up to 20 cm (Boudagher-Fadel, 2015a).

1.5.1 Foraminifera as a tool for palaeoenvironmental reconstruction

The ubiquity of diverse, well preserved tests in marine sediments (sometimes making up the bulk of calcareous sediments (Brasier and Armstrong, 1980)), and the sensitivity of individual species to ecological conditions, mean that foraminifera have been extensively utilised for biostratigraphy and palaeoenvironmental reconstruction (Murray, 1979).

Planktonic foraminifera play an important role in reconstructing global mean sea-level changes throughout the Quaternary and beyond, via oxygen isotope measurements reflecting the global ice-mass balance (e.g. Rohling et al., 2008, 2014). In Holocene salt-marsh sediments, foraminiferal assemblages provide a high-resolution record of sea-level change, as the distribution of species is highly dependent on ecological conditions, which can be related to salinity and therefore tidal inundation (e.g. Scott and Medioli, 1978; Gehrels, 1994). This level of stratigraphic detail is rarely preserved in Pleistocene deposits; nevertheless, foraminiferal assemblages can support the identification of interglacial sea-level deposits (Cann et al., 1988; Sejrup et al., 1991; Scourse et al., 1999; Read et al., 2007; Bates et al., 2010; Roe and Preece, 2011). This presents an opportunity for foraminifera to provide chronological control for interglacial sea-level deposits using AAR.

1.5.2 Foraminifer tests as a substrate for AAR

Calcareous foraminifera (those which secrete calcium carbonate tests) have been found to retain endogenous protein over geological timescales, making them a suitable target for AAR. This section discusses the mechanisms of biomineralisation in calcareous foraminifera, followed by a brief history of applications of AAR to this class of biomineral.

1.5.2.1 Biomineralisation in calcareous foraminifera

The process of biomineralisation in calcareous foraminifera is poorly understood compared to other marine biominerals (De Nooijer et al., 2014). Proteins rich in acidic amino acids and glycine have been found to play a role in the biomineralisation of calcareous foraminifera (Weiner and Erez, 1984; Sabbatini et al., 2014; Tyszka et al., 2019), as has been observed in other biomineralising invertebrates (Weiner, 1979; Berman et al., 1990; Kobayashi and Samata, 2006). In

general, calcification is directed by a primary organic membrane (POM) which forms a scaffold in the shape of a new chamber, and provides the site of nucleation for biomineral growth on either side of the POM (Bé et al., 1979; De Nooijer et al., 2014) (Fig. 1.20). Chamber walls are comprised of micro-crystallites enclosed by organic films. Successive chamber formation leads to a lamellar structure of alternating crystalline and organic layers (Debenay et al., 2000). Evidence suggests that the organic fraction observed in sub-fossil foraminifera consists of these scaffold proteins entrapped in the mineral matrix during biomineralisation (Robbins and Brew, 1990).

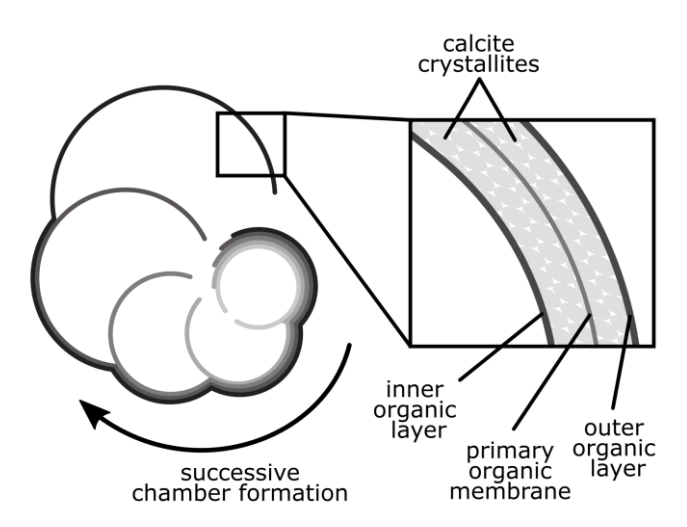


Fig. 1.20 – Formation and structure of test chambers in calcareous foraminifera (adapted from Tyszka et al. (2019)).

Following death, a range of diagenetic processes may take place which can affect the integrity of the biomineral. Mechanical breakage is typically the most common taphonomic feature, especially in high-energy depositional environments (Barbieri, 1996). Although this would not impact the integrity of the biomineral, the susceptibility of a test to breakage may reflect shell weakening by other taphonomic processes (Barbieri, 2001). Chemical alteration such as iron staining or pyrite growth (e.g. Wang and Chappell, 2001), and bioerosion or encrustation by bacteria (Barbieri, 2001), can also affect the preservation of foraminifera.

A key loss of biomineral integrity is dissolution, which can take place on timescales ranging from days (Kotler et al., 1992) to millions of years (Pearson and Burgess, 2008), depending on the sedimentary environment. For planktonic species, dissolution may take place as the test travels through the water column, especially in deep, cold waters where the solubility of calcium carbonate increases dramatically (Ben-Yaakov et al., 1974). Taphonomic alteration of calcareous foraminifer tests in intertidal flats is dominated by etching or roughening of the outer test surface due to dissolution (Berkeley et al., 2009), especially in organic-rich sediments (Berkeley et al.,

2007). In some cases dissolution can lead to the total loss of calcareous species from the fossil record (Murray and Alve, 1999). The susceptibility of a test to dissolution depends on its carbonate mineralogy, grain size, wall thickness and skeletal micro-architecture. For example, outer test chambers are typically the first to dissolve as they are thinner than internal chambers (Berkeley et al., 2009) (see Fig. 1.20). Partial dissolution may be visible under light microscopy, with tests taking on a dull, opaque appearance (e.g. Barbieri, 1996; Wang and Chappell, 2001), or a 'star-like' morphology where outer chambers are destroyed, leaving the thicker interlocular walls behind (Berkeley et al., 2009). To what extent, if any, dissolution affects the preservation of biomineral proteins in foraminifera has not been investigated.

Over longer timescales (hundreds of thousands to millions of years), overgrowth (where inorganic calcite is deposited onto the test surface), and recrystallisation from biogenic microcrystals to larger crystals with a lower surface energy, may take place (Sexton et al., 2006). Overgrowth and recrystallisation may result in an opaque, 'frosty' appearance, but alterations are not always visible under light microscopy (Edgar et al., 2013). These alterations to the integrity of the biomineral raise the potential for the occlusion of exogenous proteins, or the loss of previously closed-system endogenous proteins; some studies of foraminifer AAR have therefore targeted only tests with no visible signs of alteration (e.g. Sejrup and Haugen, 1992; Blakemore et al., 2015), although this does not necessarily guarantee that the effects of overgrowth and recrystallisation are avoided.

1.5.2.2 Applications of AAR to foraminifera

Foraminifera have been targeted for AAR since the 1970s, with several studies analysing amino acids in foraminifer-rich sediments (e.g. Wehmiller and Hare, 1971; Bada and Schroeder, 1972; Bada et al., 1973). Following work demonstrating the species-specificity of racemisation rates (King and Neville, 1977), more focus has been put on analysing single-species or single-genus samples, although the whole-sediment approach is still occasionally employed (e.g. Hearty et al., 2010; Nicholas, 2012), and may still be reliable when calcareous sediments are dominated by one taxon of foraminifera.

The stable depositional environment of deep-sea sediments has made planktonic foraminifera an ideal substrate for investigating the patterns of amino acid decomposition at diagenetic temperatures (e.g. King and Neville, 1977; Sejrup et al., 1984b; Harada and Handa, 1995; Kaufman et al., 2013). AAR of foraminifera has also been used to estimate thermal histories (Sejrup and Haugen, 1992; Kaufman, 2006) and sedimentation rates (Cann and Murray-Wallace, 1986; Macko

and Aksu, 1986) for independently dated materials in these environments. AAR has been applied to foraminifera from interglacial deposits to help reconstruct past sea-level changes in the United Kingdom and Ireland (Dowling et al., 1998; Scourse et al., 1999), the North Sea (e.g. Kristensen et al., 1998; Reinardy et al., 2017), Australia (Nicholas, 2012; Blakemore et al., 2015; Ryan et al., 2020) and Hawaii (Hearty et al., 2010).

One challenge of using foraminifera for AAR is the potential variability introduced by pooling many individuals in each species; therefore work has been carried out to develop single test methods (Hearty et al., 2004; Blakemore et al., 2015; Ryan et al., 2020). Analysing single tests enables the identification of reworked fossils (Ryan et al., 2020); however Blakemore et al. (2015) found that pooling multiple individuals improved the reliability of AAR results. An additional challenge is the high surface-to-mass ratio of foraminifer tests, which increases the possibility for contamination (Hearty et al., 2004). In bivalves, for example, smaller shells have higher variability in D/L values and higher Ser/Asx values, which are indicative of contamination (Simonson et al., 2013).

1.5.2.3 Intra-crystalline approaches to AAR of foraminifera

While chemical pre-treatments of foraminifera designed to minimise contamination are often used (e.g. 2 hour 3% H₂O₂ (e.g. Hearty et al., 2004; Kaufman, 2006; Kaufman et al., 2013), etching with dilute HCl (Murray-Wallace and Belperio, 1994; Harada et al., 1996, 1997), 1 hour 12.5% NaOCl (Nicholas, 2012)), dedicated comparisons between different protein fractions in foraminifera are limited. Stathoplos and Hare (1993) applied NaOCl treatments to various planktonic species, finding that 23-42% of the total amino acid pool represented labile material, which the study attributed to a combination of chemically accessible biomineral proteins and exogenous particles adhered to the foraminifer test. Likewise, treatment of a small number of *Elphidium* samples with 12.5% NaOCl for 48 hours by Nicholas (2012) suggested that an oxidation-resistant intra-crystalline fraction of amino acids is present in foraminifer tests. In a comparison between short (1-2 hour) ethanol, methanol, NaOCl and H_2O_2 treatments, Hearty et al. (2004) found that a 2 hour 3% H_2O_2 pre-treatment produced the lowest variability of Asx, Glx and Ser D/L in *Pulleniatina obliquiloculata*.

A detailed assessment of the behaviour of the intra-crystalline fraction of proteins in foraminifera has not yet been carried out. The aim of this thesis is therefore to investigate the behaviour of the intra-crystalline fraction of proteins in several species of calcareous foraminifera, to determine whether the IcPD approach to AAR provides benefits in reliability and precision for this class of biomineral.

1.6 Project aims

In order to investigate the behaviour of the intra-crystalline fraction of amino acids in foraminifera and their application to the geochronology of Pleistocene sea-level records, the objectives of this project are as follows:

- 1. Investigate the performance of different oxidising agents in sub-modern and naturally-aged foraminifera (*Neogloboquadrina pachyderma* (sinistral), **Chapter 3**; *Ammonia* spp., *Haynesina germanica* and *Elphidium williamsoni*, **Chapter 4**);
- 2. Explore the patterns of decomposition at high temperatures of the whole-shell and intracrystalline fraction of foraminifera (*Ammonia* spp. and *Haynesina germanica*, **Chapter 5**);
- 3. Apply the methods developed in **Chapters 3-5** to naturally-aged material from Pleistocene sea-level deposits around the United Kingdom to develop a pilot aminostratigraphic framework for foraminifera in this region (**Chapter 6**).

Chapter 2 – Routine Experimental Procedures

This chapter details, unless otherwise specified, the experimental procedures followed in **Chapters 4**, **Chapter 5** and **Chapter 6**. **Chapter 3** contains its own experimental methods.

2.1 Picking of foraminifera and species identification

Sediment samples were sieved at either 65-500 μ m or 90-500 μ m, and the most abundant species of foraminifera were wet picked using a paintbrush. Foraminifera were cleaned in bulk by repeated rinsing with 18 m Ω H $_2$ O until the water was clear, followed by 3 x 1 minute sonication treatments with rinsing between each sonication according to Miller et al. (1983), then stored at room temperature in 18 m Ω H $_2$ O or dry until required for analysis.

The benthic species analysed in this thesis (*Ammonia* spp., *Haynesina germanica* and *Elphidium williamsoni*) were identified using the identification keys in *British Nearshore Foraminiferids* (Murray, 1979). Considerable uncertainty surrounds the species-level identification of *Ammonia*; the species operationally defined as *Ammonia beccarii* contains several morphologies, and therefore potentially up to 25-30 genetically distinct species (Hayward et al., 2004). Due to difficulties separating these species based on morphology, some workers continue to use *A. beccarii* as a blanket classification of any otherwise unidentified *Ammonia* specimen. In this thesis, *Ammonia* specimens have not been identified to species level, and are referred to as *Ammonia* spp.; this is likely 'equivalent' to specimens identified as *A. beccarii* in existing literature (e.g. Scourse et al., 1999).

2.2 Oxidative pre-treatments

Pre-treatments were carried out on samples of 30-120 monospecific foraminifer tests in sterilised 0.1 mL Reactivials (Thermo Scientific) and crushed with a clean needle prior to addition of the oxidising agent. 20 μ L of oxidising agent (3 or 30% H_2O_2 w/v (VWR), or 12% NaOCl w/v (VWR)) was added to each Reactivial, with agitation after 10 minutes (for samples oxidised for 2 hours) or 1 hour (for samples oxidised for more than 2 hours), to ensure total penetration of the oxidising agent. Following removal of the oxidising agent, the samples were rinsed with 6 x 20 μ L 18 m Ω H_2O and 1 x 20 μ L HPLC-grade methanol (MeOH, Sigma), and allowed to air dry.

2.3 Demineralisation and hydrolysis

For the free amino acid (FAA) fraction, samples were demineralised with 5 μ L 2 M HCl (Aristar), with an additional 5-10 μ L 2 M HCl added if necessary to complete demineralisation. For the total hydrolysable amino acid (THAA) fraction, samples were demineralised with 8 μ l 7 M HCl (Aristar), with an additional 8 μ L 7 M HCl added if necessary to complete demineralisation. The vials were then flushed with nitrogen and heated at 110°C for 24 h. Both THAA and FAA samples were dried *in vacuo* using a centrifugal evaporator and stored at room temperature prior to rehydration for analysis.

During hydrolysis, asparagine and glutamine are irreversibly hydrolysed to aspartic acid and glutamic acid respectively; therefore these amino acids are analytically indistinguishable and reported as Asx and Glx (Hill, 1965). Additionally, some small degree of racemisation and amino acid decomposition is induced by this hydrolysis step; the temperature and duration of hydrolysis is therefore chosen to minimise hydrolysis-induced racemisation and decomposition while maximising the recovery of amino acids (Kaufman and Manley, 1998).

2.4 Chiral separation of amino acids

Samples were rehydrated with 8 μ L rehydration fluid (0.01 M HCl (Fisher), 1.5 mM sodium azide (NaN₃, VWR), 9.97 mM internal standard L-homo-arginine (Sigma)) and separated via an Agilent 1100 Series HPLC (Section 2.4.1) or an Agilent 1200 Series UHPLC (Section 2.4.2). The rehydrated samples underwent pre-column derivatisation with o-phthaldialdehyde (OPA, Sigma-Aldritch) and the chiral thiol N-isobutyryl-L-cysteine (IBLC, Sigma-Aldritch) according to Kaufman and Manley (1998). Fluorometric detection was carried out using a Xenon-arc flash lamp at a frequency of 55 Hz, with a 280 nm cut-off filter, and an excitation wavelength of 230 nm and emission wavelength of 445 nm. Standard amino acid solutions and preparative blanks were run routinely to monitor machine performance and identify potential sources of contamination.

The fluorescent derivatising agent OPA, used in both methods, does not allow for the detection of proline or hydroxyproline (Miller and Brigham-Grette, 1989), while the OPA derivative of lysine is prone to degradation during separation (Brückner et al., 1994); therefore these amino acids are not reported. A full list of amino acids which can be identified using the RP-HPLC or UHPLC methods is given in **Table 1.2**.

2.4.1 RP-HPLC method

Samples were analysed using the method developed by Kaufman and Manley (1998) with modifications by Penkman (2005) using an Agilent 1100 Series HPLC fitted with a C_{18} HyperSil BDS column (5 μ m, 250 x 3 mm). This method is carried out at 25°C and uses a ternary gradient of sodium acetate buffer (23 mM sodium acetate trihydrate (Fisher), 1.5 mM NaN₃ (VWR), 1.3 μ M ethylenediaminetetraacetic acid (EDTA, VWR), adjusted to pH 6.00 \pm 0.01 with 10 M sodium hydroxide (Fisher) and 10% acetic acid (VWR)), MeOH (Sigma) and acetonitrile (ACN, Sigma). The run time of the RP-HPLC method is 115 minutes, including flush time, and follows the solvent gradient program in **Table 2.1**.

The D-Arg peak co-elutes with another compound in all RP-HPLC chromatograms; therefore Arg D/L values are not reported and D-Arg has been excluded from total amino acid concentrations as in other studies using RP-HPLC (Powell et al., 2013).

Table 2.1 – Solvent gradient program for RP-HPLC (Penkman, 2005).

Run time (minutes)	%A (NaAc buffer)	%C (MeOH)	%D (ACN)	Flow rate (ml/min)	Temperature (°C)
0	95.0	5.0	0.0	0.56	25
31	76.6	23.0	0.4	0.60	25
95	46.2	48.8	5.0	0.60	25
95.9	0.0	95.0	5.0	0.60	25
99	0.0	95.0	5.0	0.60	25
100	95.0	5.0	0.0	0.60	25
115	95.0	5.0	0.0	0.56	25

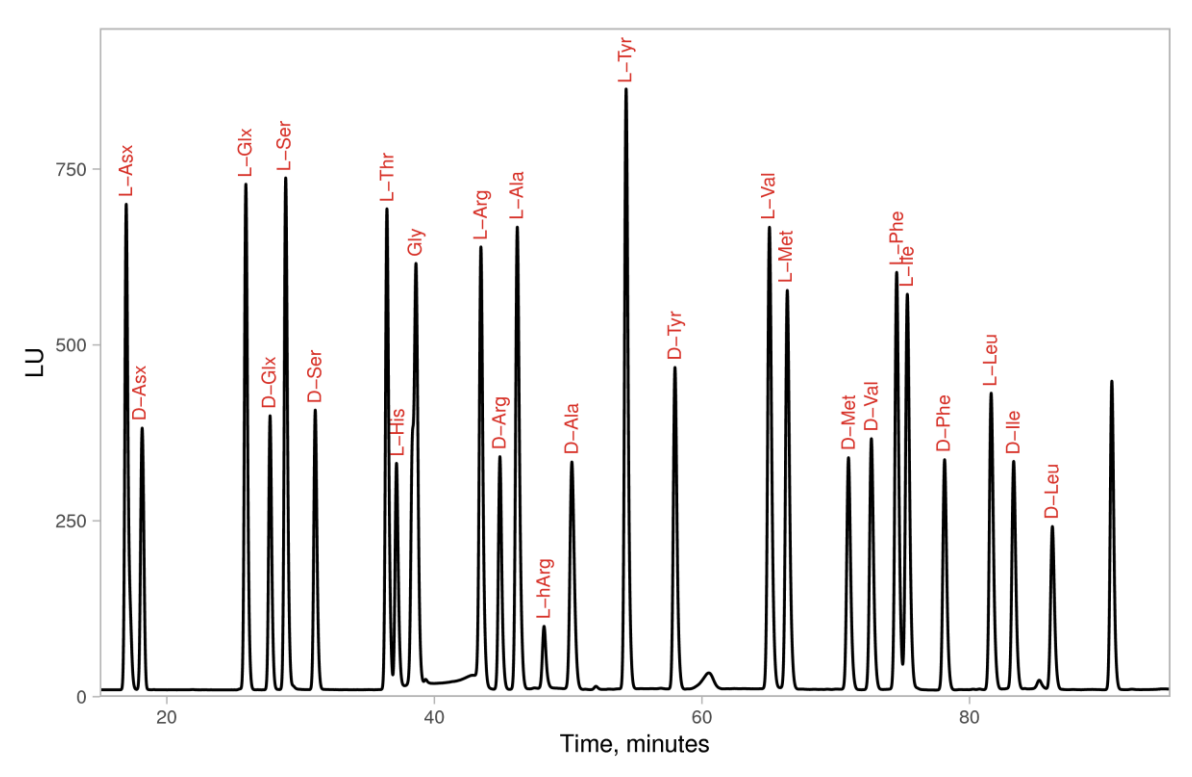


Fig. 2.1 – Typical RP-HPLC chromatogram of a 0.5 D/L standard amino acid solution with quantified amino acids labelled. L-hArg (L-homo-arginine) is the internal standard.

2.4.2 UHPLC method

Samples were analysed using a method modified from Crisp (2013) using an Agilent 1200 series Rapid Resolution UHPLC fitted with a ZORBAX Eclipse C_{18} Plus column (1.8 μ m, 100 x 4.6 mm), and a binary gradient of sodium acetate buffer (Section 2.4.1) and a mobile phase B (7.5% ACN, 92.5% MeOH v/v). The solvent gradient program was modified from Crisp (2013) to enable better separation of late-eluting amino acids for foraminifera (Table 2.2). The run time of the UHPLC method is 57 minutes, including flush time.

Table 2.2 – Solvent gradient program for UHPLC, adapted from Crisp (2013).

Run time (minutes)	%A (NaAc buffer)	%B (MeOH/ACN)	Flow rate (ml/min)	Temperature (°C)
0	90	10	1.25	28
8.8	82	18	1.25	
10			1.25	30
11	82	18	1.25	
18			1.25	28
23	78.3	21.7	1.25	
25	78.3	21.7	1.25	
27	75.2	24.8	1.25	
28.5	75.2	26	1.25	

Run time (minutes)	%A (NaAc buffer)	%B (MeOH/ACN)	Flow rate (ml/min)	Temperature (°C)
30	65	35	1.25	
40			1.25	28
46	50	50	1.30	
50			1.30	25
52	2	98	1.30	
57	95	5	1.30	

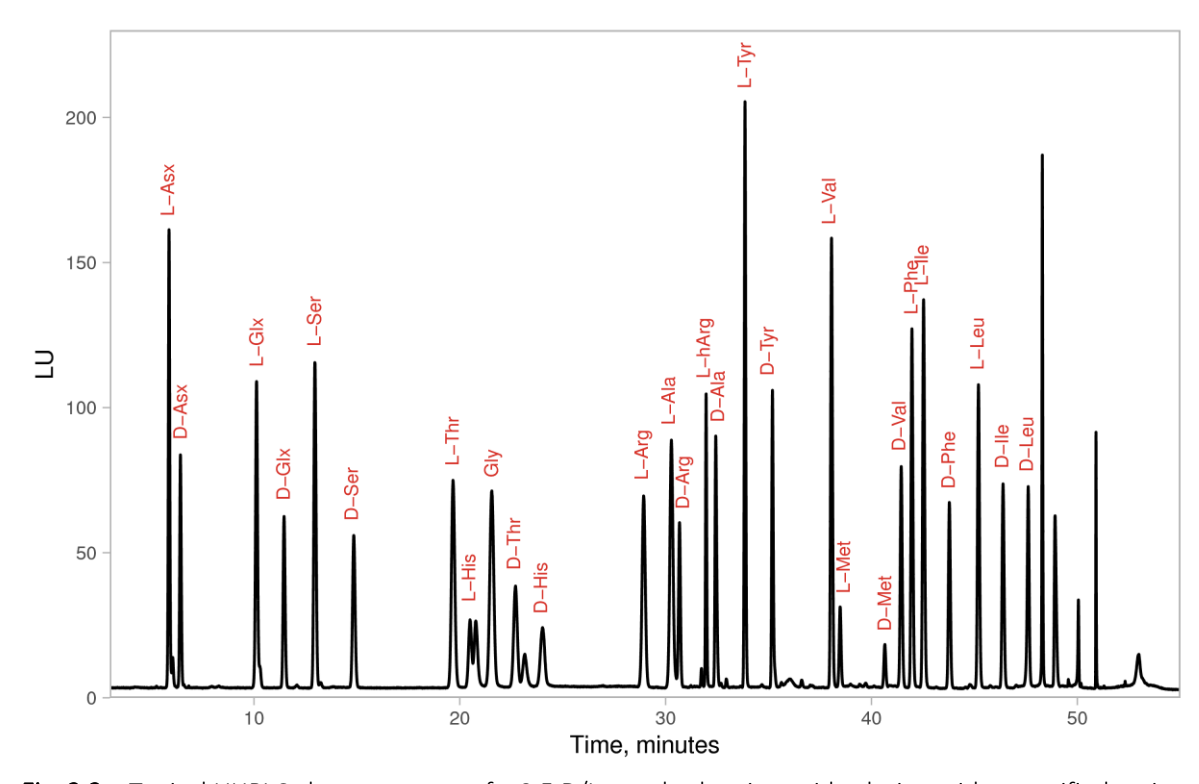


Fig. 2.2 – Typical UHPLC chromatogram of a 0.5 D/L standard amino acid solution with quantified amino acids labelled. L-hArg (L-homo-arginine) is the internal standard.

In the UHPLC method, L-Ala is more poorly resolved than in the RP-HPLC method, sometimes coeluting with D-Arg. Further modifications to the UHPLC solvent gradient program may be able to improve the separation between these two amino acids.

2.5 Data analysis

All data analysis was carried out using the programming language R, version 4.1.1 unless otherwise specified.

Chapter 3 – Assessing the intra-crystalline approach to amino acid geochronology of *Neogloboquadrina pachyderma* (sinistral)

This chapter has been published in full in Quaternary Geochronology under the citation:

Wheeler, L. J., Penkman, K. E. H., & Sejrup, H. P. (2021). Assessing the intra-crystalline approach to amino acid geochronology of *Neogloboquadrina pachyderma* (sinistral). *Quaternary Geochronology*, **61**, 101131. https://doi.org/10.1016/j.quageo.2020.101131

Analysis of samples was carried out by KP; LW carried out data analysis, interpretation and writing with guidance from KP and HPS. Supplementary information for this article can be found online.

Abstract

While amino acid (AA) geochronology has been widely applied to foraminiferal biomineral proteins, there has been limited assessment of the potential of isolating an 'intra-crystalline' fraction of proteins to improve the reliability of AA geochronology for foraminifera. In this study, bleaching experiments were carried out on the foraminifer *Neogloboquadrina pachyderma* (sinistral) from an independently dated core from the south eastern Norwegian Sea spanning the last 120 ka. Results show that this species contains a bleach-resistant fraction of biomineral proteins, and that this intra-crystalline fraction may behave as a closed system. Racemisation in both the intra-crystalline and whole-protein fractions was found to systematically increase with time.

Isoleucine epimerisation showed reliable trends with depth when analysed by ion exchange chromatography (IEC); analysis by reverse-phase liquid chromatography (RP-HPLC) resulted in reliable age-D/L relationships for aspartic acid, glutamic acid and alanine.

Isolating the intra-crystalline fraction with a 48 hour bleach treatment reduces the influence of contamination in younger material. Therefore this paper recommends that the intra-crystalline approach is used when analysing *Neogloboquadrina pachyderma* (sinistral) for AA geochronology, especially for younger samples. Material-specific regression equations developed in this study successfully convert IEC A/I to RP-HPLC D/L values for aspartic acid, glutamic acid and alanine, enabling integration of geochronologies developed using different methods for this class of biomineral.

3.1 Introduction

Amino acid (AA) geochronology relies on the retention of biomineral proteins in a closed system for the duration of diagenesis (Brooks et al., 1990; Collins and Riley, 2000). In certain biominerals, the majority of biomineral protein exists as an *inter*-crystalline 'mesh' between inorganic crystallites (Towe, 1980; Gries et al., 2009). As this inter-crystalline protein is exposed to the external environment, it is susceptible to leaching, contamination or fluctuating environmental conditions, which can influence the rate of protein diagenesis and confound the interpretation of AA geochronology (Sykes et al., 1995).

These inter-crystalline proteins are vulnerable to oxidation, which can be exploited experimentally by exposure to an oxidising agent such as NaOCI (bleaching) (Sykes et al., 1995; Penkman et al., 2008). Conversely, *intra*-crystalline proteins form part of the crystal matrix (Towe, 1980; Berman et al., 1988; Miller et al., 2000) and therefore may be better protected from external influences than inter-crystalline protein. Any residual protein remaining after oxidation is operationally defined as intra-crystalline (Sykes et al., 1995), although depending on the biomineral structure this fraction may also contain well-protected inter-crystalline protein (e.g. chitin in ostracodes (Bright and Kaufman, 2011a)). The adherence of a biomineral's intra-crystalline protein to a closed system depends on the biomineral's structure and relationship to the organic fraction. Investigations of a range of biominerals have found that this intra-crystalline protein diagenesis (IcPD) approach provides more reliable chronological information than the whole-shell approach in various mollusc shells (Penkman et al., 2008; Demarchi et al., 2013c; Ortiz et al., 2015, 2019) coral (Hendy et al., 2012; Tomiak et al., 2013), ostrich eggshell (Brooks et al., 1990; Crisp et al., 2013) and enamel (Dickinson et al., 2019)), while some other biominerals have shown little or no improvement with the IcPD approach (Penkman et al., 2008; Bright and Kaufman, 2011b; Ortiz et al., 2017).

Foraminifera are single-celled organisms found worldwide mainly in marine and estuarine sediments, with widespread applications in Quaternary palaeoenvironmental reconstructions (Boudagher-Fadel, 2015a). Due to the abundance of foraminiferal shells (tests) in marine environments, amino acid racemisation of foraminifera has been identified as a technique potentially well suited to dating marine sediments (Sejrup et al., 1984a; Kaufman, 2006). AA geochronology was first applied to foraminifera in the early 1970s (Wehmiller and Hare, 1971; Bada and Schroeder, 1972; Bada et al., 1973), and has since been applied to a wide range of species of foraminifera (see Kaufman et al., 2013).

While targeted bleaching treatments have been used to remove suspected contamination during preparation of foraminifer tests for AAR (Hearty et al., 2004; Nicholas, 2012; Kaufman et al., 2013), in-depth studies of the IcPD approach are limited (Stathoplos and Hare, 1993; Watson, 2019). In this study we compare the whole-protein and IcPD approaches to AAR on *Neogloboquadrina pachyderma* (sinistral) (hereafter Nps), a species of planktonic foraminifer ubiquitous in the polar waters of both hemispheres (Spindler, 1996). Nps has been the subject of detailed investigations of its racemisation properties (Sejrup et al., 1984a; Macko and Aksu, 1986; Sejrup and Haugen, 1992; Kaufman et al., 2008, 2013; Adler et al., 2009; Kosnik et al., 2013; West et al., 2019). Early work on Nps used only sonication to clean tests (Sejrup et al., 1984a; Macko and Aksu, 1986; Sejrup and Haugen, 1992), while more recent protocols have added a pre-treatment with a weak oxidising agent to remove labile and/or exogenous amino acids (Kaufman et al., 2008, 2013; Adler et al., 2009; West et al., 2019). However the IcPD approach has not yet been fully applied to this species of foraminifer. This study therefore aims to test whether an intra-crystalline protein fraction can be isolated from Nps through bleaching, and whether the IcPD approach provides more a reliable chronology than the whole-shell approach for this biomineral.

Early AA geochronology carried out on Nps focused on isoleucine epimerisation (Sejrup et al., 1984a; Macko and Aksu, 1986; Sejrup and Haugen, 1992) as the two epimers, L-Ile and D-Aile, can be separated using ion-exchange liquid chromatography (IEC) without the use of chiral columns or derivatising agents (Schroeder and Bada, 1976). However, the development of reverse-phase liquid chromatographic (RP-HPLC) techniques have enabled the enantiomeric separation of a wider range of amino acids (Kaufman and Manley, 1998; Powell et al., 2013); more recent studies on Nps using RP-HPLC have focused on the racemisation of Asx and Glx (e.g. Kaufman et al., 2008, 2013). For simplicity the term 'racemisation' will be used to refer collectively to racemisation or epimerisation of amino acids in this paper, as both involve inter-conversion at the α -C of an amino acid.

Whitacre et al. (2017) developed regression equations to convert isoleucine epimerisation (A/I) results from IEC to equivalent RP-HPLC D/L values for five amino acids (Asx, Glx, Ala, Val, Ile) for bivalve, eggshell, gastropod and whole-rock samples. This enables IEC data to be compared with data obtained by RP-HPLC for these biominerals. Pooled equations were developed for application to biominerals not included in the original study. As both separation techniques were used in the analysis of material in this study, in addition we evaluate the methods developed by Whitacre et al. to extend them to these foraminifer tests.

This study therefore seeks to answer three key research questions:

- 1. Does Nps have an intra-crystalline fraction of biomineral protein that can be isolated by exposure to NaOCl, and if so, what is the ideal duration of this treatment (Section 3.3.1)?
- 2. Does analysis of the intra-crystalline fraction of amino acids show an improvement in the dating performance of these amino acids, compared with the whole-protein fraction of amino acids (Section 3.3.2)?
- 3. Can A/I values measured by IEC be confidently converted to D/L values for other amino acids for Nps (Section 3.3.3)?

3.2 Materials and Methods

3.2.1 Location

MD99-2288 and MD99-2289 are two giant piston cores taken from the same location (64°39 N 04°12 E) in the Nyegga region of the Vøring Plateau, in the mid-Norwegian continental margin (Fig. 3.1), raised during the 1999 IMAGES V cruise (Hjelstuen et al., 2010). The cores are 32.21 m and 23.69 m long respectively. They were taken at a water depth of 1262 m on the northern escarpment of the Storegga Slide, a site of semi-regular submarine landslides taking place over the last 2.5 Ma (Bryn et al., 2005). Sedimentation on the Vøring Plateau is largely controlled by the advance and retreat of the Scandinavian Ice Sheet and its impact on regional ocean currents (Dahlgren and Vorren, 2003). Current bottom-water temperatures in the Norwegian Sea measure approximately -0.5°C to -1°C (Hovland et al., 2005). Palaeotemperature estimates for the Norwegian Sea suggest that bottom-water temperatures have fluctuated by up to 2-4°C between glacial and interglacial periods (Sejrup and Haugen, 1992; Bauch et al., 2000; Dwyer et al., 2000) due to changes in North Atlantic deep water formation in the northern Norwegian Sea (Sarnthein and Altenbach, 1995). In general there is a reduction in racemisation rates in glacial as compared to interglacial periods (e.g. Miller et al., 1997; Penkman et al., 2011; Ortiz et al., 2015), but as the purpose of this study is to compare protein fractions and amino acids between samples with the same diagenetic history, these temperature fluctuations will not impact the interpretation of these results.

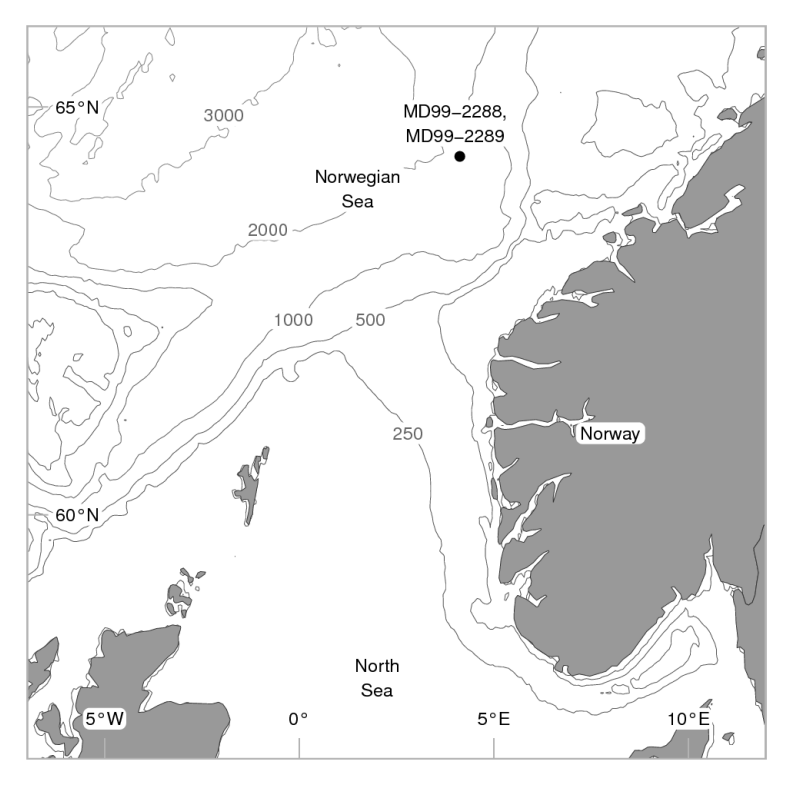


Fig. 3.1 – Location of MD99-2288 and MD99-2289 IMAGES cores in the Norwegian Sea. Isobath depths in metres; bathymetry data from NOAA.

3.2.2 Age model

MD99-2288 and MD99-2289 were matched by magnetic susceptibility and spliced at 2303.5 cm (MD99-2288)/2270.0 cm (MD99-2289) (Brendryen, 2011); therefore the established chronology for MD99-2289 was applied to MD99-2288 with a 33.5 cm correction. Chronological control for the core MD99-2289 is provided by AMS radiocarbon dating between 120 and 1300 cm (Berstad, 2003; Becker et al., 2018), correlation between the NGRIP δ^{18} O record and XRF core scanning results for Ca and Ti/K from 1441 to 1863 cm (Brendryen et al., 2010; Brendryen, personal communication 2019), and one identified tephra zone, the Faroe Marine Ash Zone II, at 1064 cm and 26.69 \pm 0.39 ka BP (Nilsen, 2014). An age depth model was constructed for the 120-1863 cm range of the spliced core using the Bayesian age modelling R package 'Bacon' (v. 2.3.7) (Blaauw and Christeny, 2011) using the Marine13 calibration curve (Reimer et al., 2013) and a 405 year reservoir correction for the ¹⁴C ages as used by Becker et al. (2018). As no uncertainties were provided for the NGRIP tie points, a 1.2 ka uncertainty was applied to the model based on calculated uncertainties for NGRIP chronology (Svensson et al., 2008). While this may result in an underestimation of the age uncertainty in the latter half of the core, it is sufficient to explore the racemisation trends for Nps protein in this study. The output of the model (**Fig. 3.2**) shows a

dramatic increase in sedimentation rate at ca. 1250 cm (~30 ka). The radiocarbon ages used and modelled ages for each sampling depth can be found in the supplementary information.

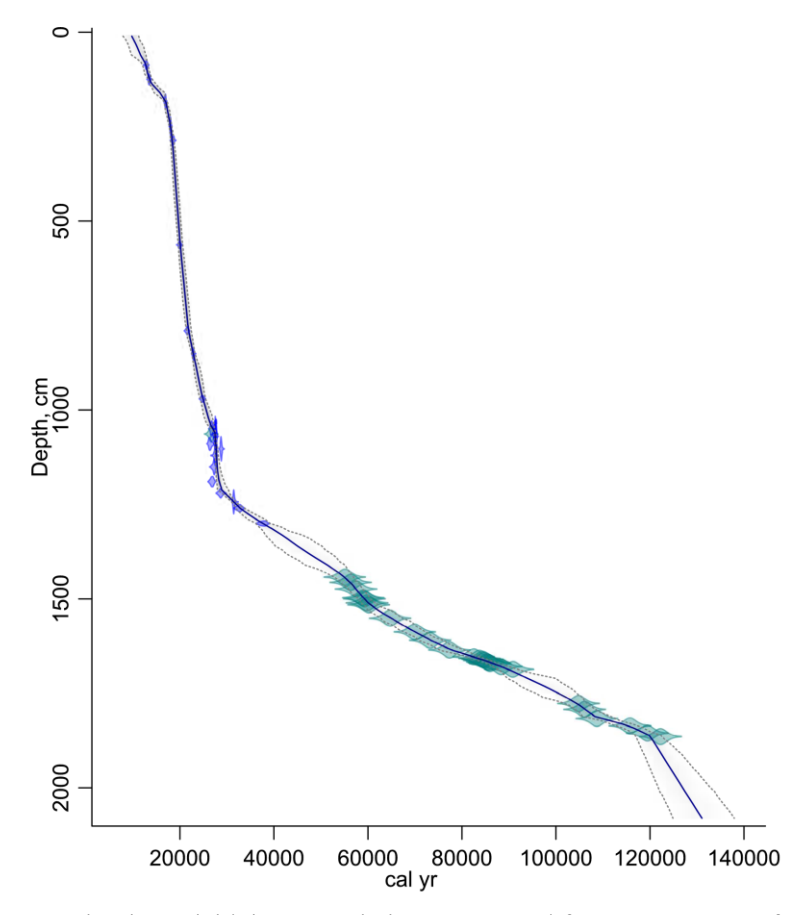


Fig. 3.2 – Bayesian age depth model (Blaauw and Christeny, 2011) for 120-1863 cm of core MD99-2289. Radiocarbon ages are shown in blue; NGRIP tie points and tephra zones are shown in teal. The dark blue line shows the model's weighted mean age. Dashed lines represent the model's 95% probability intervals.

3.2.3 Preparation of foraminifera

Foraminifera were collected at regular intervals from the >150 μ m fraction of both cores. While records of the core from which each sample was collected have unfortunately been lost, it is assumed for this study that samples between 10-2200 cm were taken from MD99-2289 and samples between 2300-2985 cm were from MD99-2288 (Brendryen, personal communication 2019). A full record of samples taken can be found in the supplementary information. For IEC analysis, 100 to 150 individuals were pooled for each analytical sample, while 30 to 50 individuals were pooled for RP-HPLC. All samples were cleaned by sonication according to Miller et al., (1983).

3.2.3.1 Isolation of the intra-crystalline fraction

To initially determine the stability of the intra-crystalline fraction of Nps biomineral proteins during prolonged oxidation, foraminiferal samples were taken from three depths (250 cm, 500 cm and 1450 cm) for extended bleaching experiments. Oxidation treatments using NaOCl (bleach) were carried out on Nps between 24 hours and 336 hours (1450 cm) or 360 hours (250 cm and 500 cm).

 $30-50~\mu L$ NaOCI (12%~w/v) was added to each sample; samples were shaken every 24 hours to aid penetration of the bleach into the biomineral. At the end of the bleaching period the bleach was pipetted off, the sample rinsed six times with ultrapure water and once with HPLC-grade methanol, then air dried prior to demineralisation. Samples analysed by IEC were dried for 15 minutes at 60° C; samples analysed by RP-HPLC were dried for 5-10 minutes at 110° C. This difference in procedure reflects the standard protocols of the different laboratories in which the analyses were carried out: IEC at the University of Bergen and RP-HPLC at the University of York.

3.2.3.2 Analysis of racemisation trends in Nps

Based on the results of the extended oxidation experiments (Section 3.3.1), a 48 hour NaOCl exposure was chosen to prepare the rest of the 'bleached' samples in this study. To assess differences between the diagenesis of the whole-protein and intra-crystalline protein fractions of Nps, unbleached and bleached samples from a range of depths throughout the cores were analysed. Depending on the amount of material available at each depth, 1-3 replicate samples were prepared for each treatment.

Procedural blanks were collected and analysed for each experiment to quantify background levels of amino acid contamination; due to the sample sizes used, corrections for contaminants identified in the blanks were not necessary.

3.2.4 Amino acid analysis

Only the total hydrolysable amino acid (free and bound amino acids; THAA) fraction was analysed to conserve material. Samples were demineralised with 8 μ L 7 M HCl, with addition of a further 8 μ L HCl if necessary to complete demineralisation. Samples were hydrolysed by heating at 110°C for 22 hours in nitrogen-flushed vials, then dried at 80°C for 15 minutes prior to rehydration for analysis by IEC, or dried overnight under vacuum prior to rehydration for analysis by RP-HPLC.

Separation of the hydrolysed amino acids was carried out either using IEC (at the University of Bergen) or RP-HPLC (at the University of York). During hydrolysis asparagine and glutamine are irreversibly hydrolysed to aspartic acid and glutamic acid respectively; therefore these amino acids are analytically indistinguishable and reported as Asx and Glx (Hill, 1965). The fluorescent derivatising agent *o*-phthaldialdehyde (OPA), used in both methods, does not allow for the detection of proline or hydroxyproline (Miller and Brigham-Grette, 1989), while the OPA derivative of lysine is prone to degradation during separation (Brückner et al., 1994); therefore these amino acids are not reported for either method.

3.2.4.1 Separation by ion exchange liquid chromatography (IEC)

For analysis using IEC, the internal standard norleucine was added with the 7 M HCl used for demineralisation. Samples were rehydrated with 100 μ L pH 2 buffer before being separated on an automatic amino acid analyser with post-column OPA derivatisation and fluorometric detection according to the methods of Sejrup and Haugen (1992). Due to the poor separation of Ser and Thr by IEC, these two amino acids are reported together for this technique. The only amino acid for which chiral information is available using IEC is IIe; this is reported as A/I.

3.2.4.2 Separation by reverse-phase high performance liquid chromatography (RP-HPLC)

For analysis using RP-HPLC, samples were rehydrated with 8-10 μ L rehydration fluid (2.38 M HCl, 0.171 mM NaN₃, 9.97 mM internal standard L-homo-arginine). The rehydrated samples underwent pre-column derivatisation with OPA and the chiral thiol *N*-isobutyryl-L-cysteine (IBLC), followed by chiral separation and fluorometric detection following a modified method of Kaufman and Manley (1998) using an Agilent 1100 Series HPLC fitted with a C₁₈ HyperSil BDS column. The D-Arg peak coeluted with another compound in all RP-HPLC chromatograms; therefore Arg D/L values are not reported and D-Arg has been excluded from total amino acid concentrations as in other studies using RP-HPLC (Powell et al., 2013).

3.2.4.3 Data screening

A range of diagnostic criteria can be used to assess the integrity of AAR data, such as Ser, Thr or Gly abundance (e.g. Miller and Brigham-Grette, 1989; Sejrup and Haugen, 1992; Kaufman, 2000),

expected depth or age trajectories (Wehmiller et al., 1976; Kosnik and Kaufman, 2008), covariance between concentrations or D/L values for different amino acids (e.g. Kaufman, 2000; Preece and Penkman, 2005), and the variability of replicate samples (Kosnik and Kaufman, 2008). Cut-offs for sample exclusion are determined empirically, and are therefore potentially somewhat subjective, but it is important that exclusion criteria, once determined, are applied uniformly to the data set to minimise systematic bias (Kaufman, 2006). D/L values lying far above or below the general trend could be indicative of a compromised sample, but as some natural variability due to reworking or intrusion is inevitable (McCarroll, 2002) only extreme outliers were excluded from this study.

The following screening criteria were chosen:

- 1. High concentrations of Gly (> 50%), which indicate contamination resulting from human handling (Sejrup and Haugen, 1992). High Ser and Thr concentrations were also considered, but poor separation of Ser and Thr using IEC precluded using these amino acids as criteria.
- 2. Deviation of increasing trend of A/I values for IEC, and D/L values of Asx, Glx and Ala (the three amino acids with the best chromatographic separation) for RP-HPLC.

Outliers were identified and excluded from the dataset according to the criteria listed in **Table 3.1**. On average, 6.0% of samples were excluded from the data set using these criteria. A full list of the samples excluded and the criteria used to exclude each sample is available in the supplementary information.

Table 3.1 – Screening criteria used to identify outliers and total number of samples excluded by each criterion for each analytical method.

	li li	EC	RP-HPLC		
Unbleached (U) or bleached (B):	U	В	U	В	
1. > 50% Gly	0	0	2*	2*	
2. Deviation of D/L from depth trend	5	4	3	3	
Total samples analysed	69	75	53	51	
% Removed	7.2	5.1	5.7	5.9	

^{*}Only one of two analytical replicates found to have > 50% Gly, indicating issues with chromatographic separation rather than contamination.

3.2.5 IEC A/I to RP-HPLC D/L conversion

Whitacre et al. (2017) developed linear regressions to convert IEC A/I data into D/L values for five amino acids (Asx, Glx, Ala, Val, Ile) equivalent to those measured by RP-HPLC. Biomineral-specific equations were found to minimise errors associated with the conversion by accounting for

variations in diagenetic patterns and chromatographic separation between biominerals; however 'pooled' regressions were also developed for use with sample types not represented in the original study:

$$log_2(Asx D/L) = 0.36 \times log_2(A/I) - 0.3$$

 $log_2(Glx D/L) = 0.64 \times log_2(A/I) - 0.5$
 $log_2(Ala D/L) = 0.62 \times log_2(A/I) + 0.22$
 $log_2(Val D/L) = 0.94 \times log_2(A/I) - 0.22$
 $log_2('RP' Ile A/I) = 0.996 \times log_2(A/I) - 0.034$

As foraminifera were not included in the original study, the pooled regressions were used to convert IEC A/I values into predicted Asx, Glx, Ala, Val D/L and RP-HPLC equivalent Ile A/I values, and compared with the values actually measured by RP-HPLC, in order to test the efficacy of the pooled equations for Nps.

New linear regressions were then carried out on \log_2 -transformed Nps data. Unlike the data used by Whitacre et al. (2017), analyses carried out in this study were not paired, as this comparison had not been the original intention of the study. Therefore average D/L values for each depth and bleaching treatment were used to develop the regressions. This means that the errors associated with the derived conversions are likely to be higher in this study. No significant differences between separate regressions run on bleached and unbleached material were found, so pairs of IEC and RP-HPLC data where the depth and bleaching treatment were the same were combined to increase the sample size for the models. Between 30 and 32 averaged D/L values were used for each regression. Following Whitacre et al. (2017) the following criteria were used to assess the quality of each model: the adjusted R² value, 1 and 2 σ prediction uncertainties, and the Akaike information criterion (AICc), a measure of model quality which penalises for overparameterisation. All statistical analysis was carried out using the statistical programming language 'R' version 3.6.2. Analytical scripts are included as supplementary information.

3.3 Results and discussion

3.3.1 Testing oxidation times

3.3.1.1 The effect of bleaching on amino acid concentration

If Nps biomineral contains an intra-crystalline protein fraction resistant to oxidation, then bleaching via exposure to NaOCl should cause an initial decrease in the total hydrolysable amino acid concentration ([THAA]), followed by a plateau once the intra-crystalline fraction has been isolated.

The presence of amino acids after the longest bleaching duration shows that Nps contains a bleach-resistant intra-crystalline protein fraction (**Fig. 3.3**), as has been observed in other species of foraminifera (Watson, 2019). While the variability of [THAA] in the extended Nps bleaching experiments is high, the similarity between unbleached and bleached [THAA] suggests that the majority of the inter-crystalline protein fraction has been lost by 18 ka, as has been observed in other biominerals (Sykes et al., 1995; Penkman et al., 2008; Ortiz et al., 2015, 2017).

The samples with much higher than average [THAA] (> 0.9 nmol / foram) at 250 cm (and seen in some unbleached samples at other depths, see Section 3.3.2) may be due to some between-shell variability in the survival of inter-crystalline protein (as seen in gastropods (Penkman et al., 2008), although given that each sample in this study consists of 100 individual tests this interpretation is unlikely. An alternate explanation may be due to modern laboratory contamination; however if this was the case these samples would have a correspondingly low A/I value, which is not seen (Fig. 3.5). This variability is therefore most likely due to the challenges in accurately measuring amino acid concentration, especially at very small sample sizes (Powell, 2012).

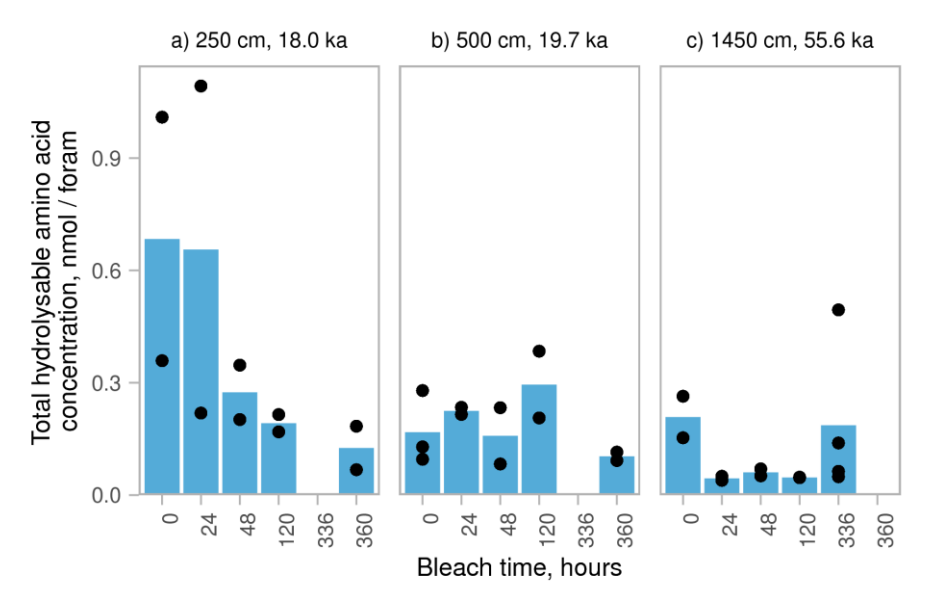


Fig. 3.3 – Trends in concentration of total hydrolysable amino acids ([THAA]) with increasing bleach time for Nps at three core depths: a) 250 cm, b) 500 cm and c) 1450 cm. Dots show individual replicates; bars show means of all replicates at each time and depth point. Where data are absent, this is because experiments of this duration were not carried out.

3.3.1.2 The effect of bleaching on amino acid composition

The biomineral protein of Nps is dominated by Asx and Gly, with smaller contributions from Ser \pm Thr, Ala, Glx, Val, Leu and Ile (**Fig. 3.4**). Phe, His, Arg and Tyr were not resolved using IEC, but observed in small amounts (total contribution from all four amino acids \pm 1 \pm 3 %) in samples analysed by RP-HPLC (see supplementary information). This composition is consistent with other foraminifera (King and Hare, 1972a; Weiner and Erez, 1984; Robbins and Brew, 1990). The high abundance of Asx indicates the presence of acidic proteins involved in biomineral formation (Weiner, 1979), while Gly and Ala likely represent silk-like proteins found in other biominerals (Pereira-Mouriès et al., 2002; Gotliv et al., 2003).

Differences in the composition of amino acids between the whole-shell and intra-crystalline fractions have been found in some mollusc shells (Penkman et al., 2008; Demarchi et al., 2013c; Ortiz et al., 2015; Pierini et al., 2016), indicating the presence of different proteins in different fractions of those biominerals. Other biominerals do not have significant differences between the two fractions (e.g. ostracodes (Ortiz et al., 2013), ostrich eggshell (Crisp et al., 2013)). The composition of amino acids is quite variable for Nps, especially for Ser + Thr and Gly, confounding a clear assessment of the effect of bleaching on composition, with no clear patterns emerging from the extended bleaching treatment (**Fig. 3.4**). The apparent stability of both the concentration and

composition of the intra-crystalline amino acid pool over extended exposure to bleach suggests that this fraction is oxidation resistant.

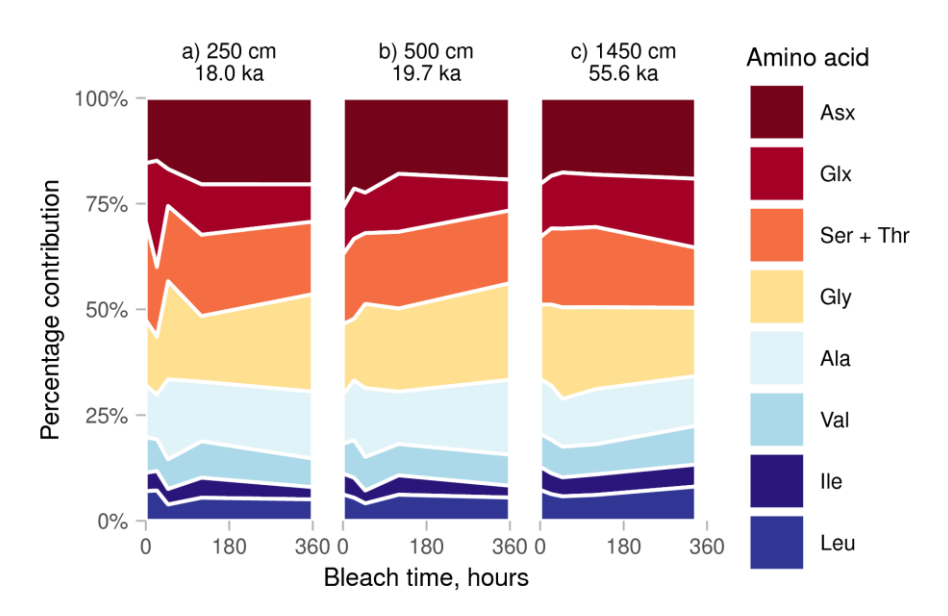


Fig. 3.4 – The effect of increasing exposure to bleach on total hydrolysable amino acid (THAA) composition of Nps tests at three core depths (analysed using IEC). While there is some variability in the THAA composition in the first 48 hours of bleach exposure, no clear compositional changes are caused by oxidation. Due to poor separation of Ser from Thr using IEC, these amino acids are reported together.

3.3.1.3 The effect of bleaching on A/I values

Differences in A/I or D/L values between the inter- and intra-crystalline fractions of biominerals may be due to the loss of more highly racemised short-chain peptides and free amino acids from an open-system inter-crystalline fraction (Penkman et al., 2008). Free amino acids in a biomineral are more highly racemised than peptide-bound amino acids due to the accelerated rate of racemisation at the terminal positions of peptides (Crisp et al., 2013; Tomiak et al., 2013). Therefore, if this fraction is more susceptible to leaching (diffusive loss) from inter-crystalline sites than intra-crystalline sites, unbleached material will show 'suppressed' A/I or D/L values compared with bleached material. This pattern has also been observed in some molluscs (e.g. Penkman et al., 2008; Demarchi et al., 2013c; Ortiz et al., 2015; Pierini et al., 2016) and ostrich eggshell (Crisp et al., 2013).

As the extended bleaching experiments for Nps were analysed by IEC only, the only amino acid for which racemisation data are available is Ile. At 250 cm the A/I value increases slightly between 24 and 48 hours and then plateaus (**Fig. 3.5a**), indicating that bleach-induced racemisation is not taking place. Due to the variability of the data there is no clear effect of bleaching on A/I at 500 and

1450 cm (**Fig. 3.5b**, **c**); however, lower A/I values in unbleached Nps are also seen in the down-core trend for ages greater than ~60 ka (**Fig. 3.8**). This suggests that the remaining inter-crystalline protein may behave as an open system even after the initial loss of protein during early stages of diagenesis; this may be due to the progressive generation of highly racemised free amino acids via hydrolysis.

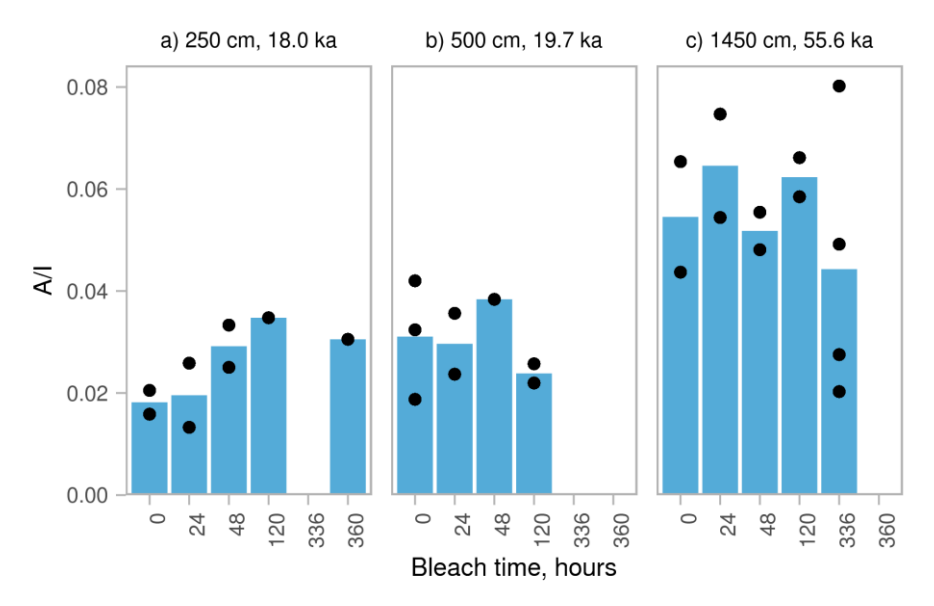


Fig. 3.5 – Trends in A/I value with increasing bleach time for Nps at a) 250 cm, b) 500 cm and c) 1450 cm. Dots show individual replicates; bars show means of all replicates at each time and depth point. Where data are absent, this is because experiments of this duration were not carried out, with the exception of 360 hours at 500 cm, where none of the samples had resolved A-Ile peaks. An increase in A/I is observed between 24-48 hours at 250 cm, while bleaching has no clear effect on A/I at 500 cm and 1450 cm.

Based on the results of these extended bleaching experiments, a 48 hour NaOCl exposure was chosen for the rest of the samples in the study, as this treatment is sufficient to isolate the intracrystalline fraction of amino acids in Nps.

3.3.2 Comparison of down-core diagenetic trends in racemisation between unbleached and bleached Nps

Samples of Nps were taken for analysis by IEC and RP-HPLC at regular intervals down the cores to enable a more detailed investigation of any amino acid trends and to compare the behaviour of the whole-protein and intra-crystalline fractions for this class of biomineral. A full list of intervals sampled can be found in the supplementary information.

3.3.2.1 Trends in concentration and composition

There is substantial variability in both the [THAA] and composition of amino acids for both unbleached and bleached samples through the cores (Fig. 3.6, Fig. 3.7). In general, the concentration of bleached samples is slightly lower than concentration of unbleached samples (Fig. 3.6), indicating that the majority of protein in naturally-aged Nps is in the intra-crystalline fraction. With the exception of a few relatively young samples having higher than average [THAA], the concentration of amino acids appears to be relatively stable over the timescale represented by this core.

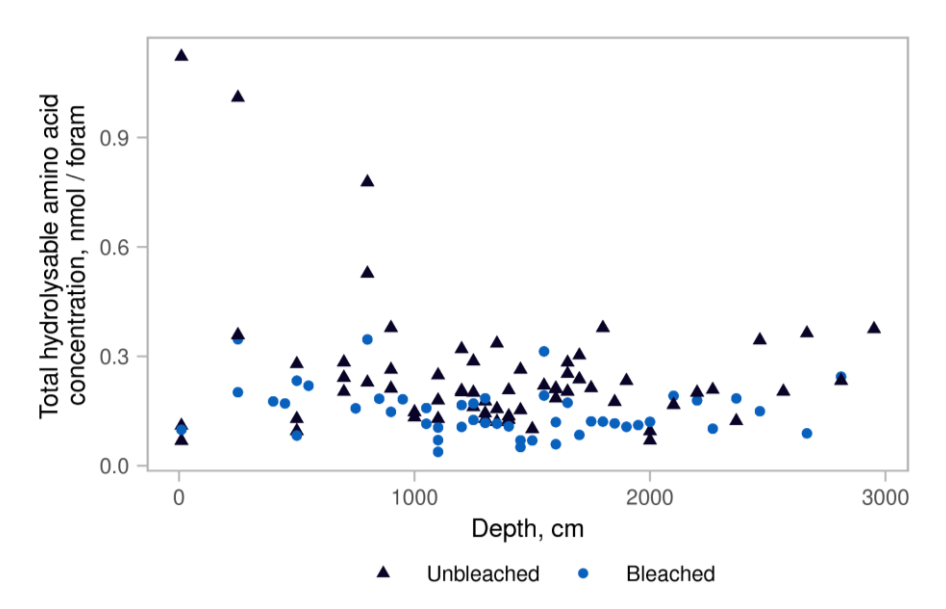


Fig. 3.6 – Down core trends in total hydrolysable amino acid concentration of bleached and unbleached Nps tests (analysed using RP-HPLC).

As was seen in the extended bleaching experiments, there is no clear difference between the composition of whole-protein and intra-crystalline protein fractions of Nps (Fig. 3.7). Neither fraction shows a systematic change in amino acid composition down core. This indicates that both the whole-shell and intra-crystalline fractions remain relatively stable during diagenesis. While some work has found differential loss of acidic proteins from a range of planktonic species within ~300 ka (Robbins and Brew, 1990), this trend is not seen here over the 120 ka studied.

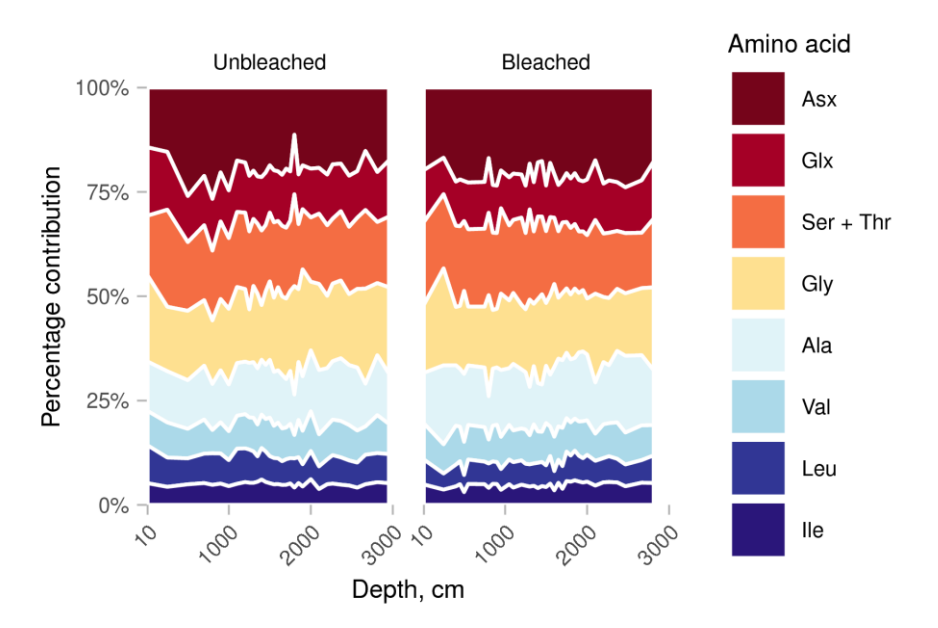


Fig. 3.7 – Down-core compositions of unbleached and bleached (48 h) Nps tests analysed by IEC, showing a relatively stable composition of both the whole and intra-crystalline fractions of amino acids. Due to poor separation of Ser from Thr using IEC, these amino acids are reported together.

3.3.2.2 Trends in racemisation

As determined by IEC, the A/I value of Nps increases with age, with the rate of racemisation slowing over time in both bleached and unbleached samples (Fig. 3.8). Due to the change in sedimentation rate at ~30 ka in the cores (see Fig. 3.2), plots of D/L against age and depth are included to show more clearly the trends in racemisation during the younger section of the core (Fig. 3.8, Fig. 3.9, Fig. 3.10). In the first ~60 ka (1550 cm) of the core, the extent of racemisation for bleached and unbleached Nps are similar, with bleached Nps having a slightly higher degree of racemisation (Fig. 3.10, presented separately for clarity). Older than ~60 ka, the levels of racemisation are lower for unbleached Nps than bleached Nps. This may be due to the loss of free amino acids from the unbleached biomineral, effectively 'suppressing' the rate of racemisation (see Section 3.3.1.3).

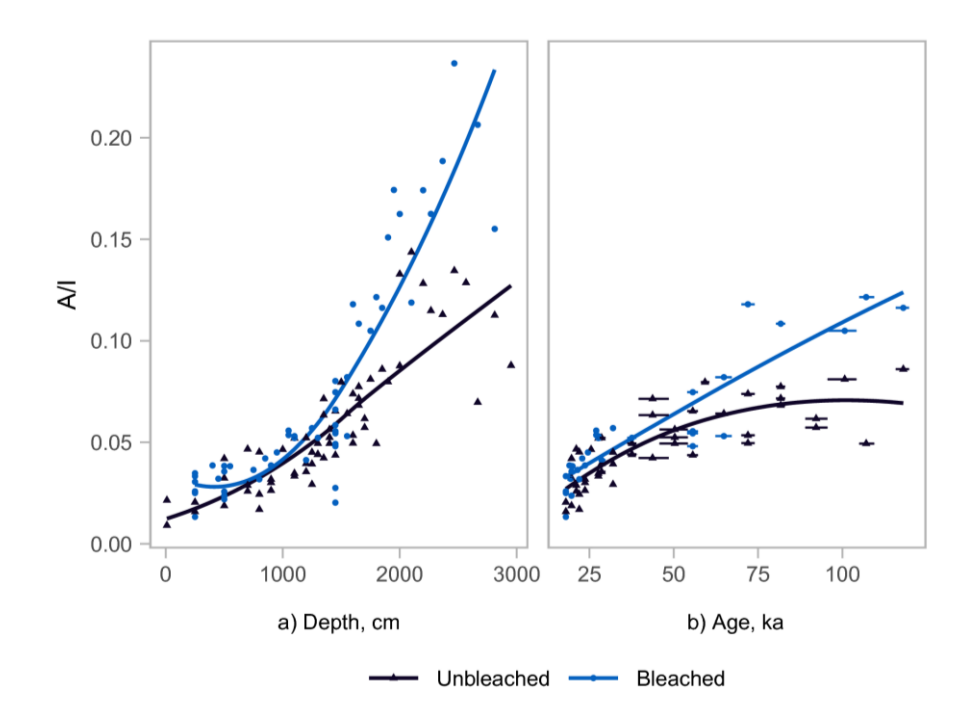


Fig. 3.8 – Downcore trends in A/I for Nps analysed by IEC: a) A/I against depth showing samples taken between 10-2951.5 cm (corrected depth); b) A/I against age for samples taken between 120-1863 cm, the range of the age model for the core (see Fig. 3.2). Horizontal lines show 1σ age error from age model. Bleached samples were subjected to 48 h NaOCl exposure. A locally weighted smoothing (loess) function has been applied (solid line) to highlight the differences between the racemisation trends for bleached and unbleached Nps.

Of the amino acids analysed using RP-HPLC, Asx and Glx showed the clearest racemisation trends (**Fig. 3.9i**, **ii**). While previous studies of amino acid racemisation in Nps using RP-HPLC have focused on Asx and Glx only (Kaufman et al., 2008, 2013), Ala also showed clear trends in racemisation in this core after ~25 ka (**Fig. 3.9iv**), suggesting that Ala could be used to provide additional chronological control for Nps in older material.

For most amino acids separated by RP-HPLC, the D/L values were similar between bleached and unbleached Nps, with bleached material having slightly higher D/L values in older (> 60 ka) samples, suggesting some loss of highly-racemised free amino acids from the inter-crystalline fraction (Fig. 3.9). Ser has substantially higher D/L values (Fig. 3.9, Fig. 3.10iii) in the bleached samples. This may be due a result of Ser having a higher abundance in the free amino acid pool as a result of the lability of Ser-X peptide bonds (Hill, 1965) results in a greater 'suppression' of Ser racemisation than other amino acids in the whole-protein fraction. As L-Ser is a common laboratory contaminant, the increase in Ser D/L on bleaching may also be in part due to the removal of exogenous amino acids.

As also seen in studies of the kinetics of amino acid racemisation in other biominerals (Penkman et al., 2008; Demarchi et al., 2011, 2015), Ser racemises the most quickly of all the amino acids due to its ability to racemise in-chain (Demarchi et al., 2013a), plateauing at ~30 ka at a D/L of around 0.3 for bleached samples (Fig. 3.9 and Fig. 3.10iii). This plateau may be due to the comparative instability of Ser (Bada et al., 1978) resulting in apparent 'steady-state' behaviour of racemisation as the rates of Ser racemisation and decomposition converge (Schroeder and Bada, 1977). Asx, Glx and Ala show a similar trend to Ile, with rapid initial racemisation in the first ~30 ka followed by a slowing of the observed rate of racemisation (Fig. 3.9 and Fig. 3.10i, ii, iii). This 'two-stage' racemisation pattern is consistent with observations of racemisation kinetics in foraminifera (Wehmiller and Hare, 1971; Harada and Handa, 1995; Kaufman, 2006), and with other biominerals (see Clarke and Murray-Wallace, 2006).

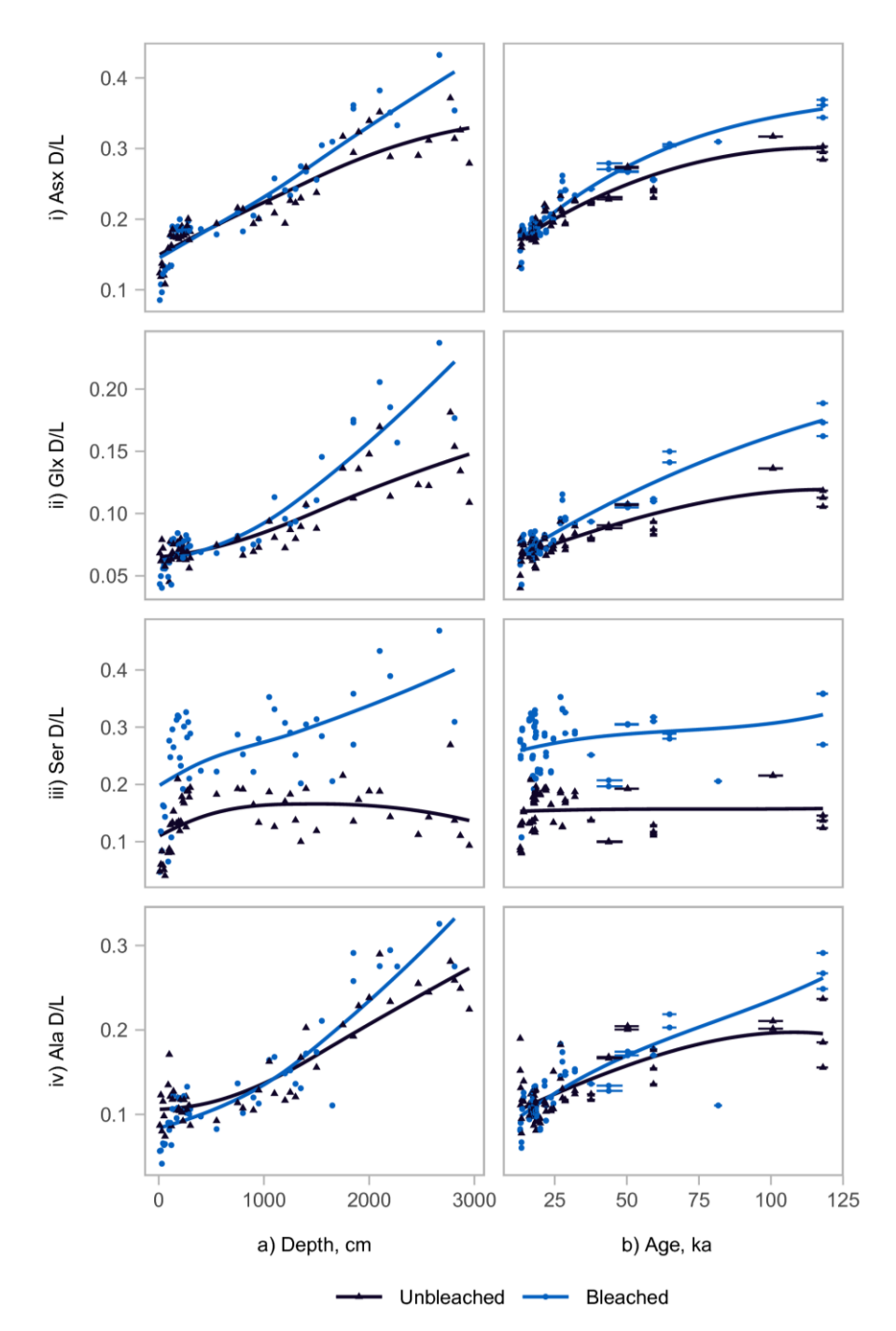


Fig. 3.9 – Trends in racemisation for four amino acids (i) Asx, ii) Glx, iii) Ser, iv) Ile) analysed by RP-HPLC. a) D/L against depth showing samples taken between 10-2951.5 cm (corrected depth); b) D/L against age for samples taken between 120-1863 cm, the range of the age model for the core (see **Fig. 3.2**). Horizontal lines show 1 σ age error from age model. All four amino acids have higher D/L values for bleached than unbleached Nps in older samples. Bleached samples were subjected to 48 h NaOCl exposure. A locally weighted smoothing (loess) function has been applied to highlight the differences between the racemisation trends for bleached and unbleached Nps.

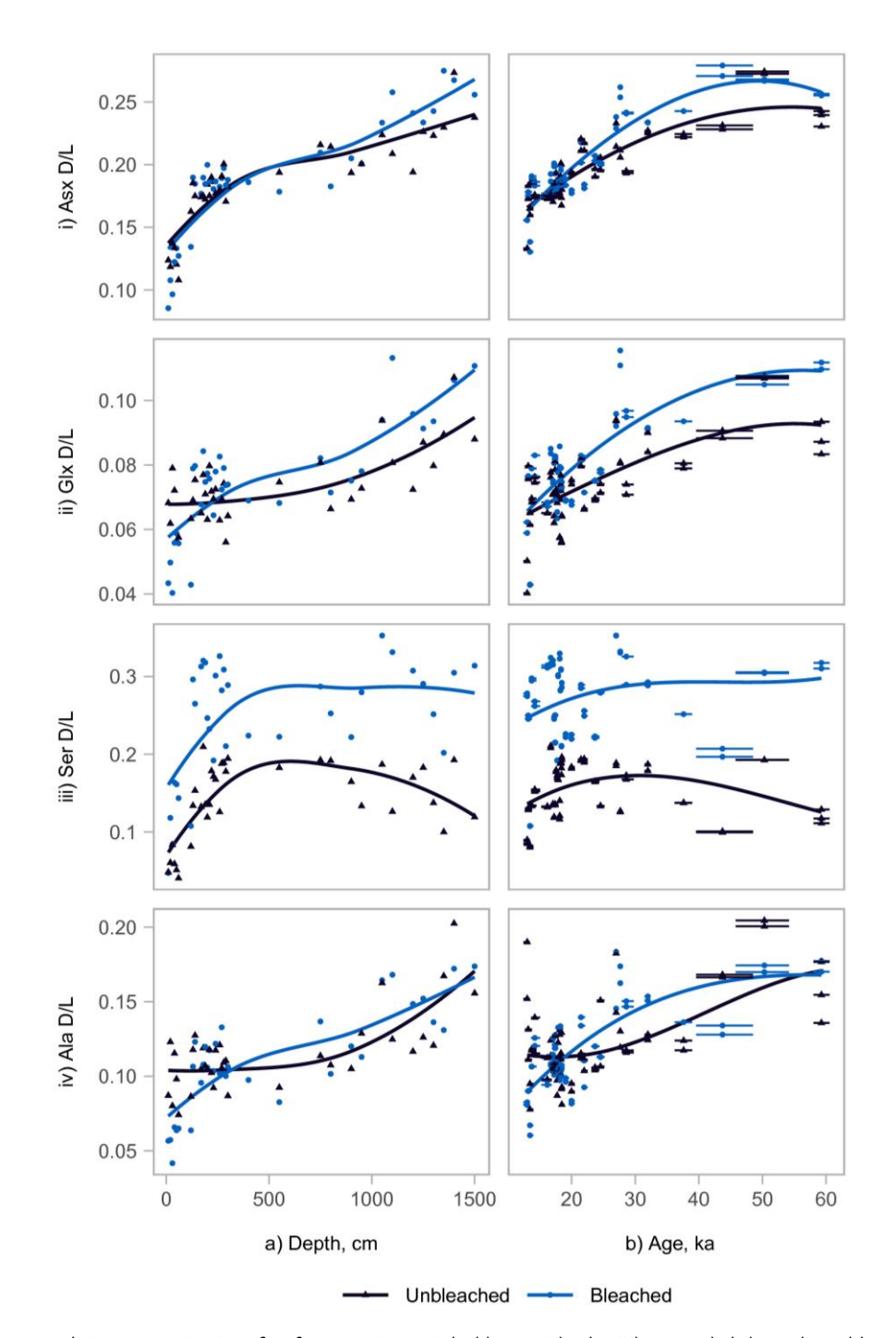


Fig. 3.10 – Trends in racemisation for four amino acids (i) Asx, ii) Glx, iii) Ser, iv) IIe) analysed by RP-HPLC for the youngest part (10-60 ka, 10-1500 cm) of the core: a) D/L against depth; b) D/L against age. Horizontal lines show 1σ age error from age model. During this early stage of racemisation D/L values are similar between bleached and unbleached Nps for Asx, Glx and Ala. Bleached samples were subjected to 48 h bleach exposure. A locally weighted smoothing (loess) function has been applied to highlight the differences between the racemisation trends for bleached and unbleached Nps.

Of these three amino acids, Asx racemises the most quickly in Nps, reaching a D/L of \sim 0.3 by 120 ka, while Glx racemises more slowly, reaching a D/L of \sim 0.15 over the same period. The apparent racemisation rate of Ala is intermediate, reaching a D/L of \sim 0.2 by 120 ka. This order of apparent

racemisation rate (Ser > Asx > Ala > Glx \sim Ile) is consistent with the results of high-temperature decomposition experiments carried out on other biominerals (e.g. Kimber and Griffin, 1987; Ortiz et al., 2017; Dickinson et al., 2019). Studies of Asx and Glx racemisation trends in heated and naturally-aged planktonic foraminifera have found that Asx racemises more quickly than Glx (Hearty et al., 2004; Kaufman, 2006; Kaufman et al., 2013); however a study of *P. obliquiloculata* investigating a wider range of amino acids found that Ile racemised more quickly than Glx, in contrast to the results of this study, which observed similar apparent racemisation rates between Ile and Glx (Harada and Handa, 1995).

If the intra-crystalline fraction better approximates a closed system than the whole-protein fraction, then there should be fewer environmental influences on racemisation in the intra-crystalline fraction, resulting in lower variability between D/L values at any given horizon for bleached samples (Penkman et al., 2008). For Nps, bleaching results in a decrease in variability between similar-age samples during early stages of diagenesis (Fig. 3.11). This result is consistent with the reduced effect of bleaching on total amino acid concentration in older material (Section 3.3.1.1), suggesting that the majority of the inter-crystalline protein is leached from the biomineral during early stages of diagenesis. While these reductions in variability on bleaching are not seen in older material, the observed increase in D/L values in the intra-crystalline fraction suggest that the IcPD approach also limits the effects of leaching and contamination in older samples.

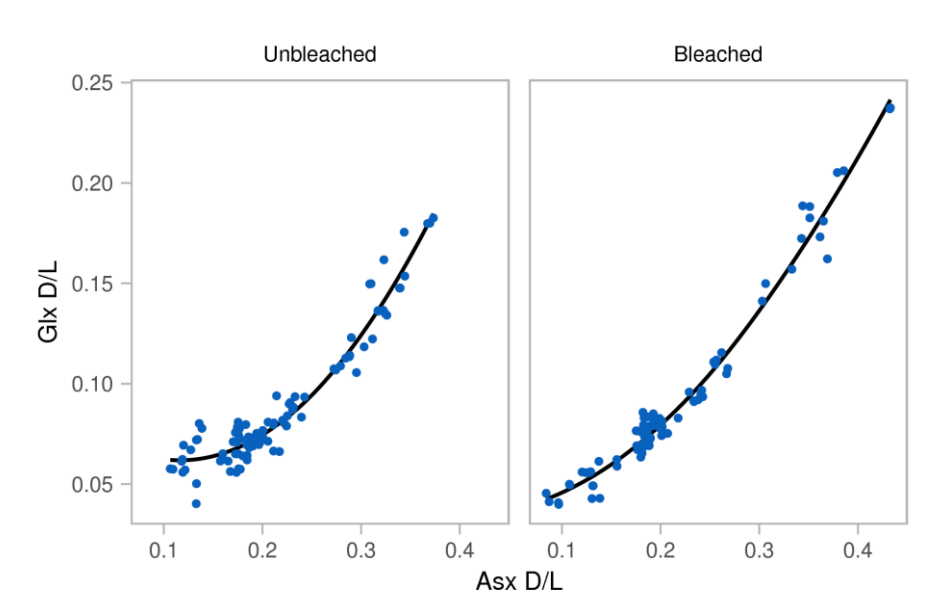


Fig. 3.11 – Covariance of Asx and Glx D/L for bleached and unbleached Nps analysed by RP-HPLC, showing decreased variability of D/L values on bleaching for young material (Asx D/L < 0.2). A locally weighted smoothing (loess) function has been applied to show the general trends of the data.

3.3.3 IEC A/I to RP-HPLC D/L conversions

Conversion from IEC Ile A/I and equivalent RP-HPLC amino acid D/L was carried out using the pooled regressions developed by Whitacre et al. (2017), as well as Nps-specific regressions derived using the Nps data set. Due to the poor separation of L-Ile and D-Aile using RP-HPLC (Powell et al., 2013; Wehmiller, 2013a), direct comparison between IEC Ile A/I and RP-HPLC Ile A/I was not possible using this data set.

When applied to the Nps data set, the 2σ prediction uncertainty for the pooled regressions were ± 23 to 42% depending on the amino acid, similar to the ranges found by Whitacre et al. for other biominerals (**Table 3.2**). While Whitacre et al. (2017) found that creating material-specific models reduced the 2σ prediction uncertainty compared with pooled regressions, this has not been observed for Nps – perhaps due to the use of averaged rather than paired analyses. For Asx, Glx and Ala the 2σ prediction uncertainty was ± 24 -35% when using the Nps-specific regression. Conversely, Val and Ile had much higher 2σ prediction uncertainties for the Nps-specific regression, highlighting the poorer chiral separation of both Val and Ile by RP-HPLC for this biomineral (**Fig. 3.12**). The pooled regressions did, however, slightly overestimate Asx, Glx and Ala D/L values (**Fig. 3.12**).

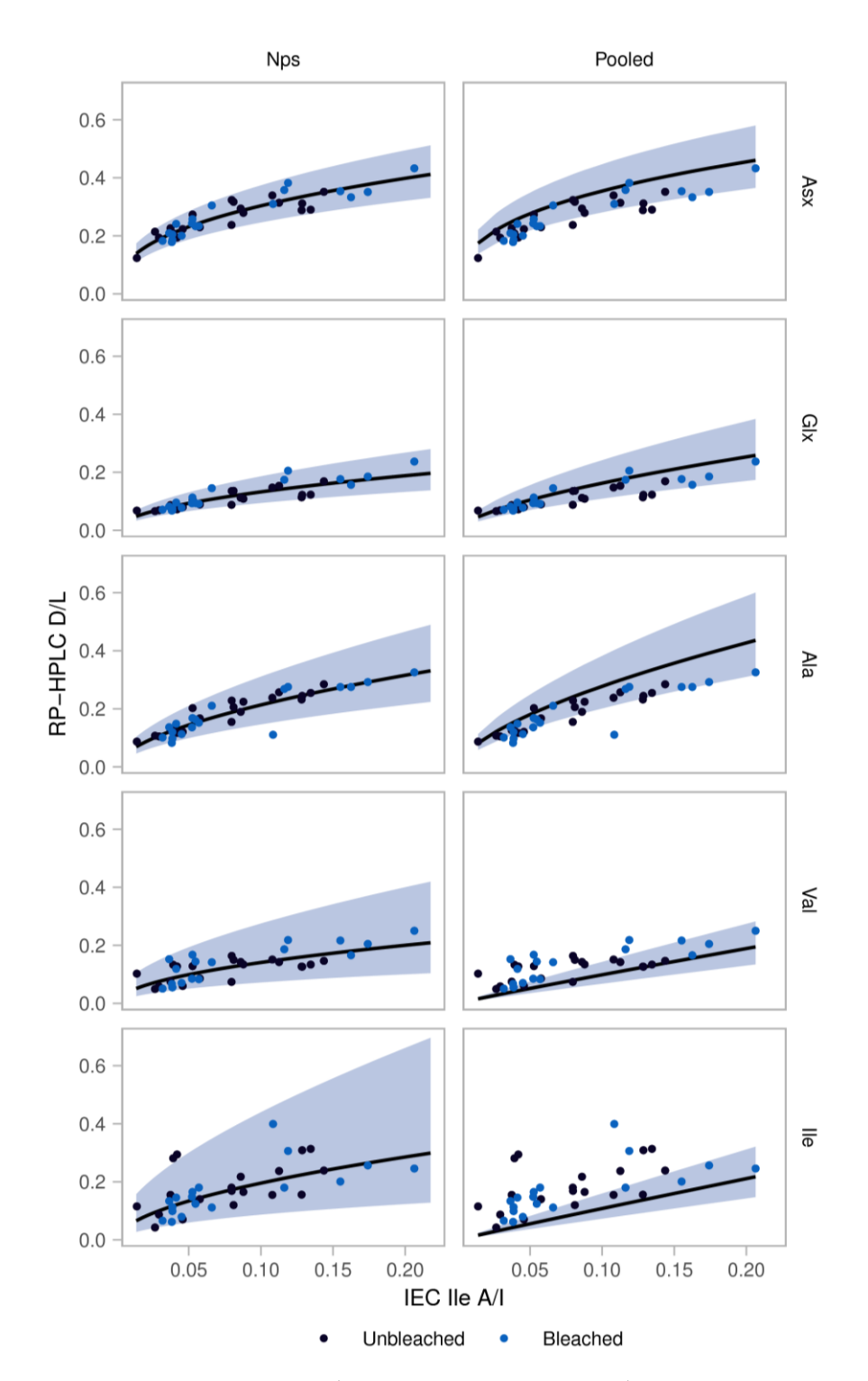


Fig. 3.12 – Relationship between IEC IIe A/I and RP-HPLC amino acid D/L values, modelled by log_2 -transformed linear regressions. Lines represent the Nps-specific and pooled linear regressions; shaded envelopes are 2σ prediction uncertainties using a 'dummy' data set for the Nps-specific regressions (as used by Whitacre et al. (2017)) and the Nps data set for the pooled regressions.

Table 3.2 – Results of linear regressions using \log_2 transformed A/I and D/L values. PU refers to the prediction uncertainty calculated using the Nps data set for the pooled regression, and a 'dummy' data set for the Nps-specific regression (as used by Whitacre et al. (2017)). Success rate refers to the proportion of predicted ranges which included the D/L value measured by RP-HPLC.

	Pooled regression				Nps-specific regression					
	1σ PU	2σ PU	AlCc	Success rate (%)	Slope	Intercept	R ²	1σ PU	2σ PU	AlCc
Asx	0.24	0.24	-239	69	0.41 ± 0.03	-0.35 ± 0.14	0.83	0.23	0.24	-24
Glx	0.41	0.42	126	94	0.51 ± 0.05	-1.22 ± 0.2	0.76	0.36	0.38	3
Ala	0.33	0.33	-16	78	0.59 ± 0.05	-0.21 ± 0.2	0.84	0.33	0.35	-2
Val	0.39	0.40	43	31	0.51 ± 0.10	-1.13 ± 0.4	0.44	0.77	0.82	48
lle	0.41	0.42	59	27	0.49 ± 0.13	-0.82 ± 0.6	0.31	0.98	1.05	57

The results of this analysis show that the Nps-specific regressions can confidently convert Nps IEC A/I values into equivalent D/L values for Asx, Glx and Ala over the ranges tested, with similar prediction uncertainty ranges as for the pooled regressions developed by Whitacre et al. (2017). Due to the poor separation of Val and Ile for Nps it was not possible to validate the regressions for these amino acids. Due to the overestimation of Asx, Glx and Ala D/L values using the pooled regressions and the similar prediction uncertainties between the Nps-specific and pooled regressions, we recommend that the Nps-specific regressions developed in this paper are used to convert Nps A/I values to D/L Asx, Glx and Ala values.

3.4 Conclusions

Bleaching experiments show that Nps tests contain an intra-crystalline fraction of amino acids which is resistant to extended exposure to bleach. A 48 hour treatment with 12% w/v NaOCl isolates the intra-crystalline fraction in Nps, with a greater proportion of amino acids being removed by bleaching in younger samples. Bleaching results in slightly increased Ile, Asx, Glx and Ala D/L values in older samples, indicating that the inter-crystalline fraction of amino acids behaves as an open system during diagenesis. Additionally the variability of D/L values is lower for bleached Nps than unbleached Nps in samples where Asx D/L < ca. 0.2. This suggests that the IcPD approach limits the influences of leaching on racemisation trends for younger Nps, while older material may also benefit from bleaching by minimising the potential impact of contamination.

Given this dataset, it is therefore recommended that a bleaching step is included during the preparation of Nps foraminifera for amino acid dating, if sufficient sample mass is present to

compensate for the reduction in concentrations caused by oxidation of the inter-crystalline fraction.

IEC A/I values were successfully converted to RP-HPLC D/L values for Asx, Glx and Ala in Nps using material-specific regression equations with a ± 24 -38% 2σ prediction uncertainty depending on the amino acid.

Acknowledgements

Funding for this study was provided by the Marie Curie Foundation (to HPS & KP) with additional funding for KP provided by the Leverhulme Trust (PLP-2012-116). This study is part of a project that has received funding from the European Research Council (ERC) under the European Union's Horizon 2020 research and innovation programme (grant agreement No. 865222).

Many thanks to Vigdis Clausen-Hope for technical support, Matthew Kosnik for assistance with linear regression modelling, Natasha Barlow for help with the geological context of the material, to Jo Brendryen for supplying the NISP tie points used in the age model, and to Jo Brendryen and Haflidi Haflidason for additional information about the cores used in this study. The authors are grateful to Kirsty High for her comments on the draft manuscript, and to José Ortiz and an anonymous reviewer for their reviews, which greatly improved the manuscript.

Data Availability: All amino acid data from this study are available through the NOAA repository: ftp://ftp.ncdc.noaa.gov/pub/data/paleo/aar/.

Chapter 4 – Testing the effect of oxidising pre-treatments on amino acids in sub-modern and Pleistocene foraminifera

The oxidation experiments carried out on sub-modern *Ammonia* spp. and *H. germanica* in **Section 4.3** of this chapter form part of the following paper:

Millman, E., Wheeler, L. J., Billups, K., Kaufman. D., Penkman, K. E. H. (2022). Testing the effect of oxidizing pre-treatments on amino acids in benthic and planktic foraminifera tests. *Quaternary Geochronology*, **73**, 101401, https://doi.org/10.1016/j.quageo.2022.101401

The full manuscript can be found in **Appendix 1.** Experiments related to benthic species (*Ammonia* spp. and *H. germanica*), and associated data analysis and interpretation, were carried out by LW. Experiments related to planktic species (*G. truncatulinoides*, *G. tumida* and *P. obliquiloculata*), and associated data analysis and interpretation, were carried out by EM. The manuscript was cowritten by EM and LW, with guidance and insight from KB, DK and KP.

4.1 Introduction

Pre-treatments with NaOCl have successfully isolated an intra-crystalline fraction of amino acids in a range of biominerals (e.g. various molluscs (Penkman et al., 2008, 2011; Demarchi et al., 2013c, 2013b; Ortiz et al., 2015, 2018), corals (Hendy et al., 2012), ostrich eggshell (Crisp et al., 2013) and tooth enamel (Dickinson et al., 2019)), including the planktonic foraminifer *Neogloboquadrina pachyderma* (sinistral) (**Chapter 3**). H_2O_2 is a weaker oxidising agent than NaOCl, and is routinely used in the pre-treatment of foraminifera for AAR to remove contaminant amino acids (Hearty et al., 2004, 2010; Kaufman et al., 2008, 2013; West et al., 2019; Ryan et al., 2020). In experiments carried out on various mollusc species, H_2O_2 was found to be less effective at isolating the intra-crystalline fraction of amino acids than NaOCl (Penkman et al., 2008), while no systematic differences between H_2O_2 or NaOCl pre-treatments were found for sub-fossil ostracodes (Bright and Kaufman, 2011a). Comparisons between H_2O_2 and NaOCl pre-treatments in foraminifera are limited to one preliminary investigation of pre-treatments in *P. obliquiloculata*, which found that a short H_2O_2 pre-treatment reduced D/L variability compared to sonication or short exposures (1-2 hours) to ethanol, methanol or NaOCl (Hearty et al., 2004).

In this chapter, oxidation experiments using NaOCl and H₂O₂ were carried out on three species of foraminifera commonly preserved in Pleistocene sea-level deposits (*Ammonia* spp., *H. germanica* and *E. williamsoni*), to determine whether an intra-crystalline fraction of amino acids can be isolated in these species. Extended oxidation experiments using NaOCl were carried out on *Ammonia* spp., *H. germanica* and *E. williamsoni* taken from surficial salt marsh deposits in the UK; these were carried out alongside high-temperature decomposition experiments on *Ammonia* spp. and *H. germanica* (reported in **Chapter 5**).

The effect of bleaching is less pronounced in older *N. pachyderma* (s) (Section 3.3.2), a pattern which is also seen in other biominerals (Penkman et al., 2008; Bright and Kaufman, 2011a; Dickinson et al., 2019). Oxidation experiments were therefore carried out on *Ammonia* spp. and *H. germanica* taken from a mid-Pleistocene sea-level deposit, in order to investigate the effect of different oxidative pre-treatments in naturally-aged foraminifera. In particular, this suite of experiments focused on whether an oxidative pre-treatment reduced the variability of D/L values between replicates, a pattern which has been observed in many biominerals (e.g. some mollusc species (Sykes et al., 1995; Penkman et al., 2008), ostrich eggshell (Crisp et al., 2013) and enamel (Dickinson et al., 2019)), but not all (e.g. some other mollusc species (Penkman et al., 2008; Ortiz et al., 2017)) and ostracodes (Bright and Kaufman, 2011a)).

4.2 Materials and Methods

4.2.1 Sample collection

Surficial sediment samples (0-5 cm) were collected from tidal flats at the Humber Estuary, Hull, UK (Lat: 53.642, Long: -0.183) and the Ythan Estuary, Aberdeen, UK (Lat: 57.313, Long: -1.995). Large numbers of *Ammonia* spp. and *Haynesina germanica* were found in the Humber Estuary sample, which were used for the oxidation experiments carried out in **Section 4.3** (see **Table 4.1**), as well as the high-temperature experiments detailed in **Chapter 5**. Sufficient numbers of *Elphidium williamsoni* for a shorter suite of oxidation experiments were present in the Ythan Estuary samples, which are also presented in **Section 4.3**. Although these samples were not independently dated, they most likely represent a modern assemblage of foraminifera. However, reworking of the saltmarsh sediment is a possibility (Figueira and Hayward, 2014). Radiocarbon dating of basal peats gives a maximum age of a few thousand years for each site (Long et al., 1998; Smith et al., 1999); therefore the foraminifera are no older than Holocene in age. To reflect the degree of uncertainty in their age, these samples are referred to as 'sub-modern'.

Samples were collected from various horizons from mid-Pleistocene deposits at Northam Pit, Eye Green, Peterborough, UK (Lat: 52.617, Long: -0.184). One sample (NP-1, at 1.9 m OD) was found to have large numbers of *Ammonia* spp. and *H. germanica*, so material from this sample was used for all pre-treatment experiments; *E. williamsoni* was represented only in small numbers at Northam Pit. OSL dating of overlying sediments gives a minimum age of MIS 7 (243-191 ka (Lisiecki and Raymo, 2005)) for these foraminifera (Bateman et al., 2020, p. 15). Additional geological context for this site and the application of AAR to its chronology can be found in **Section 6.2.1**.

4.2.2 Preparation and analysis

30-50 foraminifer tests from the 90-500 μ m fraction (Humber Estuary and Ythan Estuary) or 212-500 μ m fraction (Northam Pit) were used for each sample. For the sub-modern material, pretreatments were carried out using sonication only ('unbleached'), 3% or 30% w/v H₂O₂ (weak oxidising agent) or 12% w/v NaOCl (strong oxidising agent), for a range of durations (**Table 4.1**). Due to limitations in the number of *E. williamsoni* tests, only pre-treatments with NaOCl were carried out. 2 hour pre-treatments with 3% or 30% H₂O₂ or 12% NaOCl were carried out on the Pleistocene material in addition to a sonication-only treatment.

Table 4.1 – Oxidising pre-treatments carried out on sub-modern and Pleistocene *Ammonia* spp., *H. germanica* and *E. williamsoni*. See **Section 4.2.1** above for additional site information.

			Treatment duration (hours)				
Species	Location	Age	Unbleached	3% H ₂ O ₂	30% H ₂ O ₂	12% NaOCI	
Ammonia spp.	<i>mmonia</i> spp. Humber		0	2, 4	4	4, 24, 48,	
	Estuary					96, 192	
	Northam Pit	Pleistocene	0	2	2	2	
H. germanica	Humber	Sub-modern	0	2, 4	4	4, 24, 48,	
	Estuary					96, 192	
	Northam Pit	Pleistocene	0	2	2	2	
E. williamsoni	Ythan	Sub-modern	0	-	-	24, 48, 96,	
	Estuary					192	

Pre-treatment, demineralisation and hydrolysis were carried out according to **Section 2.2** using 20 μ L of the chosen oxidising agent. Unbleached samples were subjected to a second round of sonication (3 x 1 minute, rinsing with 18 m Ω H₂O between each sonication) following crushing of the foraminifer tests, then allowed to air dry overnight before demineralisation. To conserve material, only the total hydrolysable amino acid (THAA) fraction was analysed, as this fraction has higher amino acid concentrations than the free amino acid (FAA) fraction.

Analysis of sub-modern *Ammonia* spp. and *H. germanica* was carried out via RP-HPLC according to **Section 2.4.1**. Analysis of sub-modern *E. williamsoni*, and Pleistocene *Ammonia* spp. and *H. germanica*, was carried out via UHPLC according to **Section 2.4.2**.

4.3 Results of sequential oxidation of sub-modern foraminifera

4.3.1 Amino acid concentration

For all three species studied, treatment with 12% NaOCI results in an up to 90% decrease in the total concentration of amino acids ([THAA]) within at least 4 hours for sub-modern *Ammonia* spp. and *H. germanica*, and at least 24 hours (the first bleaching timepoint used) for *E. williamsoni* (**Fig. 4.1**). This suggests that the residual fraction of amino acids represents intra-crystalline material. The rapid oxidation of inter-crystalline proteins from these species (compared to 48-72 h typically required for other biominerals (e.g. Penkman et al., 2008; Crisp et al., 2013)) likely reflects the thin shell structure of foraminifer tests, as well as their large surface-to-mass ratio enabling rapid penetration of the oxidising agent (e.g. Hearty et al., 2004). The concentration of THAA in *Ammonia* spp. and *E. williamsoni* remains stable up to 192 h, while there appears to be further gradual loss of amino acids after prolonged bleaching (> 96 h) in *H. germanica*, indicating possible etching of the mineral matrix (Penkman et al., 2008; Hendy et al., 2012; Dickinson et al., 2019).

The effect of H_2O_2 on [THAA] (for *Ammonia* spp. and *H. germanica*) depends on the species. In *Ammonia* spp., the variability of [THAA] in the unbleached samples precludes a quantitative comparison of the proportion of amino acids removed by each oxidation pre-treatment. A smaller proportion of amino acids is removed by the 4 h 3% H_2O_2 and 30% H_2O_2 treatments than the 4 h 12% NaOCl treatment. This suggests that H_2O_2 is not a strong enough oxidizing agent to isolate the bleach-resistant intra-crystalline fraction in *Ammonia* spp. within 4 h; longer H_2O_2 pre-treatments were not carried out. Conversely, the 4 h treatments with 3% H_2O_2 , 30% H_2O_2 and 12% NaOCl all remove a similar proportion of amino acids in *H. germanica*. This is similar to the behaviour of ostracodes (Bright and Kaufman, 2011a); by comparison, H_2O_2 is unable to isolate the intracrystalline fraction, even after extended exposure, in various species of mollusc shells (Penkman et al., 2008).

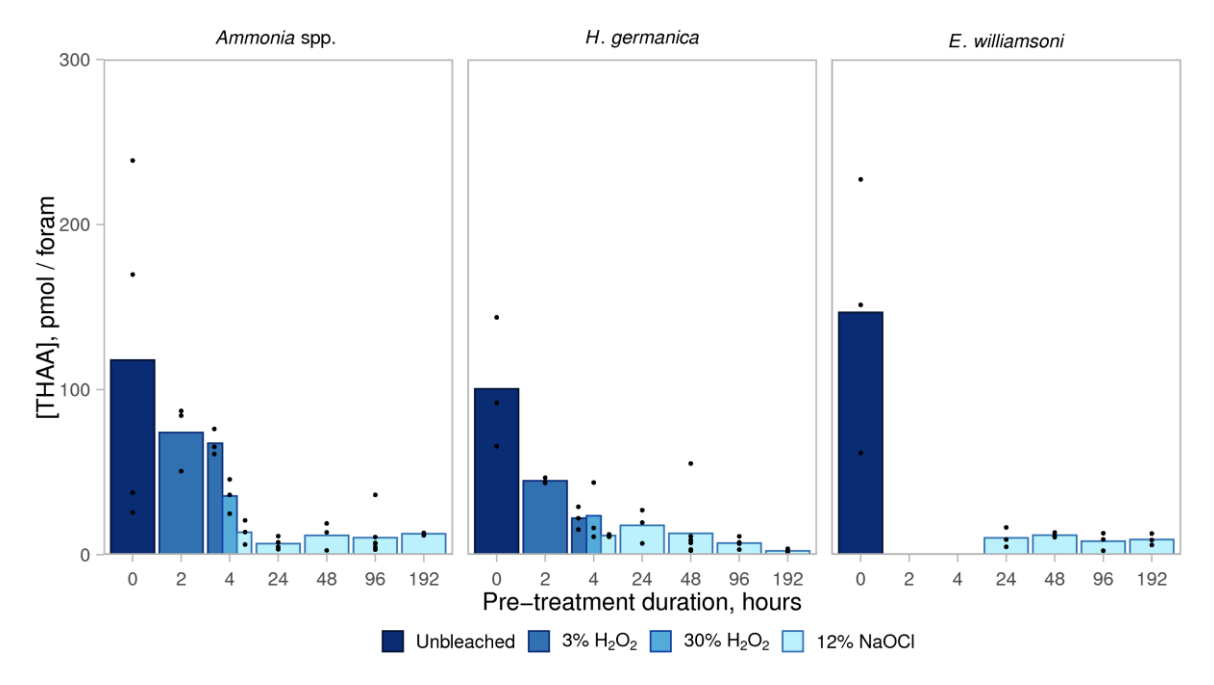


Fig. 4.1 – Concentration of total hydrolysable amino acids ([THAA]) in unbleached (H₂O sonication only) and oxidized (H₂O₂ or NaOCl) samples of sub-modern *Ammonia* spp., *H. germanica* and *E. williamsoni*. Weak oxidation (H₂O₂) experiments were not carried out for *E. williamsoni*. Dots show individual replicates; bars show means of all replicates.

4.3.2 Amino acid composition

The relative proportion of nine amino acids best resolved by RP-HPLC and UHPLC is shown for submodern *Ammonia* spp., *H. germanica* and *E. williamsoni* over the course of prolonged exposure to NaOCI (Fig. 4.2). The composition of the three species is dominated by Asx and Gly, with lesser contributions from Glx, Ser, Val, Leu and Ile. Ala contributes a similar proportion of amino acids to this second group in *Ammonia* spp. and *H. germanica*; the apparently lower proportion of Ala in *E. williamsoni* is due to its poorer separation using UHPLC (see Section 2.4.2). Overall, the composition of all three species is similar to *N. pachyderma* (s) (Section 3.3.1.2) and some other species of foraminifera (King and Hare, 1972b; Weiner and Erez, 1984; Robbins and Brew, 1990), although for the species investigated by Millman et al. (2022) (*G. truncatulinoides*, *G. tumida* and *P. obliquiloculata*) the proportion of Gly is much lower and Ala much higher than *Ammonia* spp., *H. germanica* and *E. williamsoni*.

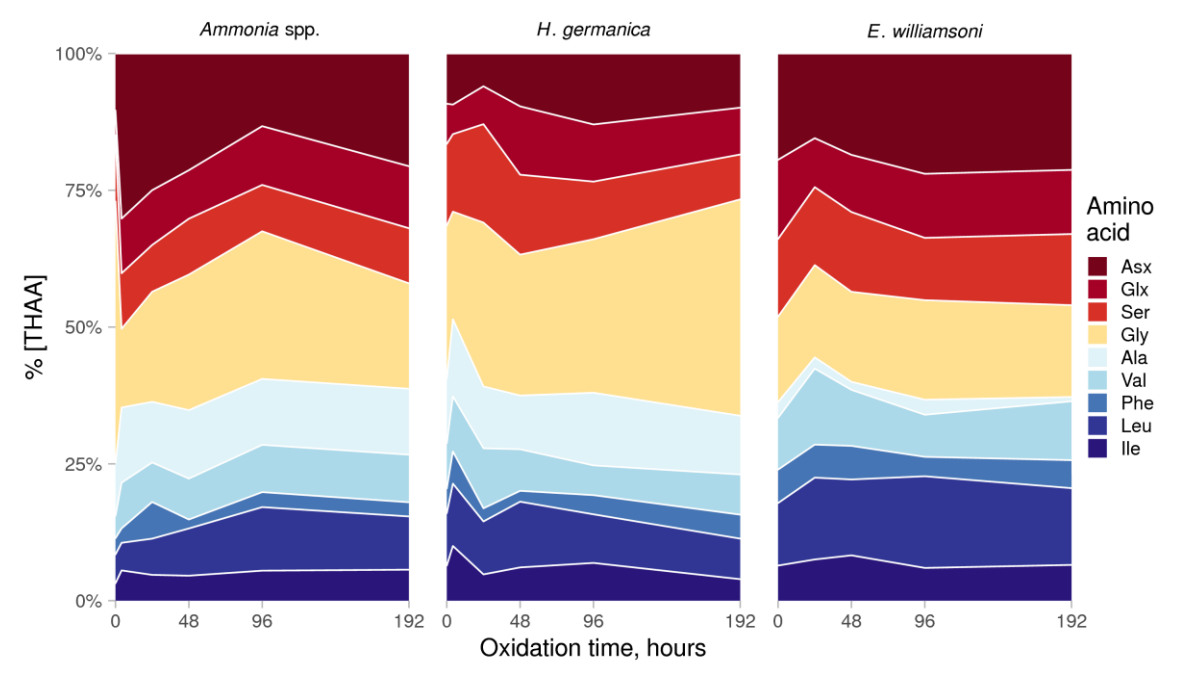


Fig. 4.2 — Relative proportion of well-resolved amino acids (% [THAA]) in sub-modern *Ammonia* spp., *H. germanica* and *E. williamsoni* over the course of extended exposure to 12% w/v NaOCl. Amino acids are shown in order of elution. The *E. williamsoni* samples were analysed using UHPLC, which resolves amino acids somewhat differently to RP-HPLC (see **Section 2.4**); therefore its composition is not directly comparable to *Ammonia* spp. or *H. germanica*. Poorly resolved amino acids (Thr, His, Arg and Met) have been excluded.

The effect of oxidation time on the composition of the three species is somewhat inconsistent. For *Ammonia* spp., after a rapid decrease in % Gly between 0-4 h of NaOCl exposure, % Asx decreases and % Gly increases between 4-96 h, followed by a slight reversal of this trend between 96 and 192 h. *H. germanica* shows a general trend of increasing % Gly over time, with % Asx, Glx and Ser decreasing somewhat, and the hydrophobic (later-eluting) amino acids Ala, Val, Phe, Leu and Ile having little change in % [THAA] over time. With the exception of a higher % Val and lower %Asx at 24 h, there is little change in composition over time for *E. williamsoni*. These results are likely due, at least in part, to the between-replicate variability of composition, illustrated for Asx and Gly in Fig. 4.3 (see Appendix 2 for the % contribution of Glx, Ser, Phe and Ile to [THAA]). To understand whether the differences in composition change with NaOCl exposure genuinely differ between the species, a larger number of replicates for each time point would be required.

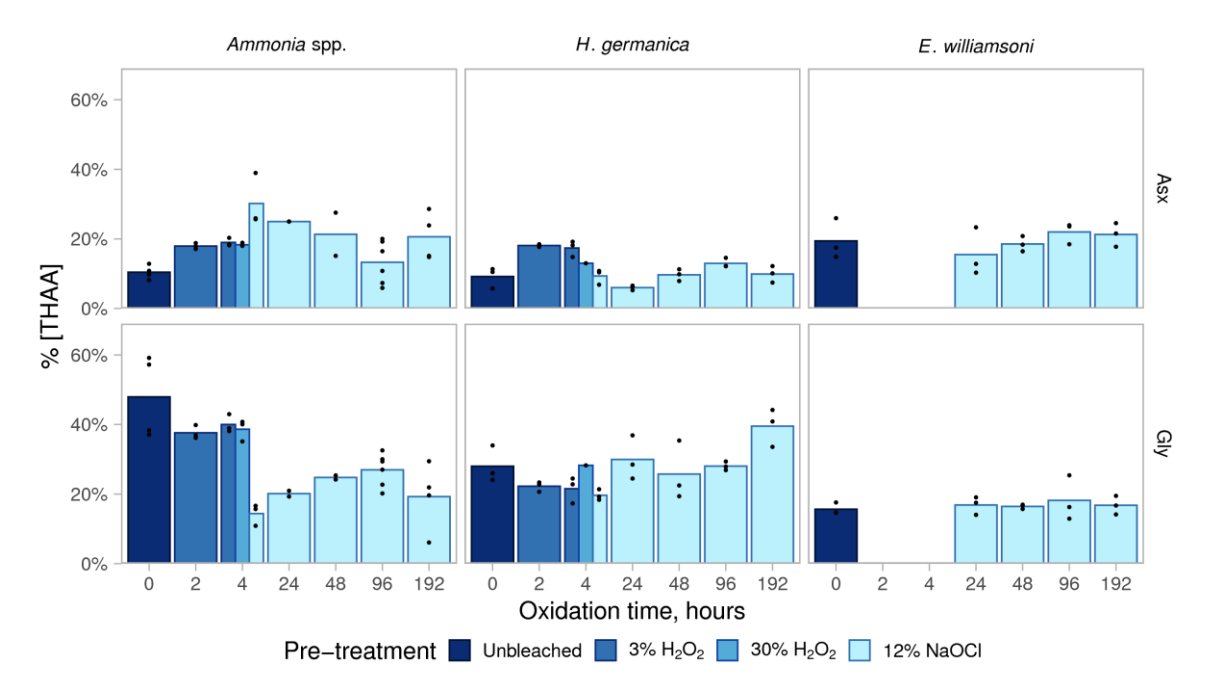


Fig. 4.3 – Proportion of Asx and Gly in unbleached (H_2O sonication only) and oxidized (H_2O_2 or NaOCl) samples of sub-modern *Ammonia* spp., *H. germanica* and *E. williamsoni*. Weak oxidation (H_2O_2) experiments were not carried out for *E. williamsoni*. Error bars show ± 1 standard deviation (σ). Dots show individual replicates; bars show means of all replicates. The corresponding proportion of Glx, Ser, Phe and Ile is given in **Appendix 2**.

Fig. 4.4 shows the effect of oxidising agent strength on *Ammonia* spp. and *H. germanica* samples subjected to a 4 h pre-treatment (these experiments were not carried out on *E. williamsoni* due to limited material). For *Ammonia* spp., increasing the strength of the oxidising agent increases % Asx, Glx and Ala, and decreases % Gly; when treated with 12% NaOCl, the composition is more similar to naturally-aged (sub-fossil) material compared to weaker oxidative pre-treatments (see Section 4.4.2). By contrast, there is relatively little difference between pre-treatments in naturally-aged *Ammonia* spp. and *H. germanica*, *N. pachyderma* (s) (Section 3.3.1.2), or various species of planktic foraminifera (Millman et al., 2022). The pattern for *H. germanica* differs to *Ammonia* spp. Samples treated with 3% and 30% H₂O₂ have a lower % Ala and higher % Asx than the unbleached samples, but the samples treated with 12% NaOCl have a more similar composition to the unbleached samples. This may be due to the large inter-replicate variability of composition, especially for Asx and Gly (Fig. 4.3).

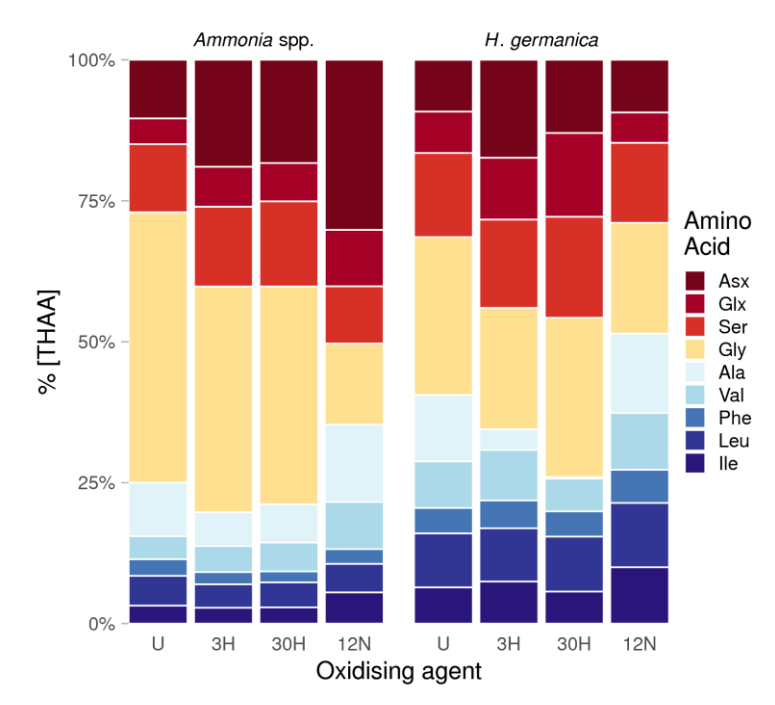


Fig. 4.4 – Relative proportion of amino acids (% [THAA]) in sub-modern *Ammonia* spp. and *H. germanica* treated with an oxidising agent for 4 hours. Four different pre-treatments were used: Sonication only (unbleached, U), 4 h 3% H_2O_2 (3H), 4 h 30% H_2O_2 (30H), and 4 h 12% NaOCI (12N).

4.3.3 Effect of oxidation on D/L values

Fig. 4.5 shows the D/L values of Asx, Glx, Ser, Phe and Ile for *Ammonia* spp., *H. germanica* and *E. williamsoni*, with increasing strength or duration of oxidising pre-treatment. For all three species, relatively few samples had measurable Phe or Ile D/L values, especially in the oxidised samples; this is likely due to low concentrations of D-Phe and D-Ile, which are more challenging to quantify than earlier-eluting D-Asx and D-Glx (see **Section 2.4**).

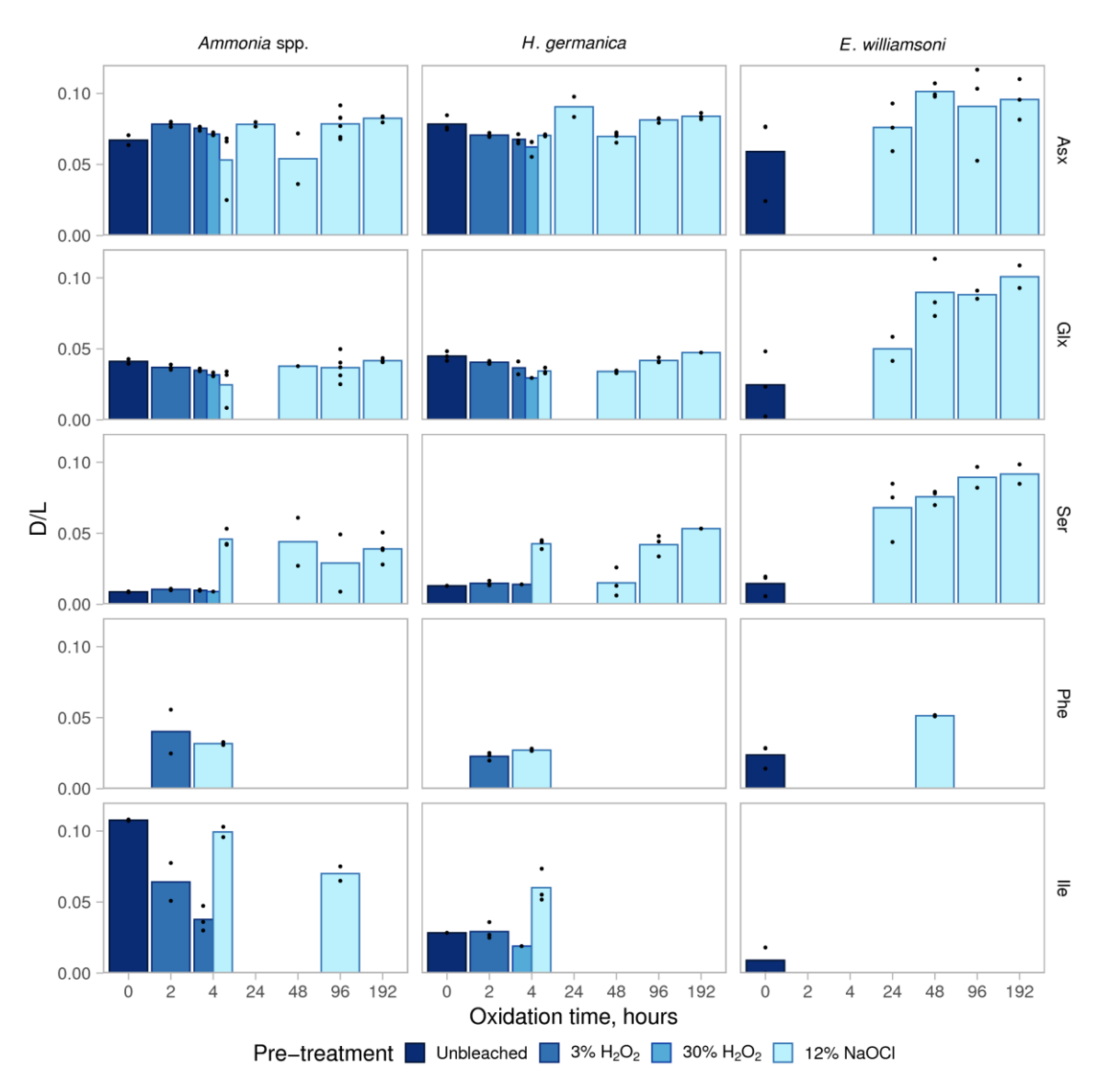


Fig. 4.5 – Asx, Glx, Ser, Phe and Ile THAA D/L in *Ammonia* spp., *H. germanica* and *E. williamsoni* treated with various oxidising agents. Weak oxidation (H_2O_2) experiments were not carried out for *E. williamsoni*; otherwise where bars are missing, it is because the respective D-amino acid was not detected in any of the samples at that time point. Dots show individual replicates; bars show means of all replicates.

In *H. germanica*, there may be a slight decrease in Asx and Glx D/L values between the sonication-only samples and samples subjected to short oxidation times (2-4 h), followed by a slight trend of increasing D/L between 4 and 192 h of bleach exposure. This pattern has been observed in other biominerals (various mollusc shells (Penkman et al., 2008), ostracodes (Bright and Kaufman, 2011a) and corals (Hendy et al., 2012)), and could indicate a catalytic effect of NaOCl on racemization following the initial removal of inter-crystalline amino acids. This, combined with the slight decrease in amino acid concentration in *H. germanica* after 92 h, suggests that the fraction of

amino acids isolated by the initial bleach exposure may not be completely resistant to chemical influences. However, given the small number of replicate analyses (n = 3-4), and relatively large overall variability in D/L values, this observation should be treated with caution.

Treatment of *E. williamsoni* with NaOCl results in an initial increase in Asx, Glx and Ser D/L, with the D/L values of Glx and Ser continuing to increase with increasing duration of NaOCl exposure. This suggests that the intra-crystalline fraction of *E. williamsoni* may not be oxidation resistant over extended timescales, with NaOCl penetrating the biomineral structure to catalyse racemisation of intra-crystalline amino acids.

4.3.4 Discussion

The oxidation experiments on sub-modern foraminifera show that NaOCl effectively removes intercrystalline proteins for all three species (Ammonia spp., H. germanica and E. williamsoni), with extended exposure to NaOCl resulting in slight further reductions in [THAA] for H. germanica. In comparison, H_2O_2 moderately reduces [THAA] in Ammonia spp. and H. germanica, depending on the concentration of H_2O_2 used and the length of the oxidative pre-treatment. The effect of increasing pre-treatment strength and duration on composition are somewhat inconsistent, with no clear patterns across the three species investigated.

The effect of pre-treatment strength and duration on D/L values was also species dependent. Samples treated with NaOCl had higher Ser D/L values than than unbleached or H_2O_2 -treated samples for both *Ammonia* spp. and *H. germanica*, while extended NaOCl exposure resulted in increasing D/L values for some amino acids in *H. germanica* and *E. williamsoni*. These results suggest that weak oxidising pre-treatments (3% or 30% H_2O_2) are somewhat less effective at removing exogenous or inter-crystalline amino acids than strong oxidising pre-treatments (12% NaOCl), and that at least some species of foraminifera may not have an intra-crystalline fraction which is resistant to prolonged exposure to NaOCl.

4.4 Results of oxidation experiments carried out on mid-Pleistocene foraminifera

Bleaching experiments carried out on *N. pachyderma* (s) (Section 3.3.1) and *P. obliquiloculata*, *G. truncatulinoides*, and *G. tumida* (Millman et al., 2022) have found that the effects of oxidation with NaOCl were more pronounced in younger material, a pattern that has also been observed in other biominerals (e.g. various molluscs (Penkman et al., 2008; Ortiz et al., 2015, 2017, 2019), ostracodes

(Bright and Kaufman, 2011a) and enamel (Dickinson et al., 2019)). A range of oxidising pretreatments were therefore carried out on mid-Pleistocene *Ammonia* spp. and *H. germanica* to investigate whether the patterns seen in sub-modern foraminifera are also seen in naturally-aged material.

Between-replicate variability was a key issue with the results of the sub-modern experiments. A larger number of replicates was therefore analysed in this suite of experiments (10 per pretreatment) to enable statistical analysis (ANOVA (analysis of variance) and two-way Tukey post-hoc analysis) of the effects of oxidative pre-treatments on naturally-aged foraminifera. Four pretreatments were investigated: sonication only ('unbleached') and oxidative pre-treatment with either 3% H₂O₂, 30% H₂O₂, or 12% NaOCl (**Table 4.1**). To limit the number of independent variables, and for comparison with oxidative pre-treatments commonly used for foraminifer AAR (Hearty et al., 2004, 2010; Kaufman et al., 2008, 2013; West et al., 2019; Ryan et al., 2020), a 2 hour duration was chosen for all oxidative pre-treatments in this suite of experiments.

4.4.1 Amino acid concentration

The [THAA] of naturally-aged Ammonia spp. and H. germanica for each of the four pre-treatments is shown in Fig. 4.6. The unbleached (sonication only) samples have substantially lower [THAA] than unbleached sub-modern samples, consistent with a loss of inter-crystalline protein during diagenesis. The lower [THAA] in H. germanica compared to Ammonia spp. is most likely due to the smaller (on average) size of H. germanica tests in the Northam Pit sample (note that as the samples were too small to be weighed accurately, concentration is reported in pmol / foram). Every oxidative pre-treatment decreased [THAA] in Ammonia spp. compared to the unbleached samples; increasing the strength of the oxidising agent (from 3% H₂O₂ to 12% NaOCl) did not lead to a further decrease in concentration, in contrast to sub-modern material (Section 4.3.1). The concentrations of H. germanica subjected to oxidative pre-treatment are essentially the same as the unbleached samples. This suggests that the majority of the inter-crystalline proteins are lost during diagenesis, as has been observed in other biominerals (e.g. Bright and Kaufman, 2011a; Kosnik et al., 2017; Ortiz et al., 2017, 2018; Dickinson et al., 2019), although not in the foraminifer P. obliquiloculata, which showed little change in concentration between ca. 2-300 ka (Hearty et al., 2004). This may indicate differences in behaviour between different foraminifer species, or that inter-crystalline protein loss occurs very rapidly (within the first few ka of diagenesis) in this biomineral class. In contrast to the sub-modern Ammonia spp. and H. germanica, a weak oxidative

pre-treatment (3% H_2O_2) was sufficient to remove the remaining inter-crystalline amino acids in this naturally-aged material.

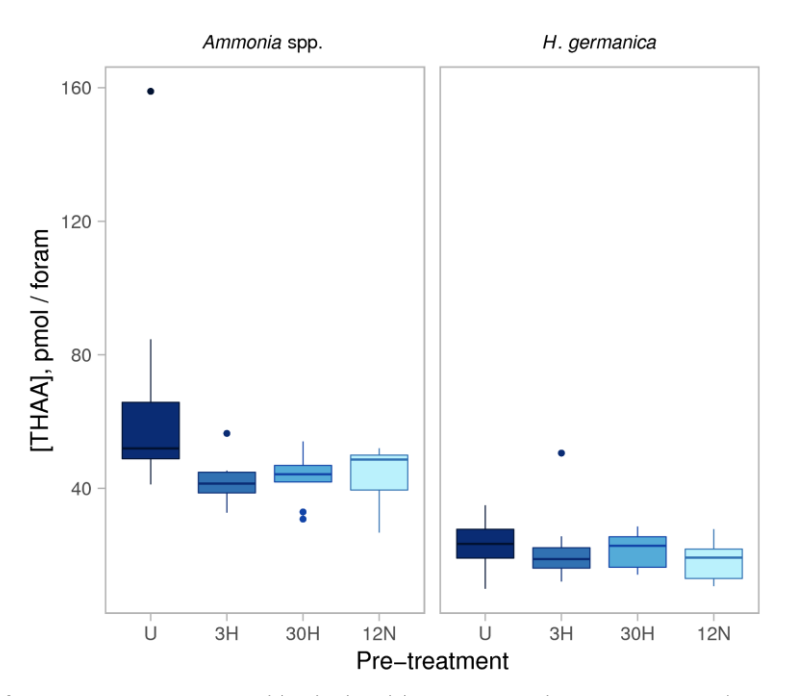


Fig. 4.6 – Effect of pre-treatment on total hydrolysable amino acid concentration ([THAA]) in Pleistocene Ammonia spp. and H. germanica (n = 10 for each pre-treatment). Boxes show the median and the first and third quartiles; the whiskers extend to the minimum and maximum values, with samples beyond 1.5 times the interquartile range treated as outliers (points). U: unbleached (sonication only); 3H: 3% H_2O_2 ; 30H: 30% H_2O_2 ; 12N: 12% NaOCl. All oxidative pre-treatments had a duration of 2 hours.

4.4.2 Amino acid composition

The average composition of mid-Pleistocene *Ammonia* spp. and *H. germanica* subjected to each pre-treatment is shown in **Fig. 4.7**; the inter-sample variability in the proportion of several key amino acids is shown in **Fig. 4.8**. The proportion of Ser is lower in the Pleistocene than sub-modern samples, due to its relative instability (Vallentyne, 1964; Sato et al., 2004). A decrease in % Ser has also been observed in high-temperature decomposition experiments of some biominerals (e.g. Demarchi et al., 2013b; Ortiz et al., 2017, 2019). The proportion of Gly is also substantially lower in the Pleistocene material, around 20% of [THAA] compared to around 40% in the sub-modern material. This is similar to a loss of Ser and Gly over ka timescales observed in the foraminiferal fraction of marine sediments, while other amino acids remain stable (Bada and Man, 1980).

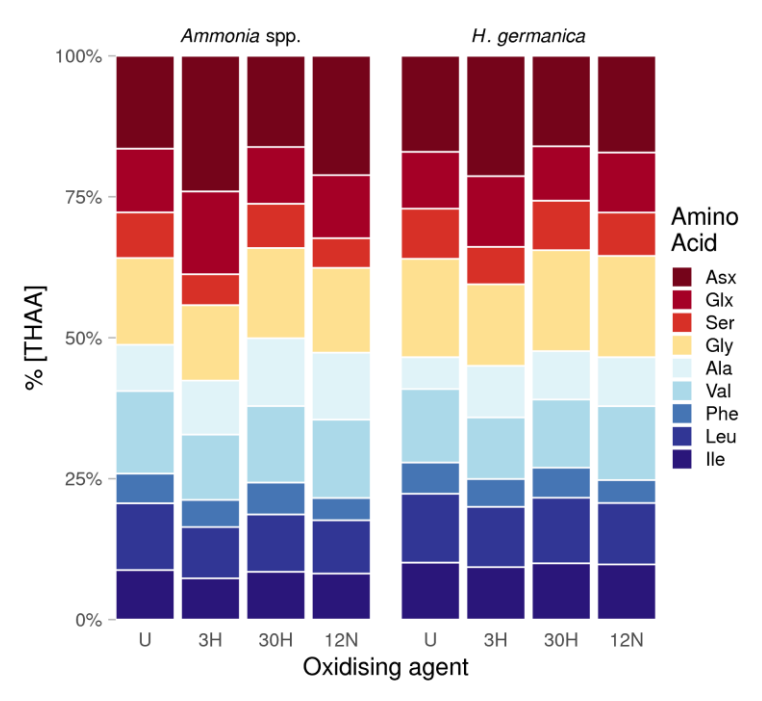


Fig. 4.7 – The effect of pre-treatment on the relative proportion of amino acids (% [THAA]) in Pleistocene *Ammonia s*pp. and *H. germanica*. U: unbleached (sonication only); 3H: 3% H_2O_2 ; 30H: 30% H_2O_2 ; 12N: 12% NaOCl. All oxidative pre-treatments had a duration of 2 hours.

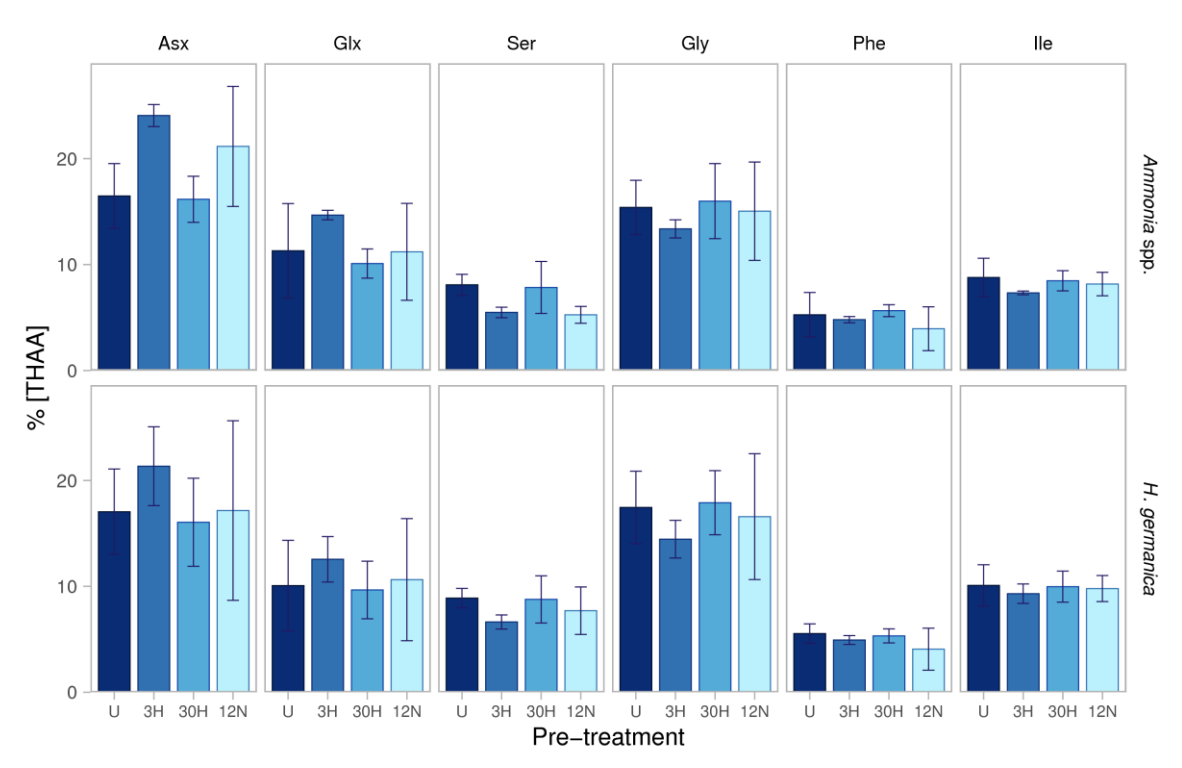


Fig. 4.8 – Variability of the relative proportion of amino acids (% [THAA]) for Asx, Glx, Ser, Gly, Phe and lle with each pre-treatment for Pleistocene *Ammonia* spp. and *H. germanica*. Error bars represent $\pm 1~\sigma$ around the average % composition. U: unbleached (sonication only); 3H: 3% H_2O_2 ; 30H: 30% H_2O_2 ; 12N: 12% NaOCl. All oxidative pre-treatments had a duration of 2 hours.

Increasing the strength of the oxidising agent does not substantially affect the composition of Pleistocene *Ammonia* spp. and *H. germanica*, at least within the 2 hour pre-treatment time used in this suite of experiments. Although the results of the sub-modern and Pleistocene oxidation experiments are not directly comparable due to differences in the pre-treatment duration, this, along with the smaller differences in concentration between unbleached and oxidised samples in the Pleistocene material (Section 4.4.1), suggests that the majority of inter-crystalline amino acids are lost from *Ammonia* spp. and *H. germanica* during burial diagenesis. This corroborates the patterns observed in planktonic foraminifera (Chapter 3, Millman et al., 2022) and other biominerals (e.g. Sykes et al., 1995; Penkman et al., 2008; Ortiz et al., 2015).

4.4.3 Effect of oxidative pre-treatments on D/L values

A key advantage of analysing only the intra-crystalline protein fraction for AAR is the lower intersample variability of D/L values in comparison to the whole-shell fraction, which is observed in many biominerals (e.g. Sykes et al., 1995; Penkman et al., 2008; Crisp et al., 2013; Dickinson et al., 2019), but not all (e.g. Penkman et al., 2008; Bright and Kaufman, 2011a; Ortiz et al., 2017). Experiments on naturally-aged N. pachyderma (s) showed modest reductions in variability between unbleached samples and samples treated with NaOCl for younger material (Section 3.3.2); likewise comparisons between H_2O_2 and NaOCl pre-treatments gave equivocal results for mid-Pleistocene to late-Holocene G. truncatulinoides, G. tumida, and P. obliquiloculata (Millman et al., 2022).

The effect of pre-treatment on the D/L values of Asx, Glx, Ser, Phe and Ile are shown in **Fig. 4.9**. For all five amino acids, an oxidative pre-treatment resulted in an increase in D/L values, with the effect being most pronounced for Ser. This is similar to the patterns seen in sub-modern material (**Section 4.3**). This indicates that an oxidising agent removes exogenous amino acids which are not removed by the sonication-only (unbleached) treatment. The substantial increase in Ser D/L, especially for *Ammonia* spp., may be due to L-Ser's high abundance in modern (laboratory) contamination (see **Section 5.3.1.1**).

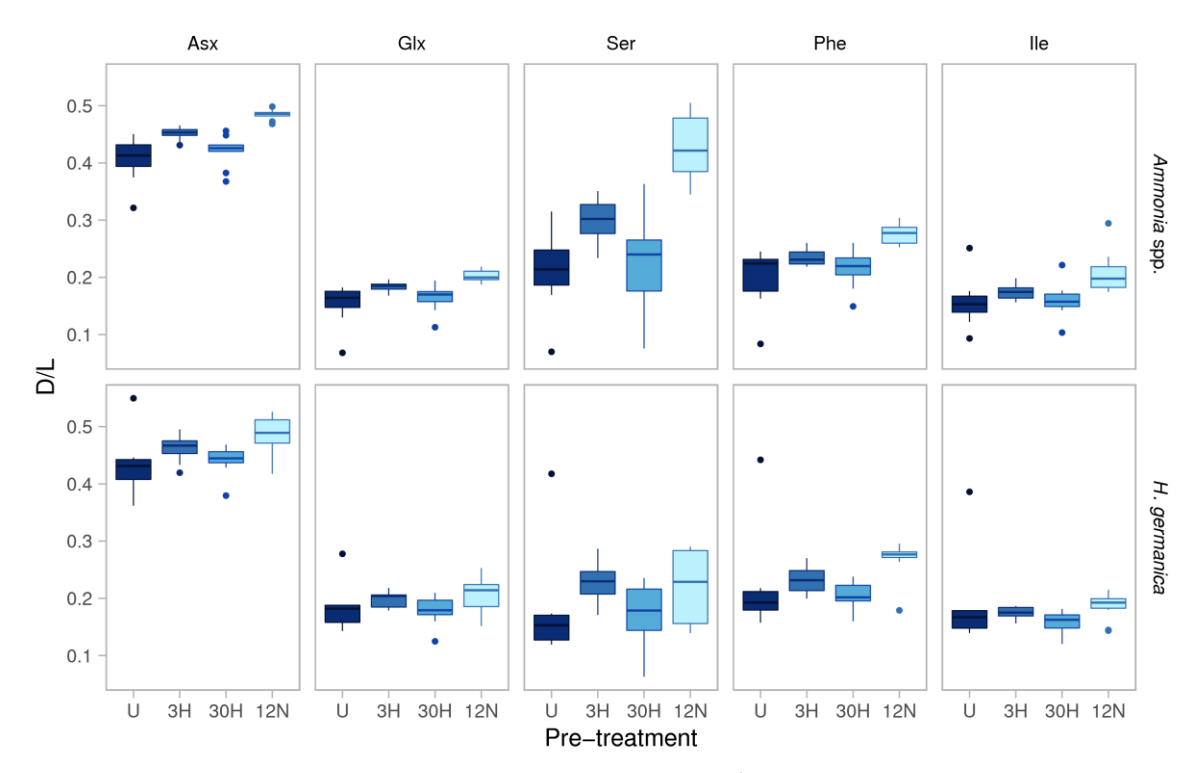


Fig. 4.9 – Effect of pre-treatment on Asx, Glx, Ser, Phe and Ile D/L of Pleistocene H. germanica and Ammonia spp. (n = 10 for each pre-treatment). Boxes show the median and the first and third quartiles; the whiskers extend to the minimum and maximum values, with samples beyond 1.5 times the interquartile range treated as outliers (points). U: unbleached (sonication only); 3H: 3% H_2O_2 ; 30H: 30% H_2O_2 ; 12N: 12% NaOCl. All oxidative pre-treatments had a duration of 2 hours.

To determine whether the differences in D/L values between each pre-treatment are statistically significant, a two-way ANOVA (analysis of variance) was carried out for each species using the D/L values of Asx, Glx, Ser, Phe and Ile. This technique compares the means of sample groups where there are two independent variables (in this case amino acid and pre-treatment). A statistically significant (p < 0.05) effect of treatment on D/L value was found for both species (**Table 4.2**). Following this result, a two-way Tukey post-hoc analysis was used to determine the significance of differences between each pair of pre-treatments (**Table 4.3**). A positive difference between means indicates that the lefthand treatment in the comparison (see table) has a significantly higher mean value than the righthand treatment; a negative difference indicates that the lefthand treatment has a significantly lower mean value than the righthand treatment. If the difference between means passes through 0, the difference between the groups is not statistically significant.

Table 4.2 – Results of two-way ANOVA for Pleistocene *Ammonia* spp. and *H. germanica*. A *p*-value of < 0.05 indicates a statistically significant result (highlighted in green). A statistically significant interaction (between pre-treatment and amino acid) shows that the effect of the pre-treatment differs between amino acids.

	Degrees of freedom	Ammo	nia spp.	H. germanica		
		F value	<i>p</i> -value	F value	<i>p</i> -value	
Pre-treatment	3	56.5	< 0.001	7.4	< 0.001	
Amino acid	4	309	< 0.001	229	< 0.001	
Interaction	12	6.7	< 0.001	0.6	0.78	

Table 4.3 – Results of two-way Tukey post-hoc analysis for Pleistocene *Ammonia* spp. and *H. germanica*. An adjusted p-value of < 0.05 indicates a statistically significant difference between the two pretreatments (highlighted in green). U: unbleached (sonication only); 3H: 3% H_2O_2 ; 30H: 30% H_2O_2 ; 12N: 12% NaOCI.

Comparison between		Ammonia	spp.	H. germanica			
treatments		Difference	Adjusted	Difference between	Adjusted		
Lefthand Righthand		between means p-value		means	<i>p</i> -value		
3H	U	0.04 to 0.02	< 0.001	0.01 to -0.02	0.72		
30H	U	0.01 to -0.01	0.45	-0.04 to 0.01	0.39		
12N	U	0.10 to 0.07	< 0.001	0.02 to 0.00	0.10		
12N	3H	0.05 to 0.03	< 0.001	0.01 to -0.01	0.050		
12N	30H	0.08 to 0.06	< 0.001	0.04 to 0.02	< 0.001		
30H	3H	-0.03 to -0.05	< 0.001	-0.03 to -0.05	0.016		

The results of this analysis show that for *Ammonia* spp., increasing the strength of the oxidising agent generally speaking increases the D/L value (with the exception of 30% H_2O_2 , which is not significantly different from unbleached and has lower D/L values than the 3% H_2O_2 treatment).

For H. germanica, there is less of a difference between the oxidative pre-treatments – the 12% NaOCl pre-treatment results in higher D/L values only when compared to the 30% H_2O_2 pre-treatment, while the 30% H_2O_2 pre-treatment results in lower D/L values than the 3% H_2O_2 pre-treatment. This is in contrast to a general trend of increasing D/L values with increasing oxidation strength and/or duration, in both sub-modern *Ammonia* spp. and *H*. germanica (Section 4.3.3), and other biominerals (Penkman et al., 2008; Bright and Kaufman, 2011a; Hendy et al., 2012; Crisp et al., 2013; Ortiz et al., 2017). A slight decrease in D/L followed by a subsequent increase over prolonged NaOCl exposure has been observed in some mollusc species (Penkman et al., 2008), thought to be due to the initial removal of highly racemised inter-crystalline FAA, followed by an increase in D/L due to the removal of inter-crystalline THAA (thus increasing the proportional effect of intra-crystalline FAA on the D/L value of the THAA fraction). It is possible that a similar mechanism is taking place here, with the initial increase in D/L between the sonication-only and 3% H_2O_2 treatments perhaps being a result of removal of exogenous amino acids, but given that this

pattern is only significant in *Ammonia* spp. and not observed in the sub-modern material, and that the differences in D/L are very small (\sim 0.03 units), this should be treated as speculative only, and may simply be due to chance.

An oxidising pre-treatment reduces the coefficient of variance (standard deviation divided by mean, CoV) for all five amino acids compared to the sonication-only pre-treatment (**Fig. 4.10**). This is consistent with comparisons between unbleached samples and samples treated with 3% H₂O₂ in *P. obliquiloculata* (Hearty et al., 2004). The difference between weak and strong oxidation pre-treatments is limited, with the 12% NaOCl pre-treatment having a higher CoV than the H₂O₂ treatments for several amino acids, a pattern also seen in comparisons between NaOCl and H₂O₂-treated foraminifera (Millman et al., 2022).

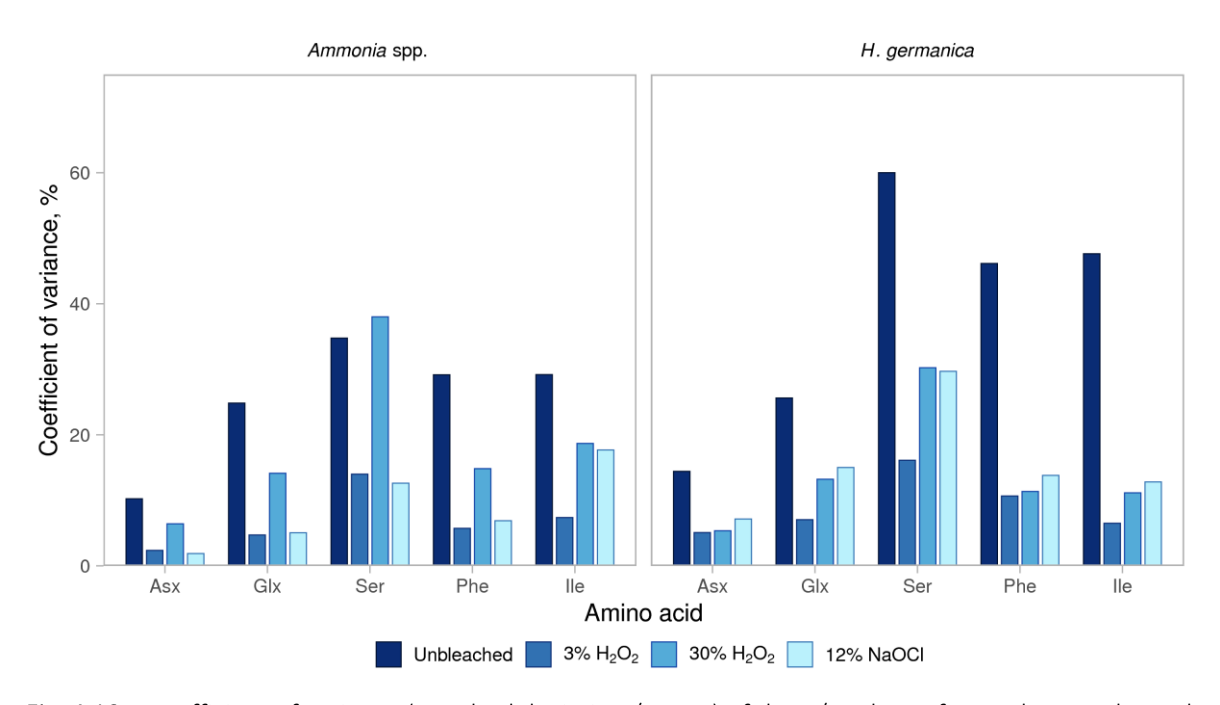


Fig. 4.10 – Coefficient of variance (standard deviation / mean) of the D/L values of Asx, Glx, Ser, Phe and Ile of mid-Pleistocene *Ammonia* spp. and *H. germanica*, subjected to a range of pre-treatments (n = 10 for each pre-treatment).

4.4.4 Discussion

In contrast to the pre-treatment experiments carried out on sub-modern material, the difference in amino acid concentration between unbleached and oxidised material was limited in Pleistocene *Ammonia* spp. and *H. germanica*, with all three oxidising pre-treatments ($3\% H_2O_2$, $30\% H_2O_2$ and 12% NaOCl) removing a similar, small, proportion of amino acids from the whole-shell fraction. This is consistent with a loss of inter-crystalline proteins during natural diagenesis, and likely also explains the similar compositions between the four pre-treatments. The loss of intra-crystalline

proteins during diagenesis has been observed in other species of foraminifera (**Chapter 3**, Millman et al., 2022), as well as other biominerals (e.g. Penkman et al., 2008; Bright and Kaufman, 2011a; Dickinson et al., 2019).

Increasing the strength of oxidising agent increased D/L values slightly for both species, with Ser D/L showing the largest effect, perhaps due to the removal of L-Ser, a common modern contaminant, by the oxidative pre-treatment. The effect of oxidation on *Ammonia* spp. was more pronounced than for *H. germanica*. The variability of D/L values was also reduced by an oxidative pre-treatment for all amino acids investigated (Asx, Glx, Ser, Phe and IIe), with the 3% H_2O_2 treatment having the lowest coefficient of variance for both species. The modest differences between the pre-treatments in Pleistocene material demonstrate that the behaviour of unbleached (whole-shell) modern and naturally-aged material can differ substantially due to the loss of inter-crystalline amino acids during diagenesis. The use of a stronger oxidising agent does not result in consistent reductions in D/L variability for either species, a result also found in comparisons between H_2O_2 and NaOCI pre-treatments of naturally-aged *P. obliquiloculata*, *G. truncatulinoides*, and *G. tumida* (Millman et al., 2022).

4.5 Conclusions

Overall, these results show that a large proportion of amino acids in sub-modern *Ammonia* spp., *H. germanica* and *E. williamsoni* are inter-crystalline, most of which are, at least for *Ammonia* spp. and *H. germanica*, lost during natural diagenesis. The remaining intra-crystalline fraction appears to be somewhat susceptible to prolonged exposure to NaOCl in *H. germanica* and *E. williamsoni*, and may not represent a closed system for these species. Increasing oxidation strength or duration increases D/L values for both sub-modern and naturally-aged material; in naturally-aged *Ammonia* spp. and *H. germanica* an oxidative pre-treatment also reduces the variability of D/L values for both species when compared to a sonication-only pre-treatment.

Unlike in molluscs (Penkman et al., 2008), the differences between weak and strong oxidising agents are limited. The 3% H_2O_2 pre-treatment has the lowest coefficient of variance of the three oxidative pre-treatments investigated here. This is consistent with findings for various planktonic species of foraminifera, which found that 3% H_2O_2 either reduced D/L variability compared to other pre-treatments (Hearty et al., 2004), or minimal differences in D/L values and variability between 3% H_2O_2 and stronger oxidising pre-treatments (Millman et al., 2022). As the use of a stronger oxidising agent (30% H_2O_2 or 12% NaOCl) does not result in consistent improvements in variability

for any of the species investigated, this suite of experiments corroborates the recommendation of a 2 hour 3% H_2O_2 pre-treatment, which additionally has the benefit of already being the most widely used oxidative pre-treatment for foraminifera (e.g. Hearty et al., 2004, 2010; Kaufman et al., 2008, 2013; Ryan et al., 2020).

Chapter 5 – Patterns of decomposition in *Ammonia* spp. and *H. germanica* at high temperatures

5.1 Introduction

In the absence of well-dated sequences of naturally-aged fossil material, high-temperature decomposition experiments have been used extensively in AAR studies to approximate the natural diagenesis of proteins in various fossil biominerals, including foraminifera (e.g. Wehmiller and Hare, 1971; Bada and Schroeder, 1972; Mitterer and Kriausakul, 1989; Sejrup and Haugen, 1992; Kaufman, 2006). This enables direct comparisons of the patterns of decomposition between different amino acids and species (e.g. Sejrup and Haugen, 1992; Kaufman et al., 2013). High-temperature experiments can also be used to assess the closed-system behaviour of the biomineral during decomposition, or to estimate kinetic parameters for racemisation and other reactions. The use of high-temperature experiments to investigate the patterns of biomineral protein decomposition, and the limitations of this approach, are summarised below in **Sections 5.1.1** and **5.1.2**.

In this chapter, the patterns of decomposition of sub-modern *Ammonia* spp. and *H. germanica* are investigated with the aim of answering the following questions:

- 1. Does isolating the intra-crystalline fraction of proteins reduce leaching (diffusive loss) of amino acids from the biomineral compared to the whole-shell fraction?
- 2. Do amino acids in *Ammonia* spp. and *H. germanica* undergo consistent patterns of decomposition, and if so which amino acids show the most reliable trends in racemisation, and would therefore provide the best chronological information in naturally-aged samples?
- 3. Does isolating the intra-crystalline fraction of proteins improve the reliability of racemisation trends for these amino acids compared to the whole-shell fraction?
- 4. Can kinetic models be used to determine the rates of racemisation for the species studied, and if so which models perform best?

5.1.1 Assessing the integrity of a biomineral system using hightemperature experiments

A key requirement for reliable AAR is the closed-system behaviour of a biomineral during its burial history - that is, no products of diagenesis should be lost and no contaminants should enter the system. In a closed system, the patterns of racemisation should be systematic and highly correlated between different amino acids, and free (FAA) and total hydrolysable (free and peptide-bound, THAA) amino acids; therefore covariance between amino acids or fractions can be used as a measure of system integrity (Penkman, 2005; Kosnik et al., 2008; Penkman et al., 2008; Hendy et al., 2012). Loss of amino acids from the biomineral may be measured directly by carrying out heating experiments in water, then analysing the amino acid content of the water (Brooks et al., 1990). This approach has been used widely in studies of intra-crystalline protein diagenesis (IcPD), to compare the whole-protein and intra-crystalline protein fractions of biominerals, and thus determine whether the intra-crystalline fraction behaves more reliably as a closed system than the whole-protein fraction, at least at high temperatures (e.g. ostrich eggshell (Crisp et al., 2013), various molluscs (Penkman et al., 2008; Demarchi et al., 2013b; Pierini et al., 2016; Ortiz et al., 2018), and enamel (Dickinson et al., 2019)). However, measuring the proportion of leached amino acids may be complicated by the presence of suspended fragments of biomineral in the supernatant water (Dickinson et al., 2019). Additionally, a biomineral which behaves as a closed system at high temperatures under controlled conditions may not show the same behaviour in the diagenetic environment (and vice versa). Nevertheless high-temperature experiments allow decomposition reactions to be observed over laboratory timescales.

5.1.2 Modelling amino acid racemisation

Kinetic models can be used to determine the kinetic parameters (e.g. rate constants and activation energies) of various amino acid decomposition reactions, most commonly racemisation. Use of these kinetic parameters to calculate the age or temperature history of a sample was proposed early in the history of AAR research (e.g. Hare, 1976). However, some discrepancies have been found between the kinetics of protein decomposition at high and ambient temperatures in some biominerals (see Section 5.1.2.3), confounding direct extrapolation of parameters determined at high temperature to sub-fossil samples.

Free amino acids and simple peptides in aqueous solution follow patterns of decomposition which can be modelled mechanistically, for example using irreversible first order kinetics for hydrolysis (Hill, 1965), or reversible first order kinetics for free amino acid racemisation (Bada et al., 1970).

These simple models have been applied to protein diagenesis to determine the kinetic parameters of hydrolysis and racemisation in a range of biominerals and model peptides (Clarke and Murray-Wallace, 2006). However, protein diagenesis takes place as a suite of complex, interrelated reactions which tend to deviate from first order kinetics, depending on the protein structure, biomineral matrix and other material-specific factors, especially at advanced stages of protein decomposition (e.g. Kriausakul and Mitterer, 1978; Miller et al., 1992; Walton, 1998). Various empirical models which take into account this deviation from first order kinetics have been developed (see Clarke and Murray-Wallace (2006) for an in-depth review of empirical models); a selection of key models are discussed below.

5.1.2.1 Reversible first order kinetics

Free amino acids in solution racemise according to reversible first order kinetics (RFOK), where the rate of racemisation is the difference between the forward rate, k_1 , and the reverse rate, k_2 . For amino acids with a single chiral centre, $k_1 = k_2$, which results in the integrated rate equation **Equation 5.1** where $K = k_1/k_2$ (= 1 for amino acids with one chiral centre), t is time, and t is a constant accounting for laboratory-induced racemisation.

$$\begin{array}{c} k_1 \\ \rightleftarrows \text{ D-amino acid} \\ k_2 \end{array}$$

$$ln\left[\frac{1+\frac{D}{L}}{1-K\frac{D}{I}}\right] = (1+K)k_1t + c$$

Equation 5.1 – Reversible first order kinetics (RFOK)

At low D/L values (< 0.1), the expression (1 - D/L) can be approximated to 1, resulting in a simplified model (**Equation 5.2**, Bada et al., 1970).

$$ln[1+D/L] = k_1t + c$$

Equation 5.2 – Simplified reversible first order kinetics

The RFOK model assumes that only one pair of reactions is taking place during decomposition: the interconversion between a single form of the L-amino acid and a single form of the D-amino acid, for which the forward and reverse rates are equal. In proteins, not only does racemisation take place when the amino acids are in a range of states, but numerous other diagenetic reactions are taking place at the same time. Conformity to RFOK in fossil biominerals is therefore more accurately described as apparent reversible first order kinetics (RFOK_a) (Clarke and Murray-Wallace,

2006). Racemisation in proteins typically only conforms to RFOK_a during the early stages of diagenesis (e.g. Wehmiller and Hare, 1971); this is because RFOK_a fails to account for the observed slowing of the racemisation rate over time in proteins. Stepped models with different racemisation rates for these 'fast' and 'slow' phases have been applied to combat this issue (e.g. Schroeder and Bada, 1976; Kriausakul and Mitterer, 1978; Harada and Handa, 1995); however, concerns have been raised about the subjectivity of assigning a point of inflection between these 'fast' and 'slow' rates (Tomiak et al., 2013).

5.1.2.2 Empirical non-linear functions

A range of non-linear functions have been proposed to model the racemisation curve in proteins more reliably than RFOK_a (see Clarke and Murray-Wallace (2006)). Rather than being based solely on chemical rationale, these functions incorporate empirical variables – typically power functions – that allow the model to be adjusted to best fit the data. The simplest of these is simple power law kinetics (SPK), where the D/L-time trend is linearised using an empirically derived exponent n (Equation 5.3), where k is the rate constant of the model.

$$D/L^{n} = kt + c$$

Equation 5.3 – Simple power law kinetics (SPK)

A special case of SPK is apparent power law kinetics (APK), where n = 2 (Mitterer and Kriausakul, 1989). However, improved fits can be found by optimising n for the substrate and amino acid under study (Goodfriend et al., 1995, 1996; Kaufman, 2006). A further modification to SPK is constrained power law kinetics (CPK, **Equation 5.4**) (Manley et al., 2000), which approaches an asymptote of 1 to take into account the racemisation reaction reaching equilibrium over time. In some cases, the natural log of the D/L term is used (**Equation 5.5**) (Clarke and Murray-Wallace, 2006; Crisp et al., 2013; Dickinson, 2018).

$$\left[\frac{1+\frac{D}{L}}{1-\frac{D}{L}}\right]^n = kt + c$$

Equation 5.4 – Constrained power law kinetics (CPK)

$$ln\left[\frac{1+D/L}{1-D/L}\right]^n = kt + c$$

Equation 5.5 – Modified form of constrained power law kinetics (CPK)

While further modifications allow D/L_0 , the degree of initial racemisation (either *in situ* or hydrolysis-induced), to be taken into account (Allen et al., 2013), the simpler models given above – where D/L_0 is assumed to be 0 – are more commonly applied (e.g. Kaufman, 2000, 2006; Manley et al., 2000; Crisp et al., 2013; Dickinson, 2018).

Power-function transformations tend to overestimate racemisation rates at low D/L values, while linear transformations tend to overestimate racemisation rates at high D/L values (Tomiak et al., 2013). The sampling range used for a transformation can therefore significantly influence calculated reaction rates (Allen et al., 2013; Crisp, 2013). In a comparison between a range of power-function transformations on various substrates, APK generally showed the weakest performance, while the performance of other models depended on the substrate, amino acid and D/L range used (Allen et al., 2013).

Due to the limitations of empirical models, model-free scaling approaches have also been applied to linearise D/L-time trends in gastropods (Demarchi et al., 2013b), corals (Tomiak et al., 2013) and ostrich eggshell (Crisp, 2013). In a comparison between a range of models, the scaling approach was found to best predict the patterns of racemisation in naturally-aged material using kinetic parameters derived from high-temperature experiments in some, but not all, biominerals (Allen et al., 2013).

5.1.2.3 Application of kinetic parameters to naturally-aged samples

"When kinetic data are used for dating calculations it should be emphasized that a small error of 1% made in the determination of activation energies will produce an error of 20% in a calculated date."

Dungworth (1976), p. 146

If high-temperature experiments are carried out at three or more different temperatures, the relationship between rate and temperature can be used to estimate the activation energy of racemisation using the Arrhenius law (**Equation 5.6**) (e.g. Bada and Schroeder, 1975; Brooks et al., 1990), where k is the rate constant, A is the pre-exponential factor, R is the real gas constant (8.314 J mol⁻¹), T is the temperature and E_a is the activation energy.

$$k = Ae^{-\frac{E_a}{RT}}$$

$$\ln(k) = -E_a/RT + \ln(A)$$

Equation 5.6 – Arrhenius equation

While the Arrhenius law technically relates only to simple reactions in the gas phase, it is assumed that the law applies sufficiently to the complex reaction kinetics of protein decomposition to allow an estimation of E_a (e.g. Crisp et al., 2013).

In theory, activation energies derived from high-temperature decomposition experiments can be used to calculate the age of sub-fossil samples with known thermal histories. However, the results of comparisons between decomposition in high-temperature experiments and naturally-aged material have been mixed. Some studies have found good agreement between decomposition patterns at high and ambient temperatures (e.g. ostrich eggshell (Brooks et al., 1990) and P. obliquiloculata (Kaufman, 2006)), while others have observed a marked deviation from ages of fossil material extrapolated from high-temperature kinetics and their measured ages (e.g. ostrich eggshell (Crisp, 2013), corals (Tomiak et al., 2013) and some molluscs (Allen et al., 2013; Demarchi et al., 2013b)), or mixed results depending on the amino acid modelled (e.g. the land snail Trochoidea (Goodfriend and Meyer, 1991) and enamel (Dickinson et al., 2019)). This deviation may be due to differing temperature sensitivities of the different decomposition reactions which take place during protein degradation, resulting in temperature-dependent activation energies. For example, the failure of high-temperature kinetic parameters to conform to the decomposition patterns of naturally-aged bone is thought to be partially due to the denaturation of collagen at high temperatures, dramatically altering its susceptibility to hydrolysis (Collins et al., 1999). Given the differences in decomposition trends at high and low temperatures, constraining hightemperature experiments with naturally-aged material can improve the reliability of derived kinetic parameters (e.g. Tomiak et al., 2013). However, independently-dated fossil material with a known temperature history is rarely available.

High-temperature experiments have been carried out on various species of foraminifera. Apparent power law kinetics were found to reliably model lle epimerisation at high temperatures in a range of foraminifer species (Mitterer and Kriausakul, 1989), while subsequent investigations into other models have found that SPK is generally the most reliable for foraminifera (Kaufman, 2006).

Attempts to derive kinetic parameters of racemisation applicable to fossil foraminifera have, as with other biominerals, generated mixed results. Studies of *P. obliquiloculata* found good concordance between the rates of racemisation derived from high-temperature experiments and independently-dated fossil material (Kaufman, 2006; Allen et al., 2013), while the kinetics of Ile epimerisation in *C. wuellerstorfi* and *N. pachyderma* at high temperatures did not extrapolate to ambient temperatures (Sejrup and Haugen, 1992). Overall, there is no 'one size fits all' model

which can be used to reliably predict racemisation in all materials, with each model having its own strengths and limitations. Therefore it is necessary to test various modelling approaches on each biomineral system to determine which, if any, of the models perform best.

Despite the issues with concordance between high- and low-temperature protein decomposition for many biominerals, high-temperature experiments are a useful tool to assess the integrity of biomineral systems, and compare the patterns of amino acid decomposition within them. High-temperature decomposition experiments were therefore carried out on *Ammonia* spp. and *H. germanica* at 110°C and 140°C.

5.2 Materials and methods

5.2.1 Oxidation and heating experiments

Ammonia spp. and H. germanica tests were taken from surface samples from the Humber Estuary (see Section 4.2.1 for additional site details). 120 monospecific individuals were picked per sample and crushed with a needle, which was cleaned with 7 M HCl between samples. As these experiments were carried out simultaneously with the oxidation experiments discussed in Chapter 4, a 24 hour pre-treatment with 12% NaOCl was used to isolate the intra-crystalline fraction, termed 'bleached' samples. Bleaching was carried out according to Section 2.2.

Samples were placed in 0.1 mL sterile Reactivials with 100 μ L 18 m Ω H₂O and heated at 110°C for 0-50 days or at 140°C for 1-48 hours (**Table 5.1**). The supernatant water was then removed and separated into two 40 μ L aliquots – one for analysis of free amino acids (FAAw) and one for analysis of total hydrolysable amino acids (THAAw). Due to the poor seal formed by the Reactivial caps, a significant proportion of the samples dried out either partially or fully (see **Table 5.1**), especially when heated at 140°C. For samples which had dried out completely only the biomineral amino acids were analysed. Where samples had partially dried out, only one 40 μ L aliquot was taken; this aliquot was used to analyse THAAw.

Table 5.1 – High-temperature experiment time points for *Ammonia* spp. and *H. germanica*. Numbers in brackets refer to samples which dried out during heating; numbers in italics refer to samples which partially dried out. U = unbleached, B = 24 h 12% NaOCl.

	LL/D	Temp-	Time points (days)									
Species	U/B	U/B	erature	0	0.04	0.17	1	2	5	10	31	50
Ammonia spp.	U	110°C				3 (1)		3	3 (1)	3	3	
	В	110°C				3 (1)		3	3 (2)	3	3	
U gormanica	U	110°C				3 (1)		3 (1)	3 (1)	3	3	
H. germanica	В	110°C				3 (1)		3 (1,1)	3 (1)	3	3	
Ammonia spp.	В	140°C		3 (1)	3 (2)	3 (3)	3					
H. germanica	В	140°C		3 (1)	3 (1,2)	3 (1)	3 (1)					
Ammonia spp.	U, B	NA	3									
H. germanica	U, B	NA	3									
Blanks	В	110°C				1	1	1, 10*	1	1	1	
	В	140°C		1	1	1	1					
	В	NA	1									

^{*}Suite of blanks carried out independently to the rest of the high-temperature experiments.

No HCl was added to the FAAw aliquot; the THAAw aliquot was demineralised with 4 μ L 7 M HCl and hydrolysed according to **Section 2.3**. Both supernatant water aliquots were dried *in vacuo* using a centrifugal evaporator prior to rehydration for analysis.

After removal of the supernatant, the samples were rinsed with 3 x 60 μ L 18 m Ω H $_2$ O and air dried, then demineralised with 10 μ L 2 M HCl, with a further 5 μ L 2 M HCl added if necessary to complete demineralisation. Half of the demineralised sample was taken for analysis of the free amino acids (FAAf), and dried *in vacuo* prior to rehydration for analysis. Hydrolysis of the remainder was then carried out according to **Section 2.3** for analysis of the total hydrolysable amino acid (THAAf) fraction.

During this suite of experiments, analytical blanks were carried out at each time point following the full bleaching and heating protocol detailed above. All blanks were bleached for 24 hours using 12% NaOCl; $100~\mu L$ $18~m\Omega$ H_2O was added to each blank before heating, as for the samples, and demineralised and hydrolysed as above. Due to the variability of these blanks, and the low concentration of some samples, especially in the free amino acid (FAA) fraction, an additional set of 10~analytical blanks was later analysed to better quantify the level of background contamination contributing to the samples. This second set of analytical blanks was treated the same as the first set of blanks (see above) and heated to 110° C for 5 days.

For samples heated to 110°C, all aliquots were analysed by RP-HPLC according to **Section 2.4.1**. The 140°C, and unheated suite of experiments, were carried out later, using the UHPLC method outlined in **Section 2.4.2**.

5.2.2 Data screening

All sample data were screened using the following three criteria (see **Section 3.2.4.3** for a discussion of data screening in AAR):

- 1. Visual inspection of chromatogram for baseline issues or column overloading, indicating a poor run or large amounts of contamination;
- 2. > 80% Gly, indicating large amounts of contamination, or loss of sample when combined with very low concentrations;
- 3. A combination of high concentration and low D/L values compared to other replicates, indicating modern contamination.

To preserve the natural variability of the data, only extreme outliers were excluded from the data set. Five subsamples in total (of 344, 0.01%) were excluded according to these screening criteria (Table 5.2).

Table 5.2 – Subsamples from high-temperature experiments excluded according to screening criteria.

Sample	Chromatography	Gly > 80%	High Concentration & Low D/L
110uABh09-THAAf	Column		
110uAdii09-inaai	overloaded		
110bHGh58-FAAw	Baseline issues	84% Gly	High concentration (~3x other replicates)
110uABh11-THAAw		92% Gly	High concentration (~3x other replicates)
			High concentration (~10x other replicates),
110uABh01-THAAf			low D/L (Asx D/L = 0.18 compared to $^{\circ}$ 0.8
			for other replicates)
			High concentration (~10x other replicates),
110bABh27-THAAf			low D/L (Asx D/L = 0.15 compared to $^{\circ}$ 0.4
			for other replicates)

Partial or full drying out of the supernatant did not significantly impact the concentration or D/L values of the samples at 110°C (ANOVA, p > 0.05). At 140°C, a significant effect of partial or full drying was found by ANOVA (p = 0.015), but a two-way Tukey post-hoc analysis did not identify any significant differences (p > 0.05) between no, partial or full drying of samples. Samples which had dried out were therefore not screened from the data set at either temperature.

A blank correction was not carried out for any samples, as the level of background contamination was only well quantified at the 5 day time point at 110°C. Instead, the average concentration of the blanks is reported in **Section 5.3.1.1**, to give an estimate of the contribution of background contamination to the samples.

5.2.3 Approach for modelling kinetic parameters

Apparent reversible first order kinetics (RFOK_a, Equation 5.1) simple power law kinetics (SPK, Equation 5.3) and constrained power law kinetics (CPK, Equation 5.4) were applied to FAA and THAA Asx, Glx and Ala, and THAA Phe and Leu, to compare rates of racemisation between amino acids and protein fractions at 110°C. As the transformation for RFOK_a mathematically excludes any D/L values > 1 for the amino acids used, samples with D/L values > 1 were excluded from all three models (Table 5.3). Optimisation of n in SPK and CPK was carried out by determining which value of n resulted in the highest R² value (i.e. the best linearisation) when applied to each data set. A range of n from 1 to 10 in increments of 0.1 was tested.

Table 5.3 – Number of samples from each fraction of the 110°C experiment with D/L values > 1, which have been excluded from the kinetic models. U = unbleached, B = 24 h 12% NaOCl.

nave been exercised in entrane introduction of anti-reaction, by 2 in 1270 indeed.									
Species	U/B	Fraction	Temperature	Asx	Glx	Ala	Phe	Leu	
Ammonia spp.	В	THAA 110°C					2	1	
	В	FAA	NA (0 hours)		2				
H. germanica	U	FAA	110°C					1	
	В	FAA	NA (0 hours)		2				
	В	THAA	NA (0 hours)			1			

5.3 Results

5.3.1 Amino acid concentration

5.3.1.1 Contribution of laboratory contamination to amino acid concentration Due to the small sample sizes used in foraminifer AAR, quantifying and minimising the amount of contamination from laboratory sources is important. While an analytical blank was originally analysed for each time point (set X), these results were more variable than expected, so a further 10 blanks (set Y) were later analysed to quantify the baseline level of modern contamination present in the samples.

In the standard protocol used for the high-temperature decomposition experiments, the needle was dipped in 7 M HCl and then rinsed with $18 \text{ m}\Omega \text{ H}_2\text{O}$ to remove any fragments of crushed biomineral between each sample. This needle was also placed into the blank vials of set X, which may have caused some cross-contamination into the blanks from fragments of biomineral not removed by this cleaning step. To test this hypothesis, placement of the needle into the blank vials was therefore omitted from set Y.

The concentration of amino acids in set Y is lower than the concentration of amino acids in set X, particularly in the 'THAAf' aliquots (**Fig. 5.1**), indicating that cross-contamination from the needle was a source of some of the amino acids observed in set X. This could also result in some cross-contamination of samples; therefore the standard protocol has been modified to specify that a freshly sterilised needle should be used to crush each sample to avoid cross-contamination; however note that the data obtained within this chapter did not use sterilised needles for each sample.

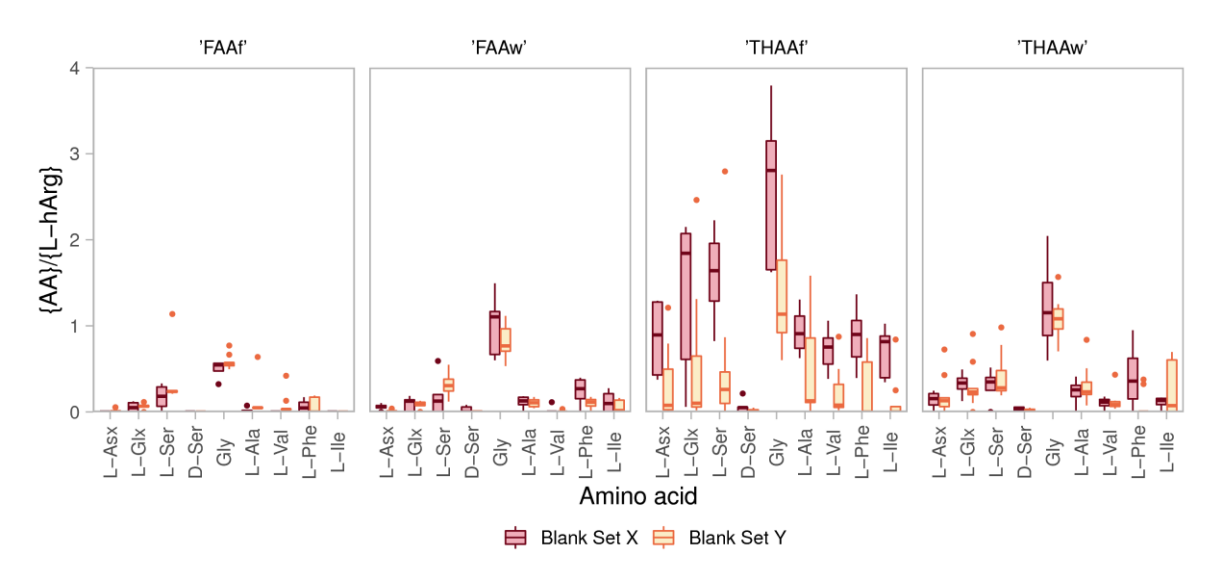


Fig. 5.1 – Relative concentrations (amino acid peak area divided by L-hArg peak area) of key amino acids in blank set X (blanks analysed alongside 110°C suite of experiments) and blank set Y (separate suite of 10 blanks heated to 110°C for 5 days). Boxes show the median and the first and third quartiles; the whiskers extend to the minimum and maximum values, with samples beyond 1.5 times the interquartile range treated as outliers (points).

The contribution of laboratory contamination to the total concentration measured in the samples varies by amino acid, with L-Ser and Gly generally having the highest proportion of laboratory contamination, particularly in the FAA fraction (**Fig. 5.1**). L-Ser is an unstable amino acid which hydrolyses and decomposes quickly; therefore high concentrations of Ser in naturally-aged samples

can be used to screen for contamination (Kosnik and Kaufman, 2008). Gly tends to be abundant in biomineral proteins (proteins with a high Gly content are thought to play a key role in the biomineralisation process (Sabbatini et al., 2014)), but as it is not a chiral molecule any contribution to its total concentration from laboratory sources is less of an issue than for amino acids used for AAR.

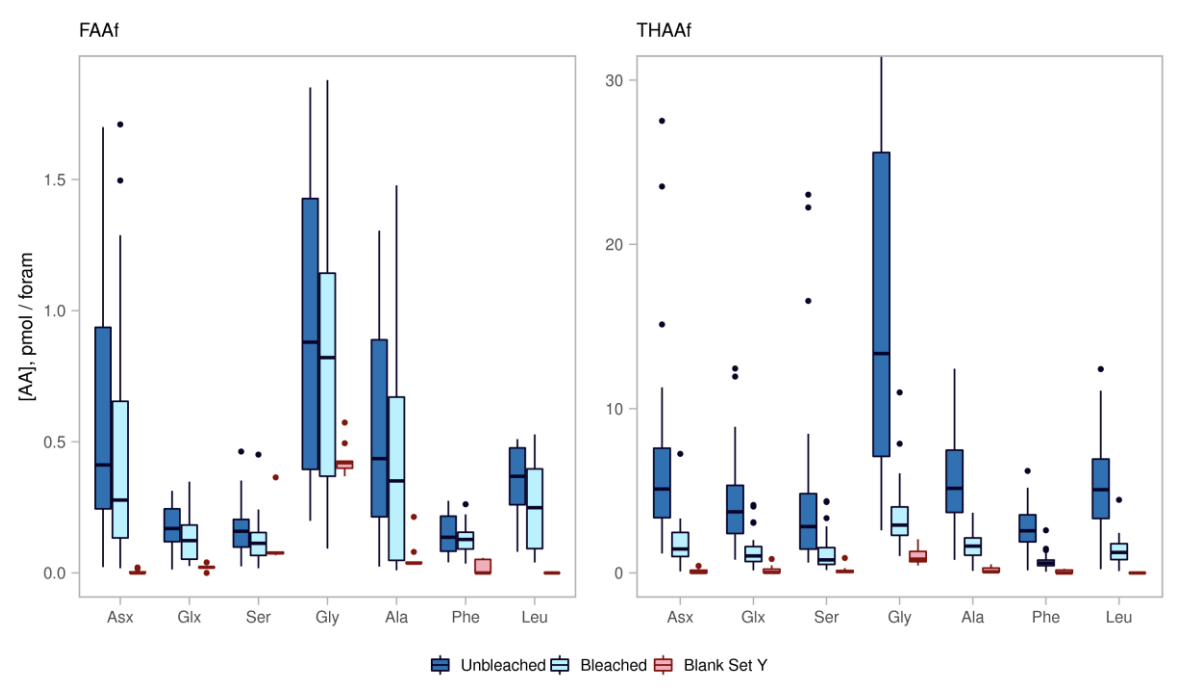


Fig. 5.2 – Concentration of key amino acids in unbleached (whole-shell) and bleached (intra-crystalline) samples and analytical blank set Y (set of 10 blanks heated for 5 days). Samples from both species (*Ammonia* spp. and *H. germanica*), and across the full range of time points at 110°C, have been combined in this figure to show the range of amino acid concentrations detected in this suite of experiments. The concentration of amino acids in the blanks is calculated using an assumed 'sample size' of 60 tests. Boxes show the median and the first and third quartiles; the whiskers extend to the minimum and maximum values, with samples beyond 1.5 times the interquartile range treated as outliers (points). The upper Gly whisker on the THAAf graph has been truncated to allow easier comparison of the lower concentration amino acids. Left: free amino acids in foraminifer fraction (FAAf); right: total hydrolysable amino acids in foraminifer fraction (THAAf).

With the exception of Gly and Ser, the blanks typically make up a small proportion of the amino acids in the foraminifer fractions, with laboratory contamination having less of an impact on the unbleached samples due to their larger concentrations (Fig. 5.2). While the data are variable, this shows that the amino acids useful for dating (Asx, Glx, Ala, Phe and Leu) are less affected by laboratory contamination than Ser and Gly. Due to the lower concentration of the intra-crystalline fraction, bleached material is more affected by laboratory contamination than unbleached material, which may explain some of the greater variability observed in the racemisation trends of

the bleached material compared to the unbleached material. To overcome this, increasing sample sizes where possible is advised, especially if carrying out an oxidation pre-treatment, and for naturally-aged samples which may have lost a large proportion of their inter-crystalline protein (see **Chapter 4**). The contribution of laboratory contamination to these small samples also highlights the importance of quantifying and reporting the background concentration of amino acids in the pre-treatment method.

5.3.1.2 Trends in amino acid concentration

In a closed-system biomineral, the concentration of free amino acids ([FAA]) should increase as hydrolysis takes place, with an overall decrease in total hydrolysable amino acids ([THAA]) occurring due to amino acid decomposition (e.g. Penkman et al., 2008; Bright and Kaufman, 2011b; Orem and Kaufman, 2011; Demarchi et al., 2013b). A decrease in the proportion of FAA has also been observed after extended heating due to decomposition of FAA in some biominerals (Penkman et al., 2008; Orem and Kaufman, 2011; Pierini et al., 2016). Conversely, an open-system biomineral will result in the leaching (diffusive loss) of some amino acids over time. FAA are smaller, and may therefore be more susceptible to leaching (Penkman et al., 2008), but leaching of peptides from biominerals has also been observed (Orem and Kaufman, 2011). The trends in amino acid concentration during heating can therefore provide a measure of the closed-system behaviour of a biomineral.

Fig. 5.3 shows the concentration of Asx, Glx, Ser and all amino acids ('total') in FAA and THAA *Ammonia* spp. over the course of the 110° C heating experiment. The orange lines show the mean (dark) and ± 1 standard deviation (σ) (pale) of the concentration of blank set Y (Section 5.3.1.1), while the bars show the mean concentration of the subsamples at each time point. A substantial proportion of amino acids in the total FAA fraction, and the bleached total THAA fraction, is laboratory contamination. The contribution of modern contamination to [FAA] is possibly underestimated in the later time points as the blanks were heated only for 5 days. The pattern of laboratory contamination is different for different amino acids — the [FAA] of Ser in the samples falls almost entirely within ± 1 σ of the laboratory contamination [FAA], and a large proportion of [FAA] and unbleached [THAA] of Gly is also accounted for in the blanks. For Asx, however, the contribution of laboratory contamination is negligible. A similar pattern to Asx is observed for Glx, Ala, Phe and Leu. *H. germanica* also shows a larger proportional contribution of laboratory contamination to Gly and Ser compared to other amino acids (Fig. 5.4).

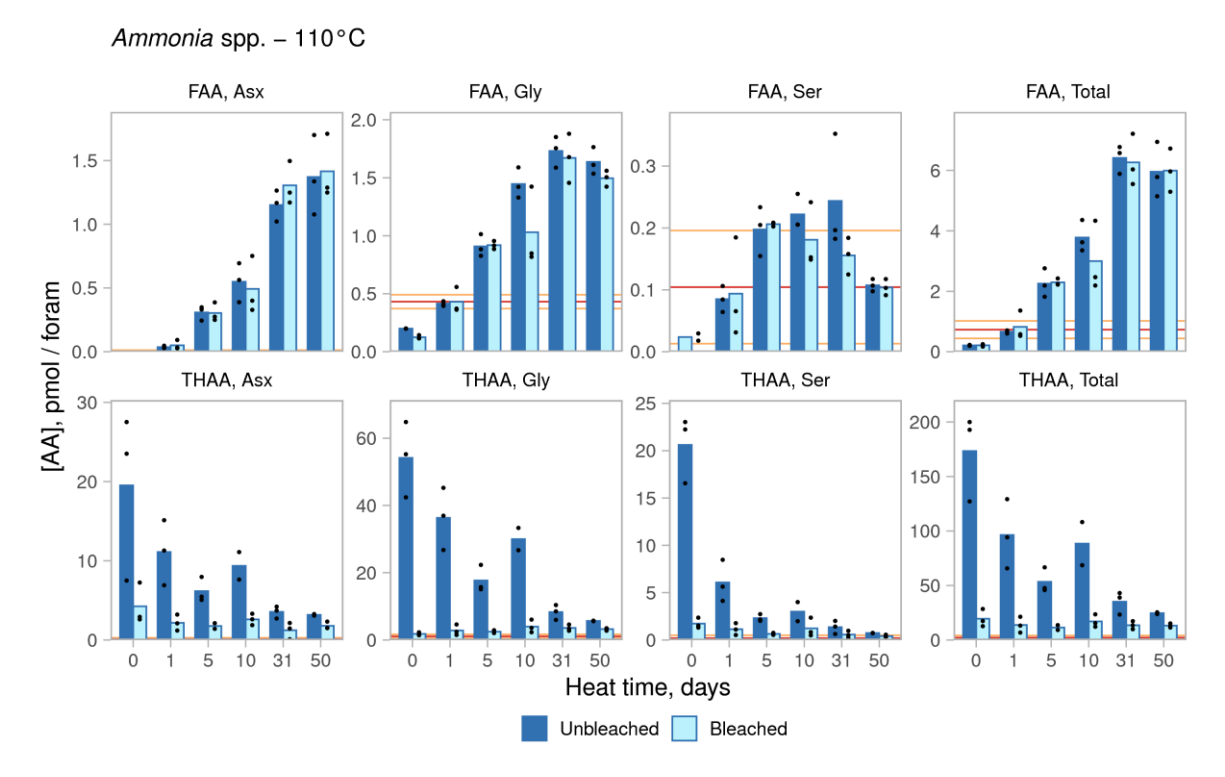


Fig. 5.3 – Concentration of Asx, Gly and Ser and total amino acids in unbleached (whole-shell) and bleached (intra-crystalline) *Ammonia* spp. during 110°C heating experiment. The bars show the average concentration of each fraction over time; the points show individual replicates. The average total concentration of amino acids in blank set Y (see **Section 5.3.1.1**), given an assumed sample size of 60 tests, is shown as a dark orange line; the pale orange lines are $\pm 1 \, \sigma$ around the mean of the blank amino acid concentration. Note the individual y-axis range for each plot. Upper: free amino acid (FAA) fraction; lower: total hydrolysable amino acid (THAA) fraction.

Although the variability of the data and contribution from laboratory contamination precludes an accurate quantification of total amino acid concentrations for *Ammonia* spp., qualitative trends can be seen. [FAA] increases over time for all amino acids except Ser, which remains within the level of modern contamination for the duration of the experiment, likely due to its relative instability (Smith and Evans, 1980). [FAA] is similar for both the whole-shell and intra-crystalline fractions of both species; this suggests that any FAA being generated from the inter-crystalline fraction is leaching out of the biomineral. If the inter-crystalline fraction behaved as a closed system then the whole-shell (unbleached) [FAA] should be higher than the intra-crystalline [FAA], as the whole-shell [THAA] is higher than the intra-crystalline [THAA]. A similar pattern has been observed in various mollusc shells, where the proportion of FAA was higher in the intra-crystalline fraction than the inter-crystalline fraction (Penkman et al., 2008), indicating that in these mollusc shells and foraminifer tests, FAA are readily leached from the inter-crystalline fraction.

The trends in [FAA] for *H. germanica* follow a similar pattern to *Ammonia* spp. (**Fig. 5.4**). However, the pattern of [THAA] differs between species. The [THAA] of the whole-shell fraction of *Ammonia* spp. decreases over the course of the experiment from a few hundreds of pmol / foram to a few tens of pmol / foram (**Fig. 5.3**). This loss of amino acids from the unbleached material indicates that the inter-crystalline fraction behaves as an open system, in contrast to the intra-crystalline (bleached) fraction, which has a consistent concentration in the tens of pmol / foram for the duration of the experiment. Conversely, in *H. germanica* both the whole-shell and intra-crystalline [THAA] remain relatively stable over the duration of the 110°C experiment (**Fig. 5.4**).

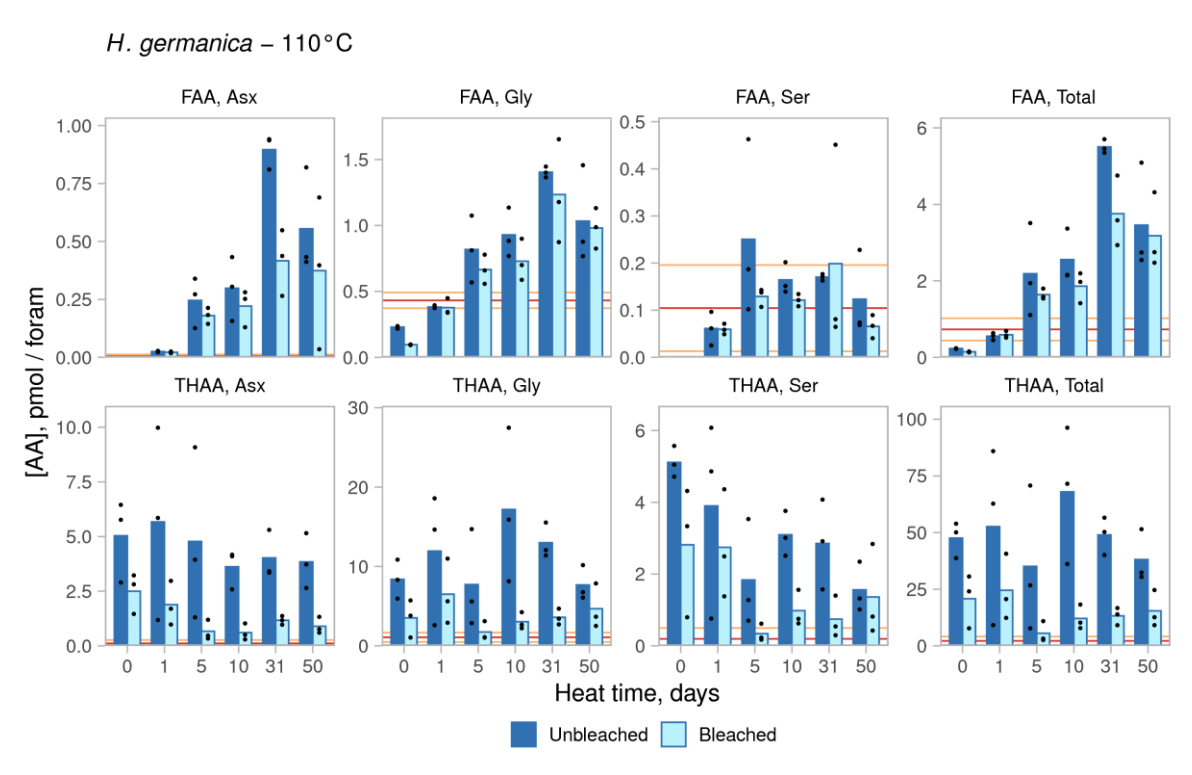


Fig. 5.4 – Concentration of Asx, Gly and Ser and total amino acids in unbleached (whole-shell) and bleached (intra-crystalline) H. germanica during 110° C heating experiment. The bars show the average concentration of each fraction over time; the points show individual replicates. The average total concentration of amino acids in blank set Y (see **Section 5.3.1.1**), given an assumed 'sample size' of 60 tests, is shown as a dark orange line; the pale orange lines are $\pm 1 \sigma$ around the mean of the blank amino acid concentration. Note the individual y-axis range for each plot. Upper: free amino acid (FAA) fraction; lower: total hydrolysable amino acid (THAA) fraction.

A decrease in [THAA] over time has been observed in a range of foraminifer and mollusc species (e.g. Wehmiller, 1980; Penkman et al., 2008; Bright and Kaufman, 2011a; Ortiz et al., 2019), with bleached material typically having more stable amino acid concentrations (Penkman et al., 2008; Ortiz et al., 2019). This pattern is followed in *Ammonia* spp., but not *H. germanica*. The higher initial [THAA] of *Ammonia* spp. compared to *H. germanica* suggests that in *H. germanica* the most

labile amino acids in the inter-crystalline fraction have already been lost from *H. germanica* prior to heating, either before sample collection or during pre-treatment. As the two species were collected from the same sediment sample, it is unlikely that the *H. germanica* tests were older than the *Ammonia* spp. tests, so this difference in behaviour may result from differences in each species' test structure.

At 140°C, the intra-crystalline fraction of *Ammonia* spp. shows a decrease in [THAA] over time (**Fig. 5.5**), likely due to the more rapid rate of protein decomposition at this higher temperature. *H. germanica* has a stable [THAA] following a drop in concentration between 0 and 1 hour of heating.

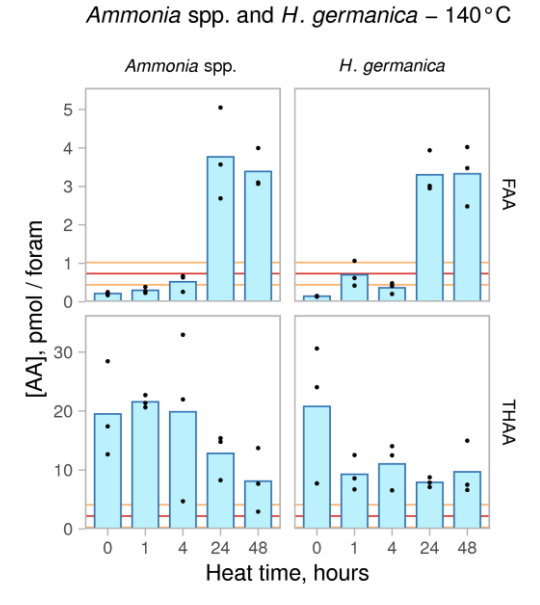


Fig. 5.5 – Total concentration of amino acids in bleached (intra-crystalline) *Ammonia* spp. and *H. germanica* during 140°C heating experiment. The bars show the average concentration of each fraction over time; the points show individual replicates. The average total concentration of amino acids in blank set Y (see **Section 5.3.1.1**), given an assumed 'sample size' of 60 tests, is shown as a dark orange line; the pale orange lines are \pm 1 σ around the mean of the blank amino acid concentration. Upper: free amino acid (FAA) fraction; lower: total hydrolysable amino acid (THAA) fraction.

Overall, the patterns of amino acid concentration over heating time are the same for the intracrystalline fractions of both *Ammonia* spp. and *H. germanica*, with relatively stable [THAA] at 110°C and a decreasing [THAA] at 140°C, and increasing [FAA] at both temperatures due to hydrolysis. However, at 110°C the unbleached *Ammonia* spp. shows a substantial decrease in [THAA] over time, which is not observed in *H. germanica*. For both species, [FAA] is similar in the whole-shell and intra-crystalline fractions, which is likely due to leaching of inter-crystalline FAA as they are hydrolysed (reducing their apparent concentration), while intra-crystalline FAA are retained within the biomineral structure.

5.3.1.3 Leaching of amino acids from the biomineral fraction

In addition to analysing the biomineral amino acids, the amino acid content of the supernatant water was analysed to measure the extent of leaching (diffusive loss) of amino acids from the whole-shell and intra-crystalline fractions of *Ammonia* spp. and *H. germanica*. However, this was hampered by several issues. Firstly, some sample vials dried out either partially or fully during heating (see **Table 5.1**), so it was not always possible to analyse the amino acid content of the supernatant water. This was a particular issue in the 140°C suite of experiments, so only the results of the 110°C suite are presented here. Secondly, the usual approach of centrifuging samples to separate the biomineral powder and supernatant (Penkman et al., 2008) proved ineffective at the small sample sizes required for foraminifera, as pipetting off the supernatant was often enough to disturb the biomineral powder. As fragments of biomineral have been observed in supernatant waters via SEM even with centrifugation to separate the supernatant (Dickinson et al., 2019), it is likely that the concentrations of leached amino acids presented here are overestimates of the true extent of leaching. However, qualitative comparisons are still useful.

Fig. 5.6 shows the concentration of Asx, Gly, Ser and all amino acids ('total') in the FAA and THAA fractions of the supernatant waters taken from *Ammonia* spp. over the course of the 110°C heating experiment. In the whole-shell fraction of *Ammonia* spp., [FAA] increases steadily in the supernatant waters (with the exception of Ser, which doesn't show a clear trend of increasing [FAA], likely due to its rapid decomposition (e.g. Hare and Mitterer, 1968; Orem and Kaufman, 2011; Demarchi et al., 2013b)). By 50 days, free amino acids represent the majority of the THAA content of the unbleached supernatant waters. Interestingly, Ser [FAA] is substantially higher than blank Ser [FAA] in the unbleached supernatant waters, in contrast to the pattern seen in the foraminifer tests. *H. germanica* follows a similar pattern (Fig. 5.7). This, along with the similar whole-shell and intra-crystalline [FAA] in the biomineral for both species, suggests that the majority of free amino acids are leached from the inter-crystalline fraction during heating.

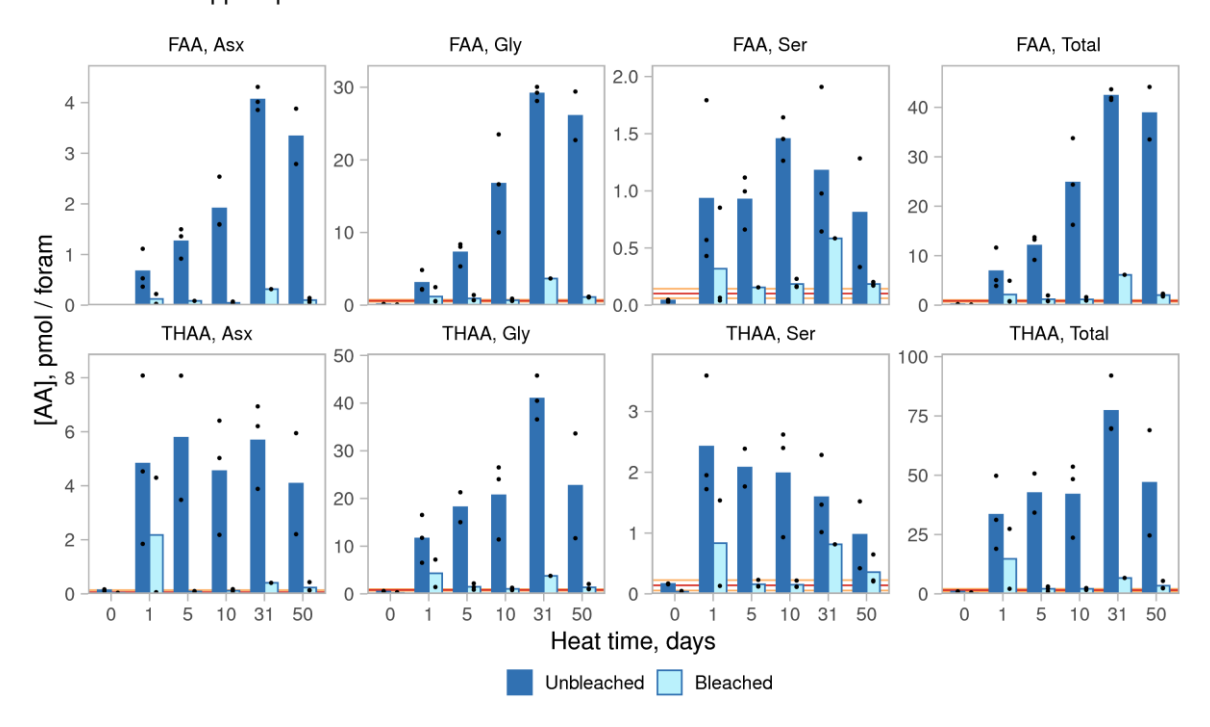


Fig. 5.6 – Concentration of Asx, Gly and Ser and total amino acids in supernatant waters from unbleached (whole-shell) and bleached (intra-crystalline) *Ammonia* spp. during 110°C heating experiment. The bars show the average concentration of each fraction over time; the points show individual replicates. The average total concentration of amino acids in blank set Y (see Section 5.3.1.1), given an assumed 'sample size' of 60 tests, is shown as a dark orange line; the pale orange lines are \pm 1 σ around the mean of the blank amino acid concentration. Note the individual y-axis range for each plot. Upper: free amino acid (FAA) fraction; lower: total hydrolysable amino acid (THAA) fraction.

The pattern for whole-shell [THAA] in the supernatant waters is less clear beyond a rapid increase between 0-1 day of heating for *Ammonia* spp. (Fig. 5.6) and possibly also *H. germanica* (Fig. 5.7), due to the variability of concentrations between replicates.

In biominerals with a closed-system intra-crystalline fraction, the proportion of amino acids detected in the supernatant water of bleached material is typically less than 5% of the intra-crystalline amino acid concentration (e.g. some gastropods and bivalves (Penkman et al., 2008; Demarchi et al., 2013c; Pierini et al., 2016; Ortiz et al., 2018), coral (Hendy et al., 2012), enamel (Dickinson et al., 2019) and ostrich eggshell (Crisp et al., 2013)). In both species, [FAA] and [THAA] is much lower in the bleached supernatant waters than in the unbleached supernatant waters, with the concentrations of most samples close to (or below) the range of modern contamination (Fig. 5.6, Fig. 5.7).

H. germanica supernatant waters - 110°C

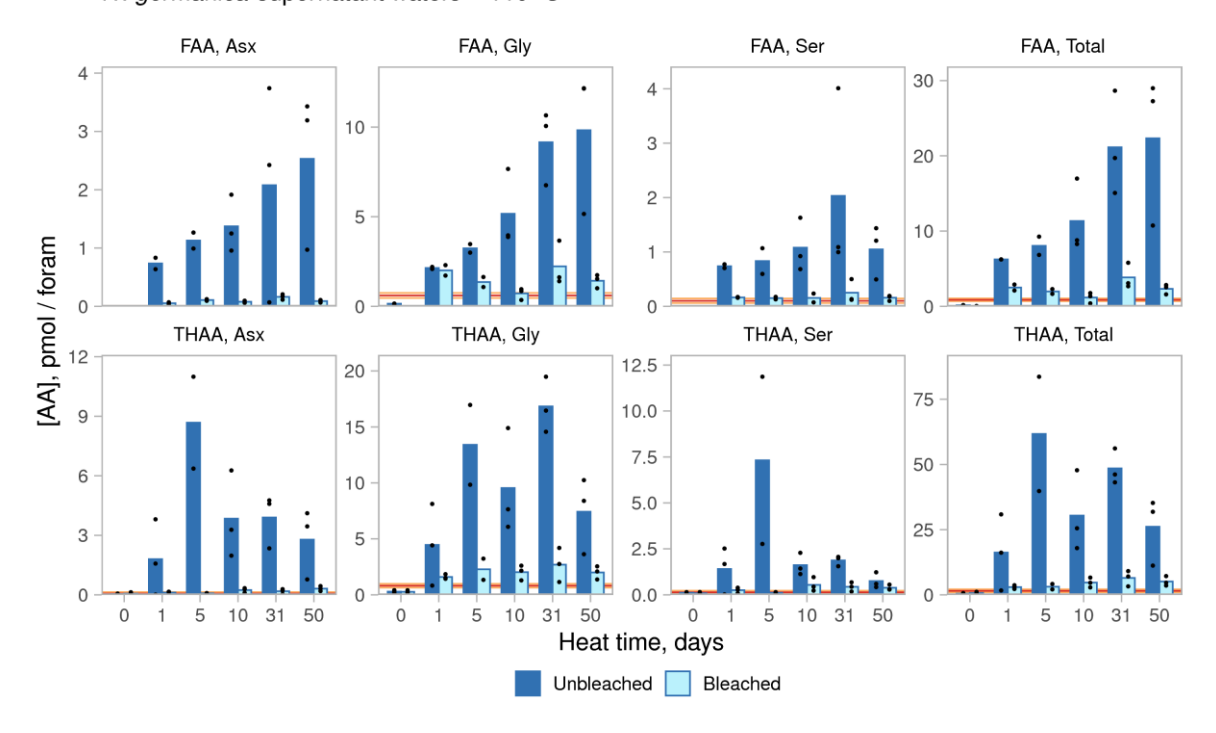


Fig. 5.7 – Concentration of Asx, Gly and Ser and total amino acids in supernatant waters from unbleached (whole-shell) and bleached (intra-crystalline) H. germanica during 110° C heating experiment. The bars show the average concentration of each fraction over time; the points show individual replicates. The average total concentration of amino acids in blank set Y (see Section 5.3.1.1), given an assumed 'sample size' of 60 tests, is shown as a dark orange line; the pale orange lines are \pm 1 σ around the mean of the blank amino acid concentration. Note the individual y-axis range for each plot. Upper: free amino acid (FAA) fraction; lower: total hydrolysable amino acid (THAA) fraction.

Fig. 5.8 shows the concentration of FAA and THAA Asx in the biomineral and supernatant waters of *Ammonia* spp. and *H. germanica* over the course of the 110°C experiment. Focusing on Asx reduces the effect of modern contamination on estimations of leaching, as this amino acid is present at very low concentrations in the blanks; the proportion of amino acids in the supernatant water is higher for Ser and Gly (**Appendix A3.1**). Isolating the intra-crystalline fraction of amino acids reduces the proportion of Asx in the supernatant water, especially in the FAA fraction, although the variability of the data precludes a quantitative comparison. The Asx observed in the supernatant waters of the bleached samples may be from leaching of free or peptide bound Asx, from biomineral fragments suspended in the supernatant water (Dickinson et al., 2019), or from a combination of these two sources.

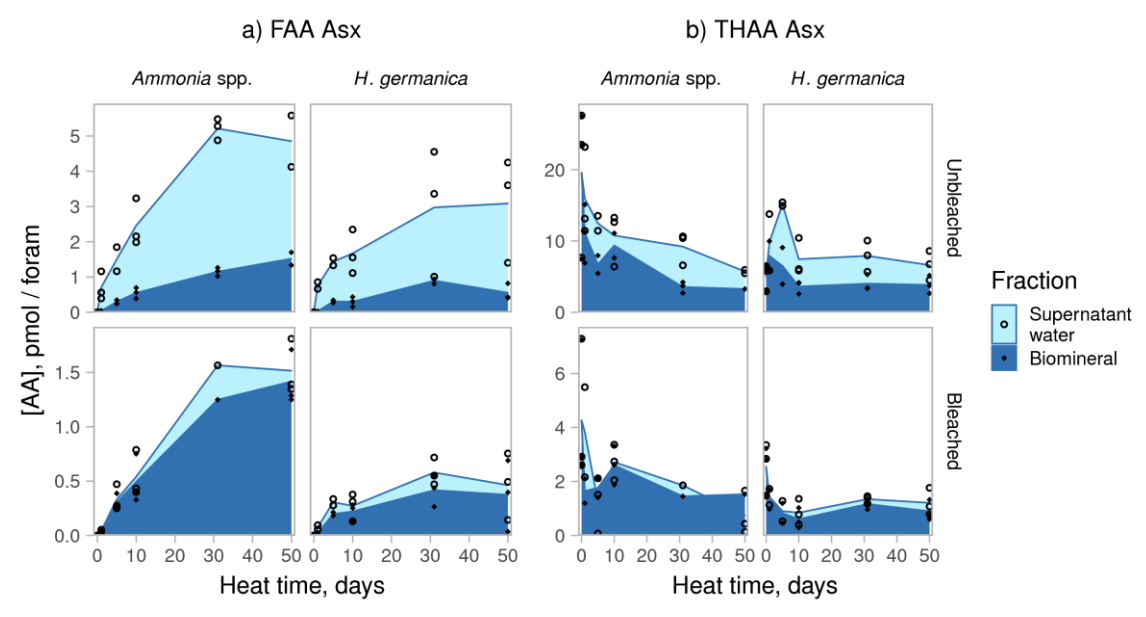


Fig. 5.8 – Concentrations of a) free (FAA) Asx and b) total hydrolysable (THAA) Asx in unbleached (whole-shell) and bleached (intra-crystalline) *Ammonia spp.* and *H. germanica* biomineral powders and the supernatant water in each vial during 110°C heating experiments. The shaded areas show the average concentration of each fraction over time; the points show individual replicates. Note the different y-axis ranges used for the unbleached and bleached graphs. Corresponding figures for Gly, Ser and all amino acids ('total') can be found in **Appendix A3.1**.

If all the Asx observed in the supernatant waters is leached from the biomineral, then in both the whole-shell and intra-crystalline fractions, the majority of the leaching of THAA appears to take place during the early stages of heating, with the increase in [FAA] in the supernatant water resulting from the hydrolysis of leached peptides or proteins. The leached amino acids observed in the bleached *Ammonia* spp. and *H. germanica* may represent a small fraction of the intracrystalline protein which is labile; if this is the case, then in naturally-aged material these labile intra-crystalline amino acids may be lost during the early stages of diagenesis, as has been observed in some other biominerals (e.g. Kosnik et al., 2017; Ortiz et al., 2017, 2019).

5.3.2 Amino acid composition

The differences in amino acid composition between the whole-shell and intra-crystalline fractions of amino acids are discussed in the extended bleaching experiments of **Chapter 4**; therefore this section focuses on changes in amino acid composition over time for *Ammonia* spp. and *H. germanica* at 110°C.

Fig. 5.9 shows the changes in the composition of *Ammonia* spp. and *H. germanica* over time during the 110°C heating experiment. For both species, the composition of the FAA fraction initially

closely resembles the composition of the blanks, with a high % Gly and small contributions from Asx, Ala and Leu. As hydrolysis of the biomineral protein proceeds, % Asx, Ala and Leu increase, while % Gly and Ser decrease. The change in FAA composition plateaus around 30 days at a similar composition to the THAA fraction, although % Ser continues to decrease over the duration of the experiment, likely due to the rapid decomposition of this unstable amino acid (Bada et al., 1978; Demarchi et al., 2013b).

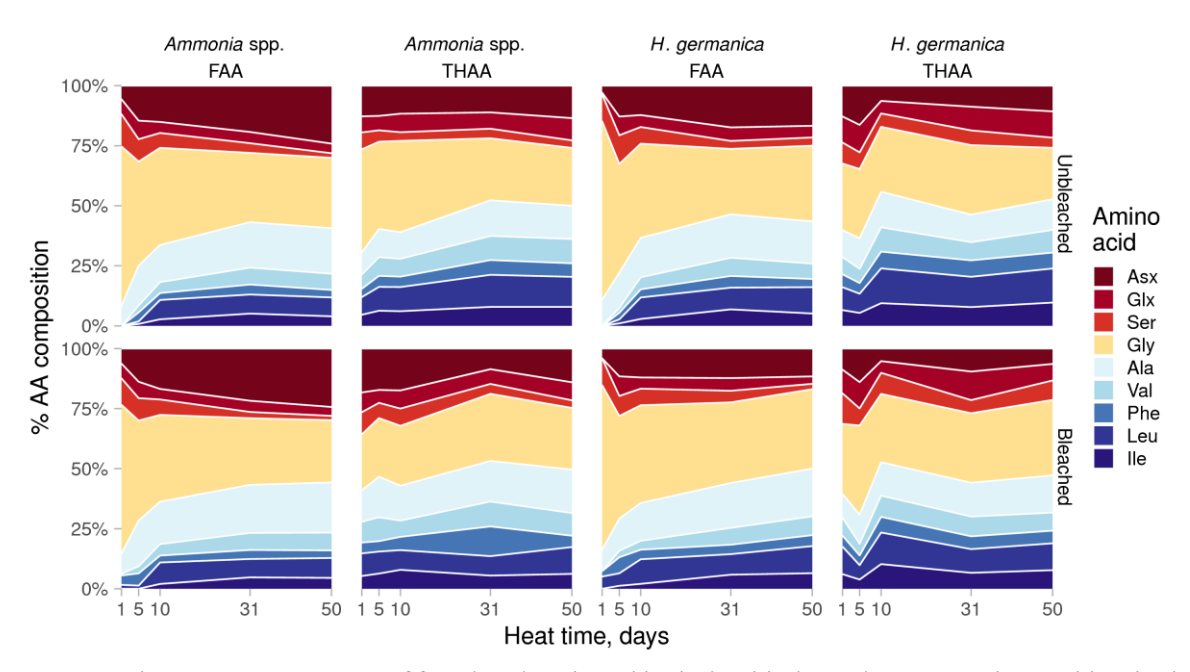


Fig. 5.9 – Change in composition of free (FAA) and total hydrolysable (THAA) amino acids in unbleached (whole-shell) and bleached (intra-crystalline) *Ammonia* spp. and *H. germanica* during 110°C heating experiment. X-axis labels show the time points for which data were collected. Arg, Tyr, Met, His and Thr are poorly resolved using RP-HPLC, and have therefore been excluded.

There is relatively little change in composition in the THAA fraction for either species (**Fig. 5.9**), although the trends for *H. germanica* are complicated by anomalous compositions at 5 days of heating in both the unbleached and bleached samples, with higher proportions of Asx (and in the bleached samples Gly) than *H. germanica* heated for 1 or 10 days. % Ser decreases in both the whole-shell and intra-crystalline fractions of *Ammonia* spp., and in the whole-shell fraction of *H. germanica* (any trend in % Ser in the intra-crystalline fraction is unclear for *H. germanica*), while % Ala increases somewhat for both species during the early stages of heating. This increase in % Ala may be due to its being a decomposition product of Ser (Bada et al., 1978). Similar patterns have been observed in high-temperature experiments of various molluscs: decreasing % Ser and increasing % Ala, decreasing or stable % Asx, and stable or slightly increasing % Glx, Gly and Leu (Demarchi et al., 2013b; Ortiz et al., 2017, 2019). The trends in composition are similar at 140°C,

with a more pronounced decrease in % Asx (for *Ammonia* spp.) and % Ser (for both species) in the THAA fraction, due to the more rapid decomposition of these relatively unstable amino acids at higher temperatures (**Appendix A3.2**).

5.3.3 Peptide bond hydrolysis

The percentage of free amino acids (FAA) in the total hydrolysable amino acid (THAA) pool was used to estimate the patterns of peptide bond hydrolysis in *Ammonia* spp. and *H. germanica*. Although this approach underestimates the rate of hydrolysis (as some proportion of free amino acids will be removed from the FAA pool through decomposition), it enables a comparison between different amino acids and fractions in each species.

The hydrolysis of Asx, Glx, Gly, Ala, Leu and all amino acids ('total') are presented in this section. Of the late-eluting amino acids, Leu has the lowest variability between replicates; the others (Phe, Val and Ile) have similar trends, but the concentration data for them is more variable, so they are not included. Free Ser is dominated by laboratory contamination (Section 5.3.1.1), therefore Ser is not presented in this section. As the [FAA] of Ser remained very low throughout the heating experiment, this suggests its rapid decomposition in the free state (Orem and Kaufman, 2011; Demarchi et al., 2013b).

Fig. 5.10 shows the percentage of amino acids in the free state in *Ammonia* spp. over the course of the 110°C experiment. Although the concentration data are quite variable, especially for the bleached material (likely due to the low amino acid concentrations in the intra-crystalline fraction, see Section 5.3.1.2), there is a clear trend of increasing % FAA over time as the biomineral proteins undergo hydrolysis. The rate of hydrolysis varies between amino acids, with similar patterns at 110°C as at 140°C (Fig. 5.11). Asx has the highest hydrolysis rate, followed by Ala and Gly, while Glx and Leu hydrolyse more slowly, a pattern seen in both coral (Tomiak et al., 2013) and the bivalve *Pecten* (Pierini et al., 2016). Conversely, in the gastropod *Patella vulgata*, Ala and Gly have higher hydrolysis rates than Asx (Demarchi et al., 2013b).

At the end of the heating experiment, % FAA is higher in the bleached than unbleached material (~50% for all amino acids at 50 days in bleached samples, compared to ~20% in unbleached samples). This suggests that free amino acids, and possibly also small peptides, are leached from the inter-crystalline fraction over time, while they are better retained in the intra-crystalline fraction.

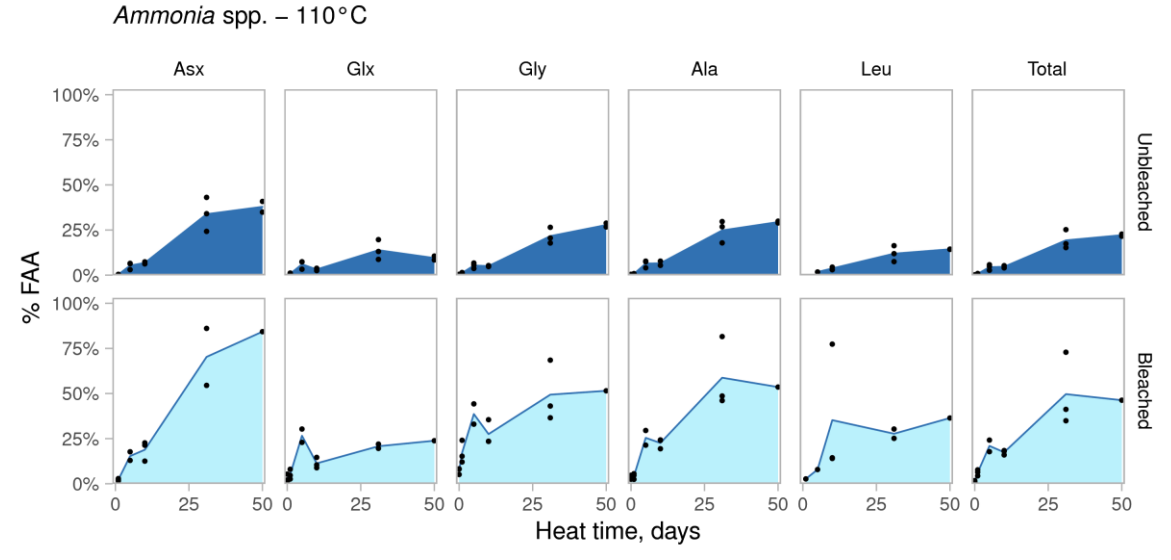


Fig. 5.10 – Percentage of amino acids in free state (% FAA) for Asx, Glx, Gly, Ala, Leu and all amino acids ('total') in unbleached (whole-shell) and bleached (intra-crystalline) *Ammonia* spp., heated to 110°C.

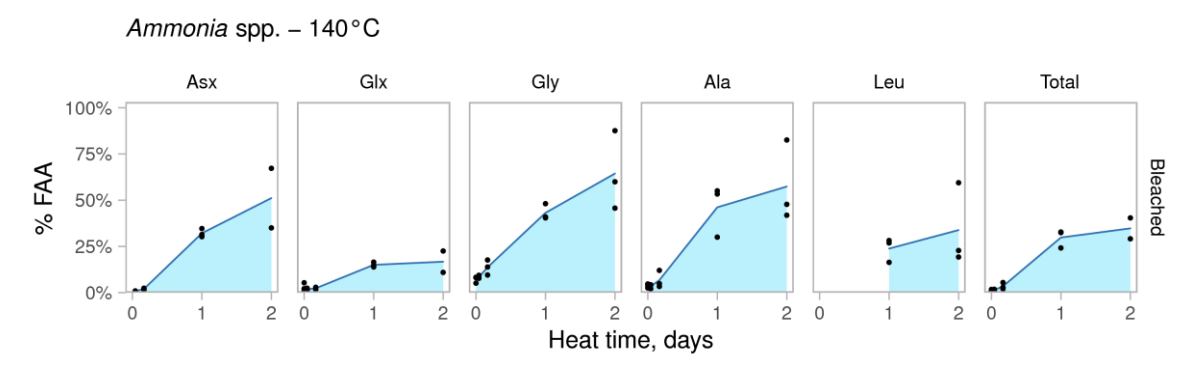


Fig. 5.11 – Percentage of amino acids in free state (% FAA) for Asx, Glx, Gly, Ala, Leu and all amino acids ('total') in bleached (intra-crystalline) *Ammonia* spp., heated to 140°C. Leu was not detected in any FAA samples heated for less than 1 day.

The trends in hydrolysis for *H. germanica* are less clear due to the higher variability in concentrations for this species, especially for the bleached fraction, where several samples have an unexpectedly high % FAA at 5 days of heating in the 110°C suite of experiments (**Fig. 5.12**). As in *Ammonia* spp., % FAA is higher in the bleached samples (~25% at 50 days for all amino acids) than the unbleached samples (~10% at 50 days). At both 110°C (**Fig. 5.12**) and 140°C (**Fig. 5.13**) there is an apparent plateauing of hydrolysis in the bleached samples. This plateau has been observed in high-temperature decomposition experiments of various mollusc species (Penkman et al., 2008; Orem and Kaufman, 2011) and may be due to the preferential hydrolysis of weak peptide bonds during early stages of decomposition.

H. germanica - 110°C

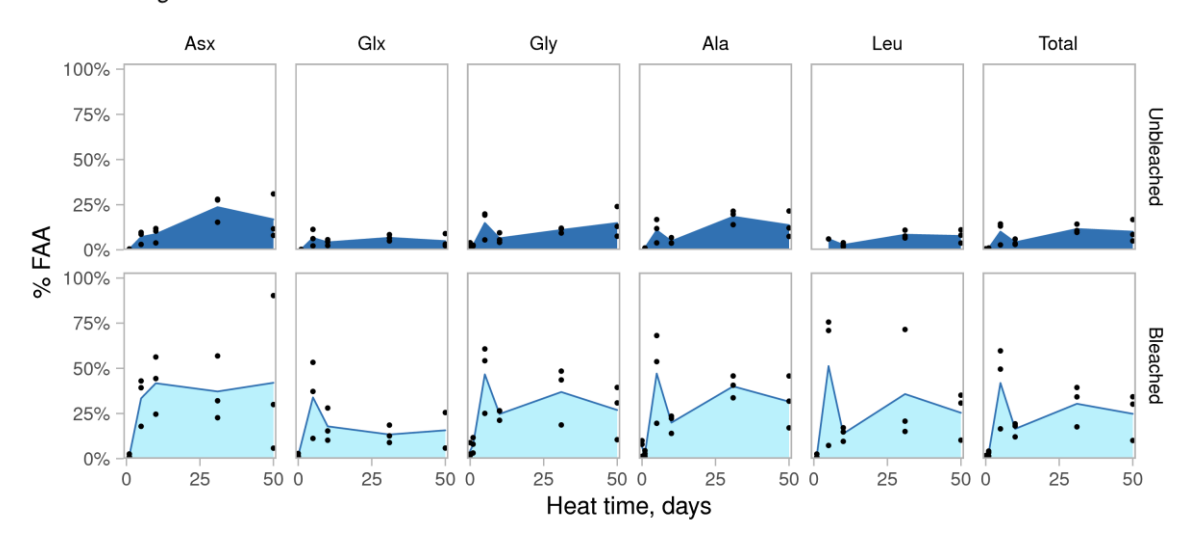


Fig. 5.12 – Percentage of amino acids in free state (% FAA) for Asx, Glx, Gly, Ala, Leu and all amino acids ('total') in unbleached (whole-shell) and bleached (intra-crystalline) *H. germanica*, heated to 110°C.

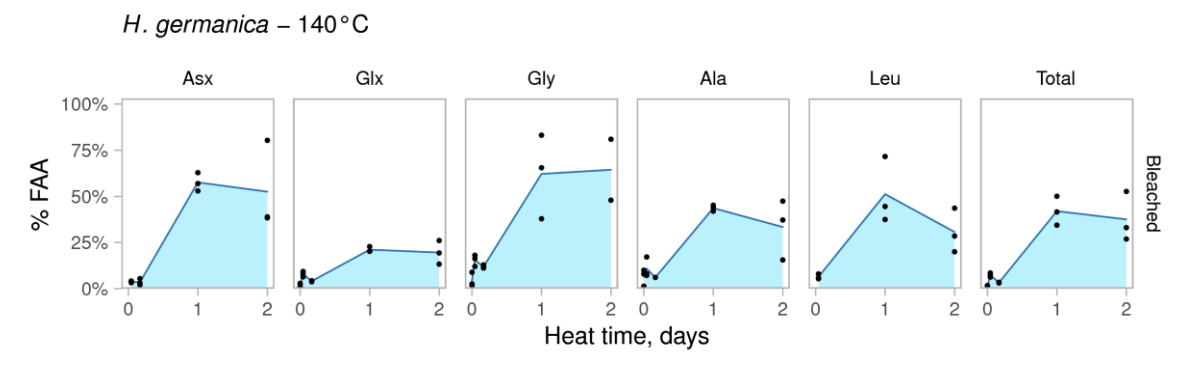


Fig. 5.13 – Percentage of amino acids in free state (% FAA) for Asx, Glx, Gly, Ala, Leu and all amino acids ('total') in bleached (intra-crystalline) *H. germanica*, heated to 140°C.

In general, the patterns of hydrolysis in *Ammonia* spp. and *H. germanica* are similar to other biominerals, with Asx, Gly and Ala hydrolysing more quickly than Gly and Leu. The slower observed rate of hydrolysis in the whole-shell fraction reflects the leaching of FAA from the inter-crystalline fraction of both species, as can be seen in the patterns of [FAA] in each fraction (Section 5.3.1.2).

5.3.4 Racemisation

5.3.4.1 General trends

FAA and THAA D/L values are presented for Asx, Glx, Ser, Ala, Val, Phe, Leu and Ile in *Ammonia* spp. and *H. germanica* heated to 110°C (**Fig. 5.14**) and 140°C (**Fig. 5.15**). Thr and His are not shown, as it is only possible to separate their D- and L-isomers using UHPLC. While L- and D-Tyr and Met can be

separated using RP-HPLC, very few samples produced D/L values for these amino acids due to their low concentrations, so they are not shown; similarly Arg is excluded as D-Arg is typically compromised by a co-eluting compound (Powell et al., 2013). Rather than applying a blank correction, samples with an amino acid concentration below the average +1 standard deviation (σ) of the independently analysed blanks (Section 5.3.1.1) are flagged as likely to be compromised. Additionally, D/L values above 1.0 (or 1.3 for Ile) are excluded (see Section 5.2.3). As RFOK_a does not allow D/L values above the equilibrium value, this exclusion criterion ensures that the models applied in Section 5.3.4.4 are compared using the same data.

Between replicates, D/L values are generally less variable than concentration values, as the ratio of D- to L-amino acids cancels out errors associated with calculating concentration, which are the same for every amino acid in a sample (Powell et al., 2013). At 110°C, Asx, Glx and Ala are well resolved by RP-HPLC for both bleached and unbleached *Ammonia* spp. (Fig. 5.14); the later-eluting amino acids (Val, Phe, Leu and Ile) are more poorly resolved, especially in the FAA fraction, and in bleached material. This is likely due to an increasingly noisy baseline towards the latter end of the chromatogram, as well as more non-amino acid peaks which can interfere with accurate determination of peak areas at very low concentrations (see Section 2.4). The unbleached THAA fraction (the fraction with the highest concentrations) has lower between-replicate variability than the other fractions, suggesting that the variability seen in the unbleached FAA and bleached FAA and THAA fractions predominantly arises from difficulties quantifying D/L accurately at very low concentrations. The same pattern of variability is seen for *H. germanica* (Fig. 5.14), although in general the results are more variable for *H. germanica* than for *Ammonia* spp.

D/L increases with time for all amino acids, with the exception of Ser. FAA Ser is dominated by laboratory contamination, so the extent of racemisation in this fraction likely represents the decomposition of contaminant amino acids introduced prior to heating. THAA Ser increases sharply, then reverses after about 10 days in both the whole-shell and intra-crystalline fractions of both species. This pattern has been widely observed in other biominerals, including ostracodes (Bright and Kaufman, 2011b), tooth enamel (Dickinson et al., 2019) and various mollusc species (Penkman et al., 2008; Demarchi et al., 2013b, 2015). The rapid initial rate of Ser racemisation is due to its ability to racemise in-chain (Demarchi et al., 2013a); its subsequent D/L reversal is thought to be caused by the dehydration of Ser to Ala (Bada and Man, 1980; Demarchi et al., 2013b; Pierini et al., 2016).

The 140°C suite follows the same general patterns of racemisation as the 110°C suite, with the exception of Ala which was poorly resolved using the UHPLC method (**Fig. 5.15**, see also **Section 2.4.2**). As expected, racemisation proceeds much more quickly at 140°C than 110°C: Asx, the fastest racemising amino acid, reaches a D/L value of ~0.9 in the FAA fraction after around 1 day of heating at 140°C, compared to around 30 days at 110°C. During the early stages of heating at 140°C (< 1 day) few samples have detectable D-amino acids in the FAA fraction, particularly for *Ammonia* spp., due to the limited extent of hydrolysis. After around 4 hours, the majority of the Ser in the THAA fraction is dominated by laboratory contamination, suggesting that Ser decomposes rapidly at this higher temperature.

As there is a more complete dataset for the 110°C suite of experiments, the patterns of D/L covariance, both between the FAA and THAA fractions, and between different amino acids, are discussed for 110°C in detail below (Section 5.3.4.2). This is followed by a comparison of the relative racemisation rates of each amino acid at 110°C (Section 5.3.4.3). The 140°C suite showed similar trends of covariance and relative rates. Due to its smaller number of time points, and as the 110°C suite is sufficient to investigate the patterns of racemisation in each species and biomineral fraction, the 140°C suite is not discussed here in detail. Additional results of the 140°C suite of experiments can be found in Appendix A3.3.

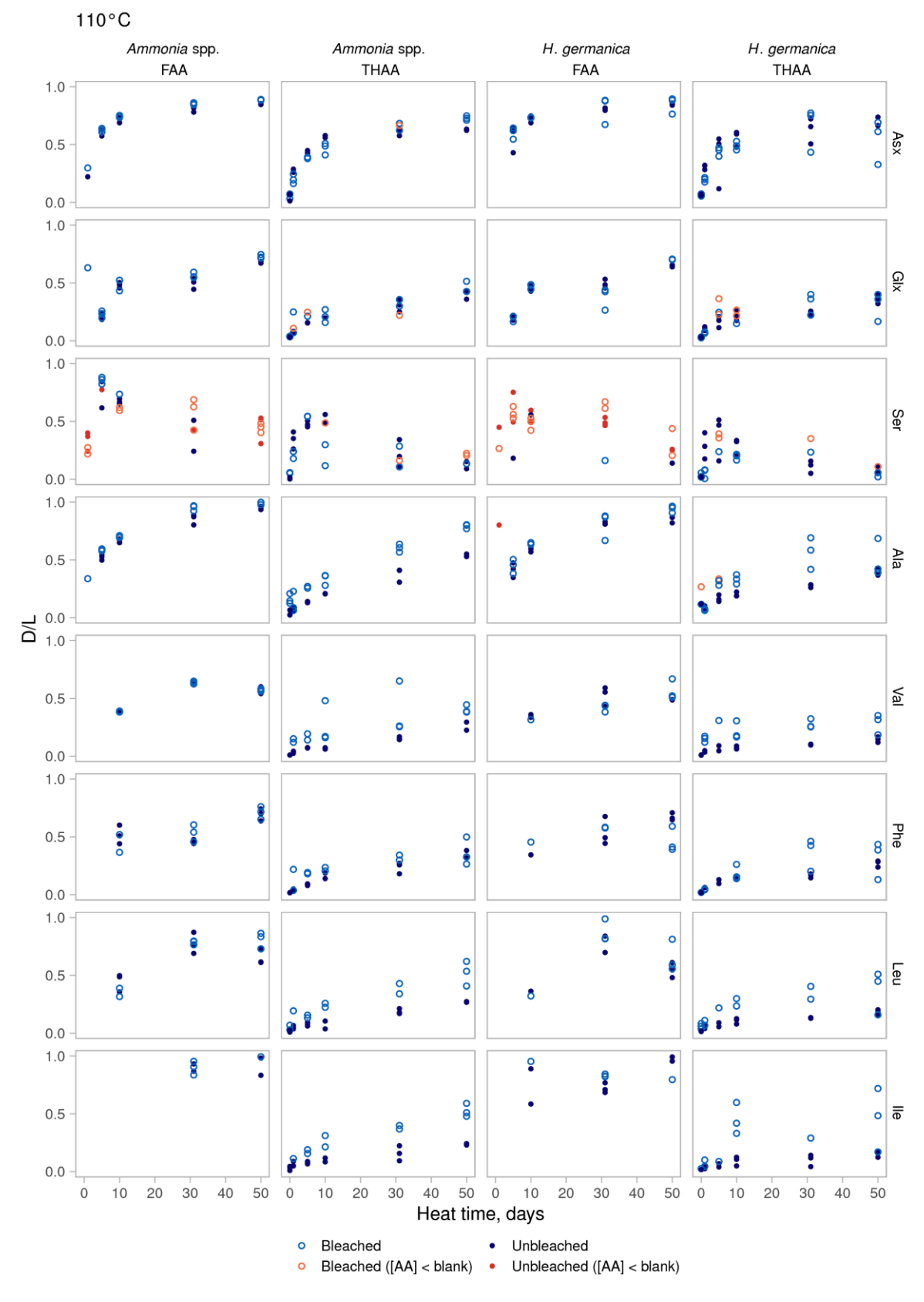


Fig. 5.14 – Racemisation of Asx, Glx, Ser, Ala, Val, Phe, Leu and Ile in the free amino acid (FAA) and total hydrolysable amino acid (THAA) fractions of unbleached (whole-shell) and bleached (intra-crystalline) *Ammonia* spp. and *H. germanica* at 110° C. Samples with an amino acid concentration below the average + 1 σ of the blanks are highlighted in orange.

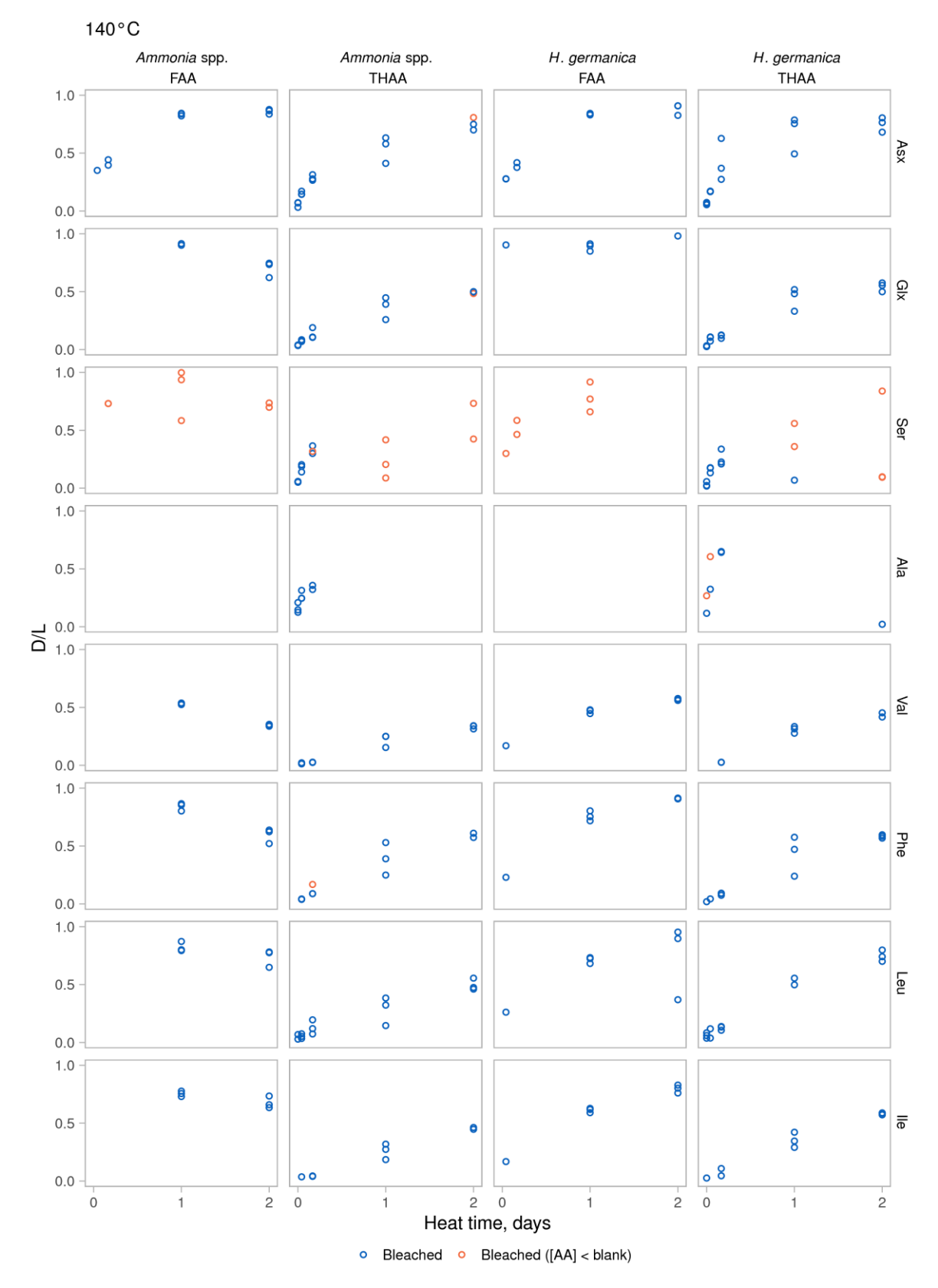


Fig. 5.15 – Racemisation of Asx, Glx, Ser, Ala, Val, Phe, Leu and Ile in the free amino acid (FAA) and total hydrolysable amino acid (THAA) fractions of bleached (intra-crystalline) *Ammonia* spp. and *H. germanica*, heated to 140°C. Samples with an amino acid concentration below the average + 1 σ of the blanks are highlighted in orange.

5.3.4.2 D/L Covariance

In a closed system, the trends in racemisation in the free and total hydrolysable fractions of amino acids should be highly correlated (Kaufman and Manley, 1998; Collins and Riley, 2000). FAA D/L values are generally higher than THAA D/L values at any given point, due to the rapid racemisation of amino acids while in terminal positions before being hydrolysed into the free state (this pattern is not seen in enamel, however (Dickinson, 2018)). The covariance of FAA and THAA D/L values can be used as a test for closed-system behaviour in biominerals (Penkman et al., 2008), and a closer correlation between FAA D/L and THAA D/L in the intra-crystalline fraction can indicate that it behaves as a more reliable closed system than the whole-shell fraction.

The covariance of FAA and THAA D/L values for Asx, Glx, Ser, Ala, Val, Phe, Leu and Ile in the 110°C suite of experiments are shown in Fig. 5.16 and Fig. 5.17 for *Ammonia* spp. and *H. germanica* respectively. In *Ammonia* spp., Asx and Ala show good FAA/THAA D/L covariance in both the unbleached and bleached material (Fig. 5.16). The relationship is poorer for the other amino acids, which is at least partly due to lower concentrations for these amino acids. The very low Ser [FAA] compared to the blanks compromises the FAA Ser D/L measurements (note the orange points in Fig. 5.16), resulting in a poor FAA/THAA D/L correlation for Ser. The poorer correlation for Glx is most likely due to the difficulty analysing free Glx (Demarchi et al., 2013b), although poor Glx FAA/THAA D/L covariance is not observed in all biominerals (Crisp et al., 2013; Dickinson et al., 2019). For the later-eluting amino acids (Val, Phe, Leu and Ile), insufficient FAA was present during early stages of heating for a FAA D/L measurement, limiting the usefulness of FAA/THAA D/L covariance as a test of predictable racemisation patterns for these amino acids over the time period measured here.

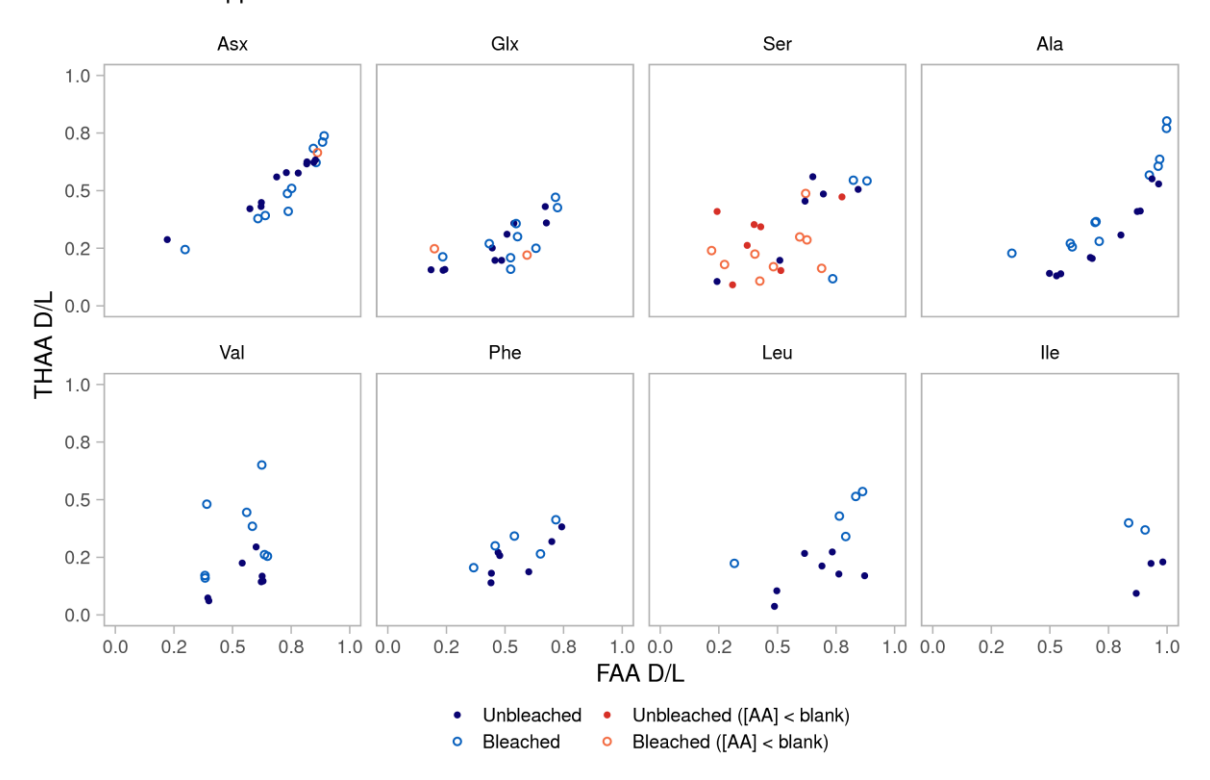


Fig. 5.16 – Covariance between D/L values in the free amino acid (FAA) and total hydrolysable amino acid (THAA) fractions for various amino acids in unbleached (whole-shell) and bleached (intracrystalline) *Ammonia* spp., heated to 110° C. Samples with either an FAA or THAA concentration below the average + 1σ of the blank are highlighted in orange.

The FAA/THAA D/L covariance for *H. germanica* is much poorer than for *Ammonia* spp. (**Fig. 5.17**), especially in the unbleached material, although generally similar behaviour is seen with Asx and Ala having better FAA/THAA D/L covariance than the other amino acids, particularly the later-eluting amino acids (Val, Phe, Leu and Ile), where fewer samples have FAA D/L values to enable comparison. This pattern may be due to the lower concentrations of amino acids in *H. germanica* (**Section 5.3.1**). For Asx, FAA and THAA D/L are more closely correlated in the intra-crystalline fraction than the whole-shell fraction (there is possibly also a slight improvement for Ala and Phe), which suggests that the intra-crystalline fraction may behave as a more reliable closed system than the whole-shell fraction in *H. germanica*.

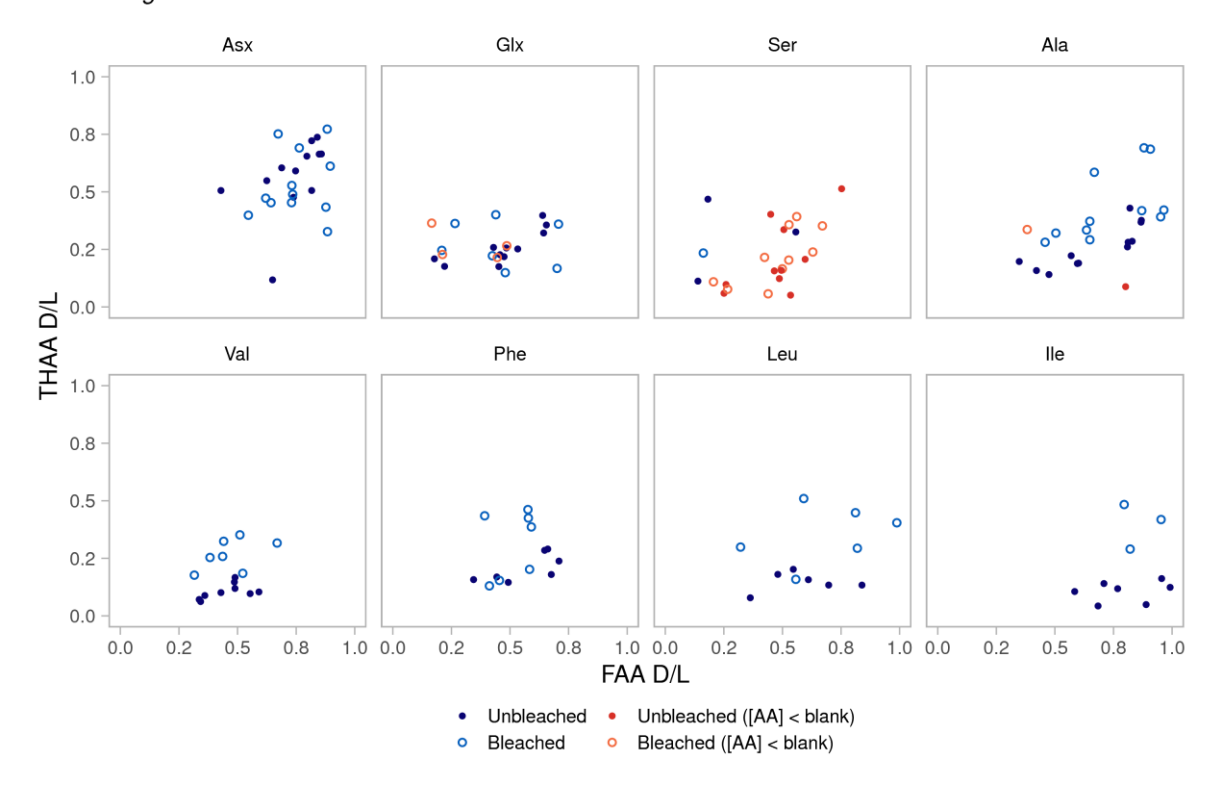


Fig. 5.17 – Covariance between D/L values in the free amino acid (FAA) and total hydrolysable amino acid (THAA) fractions for various amino acids in unbleached (whole-shell) and bleached (intracrystalline) H. germanica, heated to 110°C. Samples with either an FAA or THAA concentration below the average + 1 σ of the blank are highlighted in orange.

The covariance between D/L values of different amino acids can also be used to assess the integrity of biominerals (e.g. Kaufman, 2006; Kosnik and Kaufman, 2008; Hendy et al., 2012), especially during early time points where [FAA] is too low to provide reliable D/L values (Penkman et al., 2008). Fig. 5.18 and Fig. 5.19 show the covariance of Asx D/L against Glx, Ala, Phe, Leu and Ile for *Ammonia* spp. and *H. germanica* respectively. Both species show good covariance between Asx D/L, and Glx and Ala D/L, particularly in the FAA fraction; in the THAA fraction Asx D/L is well correlated with Glx, Ala, Phe, Leu and Ile for both species. In the THAA fraction of the whole-shell *Ammonia* spp., an inflection point of the Asx D/L trajectory is visible at ~0.6, demonstrating how the racemisation rate of Asx slows dramatically in comparison to the other amino acids. This 'two-stage' racemisation of Asx has also been observed in the foraminifer *P. obliquiloculata* (Harada and Handa, 1995).

Ammonia spp. - 110°C

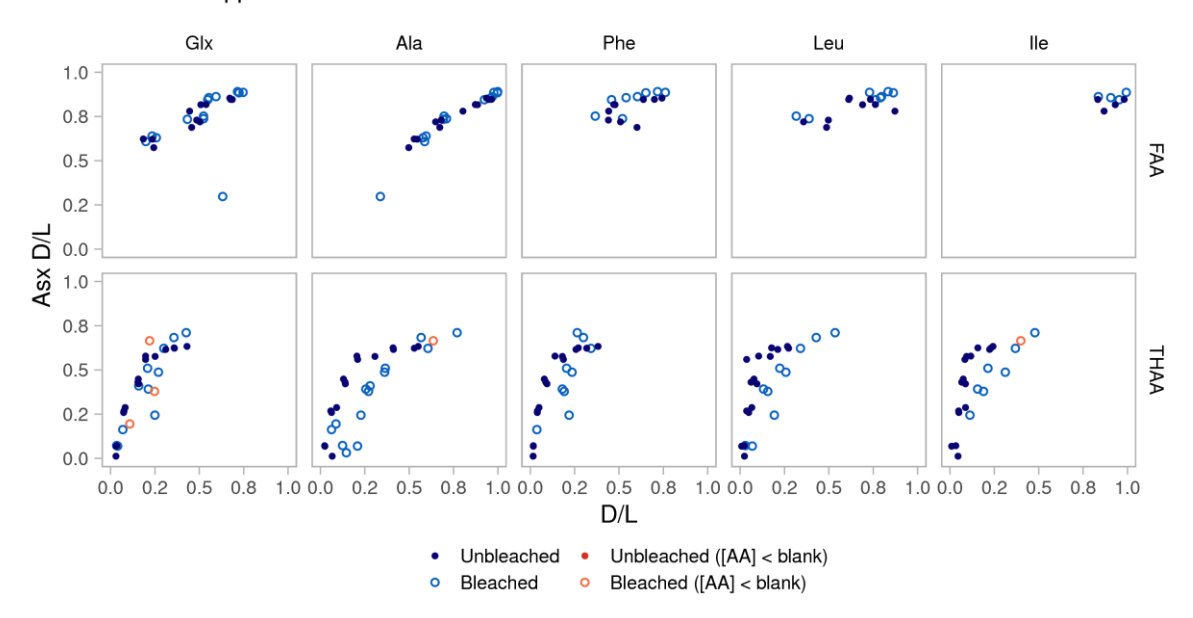


Fig. 5.18 – Covariance between Asx D/L and other amino acids in unbleached (whole-shell) and bleached (intra-crystalline) *Ammonia* spp., heated to 110° C. Samples with either Asx or another amino acid concentration below the average + 1 σ of the blank are highlighted in orange. Upper: free amino acids (FAA); lower: total hydrolysable amino acids (THAA).

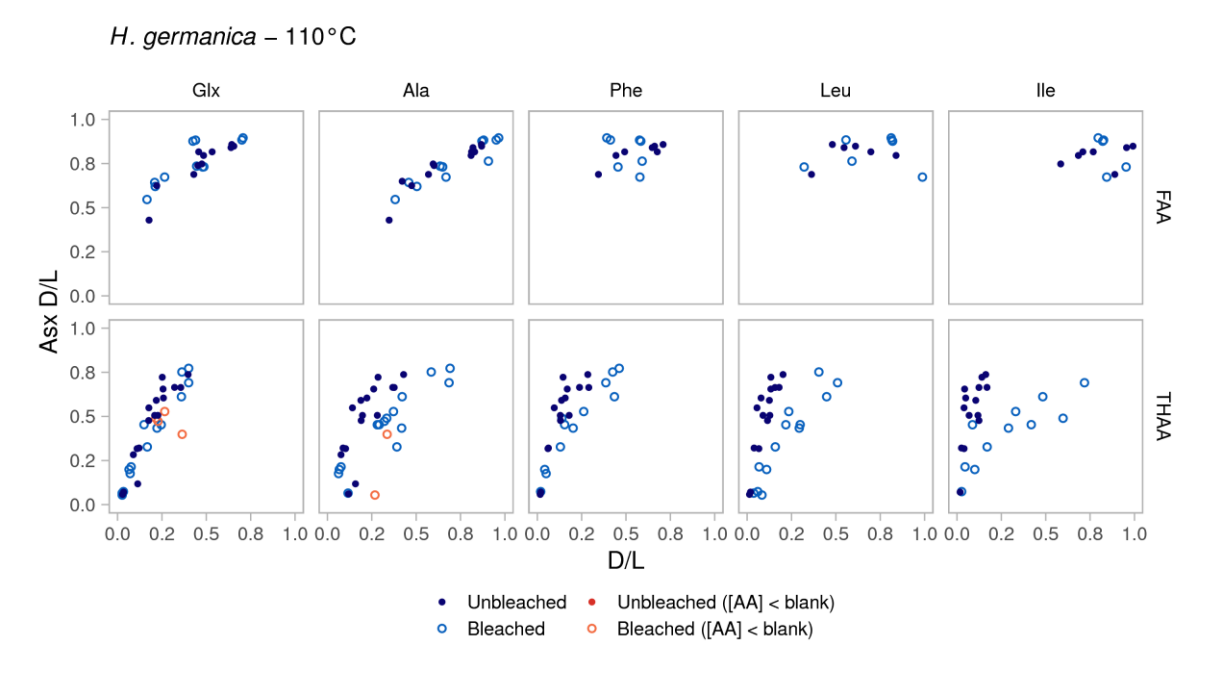


Fig. 5.19 – Covariance between Asx D/L and other amino acids in unbleached (whole-shell) and bleached (intra-crystalline) H. germanica, heated to 110° C. Samples with either Asx or another amino acid concentration below the average + 1 σ of the blank are highlighted in orange. Upper: free amino acids (FAA); lower: total hydrolysable amino acids (THAA).

Interestingly, the amino acid covariance plots show a clear deviation in the racemisation trajectory between the unbleached and bleached samples in the THAA fraction, but not the FAA fraction. This, along with the patterns of [FAA] (Section 5.3.1.3), suggests that FAA are readily leached from the inter-crystalline fraction of the biomineral, resulting in a 'whole-shell' FAA fraction comprised predominantly of intra-crystalline amino acids. For Ala, the amino acid with the best correlation with Asx, the FAA fraction shows less variance than the THAA fraction, despite the lower concentrations of FAA.

The patterns of D/L covariance between the FAA and THAA fractions, and between amino acids, of *Ammonia* spp. and *H. germanica* show that Asx, Glx and Ala, and THAA Phe, Leu and Ile, have well-correlated, systematic patterns of racemisation. The lack of early FAA Phe, Leu and Ile D/L values hindered the use of FAA/THAA D/L covariance for these amino acids; however all three amino acids showed good covariance with Asx D/L in the THAA fraction. The patterns of covariance were similar for the whole-shell and intra-crystalline FAA fractions in both species; however, in the THAA fraction the racemisation trajectory of the whole-shell and intra-crystalline fractions differed, particularly for *H. germanica*.

5.3.4.3 Relative racemisation trends

Fig. 5.20 and Fig. 5.21 show the racemisation trends of Asx, Glx, Ala, Leu and Phe for *Ammonia* spp. and *H. germanica* respectively, heated to 110°C. Ser has been excluded from this comparison due to its low concentrations in the FAA fraction and D/L reversal during this experiment in the THAA fraction (see Section 5.3.4.1).

In the FAA fraction of *Ammonia* spp. (**Fig. 5.20**), Asx and Ala are the fastest racemising amino acids; Asx has a higher racemisation rate than Ala during the initial stages of decomposition, but is overtaken by Ala in both the unbleached and bleached fractions, a pattern which has been observed in other biominerals (Penkman et al., 2008; Bright and Kaufman, 2011b; Ortiz et al., 2017, 2019). A lack of D/L values for FAA Phe and Leu at early stages of heating make comparison difficult for these amino acids; nevertheless Phe and Glx appear to have the lowest racemisation rates, while Leu has a racemisation rate intermediate between Asx and Ala, and Phe and Glx.

The patterns are slightly different in the THAA fraction of *Ammonia* spp. (Fig. 5.20); in the whole-shell material Asx has a much higher racemisation rate than the other amino acids, which follow the relative order of Ala > Glx > Phe > Leu. In the intra-crystalline fraction, the behaviour of Asx and Ala is more similar to the whole-shell and intra-crystalline FAA fractions. This makes sense given

Section 5.3.1), presumably due to leaching of inter-crystalline FAA from the whole-shell fraction during decomposition. As Ala has been found to racemise much more slowly than Asx in free amino acid studies (e.g. Bada, 1970; Smith and Evans, 1980), the relatively fast observed rate of Ala racemisation in *Ammonia* spp. and *H. germanica* may result from a contribution of racemic Ala from the rapid dehydration of free Ser (Demarchi et al., 2013b; Pierini et al., 2016). If a significant proportion of this pool of free Ala is leached from the inter-crystalline fraction of the biomineral, this may explain why the apparent rate of Ala racemisation is 'suppressed' in the whole-shell THAA fraction. Conversely to Ala, intra-crystalline THAA Leu, Phe and Glx have similar patterns to the FAA fraction, following the order Leu > Glx ~ Phe.

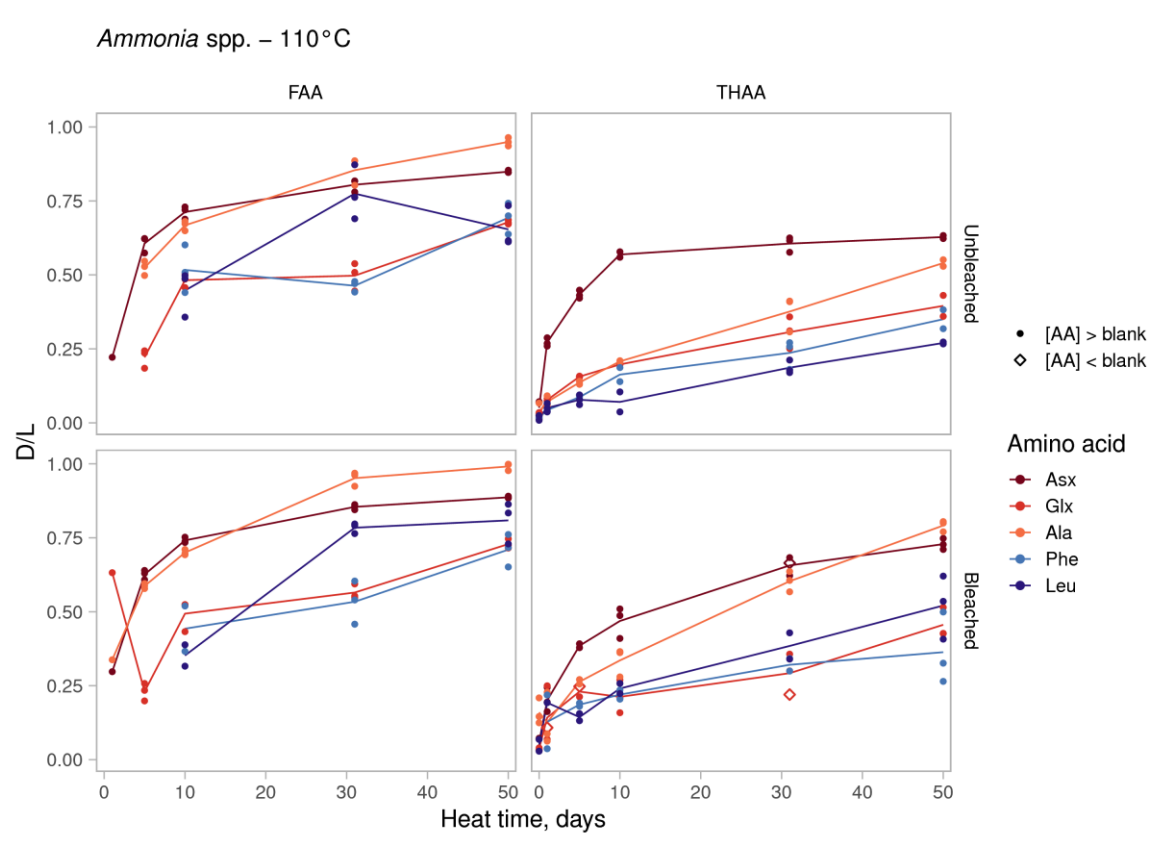


Fig. 5.20 – Comparison between racemisation of Asx, Glx, Ala, Phe and Leu in unbleached (whole-shell) and bleached (intra-crystalline) *Ammonia* spp., heated to 110° C. The solid line shows the average D/L over time; the points are individual replicates. Samples with amino acid concentrations below the average + 1 σ of the blank are shown as open diamonds. Left: free amino acids (FAA); right: total hydrolysable amino acids (THAA).

Although the D/L values are generally more variable for *H. germanica*, similar patterns in relative racemisation rates can be seen (**Fig. 5.21**). In the FAA fraction, Asx and Ala have the fastest racemisation rates, with Ala 'catching up' (whole-shell) or overtaking (intra-crystalline) Asx over the

course of the experiment. As in *Ammonia* spp., a general trend of Leu > Phe $^{\sim}$ Glx emerges for FAA. In the whole-shell THAA fraction, *H. germanica* follows a relative order of Asx >> Ala $^{\sim}$ Glx > Phe > Leu, similar to *Ammonia* spp. Although Ala doesn't overtake Asx in the intra-crystalline THAA fraction as for *Ammonia* spp., Ala has a more similar racemisation rate to Asx than in the whole-shell fraction, suggesting a greater influence of FAA in the intra-crystalline THAA fraction of *H. germanica*. The rates of racemisation for all five amino acids are similar for the two species (**Fig. 5.22**).

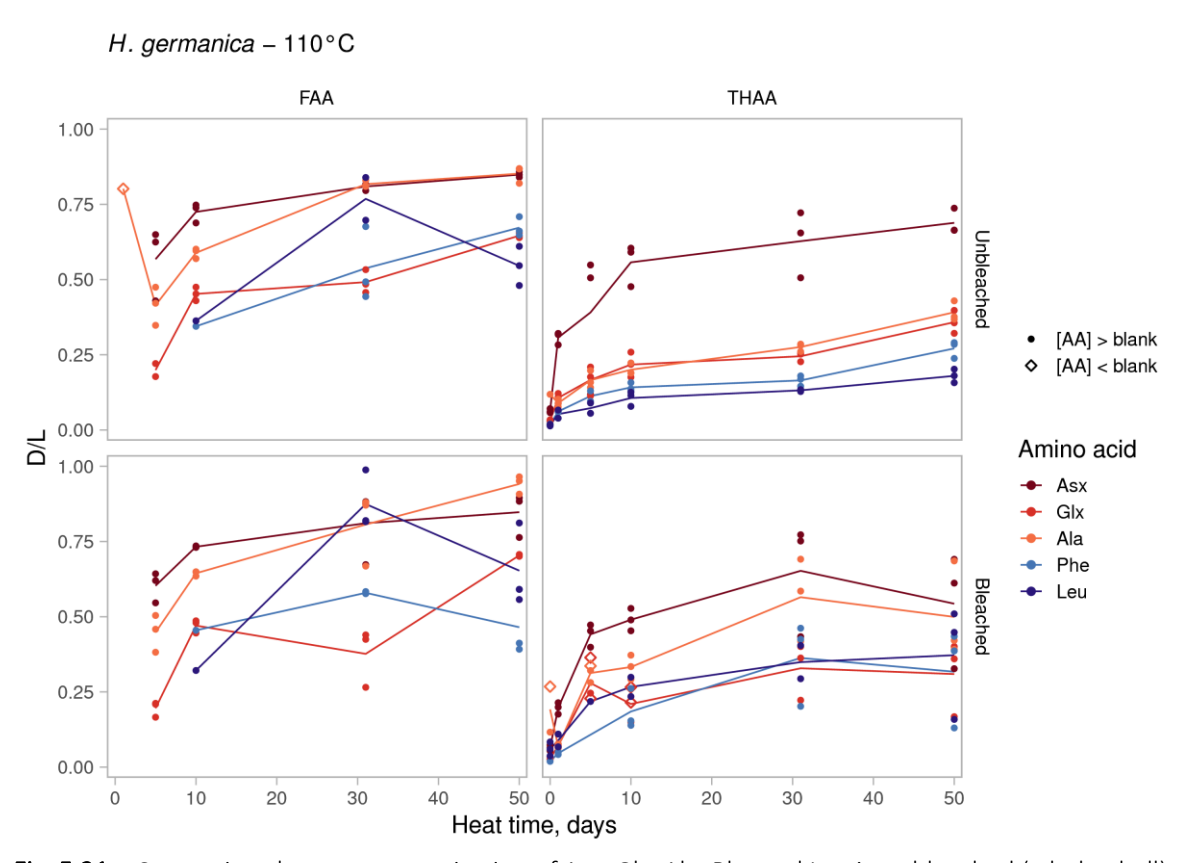


Fig. 5.21 – Comparison between racemisation of Asx, Glx, Ala, Phe and Leu in unbleached (whole-shell) and bleached (intra-crystalline) H. germanica, heated to 110° C. The solid line shows the average D/L over time; the points are individual replicates. Samples where the amino acid concentration was below the average + 1 σ of the blank are shown as open diamonds. Left: free amino acids (FAA); right: total hydrolysable amino acids (THAA).

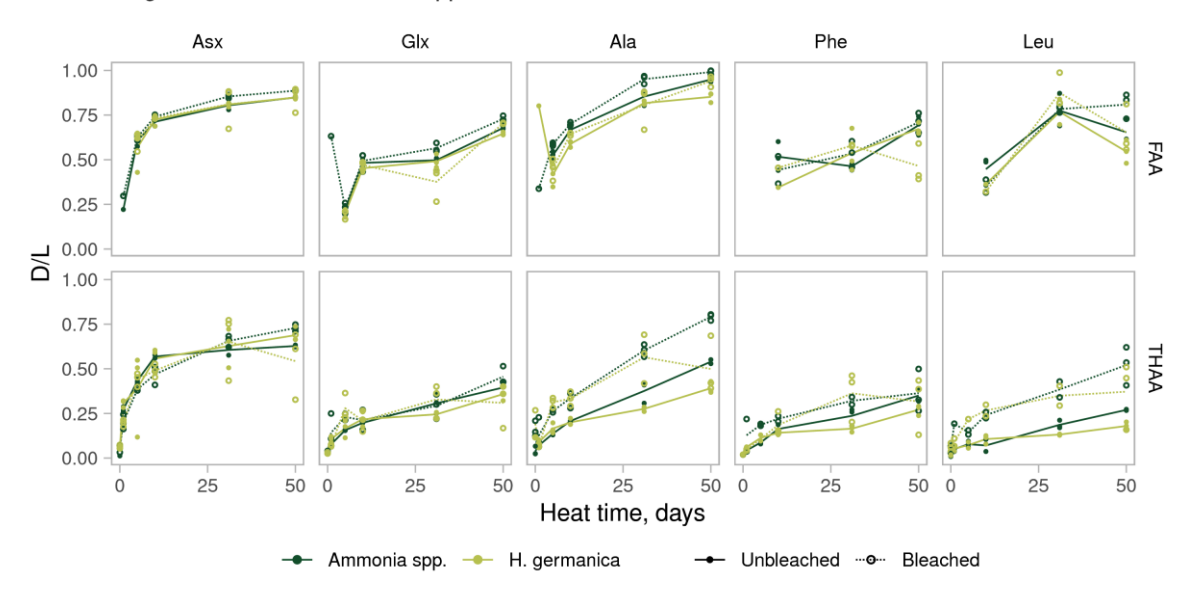


Fig. 5.22 – Comparison between racemisation of Asx, Glx, Ala, Phe and Leu in FAA and THAA unbleached (whole-shell) and bleached (intra-crystalline) *Ammonia* spp. and *H. germanica*, heated to 110°C. The solid (unbleached) and dashed (bleached) lines show the average D/L over time; the closed (unbleached) and open (bleached) circles are individual replicates. Note that samples with amino acid concentration below the average $+ 1 \sigma$ of the blank have not been highlighted in this graph.

For all amino acids in both species, the extent of FAA racemisation is higher than THAA (**Fig. 5.23**). This has been widely observed in other biominerals (e.g. various mollusc shells (Penkman et al., 2008; Demarchi et al., 2013b), ostrich eggshell (Crisp et al., 2013) and coral (Tomiak et al., 2013)), and is thought to be because free amino acids must pass through rapidly-racemising terminal positions during hydrolysis (Wehmiller, 1980; Mitterer and Kriausakul, 1984). The rates of FAA racemisation in the unbleached and bleached material are similar; conversely in the THAA fraction the unbleached D/L values are higher in the intra-crystalline fraction than the whole-shell fraction for several amino acids (Ala, Leu, possibly Phe). This could be due to the removal of laboratory contamination by bleaching (which could suppress the measured D/L values of the unbleached material), or due to the higher proportion of highly-racemised FAA retained in the intra-crystalline fraction; the latter is supported by the concentration data (**Fig. 5.3**, **Fig. 5.4**).

FAA and THAA - 110°C

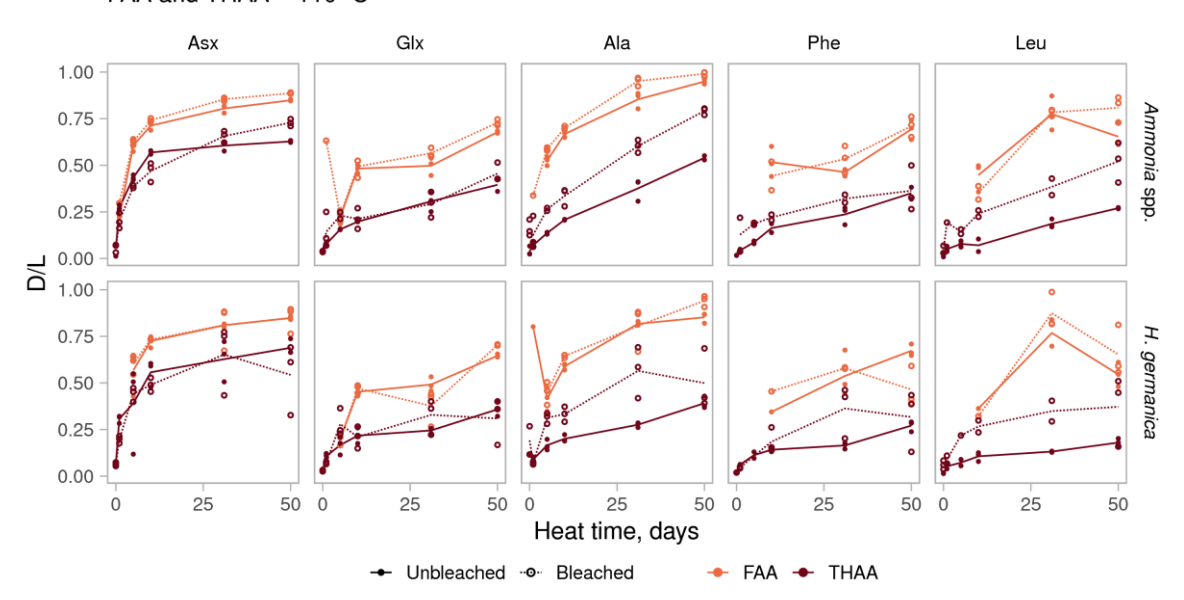


Fig. 5.23 – Comparison between amino acids (Asx, Glx, Ala, Phe, Leu) in different fractions (FAA and THAA, unbleached (whole-shell) and bleached (intra-crystalline)) of *Ammonia* spp. and *H. germanica*, heated to 110°C. The solid (unbleached) and dashed (bleached) lines show the average D/L over time; the closed (unbleached) and open (bleached) circles are individual replicates. Note that samples with amino acid concentration below the average + 1 σ of the blank have not been highlighted in this graph.

Overall, the relative rates of racemisation observed in *Ammonia* spp. and *H. germanica* follow predictable patterns, with amino acid racemisation rates typically following the order Asx > Ala > Leu > Phe ~ Glx, with Ile having a similar racemisation rate to Phe and Glx in the 140°C suite of experiments, where it was well resolved (**Appendix 3**). This general trend of faster racemisation of Asx and Ala compared to other amino acids is similar to the patterns seen in a range of other biominerals (e.g. bone (Bada and Shou, 1980), various molluscs (Penkman et al., 2008; Demarchi et al., 2013b; Pierini et al., 2016; Ortiz et al., 2017) and ostracodes (Bright and Kaufman, 2011b)), although in some biominerals the rate of Ala racemisation is similar to or slower than Phe and Glx (e.g. ostrich eggshell (Crisp et al., 2013), the bivalve *Glycymeris* (Demarchi et al., 2015) and enamel (Dickinson et al., 2019)).

In some fractions (whole-shell and intra-crystalline FAA, and intra-crystalline THAA, for *Ammonia* spp.; intra-crystalline FAA for *H. germanica*), the rapid slowing of Asx racemisation results in a higher Ala D/L at the end of the experiment, a pattern which has been observed in ostracodes (Bright and Kaufman, 2011b) and various molluscs (Penkman et al., 2008; Ortiz et al., 2017, 2019). The relative rate of Leu racemisation is quite variable, being slower than the other amino acids in the whole-shell THAA fractions of both species, but at the same rate or faster than Phe and Glx in the other fractions.

The observed rate of FAA racemisation is higher than THAA racemisation for all amino acids in both species, most likely due to amino acids in the FAA fraction having passed through terminal positions, where racemisation rates are accelerated, during hydrolysis. For the FAA fraction, and THAA Asx and Glx, the rates of racemisation between the whole-shell and intra-crystalline fractions are similar; however, for THAA Ala, Phe and Leu, the intra-crystalline fraction is more racemised than the whole-shell fraction. The differences in behaviour between the whole-shell and intra-crystalline fractions indicate that the whole-shell fraction behaves as an open system, at least with respect to FAA. Conversely, intra-crystalline FAA are more effectively retained within the biomineral, which is consistent with the observed patterns of amino acid concentration change (Section 5.3.1).

5.3.4.4 Modelling racemisation

To test the performance of kinetic models on *Ammonia* spp. and *H. germanica*, three kinetic models were applied to the data from the 110°C suite of experiments: apparent reversible first order kinetics (RFOK_a, **Equation 5.1**), simple power law kinetics (SPK, **Equation 5.3**) and constrained power law kinetics (CPK, **Equation 5.4**). The three models were applied to FAA and THAA Asx, Glx and Ala, and THAA Phe and Leu, as these amino acids showed the clearest general racemisation trends (**Section 5.3.4.1**). FAA Phe and Leu were excluded due to missing D/L values during the early stages of the heating experiment.

5.3.4.4.1 RFOK_a

RFOK_a generally performs well for Asx, Glx and Ala, and THAA Phe and Leu for *Ammonia* spp. (**Fig. 5.24**, **Table 5.4**), with THAA having higher R² values than FAA, and unbleached having higher R² values than bleached in most cases (although not for Asx). In general the rates estimated by the RFOK_a model place the rates of racemisation of the amino acids in the same order as determined visually (**Section 5.3.4.3**), with the exception of Ala, which has a much higher estimated rate than Asx in the FAA fraction, where the rate of Ala racemisation overtakes Asx during the latter stages of the experiment. This demonstrates the underestimation of the higher initial Asx rate by the RFOK_a model, which can be seen in the deviation of the D/L values from the RFOK_a line in the early time points.

For Asx and Glx, the degree of racemisation in the FAA fraction is higher than THAA, but the rates are similar. This suggests that the racemisation of FAA is driven by amino acids passing through

rapidly racemising terminal positions before being hydrolysed into the relatively slow-racemising free state.

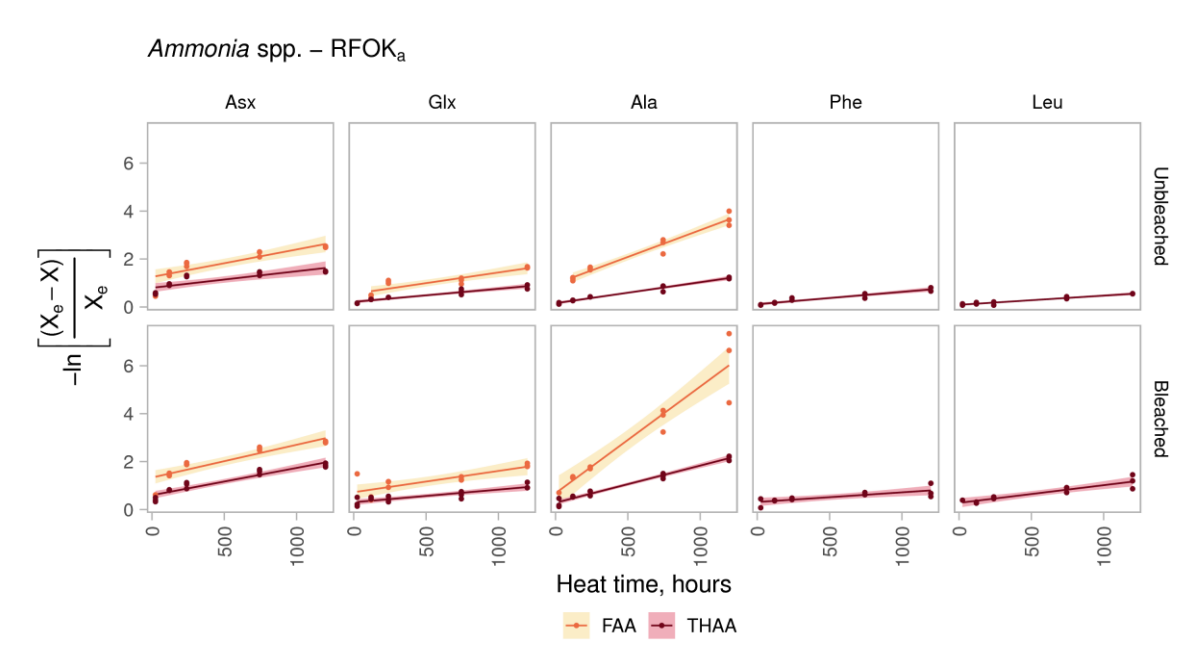


Fig. 5.24 – RFOK_a of Asx, Glx, Ala, Phe and Leu for unbleached (whole-shell) and bleached (intracrystalline) *Ammonia* spp., heated to 110°C. The solid lines show the linear regression between time and -ln[(X_e -X)/ X_e]; the shaded regions show \pm 1 σ around the linear regression. FAA Phe and Leu have been excluded due to missing FAA D/L values at early time points (see **Section 5.3.4.2**).

Table 5.4 – Results of RFOK_a linear models for unbleached (whole-shell) and bleached (intra-crystalline) *Ammonia* spp., heated to 110°C. k_1 is the rate of racemisation (slope / (1+K), where K = 1); c is the intercept; Adj. R^2 is the adjusted R^2 value. R^2 values ≤ 0.6 are highlighted in red.

	Amino	Unbleached			Bleached		
	acid	k ₁ (x10 ⁻⁴ h ⁻¹)	С	Adj. R ²	k ₁ (x10 ⁻⁴ h ⁻¹)	С	Adj. R ²
_	Asx	5.7 ± 1.0	1.25 ± 0.13	0.74	6.9 ± 0.9	1.33 ± 0.13	0.81
₹	Glx	4.4 ± 0.7	0.55 ± 0.11	0.77	4.4 ± 1.0	0.72 ± 0.14	0.60
_	Ala	11.2 ± 0.7	0.97 ± 0.10	0.96	22 ± 2	0.7 ± 0.3	0.90
	Asx	4.8 ± 1.0	0.58 ± 0.10	0.60	6.6 ± 0.7	0.44 ± 0.08	0.86
_	Glx	3.0 ± 0.3	0.17 ± 0.03	0.89	2.9 ± 0.4	0.25 ± 0.05	0.76
THAA	Ala	4.5 ± 0.2	0.13 ± 0.02	0.97	7.7 ± 0.3	0.230 ± 0.04	0.98
	Phe	2.7 ± 0.2	0.09 ± 0.02	0.91	2.0 ± 0.5	0.31 ± 0.08	0.56
	Leu	2.0 ± 0.1	0.073 ± 0.015	0.94	4.0 ± 0.5	0.212 ± 0.07	0.86

RFOK_a performs similarly for *H. germanica*, with generally good linearisation for the slowly racemising amino acids, but failing to model the rapid initial racemisation rate of Asx (**Fig. 5.25**, **Table 5.5**). For the intra-crystalline FAA fraction, Ala is predicted to have a much higher rate of

racemisation than Asx (as for *Ammonia* spp.), while in the whole-shell fraction, the racemisation rates of the two amino acids are more similar. The difference in the performance of the model between the unbleached and bleached material is more pronounced in *H. germanica* than *Ammonia* spp., with the bleached material having larger errors and smaller R² values for all fractions except FAA Ala (**Table 5.4 and 5.5**).

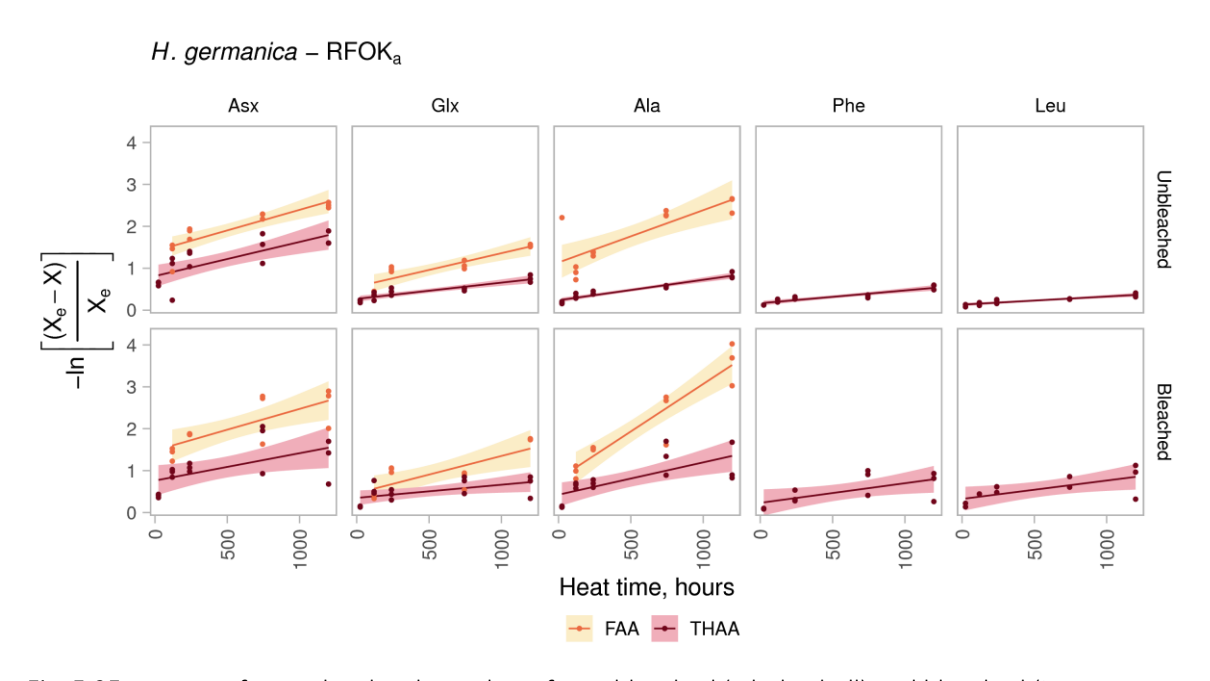


Fig. 5.25 – RFOK_a of Asx, Glx, Ala, Phe and Leu for unbleached (whole-shell) and bleached (intracrystalline) H. germanica, heated to 110°C. The solid lines show the linear regression between time and $-\ln[(X_e-X)/X_e]$; the shaded regions show \pm 1 σ around the linear regression. FAA Phe and Leu have been excluded due to missing FAA D/L values at early time points (see Section 5.3.4.2).

Table 5.5 – Results of RFOK_a linear models for unbleached (whole-shell) and bleached (intra-crystalline) *H. germanica*, heated to 110°C. k_1 is the rate of racemisation (slope / (1+K), where K = 1); c is the intercept; Adj. R^2 is the adjusted R^2 value. R^2 values ≤ 0.6 are highlighted in red.

	Amino	ino Unbleached			Bleached			
	acid	k ₁ (x10 ⁻⁴ h ⁻¹)	С	Adj. R ²	k ₁ (x10 ⁻⁴ h ⁻¹)	С	Adj. R ²	
	Asx	4.9 ± 0.8	1.41 ± 0.12	0.76	5.0 ± 1.4	1.5 ± 0.2	0.53	
₽	Glx	4.0 ± 0.7	0.56 ± 0.10	0.77	4.4 ± 1.2	0.46 ± 0.16	0.55	
	Ala	6.2 ± 1.3	1.14 ± 0.18	0.64	11.3 ± 1.3	0.80 ± 0.19	0.87	
	Asx	5.2 ± 1.0	0.61 ± 0.12	0.59	4.3 ± 1.3	0.58 ± 0.15	0.39	
4	Glx	2.3 ± 0.3	0.21 ± 0.03	0.78	2.1 ± 0.6	0.26 ± 0.07	0.39	
THA	Ala	2.44 ± 0.18	0.24 ± 0.02	0.93	3.9 ± 0.9	0.42 ± 0.11	0.52	
-	Phe	1.7 ± 0.2	0.13 ± 0.03	0.84	2.6 ± 0.9	0.19 ± 0.12	0.42	
	Leu	1.12 ± 0.15	0.104 ± 0.019	0.81	2.6 ± 0.7	0.24 ± 0.09	0.55	

The patterns seen in *Ammonia* spp. and *H. germanica* using the RFOK_a model are similar to those observed in other biominerals, with the model more effectively predicting the behaviour of slowly racemising amino acids (e.g. Manley et al., 2000; Crisp et al., 2013). The model generally performs better on the unbleached material than the bleached material, particularly for *H. germanica*, due to the lower variability of the data for the unbleached material.

5.3.4.4.2 SPK and CPK

Power law models use an exponent *n* to account for the slowing of the racemisation rate over time, and typically provide better linearisation of fast-racemising amino acids such as Asx (Clarke and Murray-Wallace, 2006; Tomiak et al., 2013). To compare the performance of power law models with RFOK_a, simple power law kinetics (SPK) and constrained power law kinetics (CPK) were applied to FAA and THAA Asx, Glx and Ala, and FAA Phe and Leu, for both species. The results for Asx are discussed here; the results for the other amino acids can be found in **Appendix A3.4**.

Fig. 5.26 shows the relationship between n and R^2 when applying SPK and CPK to Asx for each fraction and species. The value of n which produces the highest R^2 value is used and typically ranges from ~0.5-4 for Asx, depending on the model, biomineral, temperature, and D/L range used (Clarke and Murray-Wallace, 2006; Dickinson et al., 2019). In a study of the foraminifer P. obliquiloculata the optimal value of n was found to be 2.8 for Asx when using the CPK model (Kaufman, 2006).

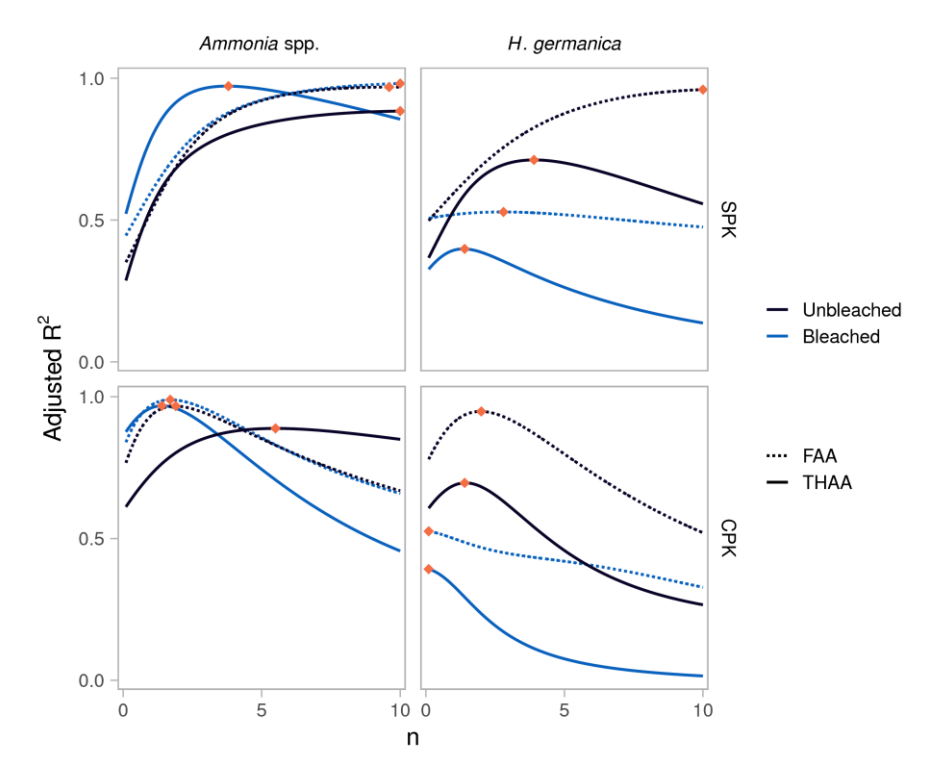


Fig. 5.26 – Optimisation of n for SPK and CPK models applied to Asx in unbleached (whole-shell) and bleached (intra-crystalline) *Ammonia* spp. and *H. germanica*, heated to 110°C. Orange diamonds show the value of n with the highest R^2 value. Optimisation was carried out with values of n between 0.1 and 10, in increments of 0.1.

The SPK model predicts much lower racemisation rates of Asx racemisation than RFOK_a for all fractions, and particularly unbleached THAA for *Ammonia spp.* (**Fig. 5.27**, **Table 5.6**). The results of the CPK model are very variable, with rates differing by several orders of magnitude between fractions, from $0.48 \pm 0.14 \times 10^{-4} \, h^{-1}$ for bleached THAA in *H. germanica* to $1.5 \pm 0.13 \, h^{-1}$ for unbleached THAA in *Ammonia* spp. (**Fig. 5.27**, **Table 5.6**). While racemisation rates vary widely between different biominerals (for example, at 110° C the racemisation rate of Asx estimated by CPK is $1.0 \times 10^{-4} \, h^{-1}$ for enamel (Dickinson et al., 2019) and $3.2 \times 10^{-1} \, h^{-1}$ for the gastropod *P. vulgata* (Demarchi et al., 2013b)), models typically estimate rates within an order of magnitude within a biomineral (e.g. Tomiak et al., 2013; Dickinson et al., 2019). For *Ammonia* spp. and *H. germanica*, there is little concordance between the k_1 values predicted for Asx by each model, even when a good linear fit (R² > 0.8) is produced (**Fig. 5.29**). Similar results are found for Glx, Ala, Phe and Leu (**Appendix A3.4**). This demonstrates the potential issues with using power law models on small, variable data sets, as even small differences in *n* can result in very large differences between predicted rates.

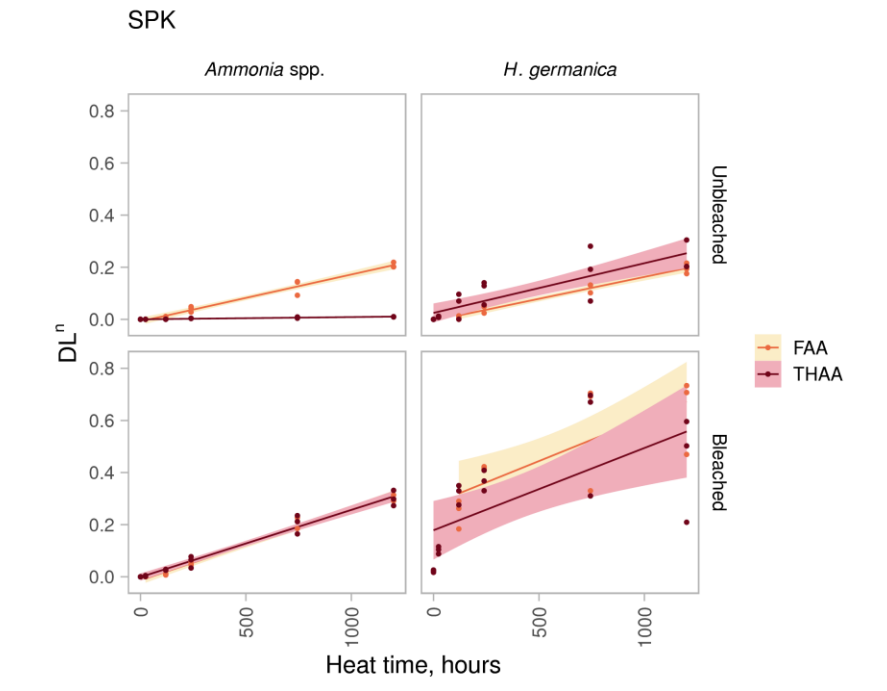


Fig. 5.27 – SPK of Asx for unbleached (whole-shell) and bleached (intra-crystalline) *Ammonia* spp. and *H. germanica*, heated to 110°C. Lines show linear regression between time and D/L^n , where the value of n is optimised to provide the highest value of R^2 (see Fig. 5.26). The shaded region shows $\pm 1 \sigma$ around the linear regression.

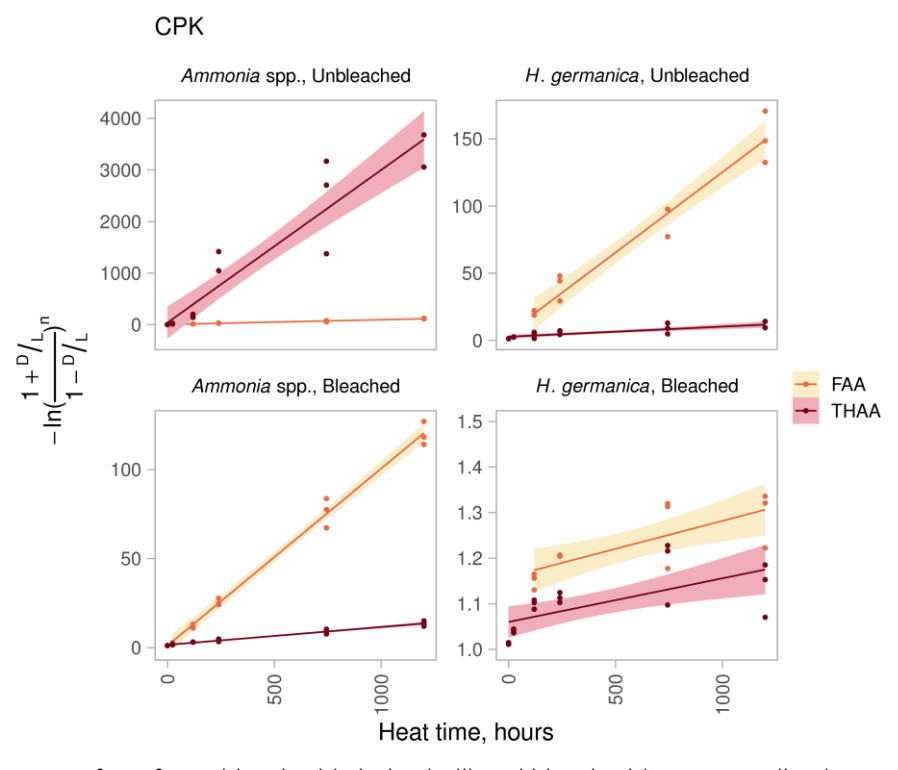


Fig. 5.28 – CPK of Asx for unbleached (whole-shell) and bleached (intra-crystalline) *Ammonia* spp. and *H. germanica*, heated to 110°C. Lines show linear regression between time and -ln([1+D/L]/[1-D/L])ⁿ, where the value of n is optimised to provide the highest value of R^2 (see Fig. 5.26). The shaded region shows \pm 1 σ around the linear regression. Note that each plot has its own y-axis range, so the slope of each linear regression should not be directly compared.

Table 5.6 – Results of SPK and CPK linear models for Asx in unbleached (whole-shell) and bleached (intra-crystalline) H. germanica and Ammonia spp., heated to 110° C. k_1 is the rate of racemisation (slope / (1+K), where K = 1); Adj. R^2 is the adjusted R^2 value. For clarity c (the intercept) has been omitted from this table; these values are given in **Appendix A3.4**. R^2 values ≤ 0.6 are highlighted in red.

		Unbleached			Bleached			
		n	k ₁ (x10 ⁻⁴ h ⁻¹)	Adj. R ²	n	k ₁ (x10 ⁻⁴ h ⁻¹)	Adj. R ²	
spp.	SPK	FAA	9.6	0.9 ± 0.05	0.97	10	1.36 ± 0.05	0.98
nia s	ß	THAA	10	0.04 ± 0	0.88	3.9	1.29 ± 0.05	0.97
Ammonia	×	FAA	1.9	460 ± 20	0.97	1.7	497 ± 15	0.99
Am	집	THAA	5.5	14800 ± 1300	0.89	1.5	50 ± 2	0.97
ica	SPK	FAA	10	0.84 ± 0.05	0.96	2.8	1.6 ± 0.5	0.53
H. germanica		THAA	3.9	0.95 ± 0.15	0.71	1.4	1.6 ± 0.5	0.40
	CP.K	FAA	2	600 ± 40	0.95	0.1	0.61 ± 0.17	0.53
	ט	THAA	1.4	38 ± 6	0.70	0.1	0.48 ± 0.14	0.39

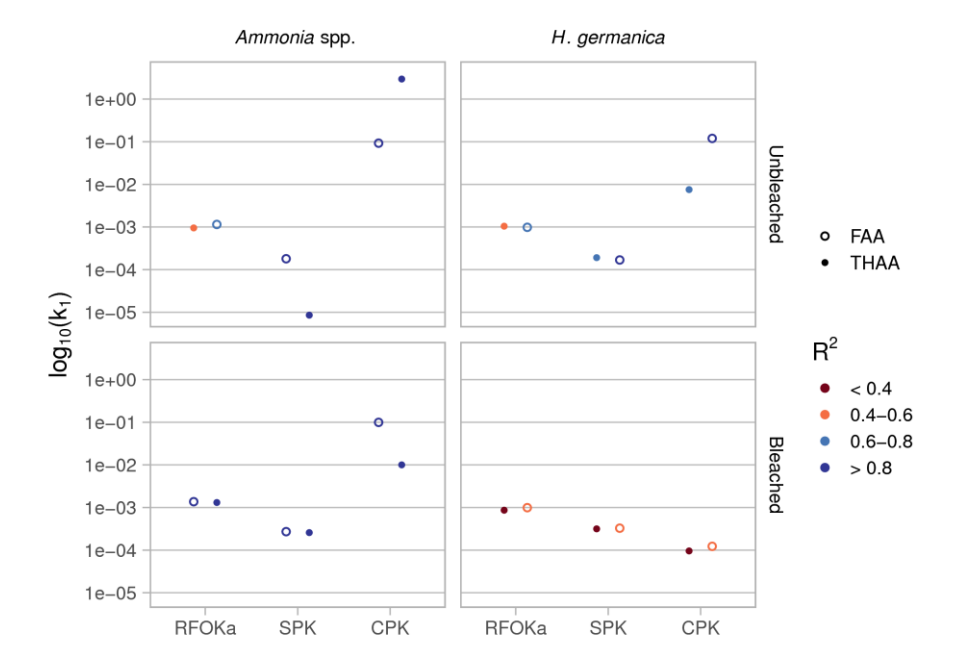


Fig. 5.29 – Comparison between k_1 of Asx, estimated by each of three models (reversible first order kinetics (RFOK_a), simple power law kinetics (SPK), and constrained power law kinetics (CPK)), for unbleached (whole-shell) and bleached (intra-crystalline) *Ammonia* spp. and *H. germanica*, heated to 110°C. Note the logarithmic y-axis scale.

Given the difficulties determining an appropriate value of n in the power law models, RFOK_a was the most successful model at estimating the patterns of racemisation in *Ammonia* spp. and H. *germanica*, despite its underestimation of the initial racemisation rate of the fast-racemising amino acid Asx. However, the large differences (orders of magnitude) in calculated rates between models

does not provide confidence in any of the approaches. The variability of the data, especially for bleached *H. germanica*, limited the successful application of any of the kinetic models.

5.4 Conclusions

High-temperature experiments were carried out on *Ammonia* spp. and *H. germanica* to assess the patterns of amino acid decomposition in the whole-shell (unbleached) and intra-crystalline (bleached) fractions of these two species of foraminifera. Changes in amino acid concentration, composition, leaching into supernatant waters, and patterns of hydrolysis and racemisation, were investigated to determine whether the intra-crystalline fraction of amino acids exhibits more reliable closed-system behaviour than the whole-shell fraction in these species, and which amino acids show the most reliable trends in racemisation. Apparent reversible first order kinetics (RFOK_a), simple power law kinetics (SPK) and constrained power law kinetics (CPK) were applied to certain amino acids to assess the utility of kinetic models in predicting the racemisation patterns of the species studied.

5.4.1 Methodological issues: sample size and sources of contamination A key issue identified in this suite of experiments was the challenge of reliably quantifying amino acid concentrations in very small samples, especially when analysing the FAA or intra-crystalline fraction (Section 5.3.1). The sample size used in these experiments was around 60 tests per sample (equivalent to 30 tests per FAA or THAA sub-sample) – it is therefore recommended that where possible larger sample sizes should be used for foraminifer AAR, especially when analysing species with smaller tests (such as *H. germanica* from the Humber Estuary sample) or samples which are likely to be highly degraded (and therefore have lower amino acid concentrations). The importance of quantifying the amount of laboratory contamination was also highlighted (Section 5.3.1.1), as internal consistency between results may not be sufficient to identify compromised samples.

The needle used to crush the foraminifer tests during preparation was identified as a possible source of cross contamination (Section 5.3.1.1); therefore for future analyses of foraminifera a fresh, sterilised needle should be used to crush each sample.

5.4.2 Closed-system behaviour in the whole-shell and intra-crystalline fractions

Open-system behaviour of the whole-shell fraction of amino acids was identified for both species, with a substantial proportion of amino acids leaching from the inter-crystalline fraction during the early stages of the heating experiment (Section 5.3.1.3). This may represent a highly labile population of amino acids, which may be lost during the initial stages of diagenesis. FAA appeared to be especially susceptible to leaching, as the concentration and racemisation rates of the whole-shell and intra-crystalline fractions were virtually identical, indicating that the whole-shell FAA pool is dominated by intra-crystalline amino acids. This is also consistent with the higher proportion of FAA in the intra-crystalline fraction compared to the whole-shell fraction during the latter stages of the experiment.

Determining closed or open-system behaviour in the intra-crystalline fraction was more challenging, however, due to the very small concentration of residual amino acids remaining after bleaching. Bleaching reduced the proportion of amino acids leached into the supernatant water; laboratory contamination and suspended biomineral fragments are likely to have contributed to the total concentration of amino acids observed in the supernatant water. Nonetheless, the proportion of leached amino acids from the intra-crystalline fraction was higher than for other biominerals with closed-system intra-crystalline fractions; therefore open-system behaviour of at least some proportion of the intra-crystalline fraction of *Ammonia* spp. and *H. germanica* cannot be ruled out.

5.4.3 Patterns of decomposition

Both *Ammonia* spp. and *H. germanica* followed predictable patterns of decomposition (**Section 5.3.3** and **5.3.4**), similar to the patterns seen in other biomineral proteins, although the trends for *H. germanica* were generally poorer, perhaps due to the smaller amino acid concentrations in this species (thus increasing the variability of the results). The composition of the THAA fraction was relatively stable, with a slight decrease in % Ser and increase in % Ala corresponding to the dehydration of Ser to Ala. The rate of hydrolysis (**Section 5.3.3**) was fastest for Asx, Gly and Ala in both species (it was not possible to determine the rate of Ser hydrolysis due to the domination of FAA Ser by laboratory contamination), a pattern also seen in other biominerals.

D/L covariance was used to determine which amino acids were best resolved for *Ammonia* spp. and *H. germanica* using RP-HPLC. Asx, Glx and Ala were found to have the best covariance trends,

both between the FAA and THAA fractions, and with each other (Section 5.3.4.2), with the whole-shell material tending to have better covariance than the intra-crystalline fraction, most likely due to the higher amino acid concentrations in this fraction. The later-eluting (more hydrophobic) amino acids Val, Phe, Leu and Ile were more poorly resolved, especially at low amino acid concentrations. The relative rates of racemisation followed predictable patterns; generally speaking Asx > Ala > Leu > Phe ~ Glx, although in some fractions Ala overtook Asx towards the end of the experiment (Section 5.3.4.3). In the 140°C experiment (analysed using UHPLC), where Ile was better resolved than at 110°C (analysed by RP-HPLC), Ile had a similar rate to Phe and Glx. This general pattern is seen in a range of other biominerals (e.g. Penkman et al., 2008; Bright and Kaufman, 2011b; Demarchi et al., 2013b; Pierini et al., 2016; Ortiz et al., 2017).

For both species, the FAA fraction had a higher racemisation degree than THAA, but similar rates of racemisation, which is consistent with the amino acids in the FAA pool having passed through rapidly racemising terminal positions during hydrolysis. In the FAA fraction, the patterns of racemisation were similar for the unbleached and bleached material, while in the THAA fraction the degree of racemisation was higher in the bleached material than unbleached for Ala, Phe and Leu, which could result from the higher contribution of FAA amino acids to the THAA pool in the intra-crystalline fraction.

5.4.4 Behaviour of kinetic models

Three kinetic models were used to explore the trends in D/L for *Ammonia* spp. and *H. germanica*: RFOK_a, SPK and CPK (Section 5.3.4.4). Generally speaking, the RFOK_a model was reasonably effective at modelling the rates of racemisation for FAA and THAA Glx and Ala, and THAA Phe and Leu, in *Ammonia* spp. and *H. germanica*, while it struggled to account for the rapid initial racemisation of Asx. The model performed poorly for all amino acids in bleached *H. germanica* except Ala, due to the variability of the data in this fraction. The two power law models tested, SPK and CPK, both performed poorly, with estimated rates differing by several orders of magnitude between fractions. This highlights the issues with applying power law models to variable datasets, as even small changes in the optimal value of *n* for these models can have large impacts on the estimated rate.

5.4.5 Overall conclusions

The experiments carried out in this chapter show that *Ammonia* spp. and *H. germanica* follow predictable patterns of racemisation at high temperatures, suggesting that they may be able to provide chronological information for Pleistocene sea-level records. The similar results seen for the whole-shell and intra-crystalline fractions corroborate the patterns seen in unbleached and bleached naturally-aged *N. pachyderma* (s) (Chapter 3), and in the extended bleaching experiments of sub-modern *Ammonia* spp., *H. germanica* and *E. williamsoni*, and naturally-aged *Ammonia* spp. and *H. germanica* (Chapter 4). The rapid loss of amino acids from the inter-crystalline fraction seen in these high-temperature experiments is concordant with the reduced effect of oxidising pretreatments on naturally-aged *Ammonia* spp. and *H. germanica* compared to sub-modern found in Chapter 4 and Millman et al. (2020, Appendix 1), suggesting that labile amino acids are lost during the early stages of diagenesis in foraminifera.

In contrast to the behaviour of many biominerals, isolating the intra-crystalline fraction of amino acids in *Ammonia* spp. and *H. germanica* did not reduce inter-sample D/L variability. The low concentrations of intra-crystalline amino acids in the bleached samples likely contributed to the increased D/L variability seen in this fraction. This result, combined with the minimal differences between H_2O_2 and NaOCl pre-treatments observed in naturally-aged material (**Chapter 4**), indicates that there is limited utility in applying a strong oxidative pre-treatment to naturally-aged foraminifera. Therefore in the development of a pilot aminostratigraphy of UK Pleistocene sites based on foraminifera (**Chapter 6**), a 2 hour 3% H_2O_2 pre-treatment was used to remove exogenous and labile amino acids, following the protocol most commonly used for preparation of foraminifera for AAR (Hearty et al., 2004, 2010; Kaufman et al., 2008, 2013; West et al., 2019; Ryan et al., 2020).

Chapter 6 – Application of AAR to foraminifera from UK Pleistocene sea-level deposits

6.1 Introduction

The relationship between global climate cycles and regional climatic responses during the Quaternary is of particular interest in an age of anthropogenic climate change (Fox-Kemper et al., 2021). Pleistocene sea-level deposits in temperate latitudes provide valuable archives of regional sea-level response to changing climates (e.g. Read et al., 2007; Bates et al., 2010; Briant et al., 2012; Candy et al., 2014; Barlow et al., 2017), which can be useful analogues for modelling and predicting future sea-level change (e.g. Rovere et al., 2016; Horton et al., 2018; Gilford et al., 2020). However, these deposits are often sparse and fragmented as a result of erosion during glacial periods, and are challenging to date due to the absence of suitable material for U-series dating at high latitudes (Hibbert et al., 2016), and difficulties identifying incomplete bleaching in trapped charge dating methods (Preusser et al., 2008). Amino acid racemisation dating (AAR) of foraminifera may therefore provide additional chronological control for these complex sequences, especially when other biomineral remains are absent.

To assess the application of AAR to foraminifera in the context of Pleistocene sea-level records, *Ammonia* spp., *H. germanica* and *E. williamsoni* from various sites across the mid-late Pleistocene were analysed using the pre-treatment method developed in **Chapter 4**, and compared with independent evidence of age provided by stratigraphic correlation, optically stimulated luminescence dating (OSL) and AAR of other biominerals. This work focuses on three regions with important Pleistocene sea-level deposits: the West Sussex Coastal Plain, the Nar Valley Clays, and the March Gravel deposits in and around Peterborough. Samples were additionally analysed from the Burtle Beds, a sequence of interglacial raised beaches in Somerset. To investigate the upper age limit of AAR on foraminifera, *Ammonia* spp., *Elphidium frigidum* and *Elphidium pseudolessoni* from Strumpshaw Fen Sandpit, an Early Pleistocene deposit, were also analysed.

This work aimed to answer the four following research questions:

1. Can robust estimates of D/L values be obtained from foraminifera from Pleistocene sealevel records?

- 2. Are the results produced by AAR of these foraminifera as expected given the existing chronology of each site?
- 3. Can these results provide age estimates for sites with currently unresolved chronology?
- 4. What recommendations should be followed when applying AAR to foraminifera in future investigations of Pleistocene sea-level records?

6.2 Materials and Methods

6.2.1 Sample locations

The locations of sites analysed in this study are shown in **Fig. 6.1**. **Table 6.1** shows the details of each horizon sampled for AAR of foraminifera at each site, along with the species analysed at each horizon.

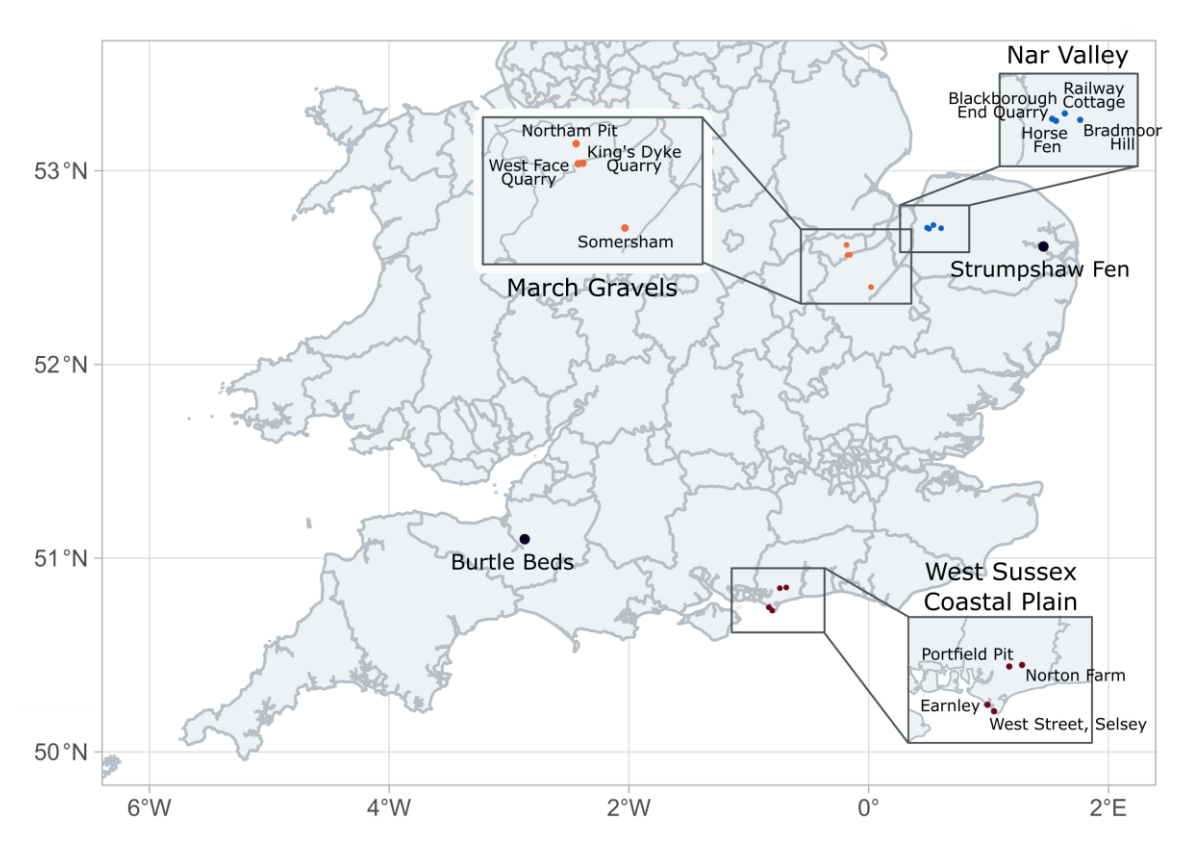


Fig. 6.1 – Location of UK Pleistocene sea-level sites analysed in this study. Study regions inset: West Sussex Coastal Plain (Section 6.3.3), Nar Valley (Section 6.3.4), March Gravels (Section 6.3.5).

Table 6.1 – Foraminifera from UK Pleistocene sites analysed in this study. *Species abbreviations: Am: *Ammonia* spp. (not identified to species level), HG: *Haynesina germanica*, EW: *Elphidium williamsoni*; Elp: *Elphidium* spp. (not identified to species level); EF: *Elphidium frigidum*; EP: *Elphidium pseudolessoni*. All samples prepared with a 2 hour 3% H₂O₂ pre-treatment and analysed using UHPLC according to **Section 2.4.2**.

Region	Site	Location (NGR, Lat/Long)	Sample code	Sample information	Species analysed*
	Portfield Pit	SU 8875 0580	PP-1.3	Borehole 1 (BH1): 1.3-1.4 m	EW
.⊑		50.845, -0.7413	PP-1.6	Borehole 1 (BH1): 1.6-1.7 m	EW, HG
West Sussex Coastal Plain			PP-1.9	Borehole 1 (BH1): 1.9-2.0 m	HG
	Earnley	SZ 825 947 50.746, -0.832	ELY-0.2	Core 1, adjacent to test pit 3: 0.18-0.20 m	Am, HG, EW
ssex C	West Street, Selsey	SZ 8448 9287 50.729, -0.804	WSS-0.3	Test Pit 7, Core 3: 30-32 cm	Am, HG
est Su	Norton Farm	SU 925 063 50.849, -0.687	NF-5.0	NOR96-BH1, Sample 7: 4.98- 5.00 m	HG, EW
>			NF-5.1	NOR96-BH1, Sample 7: 5.08- 5.10 m	HG, EW
₹	Railway	TF 71679 16581	RC-5.6	Core RC: 5.56-5.57 m	Am
/allé	Cottage	52.720, 0.540	RC-6.3	Core RC: 6.28-6.29 m	Am, HG
Nar Valley	Horse Fen	TF 69283 14353 52.700, 0.504	HF-9.9	Core 13-1: 9.90-9.91 m	Am
	Northam Pit	TF 2303 0364	NP-1	1.9 m OD	Am, HG
		52.617, -0.184	NP-4	2.45 m OD	Am
els	King's Dyke Quarry	TL 251 981 52.566, -0.156	KD-A	Section A, Top of facies FI-Fd of facies association W7	HG
March Gravels			KD-C	Section C, Top of facies association W13	Am, HG, EW
March	West Face Quarry	TL 238 979 52.565, -0.175	WF-Fa	Section F, top of facies association W7	HG
			WF-Fb	Section F, bottom of facies association W7	HG
	Somersham	TL 375 798 52.399, 0.020	SH-S1	S1/9-3, Bed H2, Section SBK	Am
Burtle Beds	Burtle Beds	ST 39233 33537 51.098 -2.869	BB-GL3	Greylake 3, Sample 2; 3.3-3.5 m	Am, HG, Elp
Norfolk	Strumpshaw Fen Sandpit	TG 34211 06829 52.609, 1.458	SF-YK11	Sample SF-YK11, base of left pit	Am, EP, EF

Along with the analyses carried out on material from Railway Cottage and Horse Fen in this study (see **Table 6.1**), the results of AAR of foraminifera from several Nar Valley sites analysed as part of the former-NERC iGlass project between 2013 and 2016 are presented in this chapter (analyses undertaken by Sheila Taylor & Kirsty Penkman, previously unpublished). A summary of the samples analysed in the iGlass project is shown in **Table 6.2**.

Table 6.2 – Foraminifera from UK sites analysed as part of the iGlass project presented in this chapter. *Species abbreviations: Am: *Ammonia* spp. (not identified to species level); HG: *Haynesina germanica*; Elp: *Elphidium* spp. (not identified to species level). All samples prepared with a 48 hour 12% NaOCl pretreatment and analysed using RP-HPLC according to Penkman et al. (2008).

Region	Site	Location (NGR, Lat/Long)	Sample code	Sample information	Species analysed*
	Bradmoor	TF 76068 14900	BH-0.2	Core BH: 0.20 m	Am, Elp
	Hill	52.703, 0.604	BH-1.2	Core BH: 1.20 m	Am, Elp
			BH-1.6	Core BH: 1.60 m	Am, Elp
	Blackborough	TF 68167 14901	BE-3.9	BQ-12-1: 3.90 m	Am, Elp
	End Quarry	52.706, 0.488	BE-5.5	BQ-12-1: 5.50 m	Am
>			BE-7.0	BQ-12-1: 7.00 m	Am, Elp
Nar Valley	Railway	TF 71679 16581 52.720, 0.540	RC-5.3	Core RC: 5.30 m	Am, Elp
ar V	Cottage		RC-6.1	Core RC: 6.10 m	Am, Elp
Z	Horse Fen	se Fen TF 69283 14353 52.700, 0.504	HF-0.2	Core HF4: 0.22 m	Elp
			HF-0.3	Core HF4: 0.30 m	Elp
			HF-1.1	Core HF2: 1.11 m	Am
			HF-3.1	Core HF4: 3.05 m	Elp
			HF-3.9	Core HF4: 3.85 m	Elp
			HF-4.5	Core HF4: 4.52 m	Am, Elp

6.2.2 Pre-treatment and analysis

Foraminifera were picked from sediment samples sieved between 65-500 μ m; analysis was carried out on monospecific samples consisting of between 25-100 foraminifer tests, depending on the size of the tests and the number of tests present in the sediment sample. Samples were prepared according to Chapter 2, with a 2 hour 3% H_2O_2 pre-treatment, and analysed using UHPLC according to Section 2.4.2. The foraminifera analysed as part of the former-NERC iGlass project (taxa originally reported by Barlow et al. (2017)) were prepared according to the IcPD (intra-crystalline protein diagenesis) protocol of Penkman et al. (2008) using a 48 hour 12% NaOCl bleaching pre-treatment. Sample sizes of between 7-100 foraminifer tests were used depending on availability, with most samples having a size of 10-30 tests. Analysis of the iGlass samples was carried out using RP-HPLC according to Penkman et al. (2008). To preserve material, only the total hydrolysable amino acid (THAA) fraction was analysed in both suites of analyses.

The foraminifera picked from Strumpshaw Fen Sandpit were heavily stained with an unknown water-soluble orange compound(s) which affected the chromatography of these samples by a process of peak suppression, previously observed with enamel samples with a high inorganic salt concentration (Griffin, 2006; Dickinson, 2018). Further dilution of these samples with L-hArg solution (see **Section 6.4** for details) was carried out up to an equivalent rehydration volume of

1280 μ L with the aim of overcoming this peak suppression. An additional solid phase extraction (SPE) step was also attempted on one sample (SF-EF86xH*) following hydrolysis, following the protocol using by Dickinson (2018). In short, a HILIC SPE cartridge (HiChron, Chromobond) with ammonium-sulfonic acid modification was conditioned with 1 mL 18 m Ω H₂O and equilibrated with 5 mL of mobile phase consisting of 80% 18 m Ω H₂O and 20% MeOH (Fisher Scientific). The rehydrated sample was diluted into 0.5 mL mobile phase, loaded onto the column, and eluted under atmospheric pressure using 2 mL mobile phase into a sterilised vial. The vial was dried by centrifugal evaporation, then rehydrated with an additional 16 μ L of L-hArg solution prior to analysis.

6.3 Results and discussion

A discussion of the data screening strategy used in this chapter, followed by an overview of the foraminifer AAR results, is given below. The results for each Pleistocene site are then discussed in detail in **Sections 6.3.3** to **6.3.6**.

6.3.1 Data screening

Following the screening criteria used in **Chapter 3**, as well as in other applications of AAR to foraminifera (e.g. Kaufman, 2006; Kosnik and Kaufman, 2008; Kaufman et al., 2013; Millman et al., in review), the following criteria indicative of modern contamination, or otherwise compromised samples, were considered for application to the Pleistocene foraminifer samples:

- 1. High concentrations of Gly (> 50%)
- 2. Deviation from general Asx vs Glx D/L covariance trend
- 3. An [L-Ser]/[L-Asx] value > 0.8

Two samples (HF4305El1bH* and HF2Am1bH*) had > 50% Gly; in these samples no D-amino acids were detected, indicating a loss of endogenous amino acids during the preparation process. An additional sample (BQ360El2bH*) with no D-amino acids detected despite having < 50% Gly was also excluded. Three samples deviated from the Asx vs Glx D/L covariance trend either of all samples (BQAm2bH* and NVRC-AB62H*) or the other replicates from the same horizon (WFFa-HG2H*); however in order to preserve and assess the natural variability of the data, these samples were not excluded from further analysis.

A large proportion of samples had an [L-Ser]/[L-Asx] value > 0.8. The proportion of samples with [L-Ser]/[L-Asx] > 0.8 was particularly high for *H. germanica* and *Elphidium* spp. samples, and for samples with lower D/L values than other replicates from the same horizon (**Table 6.3**, **Fig. 6.2**). This pattern is similar to the results of other studies of foraminifer AAR, where 20-30% of samples are generally rejected on the basis of high L-Ser concentrations, with rejection rates in some cases being as high as 60-90% (Nicholas, 2012; Kaufman et al., 2013; Ryan et al., 2020). This is higher than is typical for mollusc shells and may be due to the smaller sample sizes of foraminifera; for example, in the bivalve *Mulinia lateralis* samples of lower weights were generally found to have higher and more variable [L-Ser]/[L-Asx] values (Simonson et al., 2013).

Table 6.3 – Proportion of foraminifer samples with [L-Ser]/[L-Asx] above cut-off values of 0.8 and 1.2.

Species	Samples analysed	[L-Ser]/[L-Asx] > 0.8	[L-Ser]/[L-Asx] > 1.2	
Ammonia spp.	77	19 (25%)	11 (14%)	
H. germanica	35	20 (57%)	16 (46%)	
E. williamsoni and	2.4	21 (62%)	16 (47%)	
Elphidium spp.	34	21 (62%)	10 (4/%)	

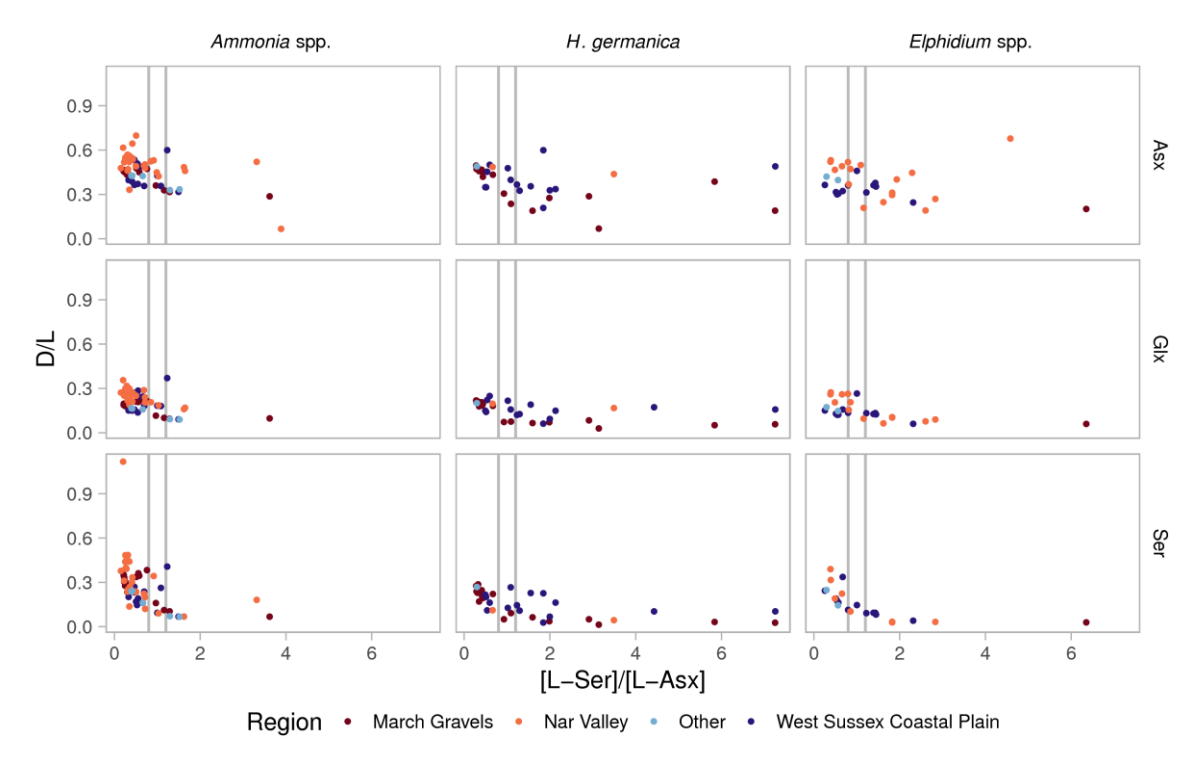


Fig. 6.2 – [L-Ser]/[L-Asx] vs Asx, Glx and Ser D/L for all Pleistocene foraminifer samples. *'Elphidium* spp.' includes both *Elphidium* spp. (not identified to species level) and *E. williamsoni*. The vertical lines show [L-Ser]/[L-Asx] values of 0.8 and 1.2.

While [L-Ser]/[L-Asx] > 0.8 is the most commonly used cut-off for screening AAR samples (e.g. Kaufman, 2006; Kosnik and Kaufman, 2008; Kaufman et al., 2013), this is an arbitrary value which may not be appropriate for all samples, depending on their age, starting compositions and patterns of diagenesis. Younger samples are therefore sometimes excluded from this screening criterion (Kaufman et al., 2013), while a cut-off of 1.2 or 1.5 is sometimes used for older samples due to their lower overall concentrations (Kaufman, 2006; Kosnik and Kaufman, 2008). Using a cut-off of 1.2 reduces the number of samples flagged by the [L-Ser]/[L-Asx] criterion; however, a substantial proportion of samples still have [L-Ser]/[L-Asx] > 1.2 (Table 6.3).

Given the large proportion of samples with [L-Ser]/[L-Asx] > 0.8 in this data set, and the purpose of this study to investigate the utility of AAR of foraminifera in providing age evidence for Pleistocene sea-level deposits, samples with [L-Ser]/[L-Asx] > 0.8 have not been removed from the data set. Instead they are flagged in further analysis to give an indication of possible contamination and a reduced confidence in the D/L values of flagged samples, and to assess whether an [L-Ser]/[L-Asx] screening criterion is appropriate for identifying outlying foraminifer samples.

An overview of all foraminifer AAR results from the UK Pleistocene sites investigated is given below in **Section 6.3.2**, with each region then discussed individually in **Sections 6.3.3** to **6.4**.

6.3.2 AAR of foraminifera from UK Pleistocene sites — overview In a closed system, D/L values should be highly correlated between amino acids (Kaufman and Manley, 1998; Collins and Riley, 2000; Kaufman, 2006; Kosnik and Kaufman, 2008; Hendy et al., 2012); therefore D/L covariance can be used as a measure of the integrity of a biomineral system, and the utility of individual amino acids to provide chronological information for naturally-aged samples. The covariance of Asx with Glx, Phe, Leu and Ile are presented below for each species (Fig. 6.3). Ala, while used routinely in AAR of other biominerals (e.g. Penkman et al., 2013; Pierini et al., 2016; Dickinson et al., 2019; Ortiz et al., 2019), suffers from interference with co-eluting compounds when analysed via UHPLC (see Section 2.4.2), so has been excluded.

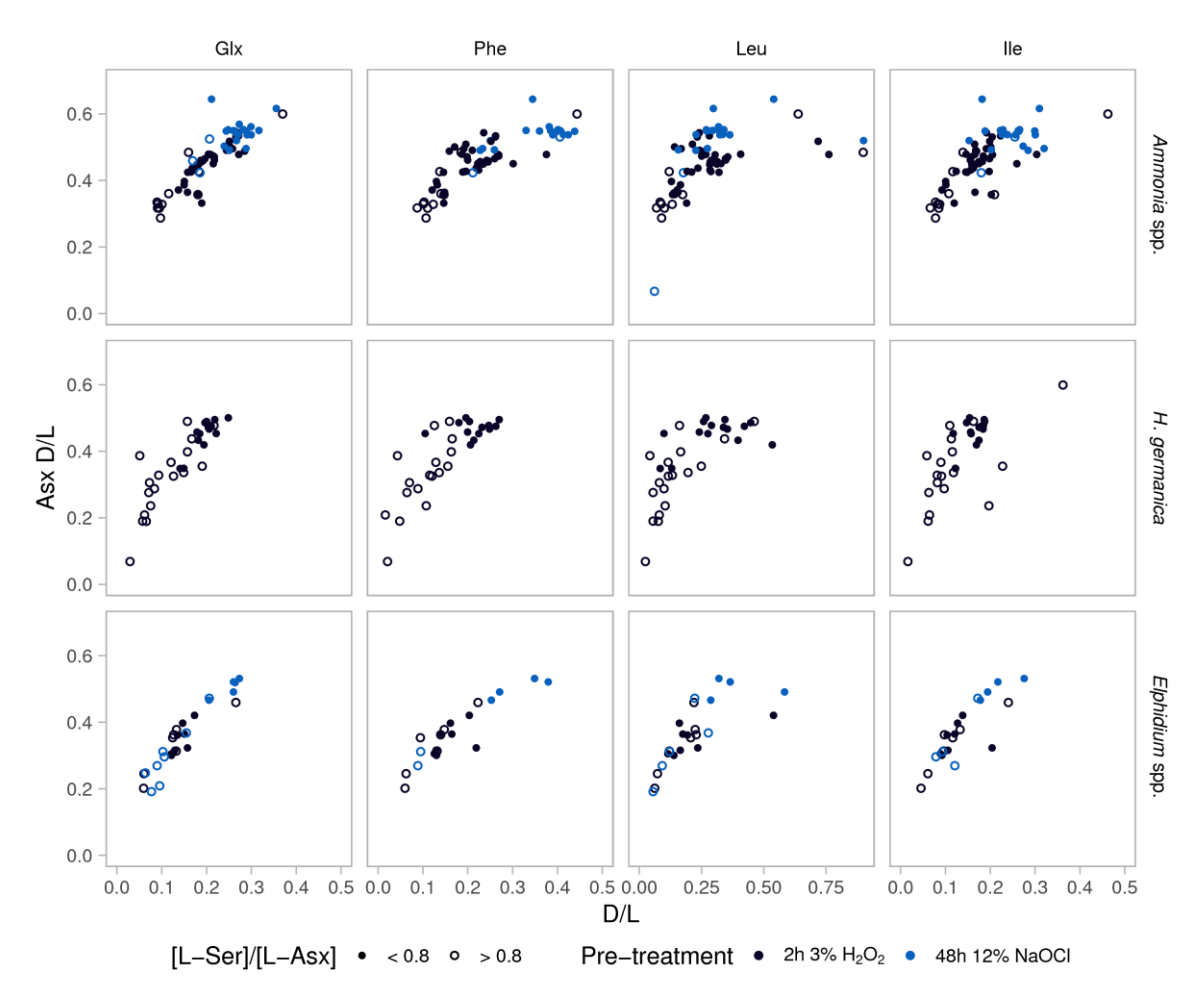


Fig. 6.3 – Covariance of Asx with Glx, Phe, Leu and Ile D/L in THAA (total hydrolysable amino acid) fraction of Ammonia spp., Elphidium spp. (including E. williamsoni) and H. germanica from UK Pleistocene sea-level sites. Samples treated with H_2O_2 (dark blue) were analysed using UHPLC; samples treated with NaOCl (pale blue) were analysed using RP-HPLC. Samples with [L-Ser]/[L-Asx] > 0.8 are shown as open circles.

Overall, Asx and Glx show the best trends in covariance, with Phe, Leu and Ile having somewhat poorer relationships with Asx, especially for *Ammonia* spp. and *H. germanica*. This is consistent with the findings of the high-temperature decomposition experiments carried out on *Ammonia* spp. and *H. germanica* in **Chapter 5**. Asx and Glx are the most commonly used amino acids in recent applications of AAR to foraminifera (e.g. Kaufman et al., 2008, 2013; Blakemore et al., 2015; Ryan et al., 2020), while Ile has the potential for comparison to earlier studies of isoleucine epimerisation in Pleistocene foraminifera (e.g. Dowling et al., 1998; Scourse et al., 1999). Asx, Glx and Ile also cover a wide range of racemisation rates (see **Chapter 5**); these three amino acids were therefore chosen as the primary focus of this study moving forward.

While amino acid D/L covariance is relatively good for all three species, within individual sites the variability of D/L values is generally quite high. The Asx vs Glx D/L covariance is shown in more detail below for *Ammonia* spp. (Fig. 6.4), *H. germanica* (Fig. 6.5) and *Elphidium* spp. (including *E. williamsoni*) (Fig. 6.6). Where a large number of replicates have been analysed, outliers can be distinguished from the main 'cluster' – for example, the results of *Ammonia* spp. from Earnley (ELY, orange triangles, Fig. 6.4, see also Section 6.3.3.1) show a cluster of 8 replicates around Glx D/L of 0.25-0.27 and two outliers: one with a Glx D/L of 0.37 and one with a Glx D/L of 0.18. Both of these outliers had an [L-Ser]/[L-Asx] value > 0.8, indicating that they may have been compromised by laboratory contamination; therefore on the basis of high [L-Ser]/[L-Asx] and deviation from the majority of replicates these samples can reasonably be excluded from an estimate of D/L values for Earnley. However, most sites only yielded enough foraminifera for 1-3 analyses, giving a lower degree of certainty about the true range of D/L values for these sites, and limiting confident identification of outlying samples.

Ammonia spp.

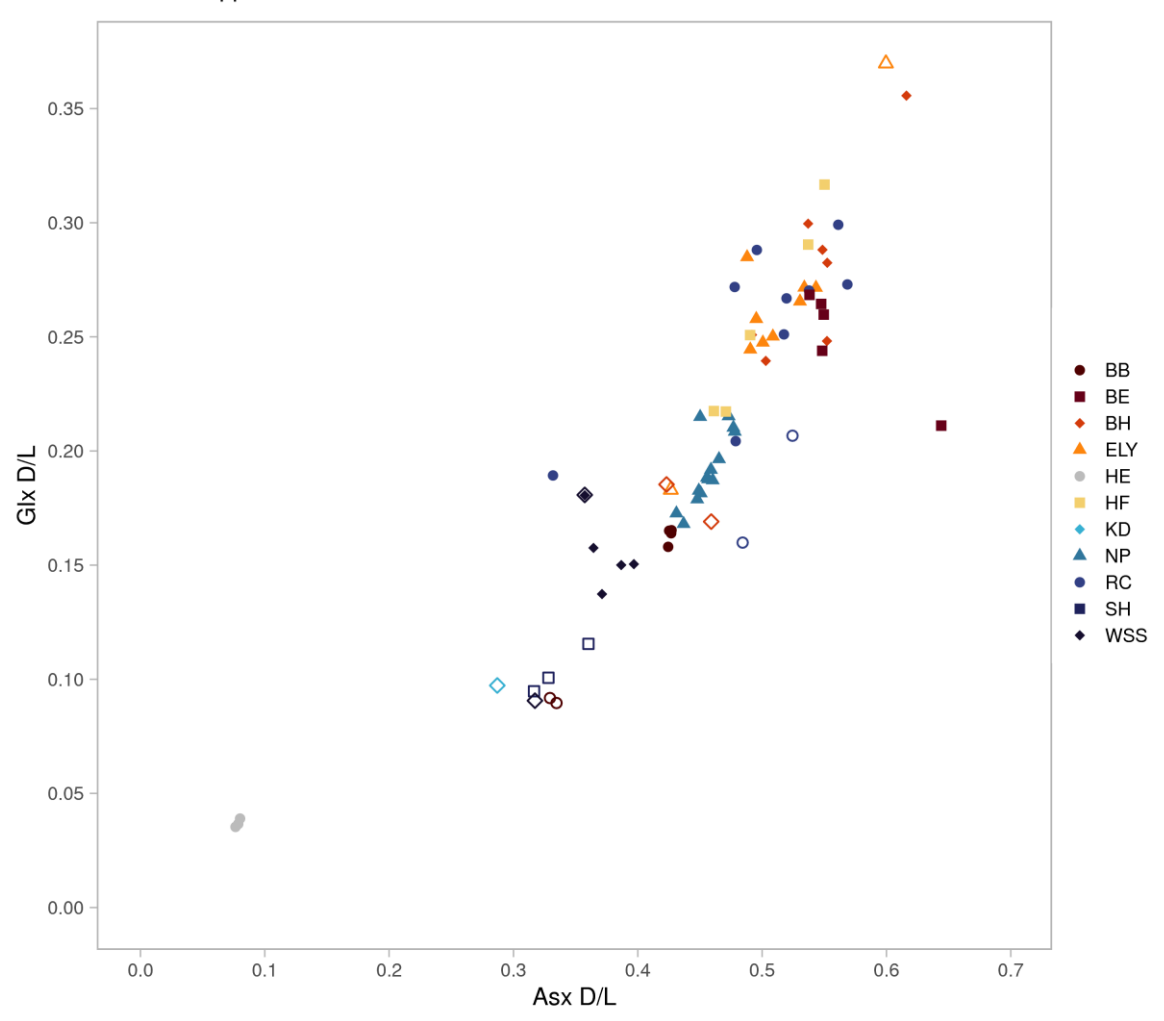


Fig. 6.4 – Asx vs Glx D/L covariance for THAA (total hydrolysable amino acid) fraction of *Ammonia* spp. samples from various UK Pleistocene sites. Samples with an [L-Ser]/[L-Asx] value > 0.8 are highlighted as open shapes. BB: Burtle Beds; BE: Blackborough End Quarry; BH: Bradmoor Hill; ELY: Earnley; HF: Horse Fen; KD: King's Dyke Quarry; NP: Northam Pit; RC: Railway Cottage; SH: Somersham; WSS: West Street, Selsey; HE: Humber Estuary, 'sub-modern' material for comparison. See **Table 6.1** and **Table 6.2** for additional site details.

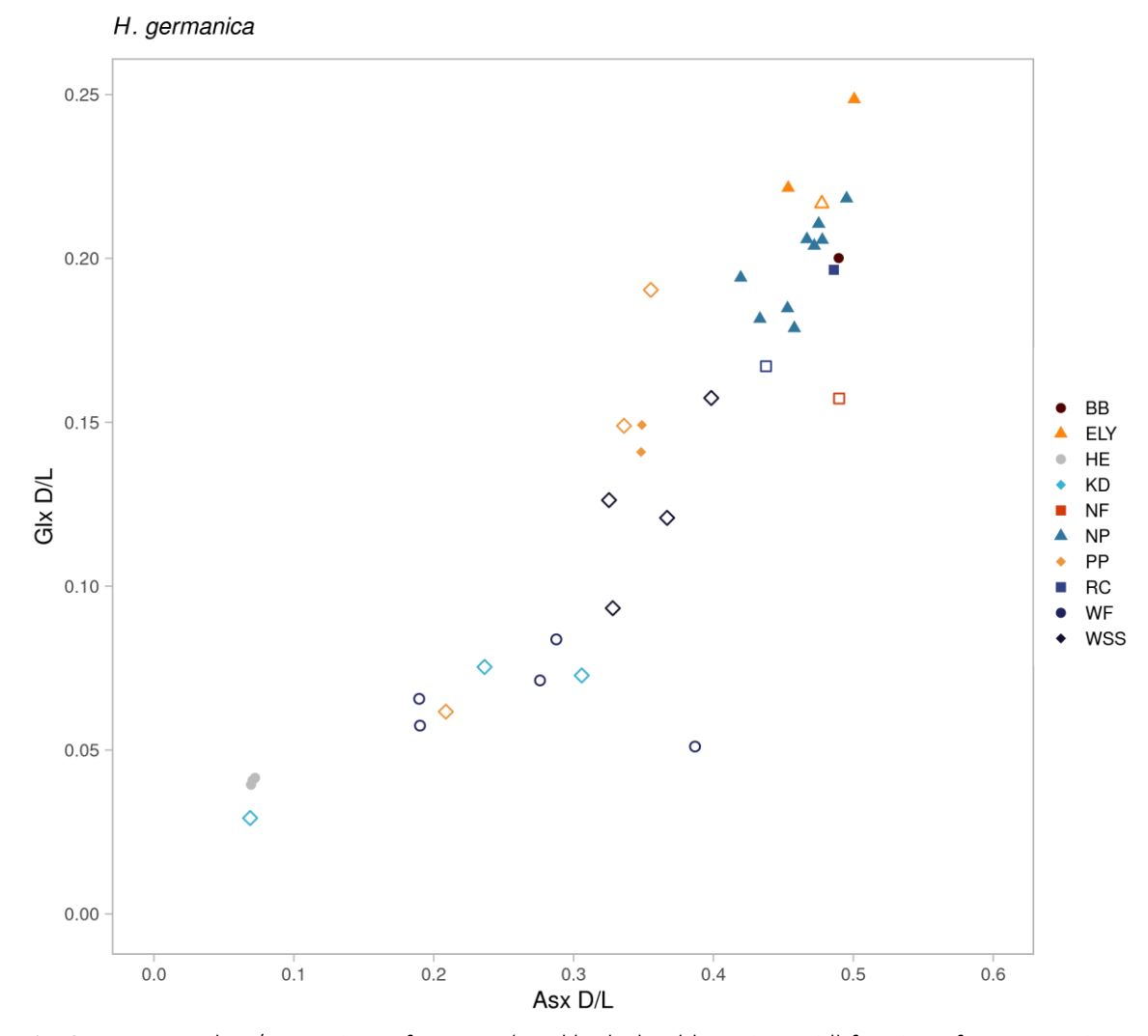


Fig. 6.5 — Asx vs Glx D/L covariance for THAA (total hydrolysable amino acid) fraction of *H. germanica* samples from various UK Pleistocene sites. Samples with an [L-Ser]/[L-Asx] value > 0.8 are shown as open shapes. BB: Burtle Beds; ELY: Earnley; KD: King's Dyke Quarry; NF: Norton Farm; NP: Northam Pit; PP: Portfield Pit; RC: Railway Cottage; WF: West Face Quarry; WSS: West Street, Selsey; HE: Humber Estuary, 'sub-modern' material for comparison. See **Table 6.1** and **Table 6.2** for additional site details.

E. williamsoni and Elphidium spp.

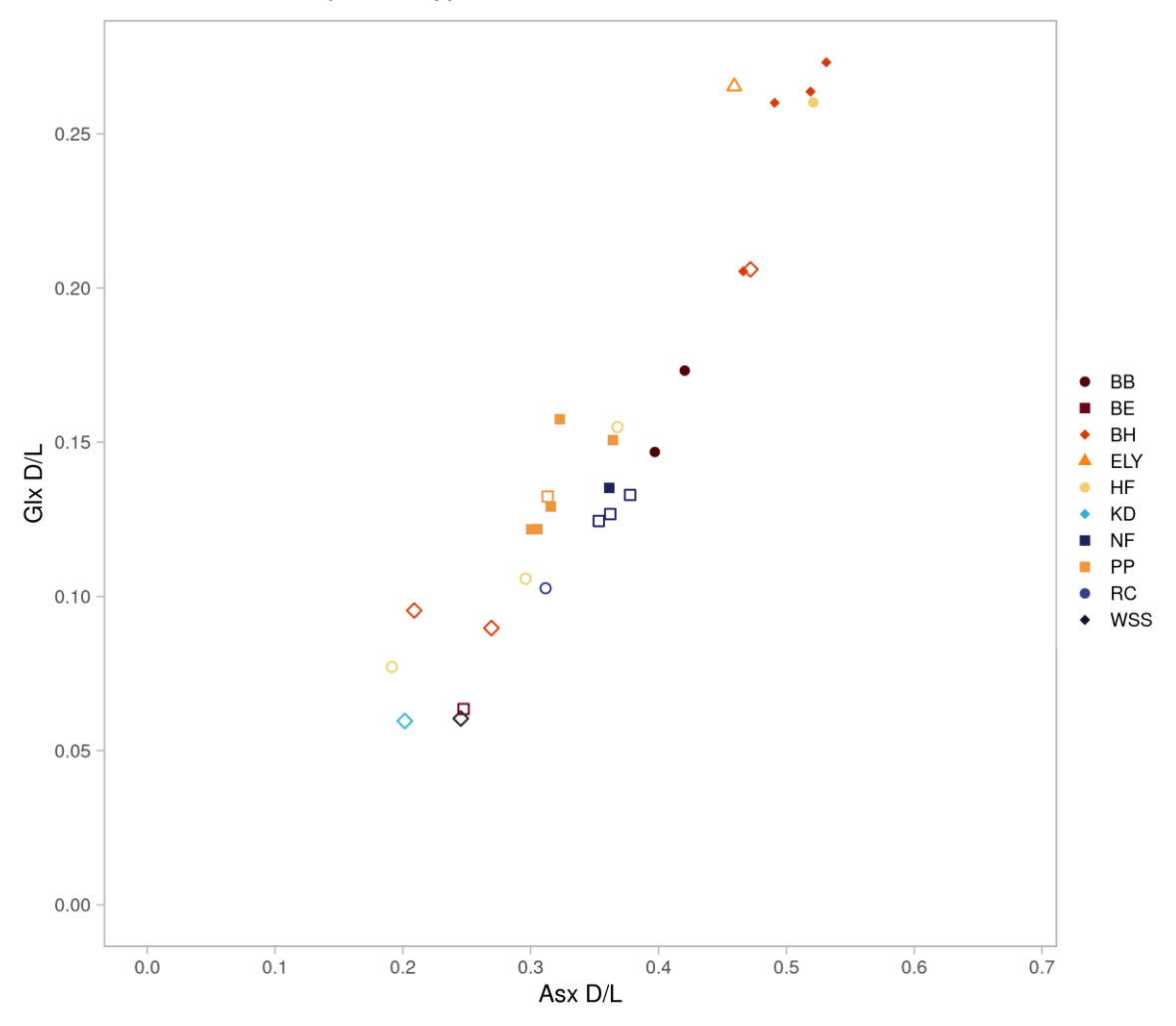


Fig. 6.6 — Asx vs Glx D/L covariance for THAA (total hydrolysable amino acid) fraction of *E. williamsoni* and *Elphidium* spp. (not identified to species level) samples from various UK Pleistocene sites. Samples with an [L-Ser]/[L-Asx] value > 0.8 are shown as open shapes. BB: Burtle Beds; BE: Blackborough End Quarry; BH: Bradmoor Hill; ELY: Earnley; HF: Horse Fen; KD: King's Dyke Quarry; NF: Norton Farm; PP: Portfield Pit; RC: Railway Cottage; WSS: West Street, Selsey. See **Table 6.1** and **Table 6.2** for additional site details.

The racemisation trajectories of the three species of foraminifera studied here (*Ammonia* spp., *H. germanica* and *Elphidium* spp.) are the same (**Fig. 6.7**), consistent with the similar patterns of decomposition observed in *Ammonia* spp. and *H. germanica* at high temperatures (**Chapter 5**). **Fig. 6.7** also shows the racemisation trajectory of Pleistocene *Bithynia tentaculata* opercula (taken from Penkman et al. (2013), Penkman (unpublished data) and Presslee (unpublished data)). The two classes of biomineral show different relative rates of racemisation between amino acids, with Glx racemising more slowly compared to Asx in opercula compared to foraminifera. For one site, Earnley (see **Section 6.3.3.1**), sufficient foraminifera were analysed for a comparison between the relative rates of racemisation of foraminifera and *B. tentaculata* opercula, although it should be

noted that these two types of biomineral may not have come from the same horizon (Richard Preece 2022, pers. comm.). *Ammonia* spp. and *H. germanica* have Asx D/L values around 0.45-0.55 at Earnley, while *B. tentaculata* opercula are more highly racemised with Asx D/L values between 0.70-0.77. The results from Earnley suggest that foraminifera racemise more slowly than *B. tentaculata* opercula, although the difference is not as pronounced as between opercula and enamel (Dickinson et al., 2019).

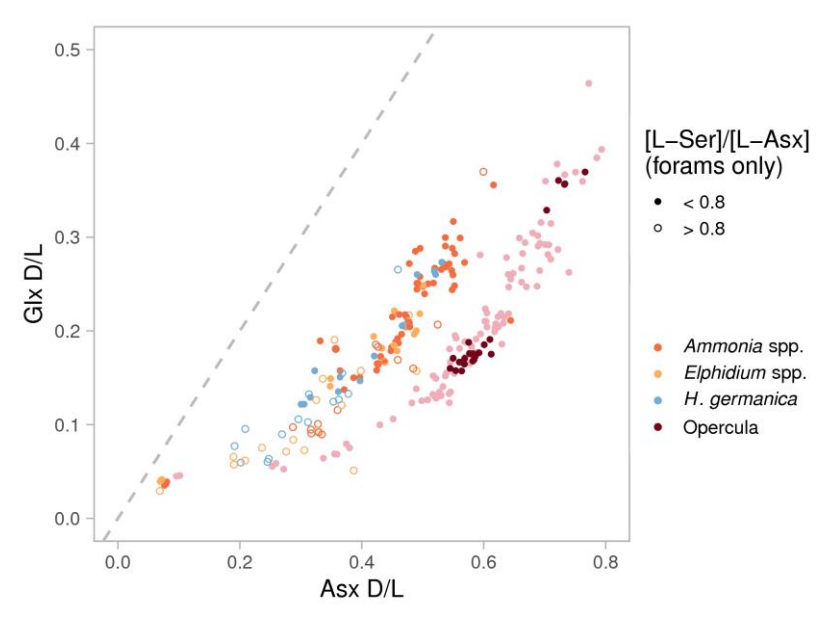


Fig. 6.7 – THAA Asx vs Glx D/L values for all foraminifer samples from UK Pleistocene sites (see **Table 6.1** and **Table 6.2**), and *B. tentaculata* opercula samples (dark red) from Horse Fen (Barlow et al., 2017), Earnley (Penkman (unpublished data); see **Table 6.4**), King's Dyke Quarry (Presslee (unpublished data); see **Table 6.6**), and West Face Quarry and Somersham (Penkman et al. (2013), Presslee (unpublished data); see **Table 6.6**). Average *B. tentaculata* opercula D/L values for UK Pleistocene sites in Penkman et al. (2013) where Glx D/L < 0.5 are shown in pale red to demonstrate the different racemisation trajectories of the two biomineral classes. Foraminiferal samples with an [L-Ser]/[L-Asx] value > 0.8 are highlighted as open circles. The dashed line shows a 1:1 relationship between Asx and Glx D/L.

Recent investigations into racemisation in foraminifera from Pleistocene sea-level records have focused on Southern Australia, which has somewhat higher mean annual temperatures (~13-16°C (Nicholas, 2012; Blakemore et al., 2015)) than the UK (~8-10°C, (Met Office, 2022)). MIS 5e (Last Interglacial) deposits typically produce Asx D/L values of ~0.5 and Glx D/L values ~0.3 for the species *Lamellodiscorbis dimidiatus* (Ryan et al., 2020) and *Elphidium crispum* (Blakemore et al., 2015). Although a direct comparison between samples of the same species or genus is not available, the D/L values (Asx D/L ~0.3-0.4 and Glx D/L ~0.15-0.20) for *Ammonia* spp. from West Street, Selsey (a site dated to MIS 5e-6 by OSL, see **Section 6.3.3.4**) are consistent with slower racemisation rates at lower temperatures.

For Earnley (Section 6.3.3.1) and Northam Pit (Section 6.3.5.1), where the large number of replicates analysed allows an assessment of the variability of D/L values in a single horizon, the range of Asx D/L values is typically ~0.1. This is substantially less than the variability found in single-foraminifer analyses of *Elphidium* from semi-enclosed basins from the Holocene and MIS 3, which typically had within-horizon ranges of ~0.2 for Asx (Nicholas, 2012). This may be due to the averaging of D/L values across many tests used in the analyses carried out in this thesis.

Overall, these results show that there is a clear racemisation signal in foraminifera from UK Pleistocene sea-level sites. To investigate whether this signal can provide chronological control for these sites, the results are compared to existing chronological evidence for each of the three regions studied: the West Sussex Coastal Plain (Section 6.3.3), the Nar Valley (Section 6.3.4) and the March Gravels and associated channel deposits around Peterborough (Section 6.3.5). The results for the Burtle Beds and Strumpshaw Fen Sandpit are discussed in Section 6.3.6 and Section 6.4 respectively.

6.3.3 West Sussex Coastal Plain

The Sussex-Hampshire coastal corridor between Bournemouth and Brighton contains an extensive succession of raised beaches representing at least four sea-level transgressions and regressions during past glacial-interglacial cycles (Bates and Briant, 2009). The West Sussex Coastal Plain has undergone regional uplift of ~70 m since the late Early Pleistocene (Westaway et al., 2006); current elevations of the raised beaches in this area therefore do not reflect palaeo sea levels. Nevertheless, these deposits represent a unique palaeontological and archaeological archive, with important implications for both environmental change and changes in human habitation in the Middle to Late Pleistocene (Bates and Briant, 2009).

Various dating schemes have been proposed for the raised beaches along the West Sussex Coastal Plain. The most recent of these schemes, from Bates et al. (2010), is followed below; however, the ages given by different dating methods do not always agree, and the chronology of the region is not fully resolved (e.g. Bates et al., 2000, 2003, 2010). The oldest raised beach identified along the West Sussex Coastal Plain is the Goodwood-Slindon Raised Beach (also known as the Westbourne-Arundel Raised Beach), which has a present elevation of ~30 m OD (Bates et al., 2007). The Goodwood-Slindon Raised Beach has been associated with MIS 13 on the basis of mammal biostratigraphy (Roberts and Pope, 2009; Bates et al., 2010), although a possible MIS 11 attribution has been suggested by early A/I (isoleucine epimerisation) analyses of gastropods (Bowen and

Sykes, 1994). The Aldingbourne and Brighton-Norton Raised Beaches (16-20 m OD and 5-9 m OD respectively (Bates et al., 2007)) are thought to represent two separate sea-level highstands within MIS 7 (Bates et al., 2010), with the Aldingbourne Raised Beach possibly representing multiple phases of deposition (Bates and Briant, 2009). The youngest raised beach, Pagham Raised Beach (0-5 m OD (Bates et al., 2007)), has been correlated with MIS 5e on the basis of OSL (Bates et al., 2010).

Sufficient foraminifera for a pilot investigation into the potential of AAR on foraminifera were recovered from four sites in the West Sussex Coastal Plain: Norton Farm (representing both the Aldingbourne and Brighton-Norton Raised Beaches), Portfield Pit (Brighton-Norton Raised Beach), West Street, Selsey (Pagham Raised Beach) and Earnley (a channel infilling not associated with any of the raised beaches) (see Fig. 6.1 for site locations). Table 6.4 summarises the existing chronological evidence present at each site. Fig. 6.8 shows the Asx vs Glx and Ile D/L covariance of these samples. The results for each site and comparison to existing chronology is discussed below.

Table 6.4 – Chronological evidence from West Sussex Coastal Plain sites. Laboratory codes for OSL dates are given in italics. IcPD: intra-crystalline protein diagenesis approach to AAR using a strong oxidative pre-treatment (NaOCl); AAR: weak oxidative pre-treatment (H_2O_2) used; A/I: isoleucine epimerisation, whole-shell approach.

Site	Horizon(s), where known	Method	Age assignment	Reference	
	Fowler's Bed 5	IcPD of B.	Pre-Anglian (> MIS 12)	Penkman	
		tentaculata		(unpublished	
		opercula		data)	
_	Unspecified	A/I of Macoma	Hoxnian (MIS 9 or 11)	(Preece et al.,	
<u>Je</u>		balthica		1990)	
Earnley	-	Pollen	Pre-Anglian or Hoxnian	West et al.	
_		stratigraphy	(MIS 9 to 13)	(1984)	
	Core 1, adjacent to	AAR of foraminif	era (this study)		
	Test Pit 3 (ELY03-C1):				
	0.18-0.20 m				
	BH16:	OSL (X1736)	MIS 6	Bates et al.	
_	6.1-6.55 m			(2010)	
arī	BH2:	OSL (X1850)	MIS 7b-8	Bates et al.	
L L	3.86-3.89 m			(2010)	
Norton Farm	Borehole 1 (NOR96-BH1),	AAR of foraminif	era (this study)		
8	Sample 7:				
	4.98-5.00 m				
	5.08-5.10 m				
	PP/95, PP/96	OSL (X382,	Minimum MIS 6 (sample	Bates et al.	
Ħ	(field codes)	X383)	nearing saturation),	(2010)	
<u>Б</u>			likely MIS 7		
Portfield Pit	Borehole 1 (BH1):	AAR of foraminifera (this study)			
or	1.3-1.4 m				
ц	1.6-1.7 m				
	1.9-2.0 m				

Site	Horizon(s), where known	Method	Age assignment	Reference
Street, Isey	SEL01-1, SEL01-2 (field codes)	OSL (<i>X549, X550</i>)	MIS 5d-6	Bates et al. (2010)
West	Test Pit 7, Core 3: 30-32 cm from base of core	AAR of foraminif	era (this study)	

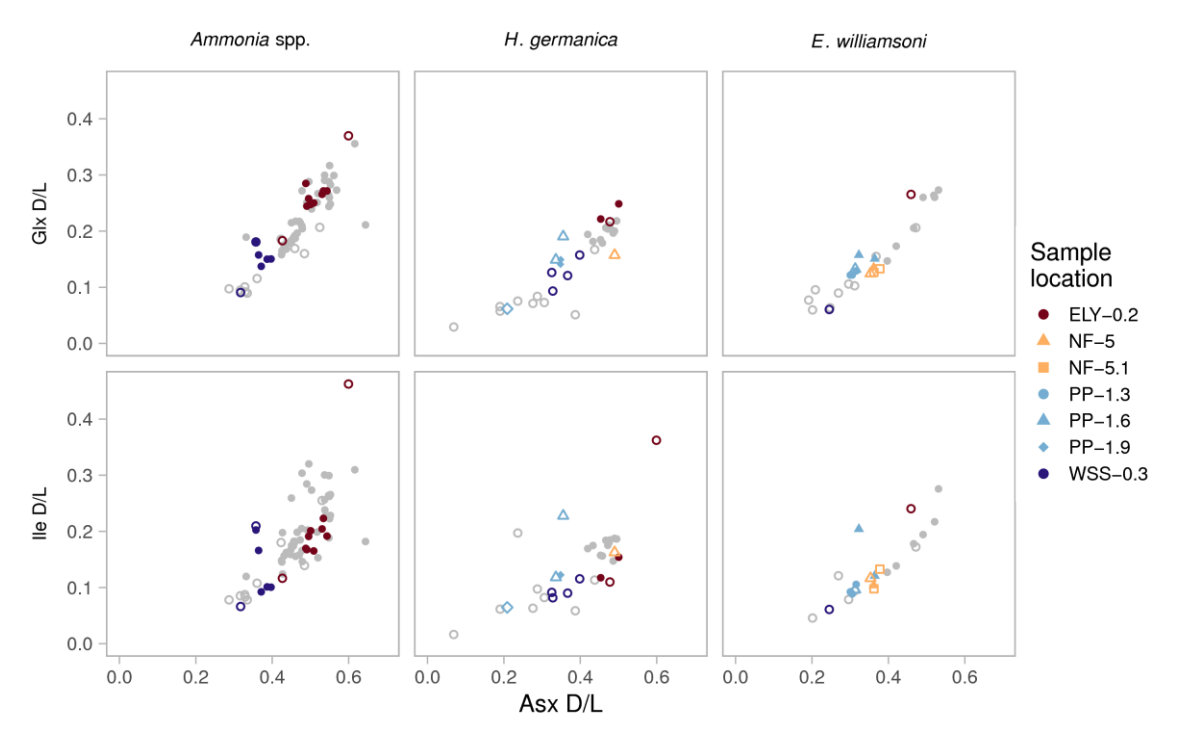


Fig. 6.8 – Asx vs Glx and Ile D/L covariance for THAA (total hydrolysable amino acid) fraction of *Ammonia* spp., *H. germanica* and *E. williamsoni* from West Sussex Coastal Plain sites. ELY: Earnley; NF: Norton Farm; PP: Portfield Pit; WSS: West Street, Selsey. Samples with [L-Ser]/[L-Asx] > 0.8 are flagged as open circles. All foraminifer AAR results are shown in grey for comparison (see **Section 6.3.2** for Asx vs Glx D/L plots of each species with all sites labelled).

6.3.3.1 Earnley

Earnley (SZ 825 947) is an infilled channel located in the foreshore of Bracklesham Bay corresponding to a marine regression from a Middle Pleistocene temperate stage, predating the raised beaches in the region (West et al., 1984). The marine infilling is commonly thought to be pre-Anglian (pre-MIS 12), or possibly MIS 11, on the basis of fossil assemblages (West et al., 1984), with A/I of a single *Macoma balthica* shell giving a tentative 'Hoxnian' (MIS 9 or 11) correlation (Preece et al., 1990). IcPD analyses of *Bithynia tentaculata* opercula place the site at the lower end of the pre-MIS 12 aminozone, suggesting a late MIS 13 age, although an early MIS 11 age cannot be ruled out (Penkman, unpublished data).

Ten *Ammonia* spp. samples, four *H. germanica* samples and one *E. williamsoni* sample were analysed from sediment taken between 0.18-0.20 m from Earnley Core 1. Eight of the ten *Ammonia* spp. samples form a close 'cluster' around Asx D/L 0.5-0.55, with two outlying samples (both of which are flagged by the [L-Ser]/[L-Asx] > 0.8 screening criterion) having substantially higher or lower D/L values (**Fig. 6.8**). These outliers can therefore confidently be excluded from the range of D/L values for Earnley. The remaining *Ammonia* spp. samples from Earnley have Asx and Glx D/L values higher than the other West Sussex sites, and similar to those from the Nar Valley sites (**Fig. 6.4**), consistent with an MIS 11 or 13 age indicated by *B. tentaculata* opercula. It is presumed that MIS 11 is more likely, assuming an MIS 9 and/or 11 age of the Nar Valley sites, although MIS 9 cannot be ruled out on the basis of the *Ammonia* spp. results. While only a small number of *H. germanica* and *E. williamsoni* samples were analysed, the average D/L values for these two species corroborate the results for *Ammonia* spp.

6.3.3.2 Norton Farm

Norton Farm (SU 925 063) contains deposits from the Aldingbourne Raised Beach to the north and the Brighton-Norton Raised Beach to the south, with OSL dating giving a range of ages within MIS 7 for both raised beaches (Bates et al., 2010).

Four *E. williamsoni* samples and one *H. germanica* sample were taken from sediment between 4.98 and 5.10 m of core NOR96-BH1, located in the Brighton-Norton Raised Beach section of Norton Farm. Of these, all but one *E. williamsoni* sample have [L-Ser]/[L-Asx] values > 0.8. Nevertheless the *E. williamsoni* samples analysed in this study cluster closely together (**Fig. 6.8**), in the same region as Portfield Pit (see **Section 6.3.3.3** below) and below the majority of samples from Earnley (see **Section 6.3.3.1** above). This is consistent with the correlation of both sites with the Brighton-Norton Raised Beach, and an MIS 7 age indicated by OSL dating. The single *H. germanica* sample deviates somewhat from the covariance trend for Asx and Glx, with a Glx D/L value within the range of the Portfield Pit samples, while its Asx and Ile D/L values are higher. In the absence of additional replicates it is not possible to determine whether this sample is an outlier for Norton Farm.

6.3.3.3 Portfield Pit

Portfield Pit (SU 8875 0580) is a gravel quarry located a few miles east of Norton Farm, containing marine sands from the Brighton-Norton Raised Beach sequence. OSL dating of overlying sediments

gives a minimum age of MIS 6 for the site, consistent with the association of the Brighton-Norton Raised Beach with MIS 7 (Bates et al., 2010).

Five *H. germanica* and six *E. williamsoni* samples were analysed from between 1.3 and 2.0 m of Borehole 1 from Portfield Pit. With the exception of one *H. germanica* sample, which has unexpectedly low Asx, Glx and Ile D/L values, and one *H. germanica* and one *E. williamsoni* sample with higher Ile D/L values than the other replicates (**Fig. 6.8**), the Portfield Pit samples have lower D/L values than Earnley (see **Section 6.3.3.1**) and similar D/L values to the Norton Farm samples (see **Section 6.3.3.2** above). As with Norton Farm, these results are generally consistent with an attribution of Portfield Pit to the Brighton-Norton Raised Beach and a likely MIS 7 age.

6.3.3.4 West Street, Selsey

The West Street site at Selsey (SZ 8448 9287) is an infilled estuarine channel correlated with the Pagham Raised Beach sequence. The northern part of the channel is characterised by marine conditions, while the southern end the channel is estuarine or near-terrestrial in character; the channel therefore potentially records a sequence of falling relative sea level during a past interglacial (Bates et al., 2009). OSL samples taken from the West Street channel give ages between MIS 5d-6 (Bates et al., 2010), corroborating an association with Pagham Raised Beach and therefore MIS 5e. *B. tentaculata* opercula from Selsey have been analysed; these come from the nearby Lifeboat Station channel (Penkman et al., 2013), which is also correlated with the Pagham Raised Beach (Bates et al., 2010). The *B. tentaculata* opercula results give an early MIS 7 attribution; whether the marine infilling of the Lifeboat Station channel occurred during the same transgression as the West Street channel is unknown, however (Bates et al., 2009).

Seven *Ammonia* spp., four *H. germanica* and one *E. williamsoni* sample were analysed from sediments taken from 30-32 cm of Core 3 from Test Pit 7 of the West Street site. The D/L values from the *Ammonia* spp. samples are quite variable, with three samples deviating from the general Asx vs Glx and Ile D/L covariance trend (**Fig. 6.8**) and a fourth sample having lower D/L values than the remaining three samples. Nevertheless, all the *Ammonia* spp. samples have D/L values lower than Earnley (see **Section 6.3.3.1**), and mostly lower than Northam Pit (see **Section 6.3.5.1**), consistent with a < MIS 7 attribution from this site from OSL, although a paucity of sites with both confident assignment to MIS 5e and robust mean D/L values for *Ammonia* spp. preclude ruling out a late MIS 7 attribution.

The single *E. williamsoni* sample has an [L-Ser]/[L-Asx] value > 0.8 so should be treated with caution, although its D/L values fall below the range for Portfield Pit and Norton Farm, consistent with an association of West Street with Pagham Raised Beach (and therefore younger than Portfield Pit and Norton Farm).

The *H. germanica* samples (which all have [L-Ser]/[L-Asx] values > 0.8) are more variable than the *Ammonia* spp. samples, precluding an estimation of mean D/L values for *H. germanica* at this site. This range is below Earnley, Northam Pit and the Burtle Beds, as for *Ammonia* spp., and similar to (for Asx), or slightly lower than (for Glx and Ile), Portfield Pit. Additional replicate analyses would be necessary to determine the relationship between West Street and Portfield Pit, which are not expected to be of the same age on the basis of correlation with raised beaches.

6.3.3.5 Discussion of West Sussex Coastal Plain results

The Asx, Glx and Ile D/L values obtained from *Ammonia* spp. and *E. williamsoni* from the West Sussex Coastal Plain sites are broadly consistent with current knowledge about the chronology of these sites, while the results for *H. germanica* are less consistent.

The *Ammonia* spp. results are consistent with an MIS 9, 11 or 13 age for Earnley and an MIS 5e or 7 age for West Street, Selsey; the large number of replicates for each site allow the variability of D/L values to be assessed and outliers identified, increasing the confidence in a reliable D/L range for these sites.

While a higher number of *E. williamsoni* samples had [L-Ser]/[L-Asx] values > 0.8, reducing the confidence of these results, Norton Farm and Portfield Pit produced results consistent with the two sites being the same age, likely MIS 7. The *E. williamsoni* results for Earnley and West Street, Selsey were also consistent with the expected ages for these sites, although as only one *E. williamsoni* replicate was analysed from each site their D/L values cannot be assessed confidently.

H. germanica samples from all four sites were analysed; however, these results are somewhat more variable than for the other species; additionally the majority of H. germanica samples had [L-Ser]/[L-Asx] values > 0.8. This poorer performance of H. germanica is consistent with the results for high-temperature decomposition experiments (Chapter 5). Earnley has the highest D/L values for H. germanica, as expected, while Portfield Pit and West Street, Selsey fall within a similar range of D/L values, with West Street possibly having slightly lower values. The single H. germanica sample from Norton Farm precludes an assessment of Norton Farm's age based on this species.

Overall, the results for the West Sussex Coastal Plain demonstrate the utility of analysing a large number of samples (ideally \geq 10) from a single horizon, to confidently identify outliers and determine the range of D/L values within a horizon. For *Ammonia* spp., the results suggest that [L-Ser]/[L-Asx] > 0.8 is an appropriate screening criterion which can be used to identify potential outliers, as the majority of *Ammonia* spp. samples which deviated from the main 'cluster' of D/L values had high [L-Ser]/[L-Asx] values. Conversely, where only a few samples were available for a single site, as for *E. williamsoni* and *H. germanica*, confident interpretations could not be made from the AAR data.

6.3.4 Nar Valley Clays

The Nar Valley is located in Norfolk, eastern England, and records a sequence of Pleistocene interglacial marine transgressions over around 20 m of elevation (Stevens, 1959). The valley is cut into Mesozoic rock and infilled with glacial till, likely laid down during MIS 12 (Anglian), with overlaying sands, silts, clays and peats referred to as the Nar Valley Freshwater Beds. In several locations across the valley, the Nar Valley Freshwater Beds are overlain by Nar Valley Clay — marine clay deposits representing one or more sea-level transgressions (Stevens, 1959; Ventris, 1996). These marine clays are thought to represent a mid to late temperate sea-level highstand of around 23 m OD (Langford and Briant, 2004).

Table 6.5 shows the existing chronological evidence for the Nar Valley Clays, along with the sampling locations of the foraminifer AAR results presented in this thesis. Previous work characterises the Nar Valley Freshwater Beds as being part a single 'Hoxnian' interglacial (e.g. Gibbard et al., 1992). More recent pollen analysis of the Nar Valley Clays has identified two separate pollen profiles, one at Bradmoor Hill and Railway Cottage, and another at the lower elevation sites of Horse Fen, Tottenhill and Blackborough End Quarry, indicating two marine transgression events (Barlow et al., 2017). Although both these pollen profiles have been assigned to sub-stages of the 'Hoxnian' pollen assemblage, additional analysis suggests the sequences may be a consequence of marine deposition during two separate interglacials, MIS 9 and 11 (Barlow et al., 2017), which are thought to have similar pollen profiles (Thomas, 2001). At Tottenhill, U-Th dating of underlying peats from the Nar Valley Freshwater Beds (Rowe et al., 1997) and preliminary A/I work on the foraminifera Ammonia beccarii and Aubignyna perlucida indicate an MIS 9 age (Scourse et al., 1999). More recently, IcPD analyses of B. tentaculata opercula from Tottenhill indicated a mid-late MIS 11 or early MIS 9 age for this site (Barlow et al., 2017). One Bithynia operculum fragment from Horse Fen was also analysed, yielding lower D/L values and therefore a

tentatively younger age for Horse Fen than Tottenhill. It is currently thought that the Nar Valley Clays represent two interglacial sea-level highstands, one in MIS 11 and one in MIS 9, although an MIS 11 age for both highstands cannot be ruled out (Barlow et al., 2017).

A lack of *Bithynia* opercula in the Nar Valley deposits limited the application of the *Bithynia* aminostratigraphy to this region (Barlow et al., 2017); therefore foraminifera, which were found at Railway Cottage (RC), Horse Fen (HF), Bradmoor Hill (BH) and Blackborough End Quarry (BE), were targeted for AAR analysis (see **Fig. 6.1**, **Table 6.1** and **Table 6.2** for site locations and horizons sampled). Some of these analyses were carried out between 2013-2016 as part of the iGlass project using the bleaching pre-treatment developed by Penkman et al. (2008). A small number of additional analyses were carried out in this thesis on material from HF and RC using an H_2O_2 pre-treatment. It is important to note that Pleistocene samples treated with NaOCl were found to have slightly higher D/L values than those treated with H_2O_2 (**Section 4.4.3**); therefore the D/L values of the iGlass samples are likely to be somewhat higher in comparison to equivalent samples treated with H_2O_2 .

Table 6.5 – Chronological evidence from Nar Valley Clay sites. IcPD: intra-crystalline protein diagenesis approach to AAR using a strong oxidative pre-treatment (NaOCI); AAR: weak oxidative pre-treatment (H_2O_2) used.

Site	Horizon(s), where known	Method Age assignment Reference					
Region	-	Pollen stratigraphy	Hoxnian (MIS 9 and/or 11), temperate	Gibbard et al., (1992) Barlow et al., (2017)			
Reg	-	Underlying Anglian clays	Maximum age of MIS 12 for Nar Valley Clays	Stevens, (1959)			
	Freshwater peat underlying Nar Valley Clay	Th/U dating	217 ± 14 ka	Rowe et al., (1997)			
Tottenhill	Nar Valley Clays Silty clay at base of Nar Valley Clay	AAR of foraminifera	MIS 9	Scourse et al., (1999)			
	Freshwater bed and shelly peat at base of core	IcPD of <i>B.</i> tentaculata opercula	Mid-late MIS 11 or early MIS 9 age	Barlow et al. (2017)			
Brad- moor Hill	Core BH: 20, 1.20, 1.60 m	IcPD of foramif	ported here)				
e Fen	Core 13-1: 10.58 m	IcPD of <i>B.</i> tentaculata opercula fragment	Mid-late MIS 11 or early MIS 9, possibly younger than Tottenhill	Barlow et al. (2017)			
Horse Fen	Core HF4: 0.22, 0.30, 3.05, 3.85, 4.52 m Core HF2: 1.11 m	IcPD of foraminifera (iGlass project, reported here)					
	Core 13-1: 9.90-9.91 m	AAR of foraminifera (this study)					

Site	Horizon(s), where known	Method	Age assignment	Reference	
Black- borough End Quarry	BQ-12-1: 3.90, 5.50, 7.00 m	IcPD of foraminifera (iGlass project, reported here)			
Railway Cottage	Core RC: 5.30 m Core RC: 6.10 m	IcPD of foramir	nifera (iGlass project, r	eported here)	
Rail	Core RC: 5.56-5.57 m Core RC: 6.28-6.29 m	AAR of foramin	ifera (this study)		

6.3.4.1 Results

The covariance of Asx with Glx and Ile D/L is shown for the Nar Valley samples in **Fig. 6.9**. For *Ammonia* spp., the majority of samples fall between Asx D/L 0.4-0.6, with a few outliers substantially higher or lower than this range, and two samples (one sample from horizon RC-5.6 and one from BE-3.9) deviating from the general Asx vs Glx or Ile D/L covariance trend. The spread of D/L values for *Elphidium* spp. is greater, between Asx D/L 0.2 and 0.55, although the majority of samples with an Asx D/L value < 0.5 are flagged by the [L-Ser]/[L-Asx] > 0.8 screening criterion, suggesting that they may be compromised by modern contamination. Only two *H. germanica* samples were analysed from the Nar Valley sites, one of which had [L-Ser]/[L-Asx] > 0.8, limiting any interpretations of the age of the Nar Valley Clays on the basis of this species.

With the exception of the samples with an [L-Ser]/[L-Asx] value > 0.8, most samples from the Nar Valley have Asx, Glx and Ile D/L values higher than sites correlated with MIS 7 (Norton Farm, see Section 6.3.3.2; Portfield Pit, see Section 6.3.3.3; Northam Pit, see Section 6.3.5.1), and within the same range as Earnley, which is thought to be MIS 11 or 13 in age (see Section 6.3.3.1). This corroborates the age assignments of MIS 9 and/or 11 produced by pollen stratigraphy, OSL and Bithynia opercula IcPD. The lack of discrimination between the Nar Valley sites in this data set could either indicate that the Nar Valley highstands analysed here fall within the same MIS (e.g. the two sea-level highstands of MIS 11) or, more likely given the spread of D/L values within each site, that the variability of D/L values in foraminifera is too high to differentiate between MIS 11 and MIS 9. As racemisation takes place at a much slower rate during glacial periods, D/L values from deposits from the early part of an interglacial are often challenging to differentiate from the later part of the preceding interglacial (Miller and Mangerud, 1985; Penkman et al., 2013).

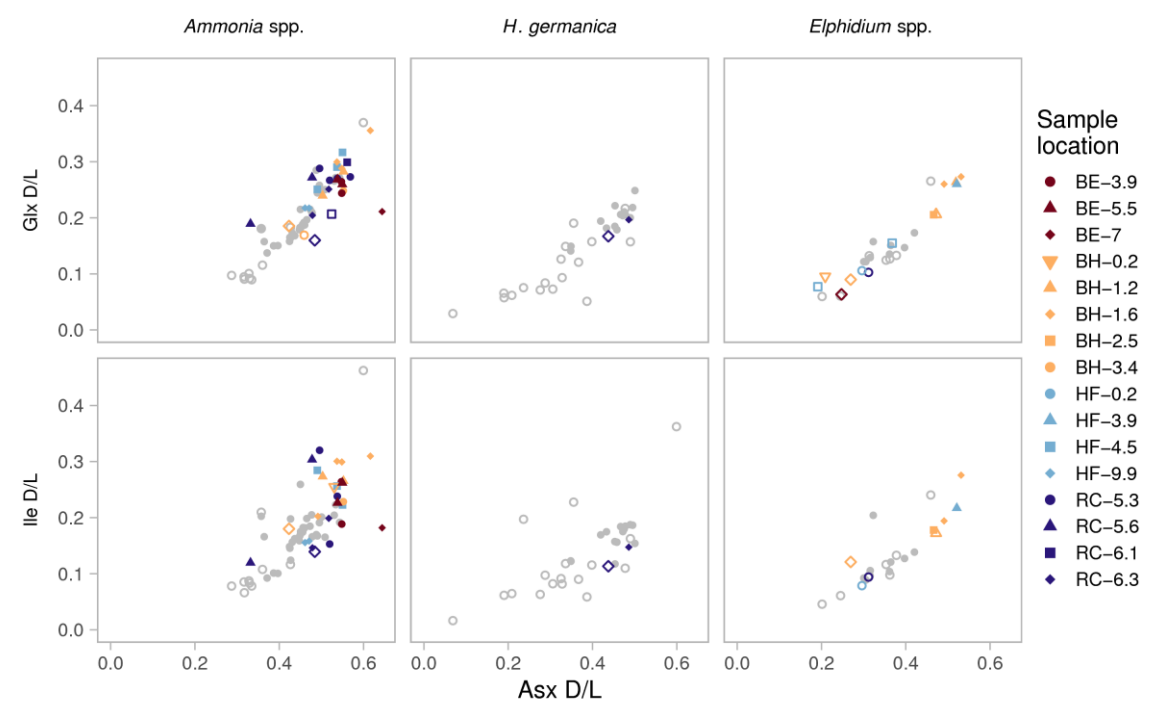


Fig. 6.9 – Asx vs Glx and Ile D/L covariance for THAA (total hydrolysable amino acid) fraction of *Ammonia* spp., *H. germanica* and *Elphidium* spp. (not identified to species level) from Nar Valley Clay sites. BE: Blackborough End Quarry; BH: Bradmoor Hill; HF: Horse Fen; RC: Railway Cottage. Samples with [L-Ser]/[L-Asx] > 0.8 are flagged as open circles. All foraminifer AAR results are shown in grey for comparison (see **Section 6.3.2** for Asx vs Glx D/L plots of each species with all sites labelled).

A possible explanation for the variability of D/L values in the Nar Valley sites is that foraminifera were taken from a range of depths in each core, as samples from higher in a core should be younger than those which are lower in the core. The relationship between core depth and Asx D/L is shown in Fig. 6.10 for the four Nar Valley cores where multiple depths were sampled. With the possible exception of Blackborough End Quarry (BE), there is no pattern of higher D/L values at lower depths. This indicates that the timescales of deposition of the Nar Valley Clays at these sites are not sufficiently long to produce measurable differences in the D/L values of foraminifera. The variability in D/L values therefore likely either results from natural age variability of the foraminifera or, given that the majority of the Nar Valley samples had sample sizes of around 10-20 tests and used the standard IcPD bleaching pre-treatment from Penkman et al. (2008), from low concentrations of amino acids measured. Further work on the Nar Valley Clays using larger sample sizes, higher numbers of replicates, and the H_2O_2 pre-treatment may yield more tightly constrained D/L values for each site. An H_2O_2 pre-treatment will also allow for more confident comparisons to other sites with similar D/L values.

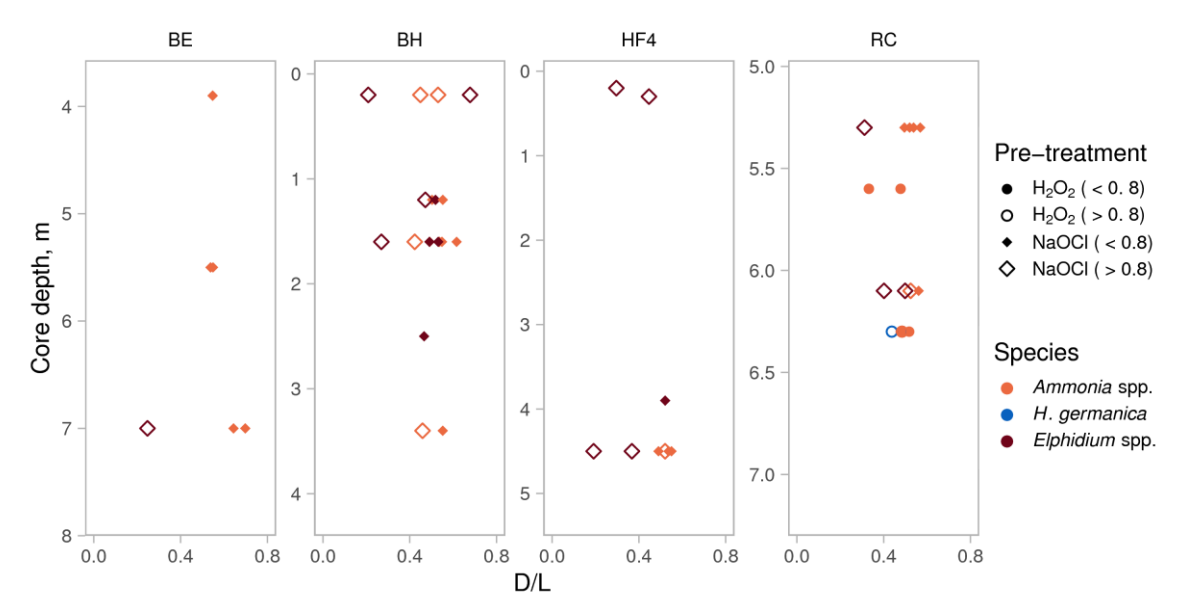


Fig. 6.10 – Asx D/L values for THAA (total hydrolysable amino acid) fraction of *Ammonia* spp., *H. germanica* and *Elphidium* spp. (not identified to species level) from Nar Valley cores. BE: Blackborough End Quarry; BH: Bradmoor Hill; HF4: Horse Fen Core 4; RC: Railway Cottage. Diamonds refer to samples treated with 2 h 3% H₂O₂; circles refer to samples treated with 48h 12% NaOCl. Samples with [L-Ser]/[L-Asx] > 0.8 are flagged as open shapes. HF2 (Horse Fen Core 2) was only sampled at one depth, so is not included. Note individual y-axis range for each plot; 'core depth' refers only to the sampling location in each core, and does not correspond to m OD.

Overall, the results from the Nar Valley foraminifera are consistent with a pre-MIS 7 age for the Nar Valley Clays, with a tentative age assignment of MIS 11 or 13 on the basis of comparative D/L values to Earnley (see Section 6.3.3.1). There is no clear discrimination between the D/L values of the four sites investigated, precluding an assessment of their relative chronology on the basis of foraminifer AAR. A substantial proportion of samples had [L-Ser]/[L-Asx] values > 0.8; these samples typically had lower D/L values than the other samples from the same horizon, suggesting that high [L-Ser]/[L-Asx] values are indicative of modern contamination, as the likelihood of samples from the same horizons being truly younger (and therefore having a naturally higher [L-Ser]/[L-Asx] value) is low.

6.3.5 March Gravels

The March Gravels are a series of outcropping sediments found across the central and western Cambridgeshire Fens. They consist of sands and gravels, contain a mix of freshwater, estuarine and marine fossils (Keen et al., 1990), and represent a post-Anglian but pre-Devensian (therefore between MIS 12 and MIS 2-5d) high sea-level phase (Langford and Briant, 2004). The chronology of the March Gravels and associated fluvial Nene River Terrace deposits has important implications

for the extent of interglacial sea-level rise and post-glacial isostatic rebound in the region during this period (Langford and Briant, 2004), as well as placing constraints on the extent of glacial ice coverage in the south of England.

Foraminifera were analysed from four sites in the March Gravels region: Northam Pit, Somersham, King's Dyke Quarry, and West Face Quarry (**Fig. 6.1**). The sedimentary context of each site is discussed below; **Table 6.6** summarises the existing chronological evidence present at each site.

Table 6.6 – Chronological evidence from March Gravel sites. Laboratory codes for OSL dates are given in italics. For King's Dyke Quarry and West Face Quarry, the original context information is given with the equivalent facies association in the revised nomenclature (Langford, in preparation) where possible (equivalence is denoted by \equiv). IcPD: intra-crystalline protein diagenesis approach to AAR using a strong oxidative pre-treatment (NaOCl); AAR: weak oxidative pre-treatment (H₂O₂) used; A/I: isoleucine epimerisation, whole-shell approach.

Si	te	Horizon(s)	Method	Age assignment	Reference	
<u> </u>	Ξ	2.4 m OD	OSL (Shfd19175)	MIS 7	Bateman et al. (2020)	
1	Northam Pit	2.5 m OD	OSL (Shfd19183)	3 ka (considered to be compromised)	Bateman et al. (2020)	
2	2	1.9 m OD 2.45 m OD	AAR of foraminifera (this study)			
	_	Unspecified	A/I of <i>C. fluminalis</i>	MIS 5e or MIS 7	West et al. (1999)	
ham	rry, Sectio)	S3 from Bed H2	IcPD of <i>B</i> . tentaculata and <i>B</i> . troschelli opercula	Mid-late MIS 7	Penkman et al. (2013)	
Somersham	(Fore Fen Quarry, Section SBK)	S1 from Bed H2	IcPD of <i>B.</i> tentaculata opercula	Mid-late MIS 7	Presslee (unpublished data)	
í	(For	S1 from Bed H2	AAR of foraminifera (this study)			
	Section A ≡ KD2	Facies A2 at Log 1 ≡ W9	OSL (Shfd96131)	MIS 6	Langford et al. (2004)	
		Facies A1 ≡ W4	A/I of <i>Littorina</i>	MIS 7 - 11	Langford et al. (2004)	
King's Dyke Quarry		Boundary of W4 and W7 (sand ribbon)	IcPD of <i>B.</i> tentaculata opercula	MIS 7	Presslee (unpublished data)	
Ž		Top of facies association W7 AAR of foraminifera (this study)				
King's	C	Sand lens at southern end of Section C ≡ W13	OSL (Shfd96130)	MIS 5e	Langford et al. (2004)	
		W4 (above left-hand side of sand lens ≡ W13)	IcPD of Littorina	MIS 7 - 11	Demarchi (2009)	
	Section	Wavy laminated sands at the top of W13 (above sand lens)	AAR of foraminifera	(this study)		

Site		Horizon(s)	Method	Age assignment	Reference	
		Unit F5 ≡ W14 Unit F6 ≡ W15 Unit G4 ≡ W14/15	OSL (Shfd030017- Shfd030021)	< MIS 5e (Devensian)	Langford et al. (2007)	
*	on F≡WF3	Organic mud bed unit from F1 ≡ W3	IcPD of Valvata piscinalis and B. tentaculata shell, and B. tentaculata opercula	MIS 7	Langford et al. (2007)	
West Face Quarry*	Section	Unit F3 ≡ W7 Top of facies association	IcPD of <i>B.</i> tentaculata opercula	MIS 7	Presslee (unpublished data)	
West F		Unit F3 ≡ W7 Top (Fa) and bottom (Fb) of facies association	AAR of foraminifera (this study)			
	1 ≡ WF5	Unit 2a ≡ W5&6	IcPD of <i>B.</i> tentaculata opercula	MIS 7, possibly late MIS 7	Penkman et al. (2013)	
	Section 1	Unit 2b ≡ W6 Unit 2c ≡ W8	IcPD of <i>B.</i> tentaculata opercula	MIS 7, possibly late MIS 7	Langford et al. (2014)	

^{*} formerly referred to as Funtham's Lane (Langford et al., 2014).

Northam Pit (TF 2303 0364) is a March Gravel exposure extending from 1.9 to 5.2 m OD and consisting of a sequence of sandy gravels with interbedded sand and silt beds (Keen et al., 1990). Palaeoecological data from the site indicate a marine proximal environment at 1.9 m OD and an estuarine environment between 1.9 m OD and 2.6 m OD, with an influx of fluvial species at 2.4 m OD. OSL dating at 2.4 m OD places Northam Pit within MIS 7; this site therefore provides an indication of relative sea level during MIS 7.

Somersham (TL 375 798) contains channel deposits from the River Great Ouse from both glacial and interglacial stages (West et al., 1994, 1999). The gravels in Section SBK are considered to be Devensian (MIS 2-5d) with fauna reworked from underlying interglacial sediments, although it is possible that the gravels were deposited during a temperate stage. A/I of *C. fluminalis* and more recently IcPD of *Bithynia* opercula give an upper age limit of MIS 7 for these gravels (West et al., 1999; Penkman et al., 2013; Presslee, unpublished data); the foraminifera analysed in this work are expected to be of the same age as the molluscs.

King's Dyke Quarry (TL 251 981) and West Face Quarry (TL 238 979, formerly referred to as Funtham's Lane (Langford et al., 2014)) are nearby sites situated on Whittlesey (or Whittlesea), a gravel-topped 'island' between 3-9 m OD, which consists predominantly of March Gravel with some outcropping of River Nene 1st Terrace deposits on its western edge (Langford et al., 2004).

The sedimentary succession at Whittlesey contains deposits spanning from MIS 8 to the Holocene, therefore recording an archive of fluvial reorganisation and sea-level change over the last three glacial-interglacial cycles. The chronology of King's Dyke Quarry and West Face Quarry are discussed in more detail in Section 6.3.5.3. The stratigraphical nomenclature of the Whittlesey quarries has been subject to several revisions (Langford et al., 2014; Langford, in preparation); where possible published dating work is given with the nomenclature provided in the original publication along with its equivalent facies association in the revised nomenclature (Table 6.1).

Fig. 6.11 shows the Asx vs Glx and Ile D/L covariance of the samples analysed from Northam Pit, Somersham, King's Dyke Quarry and West Face Quarry. With the exception of Northam Pit (NP), only a small number of foraminifera from each site were available for AAR analysis; the small number of replicates analysed, and given that all samples had [L-Ser]/[L-Asx] values > 0.8, mean that these results should be interpreted with considerable caution. The results for each site and comparison to existing chronology is discussed below.

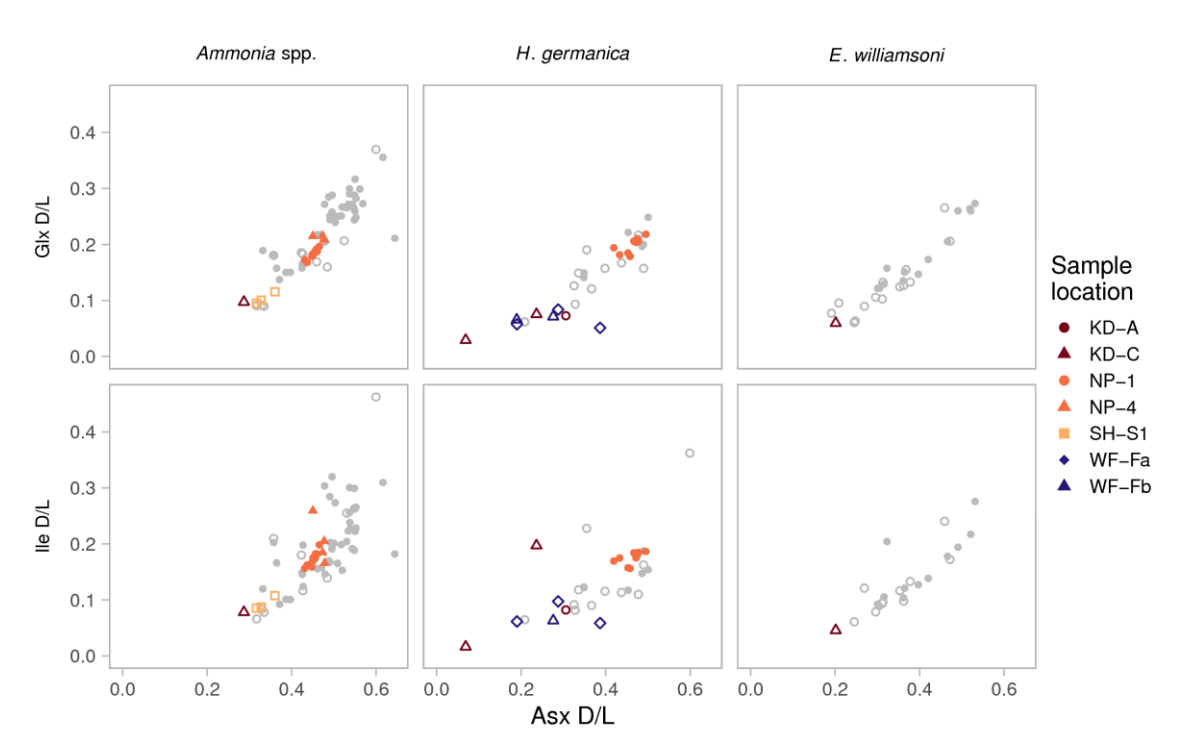


Fig. 6.11 – Asx vs Glx and Ile D/L covariance for THAA (total hydrolysable amino acid) fraction of *Ammonia* spp., *H. germanica* and *E. williamsoni* from March Gravel sites. KD: King's Dyke, NP: Northam Pit, SH: Somersham, WF: West Face Quarry. Samples with [L-Ser]/[L-Asx] > 0.8 are flagged as open shapes. All foraminifer AAR results are shown in grey for comparison (see **Section 6.3.2** for Asx vs Glx D/L plots of each species with all sites labelled).

6.3.5.1 Northam Pit

Two samples from the Northam Pit exposure yielded sufficient foraminifera for AAR analysis – NP-1, at 1.9 m OD, and NP-4, at 2.45 m OD. An OSL date at 2.5 m OD gives these samples a minimum age constraint of MIS 7; the OSL sample taken from 2.4 m OD gave an anomalously young age and is considered to have been compromised (Bateman et al., 2020).

Large numbers of *Ammonia* spp. and *H. germanica* were present in NP-1; NP-4 contained only substantial numbers of *Ammonia* spp., so no analyses of *H. germanica* were carried out for this sample. For both species, the samples from Northam Pit had higher Asx, Glx and Ile D/L values than the samples from Somersham, King's Dyke Quarry or West Face Quarry (**Fig. 6.11**). While this suggests that Northam Pit is older than the other March Gravel sites, the reliability of the D/L values for the other sites is somewhat questionable (see **Sections 6.3.5.2** and **6.3.5.3** for discussion).

Comparing the Northam Pit results to sites from other regions (Fig. 6.4), the *Ammonia* spp. D/L values are lower than the majority of the samples from Earnley (MIS 11 to MIS 13, Section 6.3.3.1) and the Nar Valley Clays (MIS 9 and/or 11, Section 6.3.4.1). While the pattern is less conclusive for *H. germanica* due to the limited number of comparative data points (Fig. 6.5), Northam Pit has higher D/L values than the majority of the samples from Portfield Pit (likely MIS 7, Section 6.3.3.3) and West Street, Selsey (likely MIS 5e, Section 6.3.3.4). These results are therefore consistent with the OSL age of MIS 7 from overlying sediments, and gives an upper age limit of MIS 9 for the Northam Pit foraminifera.

While it is higher in the stratigraphic sequence than NP-1, NP-4 has similar Asx and Ile D/L values and slightly higher Glx D/L values (statistically significant, p < 0.05). This suggests that the two samples are of similar age, with the discrepancy in Glx D/L values likely representing a limitation in the resolution of AAR in foraminifera.

6.3.5.2 Somersham Quarry, Section SBK

Three *Ammonia* spp. samples were analysed from Bed H2 in Section SBK at Somersham Quarry, a gravel deposit between -2 and 1 m OD with an ecologically mixed assemblage. This bed was likely laid down during a cold stage with fauna reworked from underlying interglacial sediment, although both the interglacial sediments and gravel could have been deposited during the same temperate stage (West et al., 1994, 1999; Langford et al., 2014). Early chronological work on Section SBK gave

a correlation with MIS 5e or MIS 7 on the basis of pollen stratigraphy (West et al., 1999); A/I measurements of *C. fluminalis* (West et al., 1999), and more recent IcPD analyses of *B. tentaculata* and *B. troschelli* opercula (Penkman et al., 2013), give a mid-late MIS 7 age for the faunas in Section SBK. IcPD analysis of *B. tentaculata* opercula from Bed H2 Section SBK (the same bed from which foraminifera were taken for analysis) also yield a mid-late MIS 7 age (Presslee, unpublished data).

All three *Ammonia* spp. samples from Somersham have [L-Ser]/[L-Asx] values > 0.8, reducing the confidence in any interpretation of their D/L values. In general, the Somersham samples have lower D/L values than the other sites for which *Ammonia* spp. was analysed (**Fig. 6.4**), with the exception of one sample from West Street, Selsey (likely MIS 5e, **Section 6.3.3.4**) and two samples from the Burtle Beds (MIS 5e or 7, **Section 6.3.6**), all of which had [L-Ser]/[L-Asx] > 0.8 and lower D/L values than the other replicates for those sites, and are therefore likely to be outliers. Given that the *Bithynia* opercula from the same horizon produce an MIS 7 age, the low D/L values for the Somersham foraminifera are not consistent with the expected chronology of the site. Additional analyses of foraminifera from Somersham may be able to identify whether these samples have been compromised.

6.3.5.3 King's Dyke Quarry and West Face Quarry

Foraminifera from two facies associations at King's Dyke Quarry (W7 of Section A \equiv KD2, W13 of Section C \equiv KD4) and one facies association at West Face Quarry (W7 of Section F) were collected for AAR analysis. A simplified schematic of the aggradational sequence of the two sites, with the foraminifer sampling locations and locations of existing chronological control indicated, is given in **Fig. 6.12**. A map of section locations at these two sites can be found in **Appendix 4**.

b) West Face Quarry a) King's Dyke Quarry OSL < MIS 5e Bithvnia IcPD = MIS 7 Bithynia IcPD = MIS 7 OSL = MIS 6OSL = MIS 5e Littorina A/I & IcPD = MIS 7 W15 W15 (channel A) W14 W10 (channel A) W5&6 (W7 W2 W7 W4 underlying Jurassic Oxford Clay underlying Jurassic Oxford Clay 'KĎ-A' 'WF-Fa' 'KD-C' 'WF-Fb'

Fig. 6.12 – Simplified schematic of the aggradational sequence of a) King's Dyke Quarry and b) West Face Quarry (formerly Funtham's Lane), with relevant existing chronological information (top) and sampling locations of foraminifera for this study (bottom). IcPD: intra-crystalline protein diagenesis approach to AAR using a strong oxidative pre-treatment (NaOCl); A/I: isoleucine epimerisation, wholeshell approach. Details of chronological work are given in **Table 6.6**. Revised nomenclature taken from Langford (in preparation); for corresponding nomenclature from original publications, see **Table 6.1**. Not to scale; locations of samples taken for AAR and OSL dating are approximate.

IcPD analyses of *B. tentaculata* opercula from the boundary of facies association W4 and W7 at King's Dyke Quarry give a minimum age of MIS 7 for W7 (Presslee, unpublished data), supported by A/I and IcPD measurements of *Littorina* shells from underlying W4 sediments giving a minimum MIS 7 age (Langford et al., 2004; Demarchi, 2009). The palaeoecological data of W7 are indicative of reworking from underlying deposits (Langford et al., 2004), with a possible correlation to the influx event recorded in facies association W7 at West Face Quarry. Facies association W13, found at Section C = KD4, is dated by OSL to MIS 5e (Langford et al., 2004). The faunal assemblage of this facies is largely estuarine, with no indication of reworking.

At West Face Quarry, IcPD analyses of *B. tentaculata* opercula give an MIS 7 age for facies associations W7 (Presslee, unpublished data), W3 (Langford et al., 2007), W5&6 and W8 (Penkman et al., 2013; Langford et al., 2014). OSL dating of overlying facies associations W14 and W15 give post-MIS 5e (Devensian) ages (Langford et al., 2007). In contrast to facies association W7 at King's Dyke Quarry, the palaeoecological data from W7 at West Face Quarry are not indicative of reworking from underlying deposits.

At King's Dyke Quarry, one H. germanica sample was analysed from facies association W7 of Section A = KD2 (abbreviated KD-A), and one Ammonia spp., one H. germanica and one E. williamsoni sample were analysed from facies association W13 of Section C = KD4 (abbreviated KD-C). At West Face Quarry, three H. germanica samples from the top of facies association W7 (WF-Fa) and two H. germanica samples from the bottom of facies association W7 (WF-Fb) were analysed.

All the samples had [L-Ser]/[L-Asx] > 0.8, and fell at the lower end of the range of D/L values across all sites, substantially lower than Northam Pit, with no clear discrimination between KD-C (expected to be MIS 5e) and KD-A and WF-F (expected to be MIS 7). The single *Ammonia* spp. sample from KD-C has similar D/L values to those for Somersham, which are also likely to be unreliable (Section 6.3.5.2 above). Given the lack of robust comparative data for *H. germanica*, it is not possible to conclude whether the samples from King's Dyke Quarry and West Face Quarry are actually younger than Northam Pit, or whether these samples are contaminated. A larger number of replicate analyses from each facies association may be able to determine whether the D/L values given by these samples are reliable; in the absence of more robust data no further age interpretation is possible.

6.3.6 Greylake 3, Burtle Beds

The Burtle Beds formation is a series of 'islands' of marine sands and gravels in various locations across Somerset, UK, deposited over several interglacials in the late Middle and Late Pleistocene. The elevation of the Burtle Beds suggests a sea-level highstand around 12 m above present mean sea level (Kidson et al., 1978). The formation has been the subject of AAR on various mollusc species, with early A/I results suggesting a probable MIS 5e correlation for the sands at the site Greylake 2 ($Patella\ vulgata\$ and $Patella\$ and $Patella\$ and $Patella\$ and $Patella\$ base of the site Greylake 1 ($Patella\$ base of the site Greylake 1 ($Patella\$ corbicula (Hunt et al., 1984)). IcPD analyses of $Patella\$ correlation with MIS 5e or late MIS 7; however, a lack of well-dated comparative data for this species limits the confidence of an age assignment for this site (Dowsett, 2017). Therefore, as foraminifera were present in large numbers at GL3, the site was targeted for AAR of foraminifera.

Six *Ammonia* spp., one *H. germanica* and two *Elphidium* spp. (not identified to species level) samples were analysed from Sample 2 (3.3-3.5 m) of the GL3 exposure (immediately above the *Peringia ulvae* samples). **Fig. 6.13** shows the Asx vs Glx and Ile D/L covariance of the Burtle Beds samples.

Two *Ammonia* spp. samples had lower D/L values than the other replicates and [L-Ser]/[L-Asx] > 0.8, indicating potential modern contamination. The remaining samples have D/L values between West Street, Selsey (likely MIS 5e) and Northam Pit (likely MIS 7) for *Ammonia* spp. (**Fig. 6.4**), while the *Elphidium* spp. samples have similar or slightly higher D/L values than Portfield Pit and Norton Farm (both likely MIS 7) (**Fig. 6.6**). The single *H. germanica* sample falls within the range for

Northam Pit (Fig. 6.5). While the results for the three species are somewhat inconsistent, overall they suggest a likely MIS 7 assignment for the base of GL3, although an early MIS 5e age cannot be ruled out.

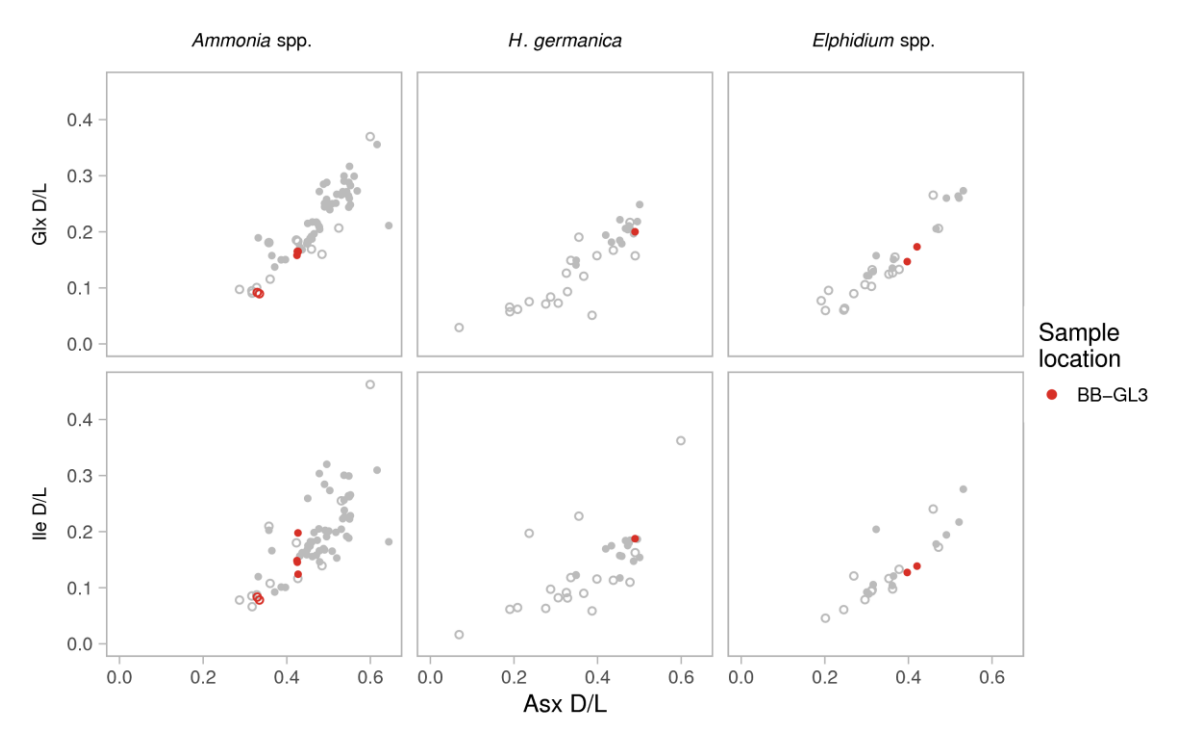


Fig. 6.13 —Asx vs Glx and Ile D/L covariance for THAA (total hydrolysable amino acid) fraction of *Ammonia* spp., *H. germanica* and *Elphidium* spp. (not identified to species level) from Burtle Beds Greylake 3. Samples with [L-Ser]/[L-Asx] > 0.8 are flagged as open shapes. All foraminifer AAR results are shown in grey for comparison (see **Section 6.3.2** for Asx vs Glx D/L plots of each species with all sites labelled).

6.4 Conclusions

Analysis of *Ammonia* spp., *H. germanica* and *Elphidium* spp. (including *E. williamsoni*) from UK Pleistocene sea-level records shows that the breakdown of proteins in all three species provides chronological information, with the relative ages given by the D/L values of foraminifera generally consistent with the known chronology of the sites investigated. Asx and Glx show the best overall trend of D/L covariance, and provide a range of temporal resolutions due to their different racemisation rates. Ile also provides supporting information, although the D/L values for this amino acid were somewhat more variable than for Asx and Glx.

The use of [L-Ser]/[L-Asx] as a screening criterion for samples potentially compromised by modern contamination was investigated. Where a large (> 5) number of samples were analysed from a

single horizon, samples with [L-Ser]/[L-Asx] > 0.8 tended have lower D/L values than the other replicates, and in general sites which deviated from the expected relative chronology (e.g. Somersham, see Section 6.3.5.2) had [L-Ser]/[L-Asx] values > 0.8 for all samples. This suggests that [L-Ser]/[L-Asx] can be used alongside other factors to identify outlying samples, although a less stringent cut-off (e.g. [L-Ser]/[L-Asx] > 1.2) may be more appropriate for foraminifera due to their small size (Kosnik et al., 2008).

For sites with a large number of replicate samples with [L-Ser]/[L-Asx] < 0.8, the range of D/L values for each site fell in the expected stratigraphic order, given the independent chronology of each site. Fig. 6.14 shows the Asx vs Glx D/L covariance for sites with five or more samples with [L-Ser]/[L-Asx] < 0.8 for a single species: Earnley; Northam Pit; Portfield Pit; West Street, Selsey and the Nar Valley Clay sites (comprising Blackborough End Quarry, Bradmoor Hill, Horse Fen and Railway Cottage). For Ammonia spp., confident D/L ranges can be derived for West Street, Selsey, Northam Pit, Earnley and the Nar Valley sites. This places them in the expected stratigraphic order, with West Street, Selsey (OSL attribution to MIS 5e, see Section 6.3.3.4) having the lowest D/L values, followed by Northam Pit (OSL attribution to MIS 7, see Section 6.3.5.1), with Earnley (IcPD attribution to MIS 11-13, see Section 6.3.3.1) and the Nar Valley Clay sites (IcPD attribution to MIS 9-11, see Section 6.3.4) falling within the same range of D/L values. In addition to generally lower abundance in the Pleistocene material, H. germanica and Elphidium spp. (including E. williamsoni) had more samples with [L-Ser]/[L-Asx] > 0.8 and higher between-replicate variability; therefore sufficient robust samples were available for only a few sites (Northam Pit for H. germanica, Portfield Pit and the Nar Valley Clay sites for Elphidium spp.). For Elphidium spp., the Portfield Pit samples had lower D/L values than the Nar Valley Clay sites, which is consistent with an MIS 7 attribution for Portfield Pit by correlation to other Brighton-Norton Raised Beach Sites (see Section **6.3.3.3**). These species therefore have the potential to give chronological information if more comparative material can be analysed.

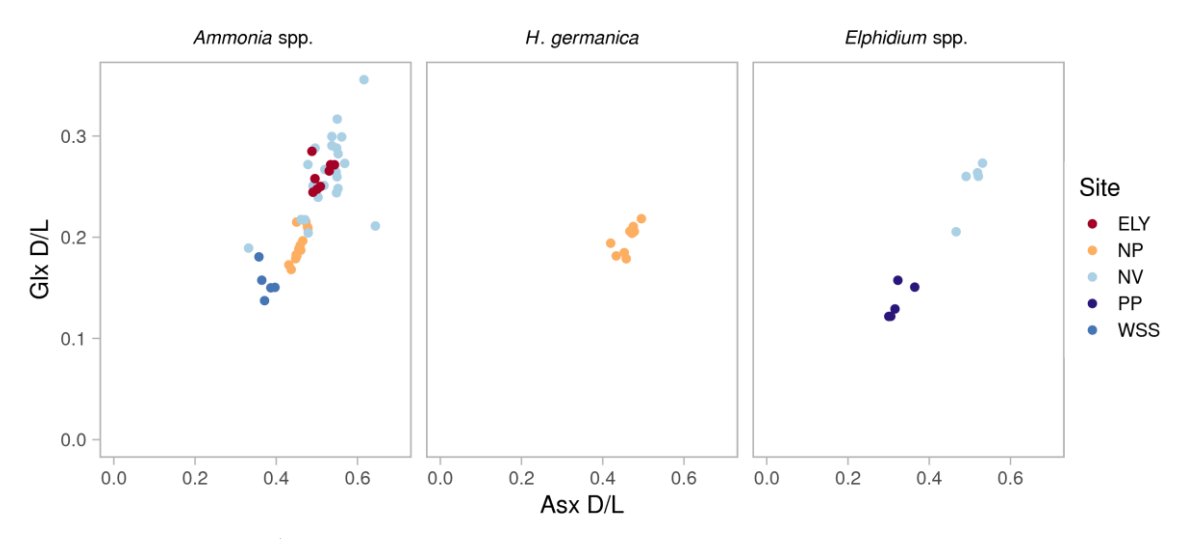


Fig. 6.14 – Asx vs Glx D/L covariance of THAA (total hydrolysable amino acid) fraction of *Ammonia* spp., *H. germanica* and *Elphidium* spp. (including *E. williamsoni*) from UK Pleistocene sea-level records with five or more samples with [L-Ser]/[L-Asx] < 0.8 (ELY: Earnley; NP: Northam Pit; NV: Nar Valley Clays (comprising Blackborough End Quarry, Bradmoor Hill, Horse Fen and Railway Cottage); PP: Portfield Pit; WSS: West Street, Selsey). Samples from these sites with [L-Ser]/[L-Asx] > 0.8 have been excluded from this figure.

To overcome the limitations of AAR of foraminifera identified in this pilot study, future development of this foraminifer-based aminostratigraphy for the UK Pleistocene should therefore focus on analysing a large number of monospecific samples (ideally 10 or more where possible), using sample sizes of between 50-100 individual tests to minimise the effect of modern contamination. The larger number of replicates will enable confident identification of outlying samples, which is of particular importance for foraminifera given the high proportion of samples with high [L-Ser]/[L-Asx] values. Another limitation is the lack of independently-dated comparative material, especially for *H. germanica* and *Elphidium* spp.; therefore where possible additional samples should be analysed from sites with well-constrained independent chronology to strengthen the aminostratigraphy.

6.4.1 Preservation of foraminifer proteins in the Early Pleistocene - Strumpshaw Fen Sandpit

Amino acids in foraminifera are known to survive well into the Pliocene in deep-sea deposits (e.g. Stathoplos and Hare, 1993; Reinardy et al., 2017), with Asx reaching D/L values of only ~0.5 by 1.5 Ma in very cold (< 0°C) ocean sediments (Kaufman et al., 2013). However, the preservation of foraminifera in terrestrial deposits from the Early Pleistocene, which experience large fluctuations in temperature due to glacial-interglacial cycles, has not to our knowledge been previously studied. Material from the East Anglian Crag group, a series of deposits representing a number of temperate sea-level highstands in the Early Pliocene to late Middle Pleistocene (Hamblin et al., 1997), was therefore targeted for AAR of foraminifera to investigate whether this class of biomineral can be used to provide age control in samples older than the Middle Pleistocene.

Correlation of Crag sites generally relies on mammal or mollusc biostratigraphy, with limited age constraints across the region (Miller et al., 1979; Lee et al., 2018; Preece et al., 2020). In recent years, IcPD analyses of molluscs and enamel have provided new insight into the age of various Crag deposits (e.g. Penkman et al., 2013; Dickinson, 2018; Preece et al., 2020). *B. tentaculata* opercula from the Weybourne Crag (part of the Wroxham Crag Formation (Rose et al., 2001)) had Asx D/L values > 0.9 and Glx D/L values ~0.7 (Penkman et al., 2013), while the marine gastropod *Nucella lapillus* produced Glx D/L values of between 0.6-0.9 depending on the Crag deposit analysed (Preece et al., 2020). Enamel racemises much more slowly than mollusc shell (Dickinson et al., 2019); for example, *Anancus arvernensis* enamel from the Red and Norwich Crags had Glx D/L values between 0.2-0.4 (Dickinson, 2018; Dickinson et al., 2019). Although limited, comparison between *Ammonia* spp. and *Bithynia* opercula from Earnley suggest that foraminifera racemise somewhat more slowly than *Bithynia* opercula (Section 6.3.2). Analysing foraminifera from Crag sites may therefore also be useful for comparing the racemisation rates of these biominerals over longer time periods.

Two East Anglian Crag sites were investigated in this pilot study into Early Pleistocene chronology using AAR of foraminifera: Strumpshaw Fen Sandpit (TG 34211 06829) and Horstead Pit (TG 25128 20718). Analyses were undertaken on material from Strumpshaw Fen Sandpit, as insufficient foraminifera were preserved in the sediments collected from Horstead Pit for AAR analyses to be carried out. The Strumpshaw Fen Sandpit deposit is ascribed to the Early Pleistocene on the basis of its stratigraphical position and the foraminiferal assemblages preserved in the lower part of the deposit. Clast lithology near the top of the section suggests it is more likely to represent Wroxham

Crag deposits rather than Norwich Crag, but this is work in progress (Adrian Read, pers. comm. 2022).

6.4.1.1 Results

One Ammonia spp., one Elphidium pseudolessoni and 4 Elphidium frigidum, as well as an additional 6 samples consisting of more poorly preserved foraminifera tentatively identified as Elphidium frigidum, were analysed from sample SF-YK11 (at the base of the left section) at Strumpshaw Fen Sandpit. However, the chromatograms of these samples suffered from 'peak suppression', a phenomenon hypothesised to be caused by the interference of inorganic species with the derivatisation step of the analysis (Griffin, 2006; Dickinson, 2018) (Fig. 6.15b). In the Strumpshaw Fen Sandpit samples, the interfering species may be iron oxides from post-depositional groundwater penetration responsible for the 'staining' of the foraminifera (Fig. 6.16), a common occurrence in Crag deposits. In enamel, solid phase extraction (SPE) was successfully used to remove interfering phosphate species (Dickinson, 2018); therefore SPE was carried out on one sample to test whether this could prevent peak suppression in stained foraminifera. This was unsuccessful, however, with the coloured compound eluting in the same fractions where amino acids were expected, and virtually no amino acids detected in the eluent (Fig. 6.15c).

Dilutions up to an equivalent rehydration volume of 1280 μ L L-hArg solution, a successful strategy used to overcome peak suppression in enamel (Dickinson, 2018) were also attempted. However, once the sample was dilute enough to overcome peak suppression, the concentrations of amino acids remaining were below the limit of quantification. Where D-Asx or D-Glx were detected, D/L values were around ~0.3 for Asx and ~0.07 for Glx – far too low for the age of the material and therefore indicative of modern contamination. No age estimation is therefore possible for these Crag samples on the basis of AAR of foraminifera.

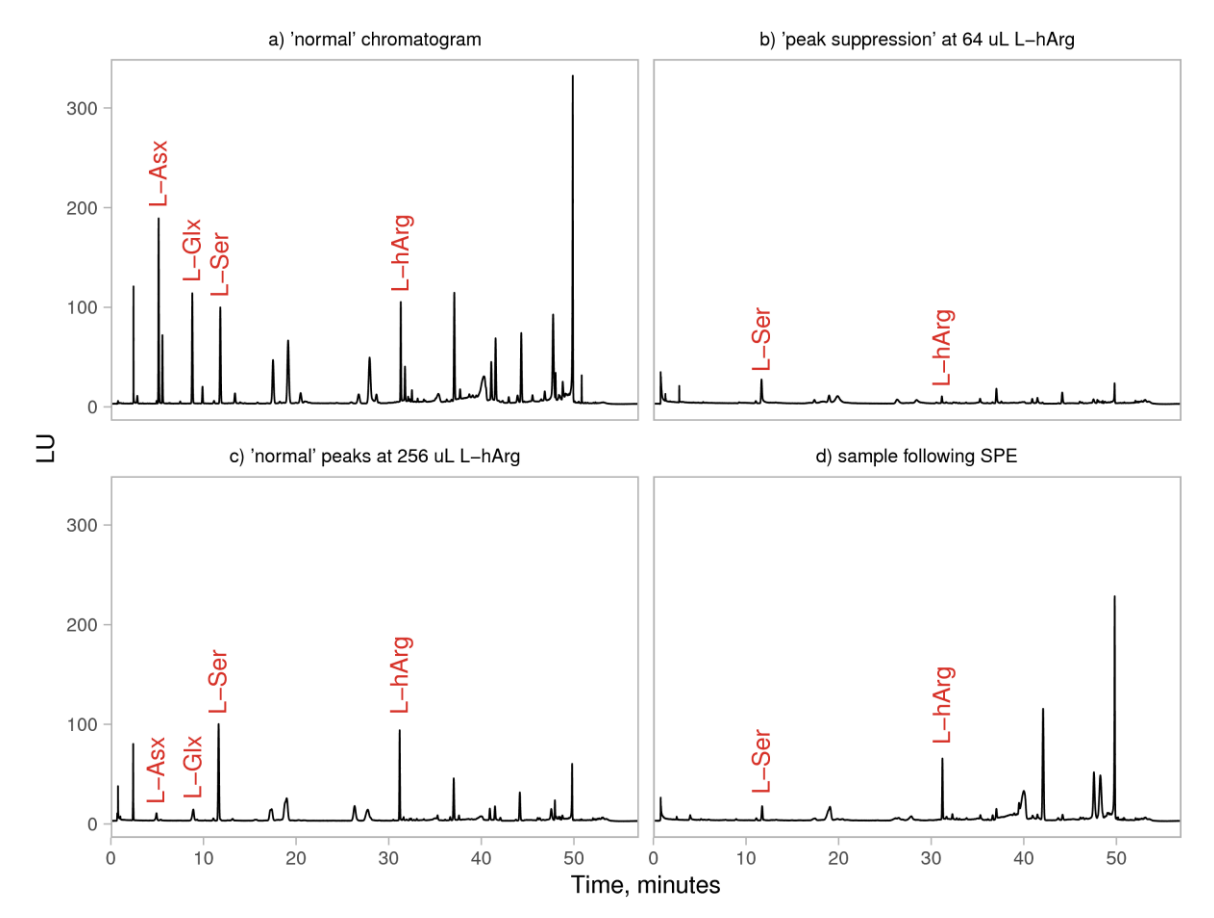


Fig. 6.15 – a) 'normal' chromatogram of an *E. williamsoni* sample, with internal standard L-hArg peak height of ~100 LU (sample no: NF-EW71H*, NEaar no: 14258); b) chromatogram of 'stained' *E. frigidum* sample (SF-EF80H*, NEaar no: 14267) rehydrated with 64 μ L L-hArg solution, showing strong 'peak suppression' (L-hArg peak ~20 LU); c) chromatogram of 'stained' SF-EF80H* rehydrated with 265 μ L L-hArg solution, showing a normal L-hArg peak but peaks of other amino acids except L-Ser close to the limit of detection; d) chromatogram of 'stained' SF-EFx86H* (NEaar no: 14723) following SPE step, rehydrated with 64 μ L L-hArg solution, showing little to no recovery of amino acids.

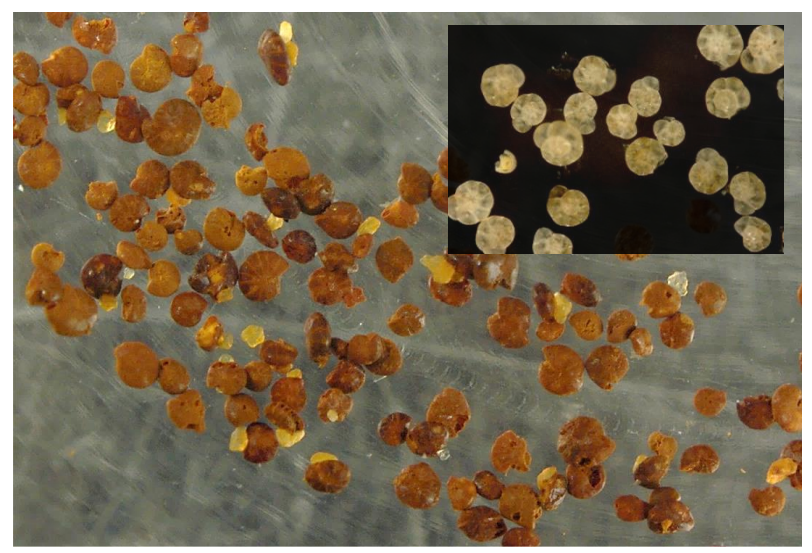


Fig. 6.16 – Foraminifera from sample SF-YK11 from Strumpshaw Fen Sandpit, showing orange-brown 'staining' from iron-containing compounds. Width of picture is approximately 1 cm. Inset: modern, 'pristine' foraminifera from the Humber Estuary with a pale, glassy appearance.

While it may be possible to develop an SPE protocol which successfully removes interfering inorganic species from foraminifer samples, this was not feasible within the timeline of this project. It should be noted that given the small sample sizes used in AAR of foraminifera any even minor loss of amino acids during SPE, or introduction of laboratory contamination from an additional preparation step, could prevent the measurement of accurate D/L values in these samples. Therefore future attempts to carry out AAR of foraminifera from Early Pleistocene sea-level deposits should focus on 'pristine' foraminifera absent of staining, in order to determine whether sufficient amounts of amino acids are preserved in this biomineral over million-year timescales under temperate conditions.

Chapter 7 – Conclusions and future work

Amino acid racemisation dating (AAR) has been widely applied to foraminifera, particularly in deep-sea environments (e.g. King and Neville, 1977; Sejrup et al., 1984b; Harada and Handa, 1995; Kaufman et al., 2013; Blakemore et al., 2015; Ryan et al., 2020). However, there have been limited investigations into the utility of foraminifera for dating Pleistocene sea-level deposits (Dowling et al., 1998; Scourse et al., 1999), or the application of the intra-crystalline approach to foraminifera (Stathoplos and Hare, 1993; Hearty et al., 2004). The aim of this thesis was therefore to determine whether an intra-crystalline fraction of proteins could be isolated in various species of foraminifera, whether analysing this fraction improved the reliability of AAR for foraminifera, and to build a foraminifer-based aminostratigraphy of UK Pleistocene sea-level deposits.

7.1 Isolation and behaviour of intra-crystalline proteins in foraminifera

An intra-crystalline fraction of proteins was isolated using NaOCl within at least 48 hours in *Neogloboquadrina pachyderma* (s) (Wheeler et al. (2021); **Section 3.3.1**), at least 24 hours in *Elphidium williamsoni*, and at least 4 hours in *Ammonia* spp. and *Haynesina germanica* (**Sections 4.3** and **4.4**).

In sub-modern material (*Ammonia* spp., *H. germanica* and *E. williamsoni*), exposure to NaOCl resulted in a dramatic reduction in amino acid concentration (**Section 4.3.1**). In *H. germanica* and *E. williamsoni*, the intra-crystalline protein fraction was found to be somewhat susceptible to prolonged exposure to NaOCl. Differences between the whole-shell and intra-crystalline fractions of all species investigated decreased with age (**Sections 3.3.2** and **4.4**), indicating a loss of intercrystalline amino acids from the biomineral system during diagenesis.

The effect of H_2O_2 , a weaker oxidising agent used routinely in the preparation of foraminifera for AAR, was tested on sub-modern and naturally-aged *Ammonia* spp. and *H. germanica* (Sections 4.3 and 4.4). In sub-modern material, H_2O_2 was less effective at removing the inter-crystalline protein fraction than NaOCl, but differences between these two oxidising agents were not observed in naturally-aged material, corroborating the results of a comparison between H_2O_2 and NaOCl in mid-Holocene to mid-Pleistocene *Pulleniatina obliquiloculata*, *Globorotalia truncatulinoides*, and *Globorotalia tumida* (Millman et al. (2022); see **Appendix 1**). This suggests that following the loss of

the majority of inter-crystalline proteins during the early stages of diagenesis, a short treatment with H_2O_2 is sufficient to isolate the intra-crystalline fraction in foraminifera.

7.2 Patterns of decomposition in foraminifera

Investigations into the decomposition of proteins in foraminifera at ambient temperatures (N. pachyderma (s), Chapter 3) and high temperatures (Ammonia spp. and H. germanica, Chapter 5) found that both the whole-shell (unbleached) and intra-crystalline (isolated with 12% NaOCI) proteins in these species underwent predictable patterns of breakdown similar to those seen in other species of foraminifera (e.g. Wehmiller and Hare, 1971; Harada and Handa, 1995; Hearty et al., 2004; Kaufman, 2006; Kaufman et al., 2013) and other biominerals (e.g. Penkman et al., 2008; Bright and Kaufman, 2011b; Ortiz et al., 2017, 2019). Open-system behaviour of the intercrystalline fraction was observed at high temperatures for both Ammonia spp. and H. germanica, with inter-crystalline proteins leaching out during the early stages of heating. This is consistent with intra-crystalline proteins making up a higher proportion of the total amino acid content in naturally-aged material (Sections 3.3.2 and 4.3.1), and has been observed in other biominerals (e.g. Penkman et al., 2008; Bright and Kaufman, 2011b; Kosnik et al., 2017; Ortiz et al., 2017, 2019; Dickinson et al., 2019). Isolating the intra-crystalline fraction reduced the proportion of amino acids leached from the biomineral, although it was not possible to confirm whether the intra-crystalline fraction behaved as a closed system during the high-temperature decomposition experiments (Section 5.3.1.3). D/L values were consistently higher in the intra-crystalline fraction than the whole-shell fraction of amino acids, for sub-modern (Section 4.3.3), naturally-aged (Sections 3.3.1.3, 3.3.2.2 and 4.4.3) and artificially heated (Section 5.3.4) material. This is most likely due to the removal of exogenous contamination, and the retention of highly racemised free amino acids in the intra-crystalline fraction, which are lost from the inter-crystalline fraction (observed in hightemperature decomposition experiments in **Section 5.3.1**).

For all the species investigated, Asx and Glx produced the most reliable racemisation trends, with Leu and Phe providing supporting information. When using RP-HPLC to separate amino acids, Ala also showed consistent racemisation trends, while Ile was more poorly resolved (Section 5.3.4, Section 3.3.2); UHPLC enabled reliable separation of Ile but poor separation of Ala (see Section 2.4). Trends in racemisation were generally poorer for *H. germanica*, most likely due to its smaller on average test size (and therefore lower amino acid concentrations) than *Ammonia* spp.; poorer results for the intra-crystalline fraction at high temperatures are also likely due to lower amino acid concentrations in this fraction compared to the whole-shell fraction (Section 5.3).

Apparent reversible first order kinetics (RFOK_a), simple power law kinetics (SPK) and constrained power law kinetics (CPK) were applied to the racemisation reactions of *Ammonia* spp. and *H. germanica* at high temperature (Section 5.3.4.4). Of the three models, RFOK_a was most effective at modelling racemisation in these species, with SPK and CPK both performing poorly with little concordance between estimated rates of racemisation. This demonstrates the issues with applying power law models to data with a relatively high degree of variability, as even small differences in the model can lead to large differences in estimated racemisation rates.

7.3 The effect of oxidising pre-treatment on D/L variability in foraminifera

7.4 Use of AAR of foraminifera to provide chronological control in UK sea-level deposits

A pilot aminostratigraphy based on *Ammonia* spp., *H. germanica* and *Elphidium* spp. (including *Elphidium williamsoni*) was developed using a range of Pleistocene sea-level sites in the UK (**Chapter 6**). This work showed that these species of foraminifera provide chronological information in the mid-late Pleistocene, with the results generally being consistent with the existing chronology of the sites investigated. Of the three species investigated, *Ammonia* spp. performed best,

consistent with high-temperature decomposition experiments (**Chapter 5.3**); *H. germanica* and *Elphidium* spp. gave supporting information.

A significant issue in the building of the aminostratigraphy was the variability of D/L values between replicate samples. A substantial proportion (25-60% depending on the species) of samples had [L-Ser]/[L-Asx] > 0.8, which corresponded to typically lower D/L values than other replicates, and a higher likelihood of deviating from general trends of D/L covariance. Where only a small number of replicates were analysed from a single horizon, this variability and the high proportion of potentially compromised samples precluded a confident measure of average D/L values for that horizon. This underlines the importance of analysing large numbers of replicate samples (\geq 10) to overcome these limitations.

7.5 Future work

7.5.1 Method development

The work carried out in this thesis demonstrates the importance of quantifying and minimising contamination when carrying out AAR on very small sample sizes (< 0.1 mg). This is particularly important when analysing the intra-crystalline fraction of proteins in naturally-aged material where a significant proportion of proteins have been lost during diagenesis. Future work may be able to accurately quantify the level of background contamination from laboratory sources to develop a blank correction protocol, including a measure of the uncertainty introduced by contaminant amino acids.

A modified version of a method for separation via UHPLC developed by Crisp (2013) was found to reliably separate Asx, Glx and Ile; however, co-elution of a non-amino acid compound with L-Ala prevented accurate D/L measurements for this amino acid. Further modifications to the method's solvent gradient program may enable better resolution of Ala in foraminifera. Additionally, while beyond the scope of this thesis, analysis using UHPLC of inter-laboratory comparison samples will enable any biases between RP-HPLC and this UHPLC method to be quantified (Wehmiller, 2013a).

7.5.2 Further development of foraminifer-based aminostratigraphy
The pilot aminostratigraphy presented in **Chapter 6** demonstrates the utility of foraminifera to
provide chronological information in UK Pleistocene sea-level deposits, especially where other
biominerals are absent. However, given the small number of samples available for analysis at some

sites, the high proportion of samples with indications of contamination, and the high between-replicate variability for some sites, it was not possible to derive a robust estimate of D/L ranges for all the sites investigated. This was especially true of Somersham (Section 6.3.5.2), King's Dyke Quarry and West Face Quarry (Section 6.3.5.3) from the March Gravel area; some uncertainty also remains for Norton Farm (Section 6.3.3.2) and the Burtle Beds (Section 6.3.6). Where material is available, additional replicates should be analysed to improve the confidence of D/L values at these sites.

As more independently-dated sites are added to an aminostratigraphy, the higher the confidence in the chronology of existing sites becomes. A set of recommendations for building on this pilot aminostratigraphy are given in Section 7.5.2.1. In the case of the foraminifer-based aminostratigraphy, the addition of material well-dated to MIS 5e and MIS 9+ will help to constrain the D/L ranges associated with each interglacial. Additionally, while only sites from the UK were analysed in this thesis, the aminostratigraphy may be extended to sea-level records from northern Europe, which fall within the same temperature regime as the UK. Analysis of 'pristine' foraminifera (those absent of inorganic compounds which may interfere with chromatography) from early Pleistocene deposits may also enable an estimation of the upper limits of AAR of foraminifera in Pleistocene sea-level deposits.

7.5.2.1 Recommendations for analysing foraminifera from Pleistocene sealevel deposits

For future applications of foraminifer AAR to dating Pleistocene sea-level deposits, the following methodological recommendations are given:

- 1. An oxidative pre-treatment should be carried out to reduce the variability of D/L values compared to a sonication-only pre-treatment. Differences between a weak (H_2O_2) and strong (NaOCl) oxidative pre-treatment are equivocal in naturally-aged material, likely due to the loss of labile inter-crystalline amino acids during diagenesis; H_2O_2 is therefore sufficient to isolate the intra-crystalline fraction. A 2 hour pre-treatment with 3% H_2O_2 is recommended for foraminifera, for comparability to existing research.
- 2. Depending on the size of the foraminifer tests present, sample sizes of 50-100 individual tests are recommended to minimise the impact of contamination. If *Ammonia* spp. is present in abundance, analyses should focus on this species; *H. germanica* and *Elphidium* spp. may also provide chronological information.

- 3. Where possible, 10 or more replicate samples should be analysed for each species from a single horizon, to allow for the identification and exclusion of outlying samples.
- 4. Asx and Glx provide the best chronological control for foraminifera, with other amino acids (Ala, Phe, Leu and Ile) providing supporting information depending on the separation method used. RP-HPLC gives better separation of Ala but poorer separation of Ile, while the reverse is true for UHPLC.
- 5. High [L-Ser]/[L-Asx] values are indicative of contamination and should be used to screen for potentially compromised samples alongside high (> 50%) Gly and, if enough replicates are analysed, deviation from Asx vs Glx D/L covariance, in keeping with screening criteria used for other biominerals (Kaufman, 2006; Kosnik and Kaufman, 2008; Kaufman et al., 2013). While an [L-Ser]/[L-Asx] cut off of 0.8 was assessed for this work, a higher value (e.g. 1.2) may be more appropriate due to the small sample sizes (and therefore higher proportional impact of background L-Ser) used in AAR of foraminifera.

Appendices

Appendix 1 – Testing the effect of oxidizing pretreatments on amino acids in benthic and planktic foraminifera tests

This manuscript, part of which is also reported in **Chapter 4**, has been published in *Quaternary Geochronology* under the following citation:

Millman, E., Wheeler, L. J., Billups, K., Kaufman. D., Penkman, K. E. H. (2022). Testing the effect of oxidizing pre-treatments on amino acids in benthic and planktic foraminifera tests. *Quaternary Geochronology*, **73**, 101401. https://doi.org/10.1016/j.quageo.2022.101401

Analysis and interpretation of benthic foraminifera (*Ammonia* spp. and *H. germanica*) was carried out by LW; analysis and interpretation of planktic foraminifera (*G. truncatulinoides, G. tumida* and *P. obliquiloculata*) was carried out by EM. The manuscript was co-written by EM and LW with guidance and insight from KB, KD and KP.

Abstract

Amino acid racemization (AAR) is a geochronological method that uses the ratio of D- to L-configurations in optically active amino acids from carbonate fossils to determine the time elapsed since the death of an organism. Although AAR techniques have been widely applied to foraminiferal tests, there have been limited dedicated assessments of the potential of isolating a bleach-resistant, intra-crystalline fraction of proteins to improve the reliability of AAR in this biomineral system. In this study, we evaluate the effect of two oxidative pre-treatments (hydrogen peroxide and bleach) on amino acid concentrations and D/L values in sub-modern benthic foraminifers (*Ammonia* spp. and *Haynesina germanica*) and well-preserved mid Holocene and mid Pleistocene planktic foraminifers (*Pulleniatina obliquiloculata*, *Globorotalia truncatulinoides*, and *Globorotalia tumida*). The oxidative pre-treatments successfully reduced the amino acid content of the foraminiferal tests to a residual fraction, and with the exception of *Ammonia* spp., neither pre-treatment substantially affected the relative proportion of individual amino acids. The bleaching pre-treatment does not consistently alter D/L values when compared to peroxide pre-treatment, but it does tend to reduce the subsample variability in D/L values, albeit only to a small degree in

an inconsistent fashion. Therefore, we recommend that a relatively weak oxidative pre-treatment with 3% hydrogen peroxide is sufficient for foraminifera-based AAR applications.

A1.1 Introduction

Amino acid racemization (AAR) is a diagenetic process that has been used as a geochronological tool for decades. AAR is the interconversion of amino acids from their L- to D- enantiomeric configuration, which starts upon the death of an organism and subsequent breakdown of proteins (Wehmiller and Hare, 1971; Bada and Schroeder, 1975). The D- to L- ratio of amino acids (D/L) is thus a measure of the extent of racemization and increases with time (and temperature), from values of ~0 in modern materials to equilibrium values of ~1 (for most amino acids), when the forward and reverse reaction rates are equal (e.g. Miller and Mangerud, 1985; McCoy, 1987). AAR is applicable to a wide range of fossiliferous material (e.g., mollusks, foraminifera, eggshell, and ostracodes), depositional environments (e.g., marine, lacustrine, and fluvial) as well as to determine stratigraphic relationships (e.g., correlations, the reworking of fossils, and detecting unconformities) (Walker, 2005; Miller et al., 2013). Since the 1970s, AAR has been used as a relative (e.g. Wehmiller, 1977, 2013b; Miller et al., 1979; Kaufman and Miller, 1992; Walker, 2005; Penkman et al., 2011, 2013) or absolute (e.g. Sejrup et al., 1984b; Macko and Aksu, 1986; Goodfriend, 1989; Hearty et al., 2004; Kosnik et al., 2013) dating tool for Quaternary deposits. In order to reliably use D/L values in fossil material to calculate the time elapsed since the death of the organism (i.e., as a geochronometer), it is essential that external influences on racemization rates and the effects of modern contamination are minimized.

To this end, one advancement in AAR geochronology is the development of the intra-crystalline protein diagenesis (IcPD) approach, which uses a chemical oxidant, bleach (NaOCl), to remove the inter-crystalline protein "mesh" between the biomineral crystallites while leaving behind proteins that are embedded within the crystallites (Towe, 1980; Sykes et al., 1995; Penkman et al., 2008). This approach provides more consistent results in mollusks, corals, and eggshells than more gentle cleaning methods involving sonication in deionized water or weak oxidation with dilute hydrogen peroxide (3% H₂O₂) (Penkman et al., 2008, 2011; Hendy et al., 2012; Crisp et al., 2013; Demarchi et al., 2013c, 2013b; Ortiz et al., 2015; Torres et al., 2016). While bleaching pre-treatments have been used during the preparation of foraminiferal tests for AAR (Nicholas, 2012; Kaufman et al., 2013), dedicated assessments of the IcPD approach to this class of biominerals are limited (Stathoplos and Hare, 1993; Hearty et al., 2004). Recently, a study detailing the effects of bleach on the tests of the planktic foraminifer *Neogloboquadrina pachyderma* (sinistral) suggested that the IcPD approach

reduces the influences of open-system behavior when compared to a sonication-only pretreatment (Wheeler et al., 2021). However, peroxide pre-treatments were not considered by Wheeler et al. (2021) for comparison with the bleach pre-treatment.

In this study, we test the effects of different oxidative pre-treatments on the amino acid composition and D/L values for several benthic and planktic foraminiferal species. Specifically, we assess the effects of sonication, various peroxide concentrations, and the addition of bleach on the composition of amino acids, the D/L values within individual amino acids, and the inter-sample variability of D/L values. This study merges data generated in two separate efforts: one focusing on benthic foraminifera from surface sediments (0-5 cm, sub-modern) and the other on planktic foraminifera from deep sea sediment cores (~6 ka to ~410 ka). The primary goal in the former study was to establish whether an oxidation-resistant protein fraction can be isolated from benthic foraminiferal tests and to assess the effects of these pre-treatments on amino acid composition and D/L values. In the latter study, the original research question asked whether or not pretreatment with bleach had a significant effect on amino acid composition, inter-species differences in D/L, and D/L variability of previously peroxide-cleaned planktic foraminiferal tests ranging in age from the mid Holocene through the mid Pleistocene. Although the study designs were independent, both approaches have similar implications for understanding the effect of oxidative pre-treatment on foraminiferal proteins, thereby warranting integration into a common framework within this paper.

A1.2 Methods

A1.2.1 Sample selection

The first set of samples involves benthic foraminifers from surface (0-5 cm) sediments collected in the Humber Estuary, a mid-latitude, coastal plain estuary formed by the Ouse and Trent rivers in the northeastern United Kingdom (**Table A.1.1**). Sample collection was carried out in February, 2018. Although these samples were not independently dated, they most likely represent a modern assemblage of foraminifera. However, reworking of the salt-marsh sediment is a possibility (Figueira and Hayward, 2014); radiocarbon dating of basal peats in the area gives a maximum age of a few thousand years (Long et al., 1998). To reflect the uncertainty in their age, we refer to these samples as 'sub-modern.' Abundant foraminiferal species include several belonging to *Ammonia* and *Haynesina gemanica*. The speciation of *Ammonia* is challenging; therefore, we refer to them collectively as '*Ammonia* spp.' (Hayward et al., 2004). The extent of AAR in *Ammonia* spp. has been

used to date Quaternary sea-level deposits (e.g. Dowling et al., 1998; Scourse et al., 1999; Nicholas, 2012; Blakemore, 2014), but to the authors' knowledge, *H. germanica* has not previously been used in foraminiferal-based AAR studies.

The second set of samples involves planktic foraminifers that were picked from three Ocean Drilling Program (ODP) sites (Sites 1056, 1059, and 1062) and one piston core (KNR140-JPC37) located on Blake Bahama Outer Ridge (BBOR) in the northwestern subtropical Atlantic Ocean (Table 1). We use three species, *Globorotalia truncatulinoides*, *Globorotalia tumida*, and *Pulleniatina obliquiloculata*, because of their relatively high abundance, large tests, resistance to dissolution (e.g. Hemleben et al., 1989), and their demonstrated applicability to AAR research (e.g. Stathoplos and Hare, 1993; Wehmiller and Hall, 1997; Hearty et al., 2004; Kaufman, 2006; Kaufman et al., 2013). By analyzing multiple species, we also assess potential inter-species differences in amino acid concentration, composition, and variability in amino acid D/L values.

At the BBOR, samples span the mid Holocene through mid Pleistocene ($^{\sim}6-410$ ka, Table 1). Mid-Holocene-samples from BBOR were initially located in the cores using published age models (Grützner et al., 2002). Early Holocene through mid Pleistocene-aged samples from Site 1056 and KNR140 JPC-37 were identified using the cores' δ^{18} O stratigraphy (Hagen and Keigwin, 2002; Billups et al., 2004). The time equivalency of the mid Holocene samples from the three BBOR sites was subsequently confirmed to within $^{\sim}1$ -2 ka (**Table A.1.1**) using rapid, low precision, 14 C analyses (Bush et al., 2013; Watson, 2019). These were conducted on mono-specific planktic foraminiferal tests at the Keck AMS facility at the University of California Irvine with calibration to calendar ages following the convention of Stuvier and Polach (1977).

Table A.1.1 – Site locations and sampling intervals.

Location	Longitude, Latitude	Water Depth (m)	Core Intervals (cm)	Sediment Depth (mcd) ¹	Age (ka) ²	Age (ka) ³
<u>Sub-modern</u>						
Humber Estuary	54°N, 0°E	-	0-5	0.00-0.05	-	-
Mid Holocene						
1056D, 1H-1	32°N, 76°W	2178	62, 64, 68, 70	0.62-0.70	6.0-6.5	4.8-5.0
1059A, 1H-1	32°N, 75°W	2997	44, 50, 54	0.44-0.56	6.0-6.5	5.0-5.4
1062B, 1H-1	28°N, 74°W	4780	62	0.62-0.64	7.1	7.0
Early Holocene						
KNR140 JPC37	31°N, 75°W	2997	150	1.50	10.5	-
<u>Late Pleistocene</u>						
KNR140 JPC37	32°N, 75°W	2997	1112	11.12	51.5	-

	Location	Longitude, Latitude	Water Depth (m)	Core Intervals (cm)	Sediment Depth (mcd) ¹	Age (ka) ²	Age (ka) ³
Mid Pleistocene							
	1056B, 5H-7	32°N, 76°W	2178	44	35.34-35.36	410	-

¹MCD stands for meters composite depth.

A1.2.2 Experimental methods

Experiments involving benthic foraminifera from the Humber Estuary were carried out at the Northeast Amino Acid Racemization (NEaar) laboratory (University of York, UK). Experiments (**Fig. A.1.1a**) consisted of a series of extended oxidation pre-treatments using hydrogen peroxide (3% and 30% w/v H_2O_2) or bleach (12% w/v NaOCl), compared to "unbleached" samples treated only by sonication in purified water.

Experiments involving planktic foraminifera from the BBOR were conducted at the University of Delaware. These experiments compared foraminifer tests oxidized for 2 h with 3% w/v H_2O_2 (referred to as "3% H_2O_2 ") to those additionally oxidized for 48 h with 12% w/v NaOCl (referred to as "12% NaOCl-addition") (**Fig. A.1.1b**). The pre-treatments used by the University of Delaware are akin to a subset of the pre-treatments by the University of York.

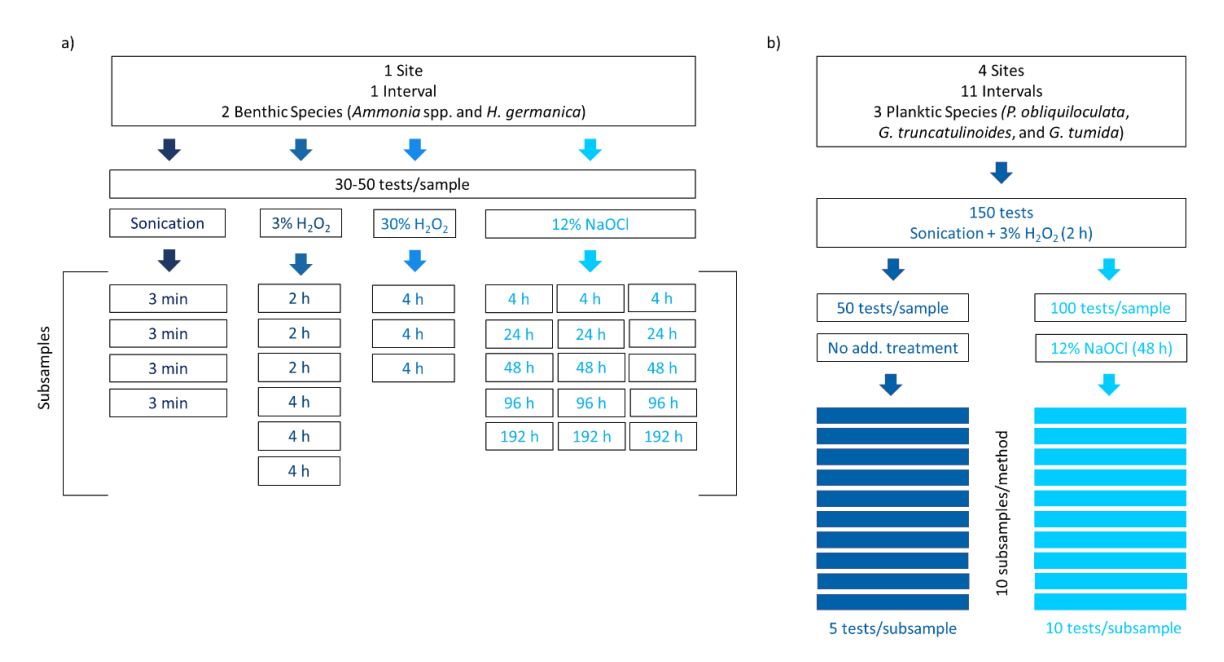


Fig. A.1.1 – Visual representation of the pre-treatment methodology for a) the sequential pre-treatment experiments (University of York) and b) the comparison between $3\% H_2O_2$ -only and the 12% NaOCl-addition pre-treatments (University of Delaware). Discussion of these methods can be found in **Sections A1.2.2.1** and **A1.2.2.2**.

²Stratigraphic ages (see **Section A1.2.1**).

³AMS ¹⁴C dates. For Site 1062, this is the average of two ages (6.68 and 7.23 ka).

A1.2.2.1 Sequential pre-treatment experiments (University of York)

Tests of *Ammonia* spp. and *H. germanica* from the surface sediments of the Humber estuary tidal flats were picked from the $63-500~\mu m$ fraction and whole tests were cleaned prior to pretreatment by sonicating repeatedly with purified water ($18.0~m\Omega$) until the water was clear. Each replicate sample consisted of 30-50 monospecific tests with 3-4 replicates for each species and pre-treatment. Each replicate was prepared separately in sterilized 0.1~mL conical-bottomed microreaction vials (Thermo Scientific). Tests were crushed in the vials with a clean needle before a second round of sonication (3~x~1~minute, rinsing with purified water between each sonication). For "unbleached" samples, no further pre-treatment was carried out prior to analysis.

Oxidative pre-treatments were carried out for various durations (2 - 192 h) using hydrogen peroxide (3% and 30% w/v H_2O_2) and bleach (12% w/v NaOCl) (**Fig. A.1.1a**). Oxidizing agent (20 μ L) was added to each replicate sample, with periodic agitation to ensure complete exposure of the biomineral to the oxidizing agent. The oxidizing agent was then removed by pipette and the biomineral rinsed with purified water six times and HPLC-grade methanol once then air dried prior to demineralization.

For the hydrolysis step, all samples were demineralized in the micro-reaction vials with 10 μ L 7 M HCl, flushed with nitrogen, and heated at 110°C for 24 h. Samples were then dried under vacuum and stored at room temperature prior to rehydration for analysis. Samples were rehydrated with 8 or 10 μ L of rehydration fluid (indicating that some samples had to be diluted and reanalyzed on the HPLC), comprising 0.01 M HCl, 1.5 mM NaN₃, and 0.01 mM L-homo-arginine (L-hArg), an internal synthetic amino acid standard used to quantify the abundance of amino acids in each vial. Amino acid enantiomers were resolved by reversed phase HPLC at the NEaar lab using a slightly modified method of Kaufman and Manley (1998) with the additions of Kaufman (2000) for analyzing microfossils. Of the total sample volume, 2 μ L of the rehydrated samples were injected into the HPLC where they underwent pre-column derivatization with o-phthaldialdehyde (OPA) and N-isobutyryl-L-cysteine (IBLC) followed by chiral separation with a C₁₈ stationary phase (Hypersil BDS, 5 μ m) and fluorometric detection (Kaufman and Manley, 1998). Procedural blanks were analyzed for each experiment to quantify background levels of amino acid contamination. Due to the limited number of replicates analyzed for each pre-treatment (Fig. A.1.1), statistical comparisons were not carried out for this series of experiments.

A1.2.2.2 Comparison between oxidative pre-treatments (University of Delaware) Bulk sediment samples from the three ODP core sites on BBOR (Table 1) were processed using standard techniques involving disaggregation in a buffered sodium metaphosphate solution, washed over a 63 μ m sieve with deionized water, and left to air dry. The sediments from the piston core were already processed according to Hagen and Keigwin (2002). From each core interval (n = 11), we aimed to pick about 150 individuals of *P. obliquiloculata*, *G. truncatulinoides*, and *G. tumida* from the >350 μ m fraction.

The 150 species-specific tests from each core interval (n = 19) were placed into individual 16 mm glass culture tubes. Each tube was filled with deionized water and sonicated briefly to loosen surface contaminants. To remove organic contaminants, the tests were soaked in 3% w/v H₂O₂ for 2 h, rinsed three times with reagent grade H₂O, decanted, and air dried under laminar flow; this is a common cleaning step in other foraminifera AAR studies (e.g. Kaufman et al., 2008). Once clean, the 150 tests of each species for each core interval were split into samples of 50 and 100 tests. The samples containing 50 tests were then subdivided into 10 subsamples composed of 5 individuals on average, which were placed into sterilized, conical bottomed 0.1 mL micro-reaction vials (e.g., Fig. A.1.1b). Subsamples were hydrolyzed, rehydrated, and analyzed using a similar procedure to the one used by the University of York (Section A1.2.2.1). The difference is that samples were hydrolyzed with 7 μL 6 M HCl, flushed with nitrogen, and heated at 110°C for 6 h, in order to minimize hydrolysis-induced racemization in the older samples. This heating time is shorter than the NEaar hydrolysis protocol, but the difference will not impact the paired comparisons as the D/L values are not being directly compared between the two studies (e.g. Dungworth, 1976; Williams and Smith, 1977). Samples were then rehydrated with 4 μL of the rehydration fluid, and all 4 μL of the sample was injected into the column for analysis. Amino acid enantiomers were resolved by reversed phase high performance liquid chromatography at the Amino Acid Geochronology Lab (Northern Arizona University, AZ) using the same parameters as above (Section A1.2.2.1).

The samples containing 100 tests were further treated with bleach following Penkman et al. (2008), with modifications. First, each group of 100 tests were divided into 10 subsamples (e.g., **Fig. A.1.1b**), each containing 9 tests on average, and placed into separate glass test tubes. Second, to isolate the intra-crystalline fraction, tests in each subsample were gently broken and 12% NaOCl was added to fill three fourths of the tube. Third, the tubes were agitated, left for 24 h, re-agitated to ensure complete exposure to the bleach, and soaked for another 24 h. After 48 h, the bleach was pipetted off and samples were rinsed with purified water 3 – 5 times before being left to dry under laminar flow. The dry fragments were transferred to conical bottomed 0.1 mL micro-reaction

vials and hydrolyzed, rehydrated, and analyzed using the same procedure as the peroxide-cleaned samples.

A1.2.3 Data screening

In this study, we focus on the D/L values of aspartic acid and glutamic acid, which are two of the most abundant amino acids in foraminiferal protein and best resolved chromatographically (Kaufman et al., 2013). However, during hydrolysis, asparagine and glutamine are irreversibly hydrolyzed to aspartic acid and glutamic acid respectively; therefore, these amino acids are analytically indistinguishable and reported as Asx and Glx (Hill, 1965). The integrity of AAR data can be assessed using a range of diagnostic criteria, such as serine (Ser) abundance, depth or age trajectories, covariance of concentrations or D/L values, and variability of replicate subsamples (Kosnik and Kaufman, 2008). Cut-offs for sample exclusion are determined empirically and are known to depend on age and taxonomy (Kaufman, 2006; Kosnik and Kaufman, 2008). Here we followed the three-step screening procedure from Kosnik and Kaufman (2008) to systematically identify subsample outliers that could influence the resulting mean D/L values for each sample.

First, the concentration of Ser, a labile amino acid which should be present only in low concentrations within fossils due to its rapid rate of decomposition, was used to identify subsamples contaminated by modern amino acids (Kaufman, 2006; Kosnik and Kaufman, 2008; Kaufman et al., 2013). Although this criterion is not applicable to the sub-modern material from Humber Estuary, because the low extent of protein breakdown means that Ser concentrations remain high, individual subsamples from the BBOR cores with L-Ser/L-Asx values ≥ 0.9 were rejected. Second, the covariance between the D/L values of Glx and Asx was visually assessed to identify subsamples with D/L values that substantially deviate from the linear relationship of all subsamples within a species (Kaufman, 2006; Kaufman et al., 2013). Third, subsamples with D/L Asx or Glx values that fell beyond $\pm 2\sigma$ of the mean of the rest of the group were rejected (Kaufman, 2006; Kaufman et al., 2013).

No outliers were identified in the estuarine data set, likely due to the small number of replicates for each pre-treatment (n = 3 – 4). Screening of the BBOR data (n = 381) resulted in the rejection of 46 (12.1%) individual data points. Of these, 14 (3.7%) were rejected based on high Ser content, 7 (1.8%) were rejected as outliers based on the expected linear Asx D/L vs. Glx D/L trend for a species, and 25 (6.6%) were rejected due to falling beyond the $\pm 2\sigma$ of the mean of the group. The rejection rate is slightly lower for the samples pretreated with hydrogen peroxide (19 out of 196

subsamples rejected, 9.7%) as opposed to samples pretreated with bleach (27 out of 185 subsamples rejected, 14.6%).

A1.3 Results

A1.3.1 Amino acid concentration

Our results show that the choice of pre-treatment affects the concentration of total hydrolysable amino acids ([THAA]) in both benthic (Fig. A.1.2) and planktic foraminifer tests (Fig. A.1.3). Regarding the benthic foraminifer tests, sequential oxidation illustrates that when treated with 12% bleach, the total concentration of amino acids decreases by ~90% in the first 4 h of bleaching, then remains at consistently low levels for the remainder of the oxidation period, regardless of species (Fig. A.1.2). This suggests that the residual fraction of proteins isolated within 4 h of bleach exposure represents a bleach-resistant intra-crystalline protein fraction. The results of the H₂O₂ pre-treatment experiments are more species dependent. In Ammonia spp., the variability of [THAA] in the unbleached samples precludes a quantitative comparison of the proportion of amino acids removed by each oxidation pre-treatment, although a smaller proportion of amino acids are removed by the 4 h 3% H_2O_2 and 30% H_2O_2 treatments than the 4 h 12% NaOCl treatment (**Fig.** A.1.2a). This suggests that H₂O₂ is not a strong enough oxidizing agent to isolate the bleachresistant intra-crystalline fraction, at least within 4 h, in Ammonia spp. Conversely, the 4 h treatments with 3% H₂O₂, 30% H₂O₂ and 12% NaOCl all remove a similar proportion of amino acids in *H. germanica* (Fig. A.1.2b). The concentration of THAA in *Ammonia* spp. remains stable up to 192 h, while there appears to be a further gradual loss of amino acids after prolonged bleaching (> 96 h) in *H. germanica*, indicating possible etching of the mineral matrix (Penkman et al., 2008; Dickinson et al., 2019).

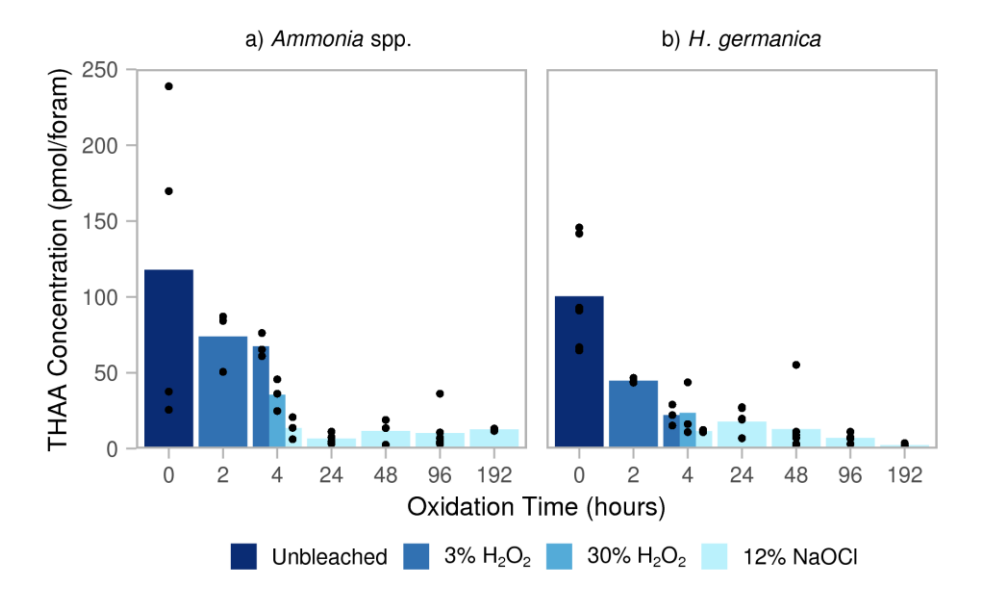


Fig. A.1.2 – Concentration of total hydrolysable amino acids ([THAA]) in unbleached (i.e., H_2O sonication only) and oxidized (i.e., H_2O_2 or NaOCl) samples of modern benthic species a) *Ammonia* spp. and b) *H. germanica* from surface sediments of the Humber Estuary. Bars reflect the average concentration derived from individual measurements (solid black circles). Due to the small number of replicates analyzed at each time point in this suite of experiments, all data points are shown as solid black points.

In comparison to the benthic foraminifer species (**Fig. A.1.2**), the planktic foraminifer species (**Fig. A.1.3**) have higher amino acid concentrations when treated with 3% H_2O_2 . This observation most likely corresponds to the larger size of the planktic species. The 24 h bleach pre-treatment reduces [THAA] by ~90% in the sub-modern, benthic foraminifera, whereas [THAA] is reduced by 41 - 72% in the down-core, planktic foraminifera. This difference could be explained by the sample age difference. For *G. truncatulinoides* and *P. obliquiloculata*, bleach reduces [THAA] by 68 - 72% in mid to early Holocene-aged samples but only 41 - 57% in mid Pleistocene-aged samples. Thus, it appears bleach removes a smaller proportion of amino acids as the age of the samples increase, indicating a loss of open-system inter-crystalline amino acids during the early stages of diagenesis. This pattern has been observed in a variety of mollusk species (e.g. Sykes et al., 1995; Penkman et al., 2008; Ortiz et al., 2015, 2017).

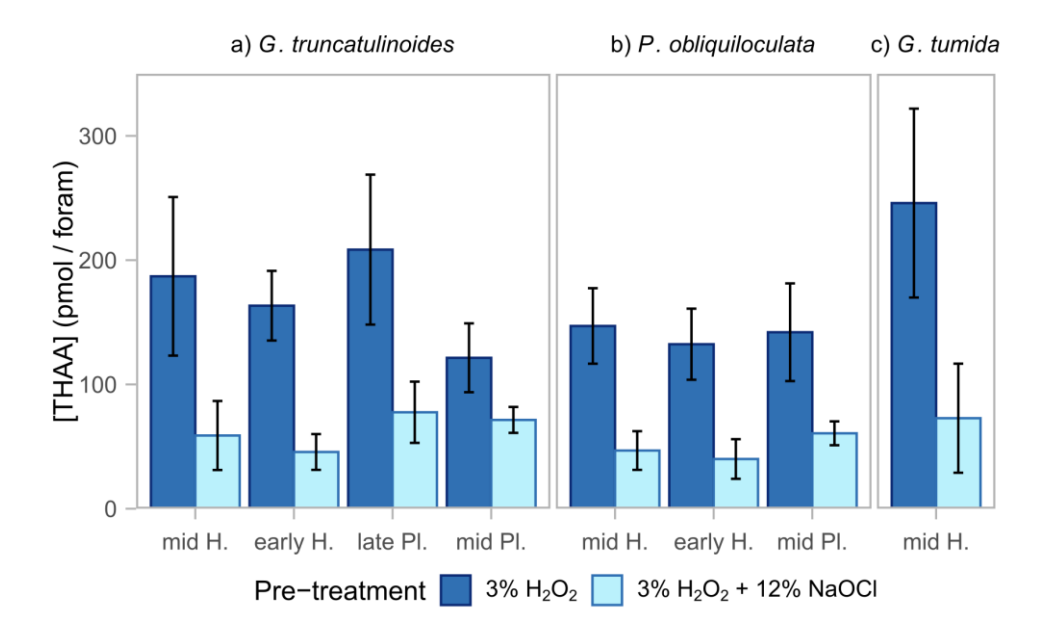


Fig. A.1.3 – Concentration of total hydrolysable amino acids ([THAA]) for a) G. truncatulinoides, b) P. obliquiloculata, and c) G. tumida pre-treated with 3% H_2O_2 only or 3% H_2O_2 plus 12% NaOCl. Mean [THAA] is separated based on sample age (mid Holocene, early Holocene, late Pleistocene, and mid Pleistocene) for each pre-treatment. Error bars represent the $\pm 1\sigma$ around the mean. All differences are statistically significant at the 95% confidence interval (P-values < 0.05).

In sum, bleaching foraminifer tests more effectively reduces [THAA] as opposed to either peroxide treatment, in both benthic and planktic foraminifer species. This reduction is more drastic in the sub-modern benthic foraminifera, where little to no diagenesis has taken place to remove the easily accessible inter-crystalline amino acids.

A1.3.2 Amino acid composition

The pre-treatment methods do not have a consistent effect on the relative proportion of individual amino acids among the foraminifera species used in the two experiments. The largest effect is observed for the benthic species Ammonia spp. (Fig. A.1.4a), where increasing the strength of the oxidizing agent increases the proportion of Asx, Glx, and Ala but decreases the proportion of Gly, especially for the 12% NaOCl treatment. In H. germanica, samples treated with 3% and 30% H_2O_2 have a lower %Ala and higher %Asx than the unbleached samples, but compositionally the samples treated with 12% NaOCl are more similar to the unbleached samples (Fig. A.1.4b). This may be due to the large inter-replicate variability of composition, especially for Asx and Gly (Supplementary Fig. A.1.12). The more similar composition of H. germanica protein between the different pre-

treatments is consistent with the similar concentrations for this species for the 4 h treatments at different oxidizing agent strengths, in contrast to *Ammonia* spp. (Fig. A.1.2).

For the planktic foraminifera, the amino acid composition is relatively similar between pretreatments and across species and ages (Fig. A.1.5). With the addition of 12% NaOCl, there is a slight reduction in the %Gly and %Phe with an increase in %Ala observed for *G. truncatulinoides*, *P. obliquiloculata*, and *G. tumida*. The small differences observed in the THAA composition of the older planktic species (in contrast to the sub-modern benthic species) could be due to the loss of easily accessible inter-crystalline proteins during the early stages of diagenesis, where afterwards the THAA composition becomes relatively stable against aging and oxidative effects.

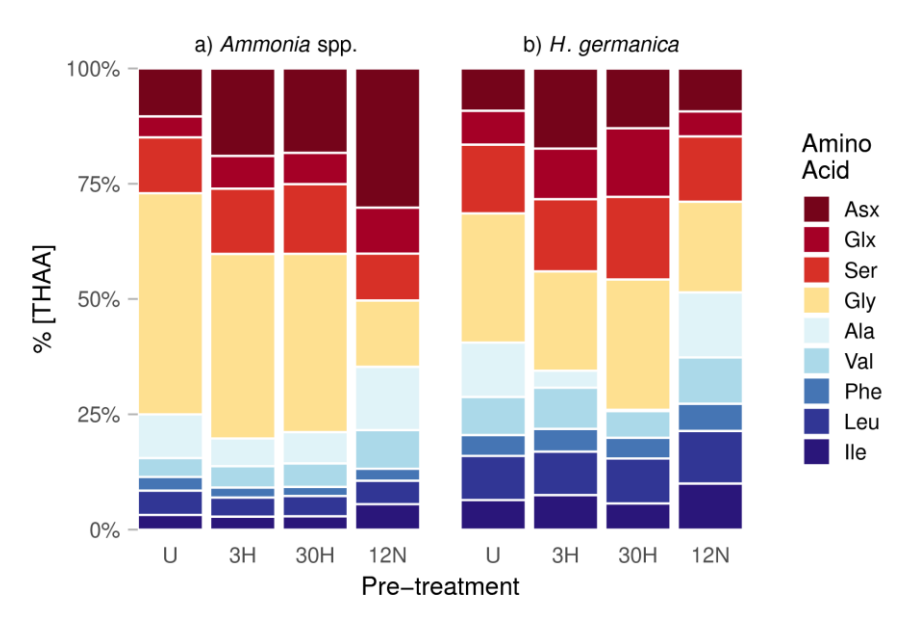


Fig. A.1.4 – Relative proportion of amino acids (%THAA) in benthic foraminifer tests from estuarine surface samples for a) *Ammonia* spp. b) *H. germanica*. Four different pre-treatments were used: H_2O sonication only (Unbleached, U), 4h 3% H_2O_2 (3H), 4h 30% H_2O_2 (30H), and 4h 12% NaOCI (12N).

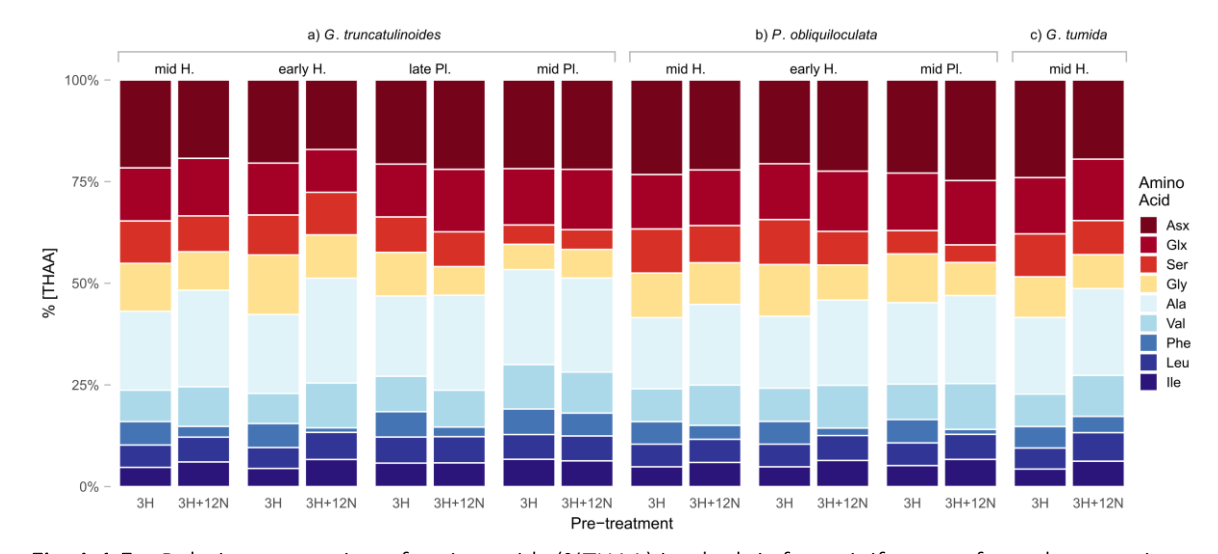


Fig. A.1.5 – Relative proportion of amino acids (%THAA) in planktic foraminifer tests from deep marine sites aged mid Holocene (H) to mid Pleistocene (Pl) for a) G. truncatulinoides, b) P. obliquiloculata, and c) G. tumida. Two different pre-treatments were used: 3% H_2O_2 only (3H) and 3% $H_2O_2 + 12\%$ NaOCl (3H+12N).

A1.3.3 D/L differences between pre-treatments

D/L values for Asx and Glx were investigated because these amino acids are the most common for AAR age or temperature reconstructions (Goodfriend et al., 1996; Kaufman, 2003b, 2006; Kaufman et al., 2008, 2013; Miller et al., 2013). Within the data scatter, there are no robust trends for pretreatment conditions in the D/L values of the benthic foraminifer samples, regardless of whether or not the samples were treated beyond sonication with H_2O (Fig. A.1.6). In *H. germanica*, there may be a slight decrease in Asx and Glx D/L values between the sonication-only samples and samples subjected to short oxidation times (2-4 h), followed by a slight trend of increasing D/L between 4 and 192 h of bleach exposure (Fig. A.1.6b). This pattern has been observed in various mollusk shells (Penkman et al., 2008) and ostracodes (Bright and Kaufman, 2011a), and could indicate a catalytic effect of NaOCI on racemization following the initial removal of inter-crystalline amino acids. This combined with the slight decrease in amino acid concentration in *H. germanica* after 92 h (Fig. A.1.2b) suggests that the fraction of amino acids isolated by the initial bleach exposure is not resistant to chemical influences. However, given the small number of replicate analyses (n = 3 -4) and relatively large overall variability in D/L values, this observation should be treated with caution.

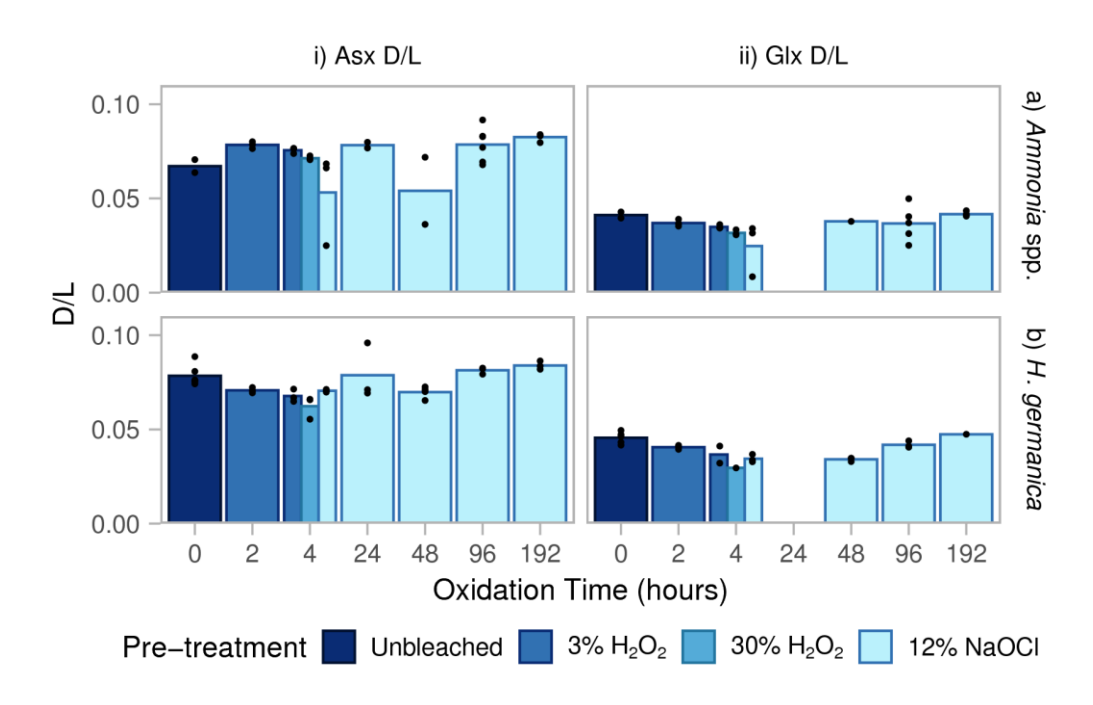


Fig. A.1.6 – Trends in i) Asx and ii) Glx THAA D/L with increasing oxidation time for a) *Ammonia* spp. and b) *H. germanica* from the estuarine surface. The top of the bar reflects the average concentration derived from individual measurements (solid black circles). Note that the gap at 24 h indicates that no Glx D/L values were collected for that particular oxidation step due to low amino acid concentrations.

For the planktic foraminifera, the addition of bleach to peroxide treated samples does not have a consistent impact on the D/L values of Asx or Glx. The differences in mean D/L between the pretreatments are fairly small (e.g., average 7% and 11% for Asx and Glx, respectively) and are not consistent in direction (Fig. A.1.7 and Fig. A.1.8; Table A.1.2). The relatively large number of subsamples measured at BBOR afford statistical analyses to support these results. Welch independent t-tests for the mid Holocene samples show that 8/14 mean D/L Asx values and 5/14 mean D/L Glx values had significant differences (P < 0.05) between the two pre-treatments (Fig. A.1.7; Table A.1.2). Unlike the mid Holocene samples, the early Holocene to mid Pleistocene-aged samples show a lack of significant change in the mean D/L values between the two differing treatment methods. The t-test results show that only 1/5 mean D/L Asx values and 1/5 mean D/L Glx values are significantly different (Table A.1.2). This indicates that the D/L values of older samples (> 10.5 ka) are less affected by the bleaching pre-treatment. Nevertheless, a pattern did emerge for species specific effects regardless of sample age. For samples that showed significant differences in their mean D/L values, bleach increased the D/L values of all P. obliquiloculata samples (5/5), decreased the D/L values of most G. truncatulinoides samples (4/5), and both increased and decreased the D/L values of G. tumida samples (Fig. A.1.7 and Fig. A.1.8).

Due to the increase in the familywise error rate when carrying out individual t-tests, a three-way analysis of variance (ANOVA) was used to confirm the results for normally distributed data, whereas individual Kruskal-Wallis tests were used for not normally distributed data (Table A.1.3). The ANOVA evaluated three variables that can contribute to differences in the D/L ratios: 1) pretreatment, 2) planktic foraminifer species, and 3) ODP site (i.e., sample age and water depth). The ANOVA and Kruskal-Wallis results align with those from the t-tests, indicating that the D/L of some Holocene-aged samples are significantly different between the two pre-treatments, whereas the D/L of Pleistocene-aged samples are not significantly different. As a whole, the Kruskal-Wallis tests for samples aged 6.0 – 410.0 ka show that the pre-treatment may have a larger effect on the D/L of Glx, possibly due to the slower racemization rate of this amino acid. The statistical results also suggest that that there are significant differences in the mean D/L arising from the species used (further explored in Section A1.3.4) and sampling site, which is expected due to varying sample age and water temperature at each site.

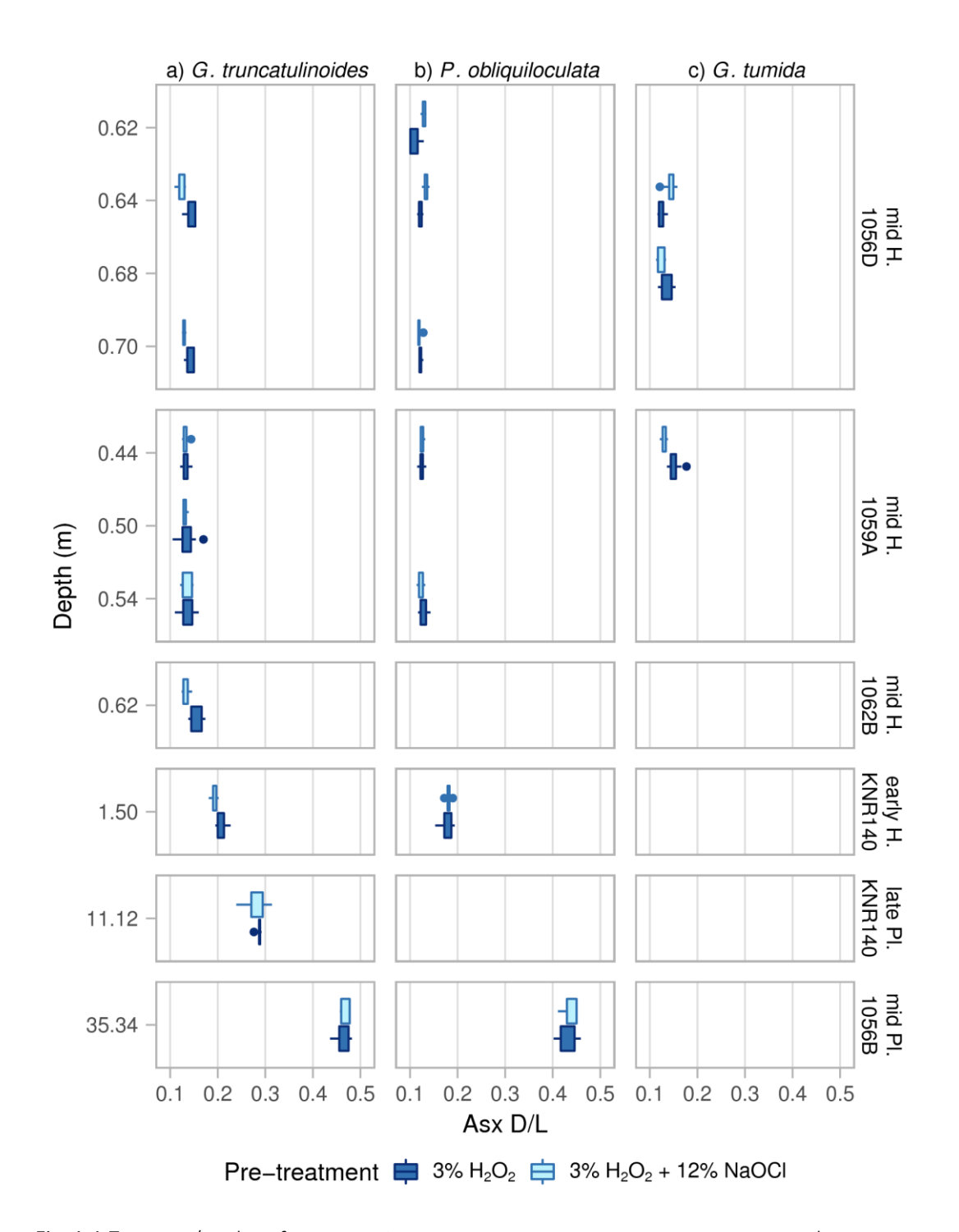


Fig. A.1.7 – Asx D/L values from ODP Sites 1056D, 1059A, 1062B, KNR140 JPC-37, and 1056B comparing the effects of bleaching on sample mean and standard deviation within a) *G.* truncatulinoides, b) P. *obliquiloculata*, and c) *G. tumida*. Samples are dated mid Holocene (H) to mid Pleistocene (Pl). The box is plotted from the first quartile to the third quartile with whiskers extending the full range and circular data points representing subsample values outside of the range by > 1.5 times the interquartile range.

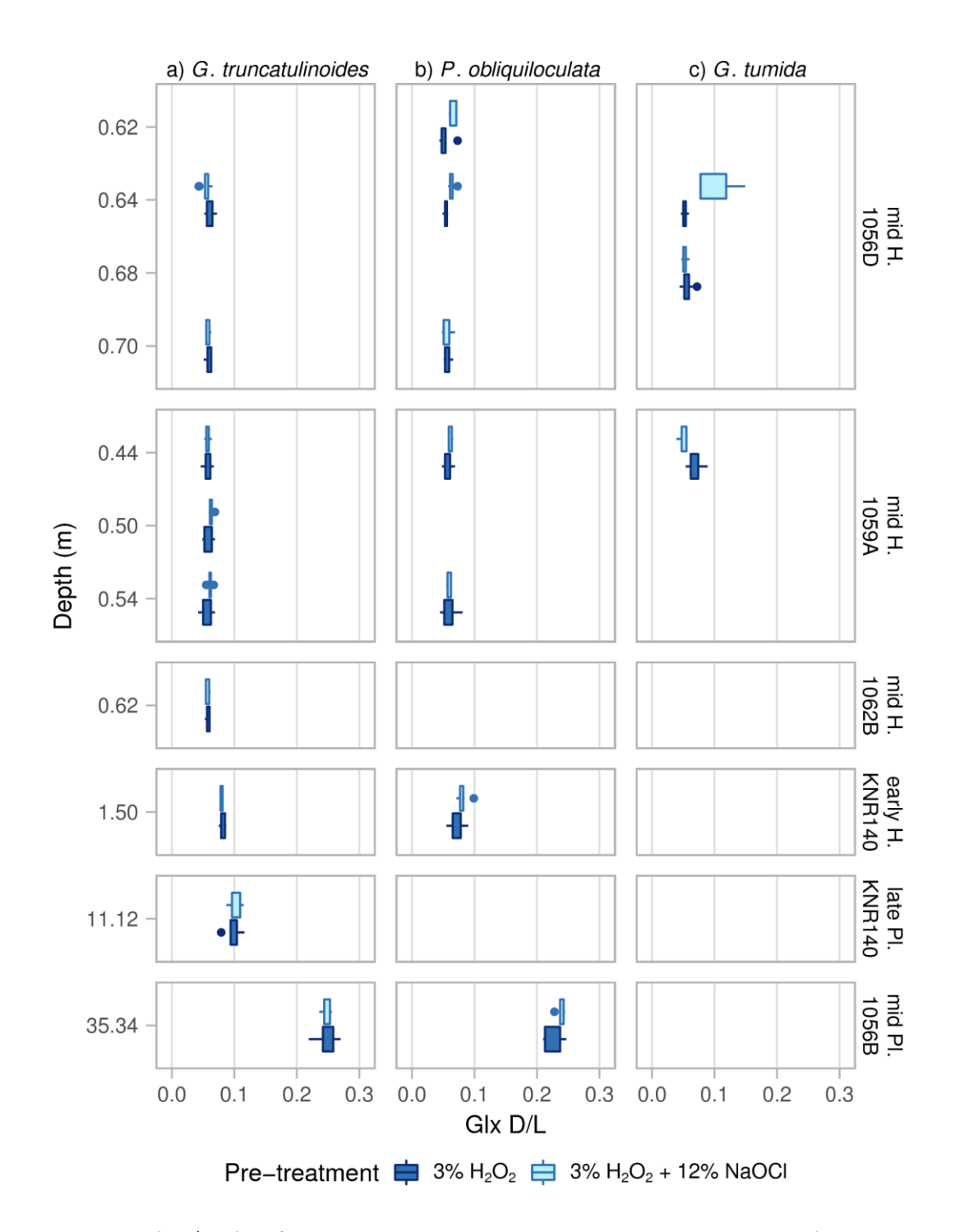


Fig. A.1.8 – Glx D/L values from ODP Sites 1056D, 1059A, 1062B, KNR140 JPC-37, and 1056B comparing the effects of bleaching on sample mean and standard deviation within a) G. truncatulinoides, b) P. obliquiloculata, and c) G. tumida. Samples are dated mid Holocene (H) to mid Pleistocene (Pl). The box is plotted from the first quartile to the third quartile with whiskers extending the full range and circular data points representing subsample values outside of the range by > 1.5 times the interquartile range.

Table A.1.2 – Mean D/L values for planktic foraminifera from the BBOR and P-values for statistical

significance between the pre-treatments.

Site	Sediment	¹ Species		D/L As	х		D/L Glx	
Site	Depth (m)	-species	H ₂ O ₂	² NaOCl	³ P-value	H ₂ O ₂	² NaOCl	³ P-value
Mid Holoc	ene (6.0-7.1 k	<u>:a)</u>						
1056D	0.62	P. obliq	0.110	0.129	0.0093*	0.053	0.064	0.0434*
1056D	0.64	P. obliq	0.121	0.134	0.0002*	0.054	0.063	0.0005*
1056D	0.70	P. obliq	0.122	0.120	0.3131	0.057	0.056	0.9175
1056D	0.64	G. trun	0.143	0.123	0.0004*	0.060	0.054	0.0715
1056D	0.70	G. trun	0.143	0.129	0.0014*	0.060	0.058	0.4209
1056D	0.64	G. tum	0.124	0.143	0.0004*	0.052	0.100	0.0002*
1056D	0.68	G. tum	0.136	0.124	0.0334*	0.057	0.052	0.2189
1059A	0.44	P. obliq	0.124	0.126	0.5682	0.057	0.062	0.1603
1059A	0.54	P. obliq	0.129	0.123	0.1310	0.060	0.060	0.9817
1059A	0.44	G. trun	0.134	0.132	0.4346	0.057	0.057	0.9568
1059A	0.50	G. trun	0.135	0.132	0.6323	0.058	0.063	0.0983
1059A	0.54	G. trun	0.136	0.136	0.9809	0.056	0.061	0.0057*
1059A	0.44	G. tum	0.152	0.130	0.0009*	0.069	0.051	0.0007*
1062B	0.62	G. trun	0.154	0.133	0.0134*	0.058	0.057	0.7570
Early Holo	cene (10.5 ka)	<u>)</u>						
KNR140	1.50	P. obliq	0.178	0.181	0.6082	0.072	0.081	0.1233
KNR140	1.50	G. trun	0.207	0.193	0.0042*	0.081	0.080	0.3287
Late Pleist	ocene (51.5 k	<u>a)</u>						
KNR140	11.12	G. trun	0.286	0.280	0.4878	0.098	0.101	0.6806
Mid Pleisto	ocene (410.0 l	ka)						
1056B	35.34	P. obliq	0.432	0.437	0.6963	0.225	0.239	0.0386*
1056B	35.34	G. trun	0.463	0.469	0.4254	0.249	0.247	0.8414

 $^{^{1}}$ P. obliq = Pulleniatina obliquiloculata, G. trun = Globorotalia truncatulinoides, G. tum = Globorotalia tumida 2 NaOCl stands for samples treated with 3% $H_{2}O_{2}$ plus 12% NaOCl.

Table A.1.3 – P-values from three-way ANOVA models used to determine whether the pre-treatments, planktic foraminifera species, and ODP sites (i.e., water depth) significantly impacted the mean D/L of Asx and Glx.

Sample Age	D/L	Asx P-value	es ¹	D/L Glx P-values ¹			
(ka)	Treatment	Species	Site	Treatment	Species	Site	
$6.0 - 10.5^2$	0.0096*	0.0000*	0.0000*	0.0081*	0.3296	0.0000*	
51.5 – 410.0	0.7753	0.0044*	0.0000*	0.2647	0.0004*	0.0000*	
$6.0 - 410.0^2$	0.1868	0.0000*	0.0000*	0.0260*	0.0219*	0.000*	

 $^{^{1}}$ P < 0.05 show a significant difference in the mean D/L between groups.

 $^{^{3}}$ P-values from independent t-tests for the difference of means. Samples with P < 0.05 show a significant difference in the means of the treatments, indicated by an asterisk.

 $^{^2}$ The Shapiro-Wilks test for normality showed that the Glx data for samples aged 6.0-10.5 ka and the whole dataset for samples aged 6.0-410.0 ka were non-normally distributed. Therefore, individual Kruskal-Wallis tests were used.

A1.3.4 D/L differences between foraminifer species

At the genus level, differences in the rate of amino acid racemization in foraminifera are well documented in the literature (King and Neville, 1977; Kaufman, 2006; Kaufman et al., 2013). Here we evaluate the effect of oxidative pre-treatments on foraminifer D/L values at the species level. We obtained sufficient tests from *P. obliquiloculata*, *G. truncatulinoides*, and *G. tumida* from six mid Holocene to late Pleistocene intervals to evaluate species differences in D/L values (**Table A.1.4**). However, we were able to obtain enough tests for only one species comparison from both the early Holocene and late Pleistocene sample sets, and none from the mid Pleistocene interval.

Akin to the ANOVA and Kruskal-Wallis results (**Table A.1.3**), the t-tests show that significant differences in the D/L values tend to exist between co-occurring planktic species in the majority of intervals (**Table A.1.4**). For D/L Asx, 8/10 intervals of both peroxide-treated and additional bleachtreated comparisons show significant differences, although not for the same species pair (**Table A.1.4**). For D/L Glx, about half of the comparisons show significant differences for the peroxide (5/10 intervals) versus the additional bleach treatments (6/10 intervals). These latter comparisons could illustrate that differences in D/L Glx values are less species-specific than D/L Asx in this range, and adding bleach does not change this result appreciatively. Alternatively, the slower racemization rate of Glx could result in smaller D/L differences between different species in this age range.

Table A.1.4 – Results of Welch's independent t-tests to evaluate species differences in the D/L values of Asx and Glx among two pre-treatments (3% H_2O_2 only versus 3% H_2O_2 plus 12% NaOCl).

Site	Sediment	Species	D/L Asx P-\	/alues²	D/L Glx P-values ²	
	Depth (m)	Comparison ¹	H ₂ O ₂	NaOCl ³	H ₂ O ₂	NaOCl ³
Mid Holoc	ene (6.0-7.1 ka)					
1056D	0.64	P. obliq vs G. trun	0.0001*	0.0068*	0.0298*	0.0058*
1056D	0.64	P. obliq vs G. tum	0.3591	0.0348*	0.2565	0.0014*
1056D	0.64	G. trun vs G. tum	0.0005*	0.0004*	0.0057*	0.0002*
1056D	0.70	P. obliq vs G. trun	0.0000*	0.0014*	0.2992	0.6660
1059A	0.44	P. obliq vs G. trun	0.0009*	0.0081*	0.9325	0.0208*
1059A	0.44	P. obliq vs G. tum	0.0001*	0.1150	0.0180*	0.0026*
1059A	0.44	G. trun vs G. tum	0.0028*	0.4641	0.0112*	0.0301*
1059A	0.54	P. obliq vs G. trun	0.1224	0.0024*	0.2867	0.3451
Early Holo	cene (10.5 ka)					
KNR140	1.50	P. obliq vs G. trun	0.0003*	0.0022*	0.0692	0.7268
Late Pleiste	ocene (51.5 ka <u>)</u>					
1056B	35.34	P. obliq vs G. trun	0.0017*	0.0336*	0.0050*	0.1108

 $^{^1}$ P. obliq = Pulleniatina obliquiloculata, G. trun = Globorotalia truncatulinoides, G. tum = Globorotalia tumida.

Focusing on the individual D/L Asx comparisons where species differences are more apparent, there is no consistent change in the species differences with the particular pre-treatment method. The difference in D/L Asx in *P. obliquiloculata* versus *G. truncatulinoides* is significant in 5/6 pairs whether or not bleach is added and is significant in the sixth comparison after bleach is added. The *P. obliquiloculata* versus *G. tumida* comparison, on the other hand, is inconclusive as the addition of bleach results in a significant difference in one of the two analysis pairs (1056D, 0.64 m) while it removes significance in the other example (1059A, 0.44 m). The difference in D/L Asx between *G. truncatulinoides* and *G. tumida* is significant for both examples when treated with peroxide only, but adding bleach appears to diminish the difference in one (1056D, 0.64 m versus 1059A, 0.44 m, respectively). These data suggest that adding bleach does not better define existing species differences in D/L Asx with respect to samples treated with peroxide only.

Samples from the BBOR also allow an examination of species-specific differences in racemization rates. We visualize these by regressing the D/L values of the same amino acid from two species against one another (Fig. A.1.9). For this purpose, we focus on results from *P. obliquiloculata* and *G. truncatulinoides* because they are present at three age horizons (mid Holocene, early Holocene and late Pleistocene) providing a common temporal reference frame. In this analysis, a slope of 1 reflects identical observed racemization rates (i.e., same D/L values for a given sample horizon), while deviations from a slope of 1 indicate slower or faster racemization rates, resulting in lower or higher D/L values, respectively, for a given time. *Globorotalia truncatulinoides* racemizes faster than *P. obliquiloculata* by 5% for Asx and 13% for Glx if pre-treated with peroxide only and 9% for Asx and 6% for Glx if pre-treated with peroxide and bleach (Fig. A.1.9). The similarity of the slopes suggests that the choice of pre-treatment has little effect on species-specific racemization rates for Asx (Fig. A.1.9a). However, bleach reduces the apparent species effect in samples with the higher D/L Glx values (i.e., older tests), resulting in a decrease in the apparent racemization rate of *G. truncatulinoides* compared to *P. obliquiloculata* (Fig. A.1.9b).

 $^{^2}$ P-values from independent t-tests of the subsamples where the null hypothesis was that the true difference in means is equal to 0. Samples with P < 0.05 (asterisk) show a significant difference in the means between species.

³ NaOCl stands for samples treated first with H₂O₂ and additionally with NaOCl.

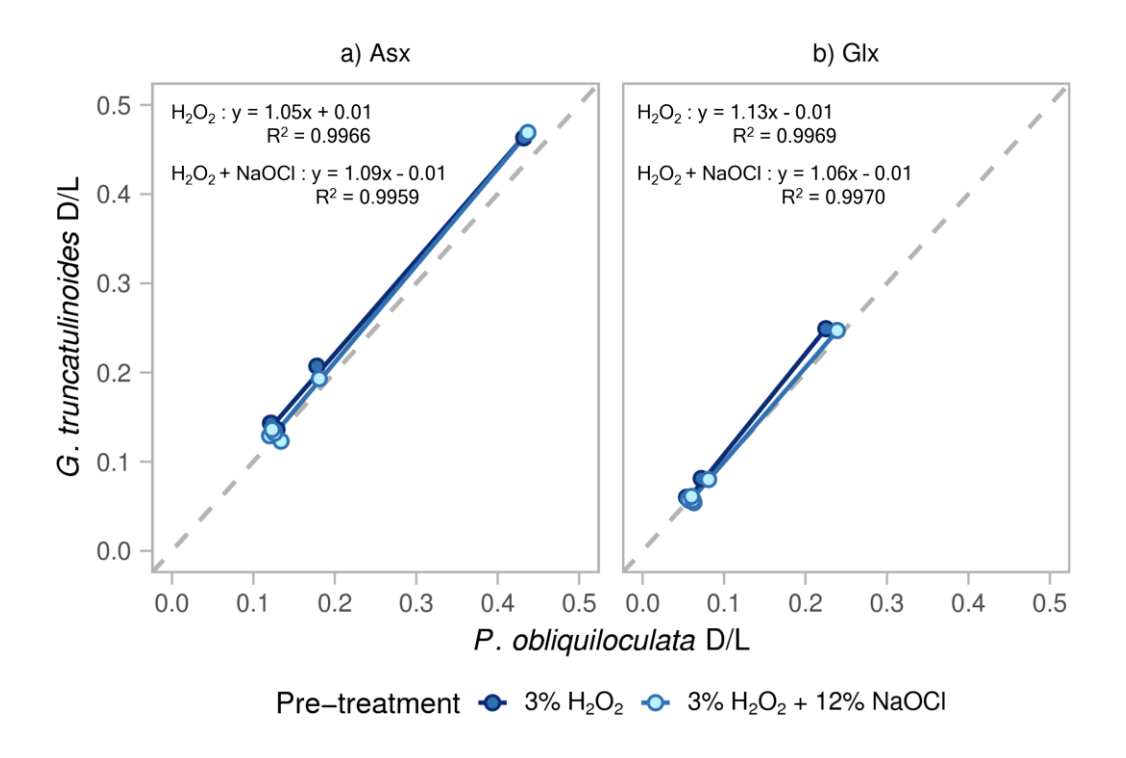


Fig. A.1.9 – Extent of racemization (D/L) in a) Asx and b) Glx measured in six coeval intervals of P. obliquiloculata and G. truncatulinoides (Table A.1.2). The slope indicates the relative racemization rates for the species where i) slope =1 indicates that both species racemize at the same rate, ii) slope > 1 indicates that G. truncatulinoides racemizes faster than F. obliquiloculata, and iii) slope < 1 indicates that F. obliquiloculata racemizes faster than F. truncatulinoides.

A1.3.5 D/L variability within planktic foraminifera

The subsamples for each interval and species in the planktic foraminifer study also afford a closer look at the effects of bleach on the replicability of sample mean D/L values. To describe this subsample variability, and to normalize it to the mean values, we use a coefficient of variation (CV). To quantify the average change (e.g., Δ CV,**Table A.1.5**) in the subsample variability between the pre-treatments for Asx and Glx, we subtract the CV for samples treated with H₂O₂-only from the CV for samples also treated with NaOCl. Accordingly, a decrease in the subsample variability is described by a decrease in the CV and indicates an improvement in replicability due to the additional bleaching pre-treatment. However, it is important to note that these statistical analyses are limited. While there are 14 mid Holocene aged samples for comparison, there are only 2 early Holocene, 1 late Pleistocene, and 2 mid Pleistocene-aged samples for comparison. We must therefore be careful when interpreting the statistics for the older samples (n = 5).

Overall, the results show that bleaching can reduce the subsample variability, although not consistently. For example, in 14 out of the 19 samples analyzed (74%), mean D/L for Asx and Glx

show an improved CV with the bleaching method (negative values in **Table A.1.5**, **Fig. A.1.10**). However, the improvement for Asx is small, on average -3.4% \pm 3.1%, with most samples falling within \pm 0.5% of the 1:1 regression line, suggesting that there is minimal difference between the CV of the two treatments. More specifically, we note that mid Holocene samples, for which we have the largest amount of data (n = 14) show the largest variations in the effect of adding bleach in comparison to the older samples (**Table A.1.5**; **Fig. A.1.10**). Less than half of these samples show noticeable reductions in their CV with bleaching (Δ CV < -4%; Fig. 10). For Asx, the late Pleistocene sample shows a notable increase in its CV after bleaching (Δ CV = 6%), while the early Holocene and mid Pleistocene samples are on or to the right of the 1:1 line (Δ CV = 0 to -4.6%). For Glx, all samples older than mid Holocene fall to the right of the 1:1 line (Δ CV = -2.8 to -5.6%), suggesting that bleach may more consistently reduce the inter-sample variability of D/L Glx.

Table A.1.5 – Average intra-sample variability in D/L values as described by the coefficient of variation (CV) compared between the 3% H₂O₂-only and 12% NaOCl-addition pre-treatments of planktic foraminiferal tests.

Site	Sediment	Species ¹	D/L As	x CV (%)		D/L Gl	D/L Glx CV (%)		
	Depth (m)		H ₂ O ₂	NaOCl ²	∆CV ³	H ₂ O ₂	NaOCl ²	∆CV ³	
Mid Holoc	ene (6.0-7.1 ka	<u> </u>			·	·			
1056D	0.62	P. obliq	10.0	3.0	-7.0	20.0	8.0	-12.0	
1056D	0.64	P. obliq	3.7	3.9	0.2*	5.5	7.7	2.2*	
1056D	0.70	P. obliq	2.7	3.3	0.6*	9.7	13.8	4.8*	
1056D	0.64	G. trun	7.9	6.7	-1.2	11.0	13.1	2.1*	
1056D	0.70	G. trun	6.1	2.3	-3.8	8.2	5.9	-2.3	
1056D	0.64	G. tum	5.6	7.8	2.2*	6.9	25.7	18.8*	
1056D	0.68	G. tum	9.5	6.6	-2.9	16.6	7.8	-8.8	
1059A	0.44	P. obliq	4.5	3.2	-1.3	12.3	5.1	-7.2	
1059A	0.54	P. obliq	6.7	5.1	-1.6	17.9	5.6	-12.3	
1059A	0.44	G. trun	5.1	4.6	-0.5	10.1	6.3	-3.8	
1059A	0.50	G. trun	15.1	2.9	-12.2	13.0	4.8	-8.2	
1059A	0.54	G. trun	10.2	7.3	-2.9	13.4	4.4	-9.0	
1059A	0.44	G. tum	8.5	4.6	-3.9	15.3	12.4	-2.9	
1062B	0.62	G. trun	8.8	6.9	-1.9	5.5	7.2	1.7*	
Early Holo	ocene (10.5 ka)				·	<u> </u>		·	
KNR140	1.50	P. obliq	7.6	3.0	-4.6	16.6	11.0	-5.6	
KNR140	1.50	G. trun	5.4	3.3	-2.1	6.9	2.7	-4.2	
Late Pleist	ocene (51.5 ka)								
KNR140	11.12	G. trun	2.1	8.1	6.0*	13.8	10.1	-2.8	

Site	Sediment	Species ¹	D/L As	(CV (%)		D/L Glx CV (%)		
	Depth (m)		H ₂ O ₂	NaOCl ²	ΔCV ³	H ₂ O ₂	NaOCl ²	ΔCV ³
Mid Pleisto	cene (410.0 ka)							
1056B	35.34	P. obliq	4.2	4.2	0.0	6.1	3.3	-2.8
1056B	35.34	G. trun	3.4	2.0	-1.4	6.2	3.0	-3.2

 $^{^{1}}$ P. obliq = *Pulleniatina obliquiloculata*, G. trun = *Globorotalia truncatulinoides*, G. tum = *Globorotalia tumida*

³ The values with an asterisk show an increase in variance with the NaOCl bleaching pre-treatment where $\Delta CV = CV_{NaOCl} - CV_{H_2O_2}$.

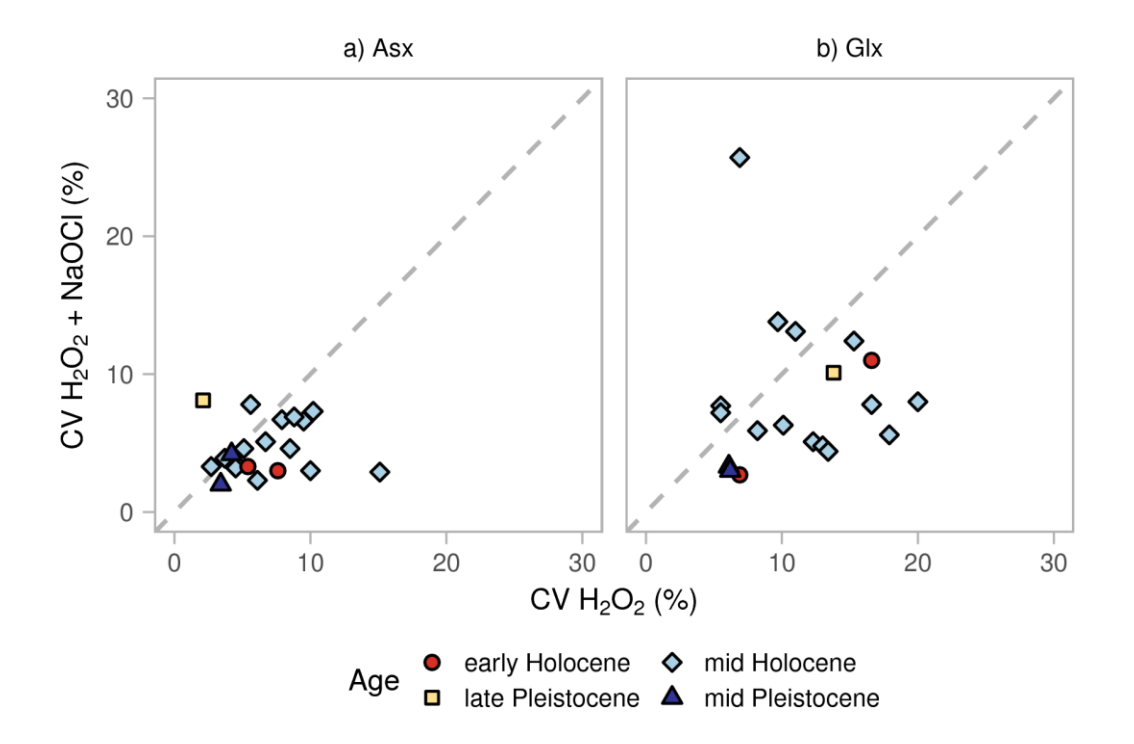


Fig. A.1.10 – Relationship between the coefficient of variation (CV) pertaining to the two pre-treatment methods in planktic foraminifera for a) Asx and b) Glx. The diagonal dashed line indicates the 1:1 relationship on which the points should fall if additional treatment with bleach does not produce a change in the CV. Points to the left of the line indicate that additional bleaching increases the CV with respect to peroxide treatment only; points to the right of the line indicate that the CV is lower after bleaching with respect to peroxide treatment only.

A1.4 Discussion

This study shows the effects of oxidative pre-treatments on biomineral amino acids within foraminiferal tests by combining the results of two studies:

1) sequential oxidation experiments involving peroxide versus bleach conducted on submodern benthic *Ammonia* spp. and *H. germanica*;

² NaOCl stands for samples treated first with H₂O₂ and additionally with NaOCl.

2) experiments testing the effects of bleach on peroxide pre-treated mid Holocene through mid Pleistocene planktic species (*P. obliquiloculata*, *G. truncatulinoides*, and *G. tumida*).

Our integrated results suggest that bleach more effectively reduces [THAA] in a sample in comparison to sonication-only treatments (Fig. A.1.2), while peroxide moderately reduces [THAA] (Fig. A.1.2 and Fig. A.1.3). These results demonstrate that bleach pre-treatment is effective in removing exogenous and/or inter-crystalline proteins in accordance with previous studies (e.g. Penkman et al., 2008, 2011; Hendy et al., 2012; Crisp et al., 2013; Demarchi et al., 2013c, 2013b; Ortiz et al., 2015, 2018). This is important because contamination by surface amino acids is of particular concern in foraminifera due to the high surface area-to-mass ratio related to test porosity (Stathoplos and Hare, 1993; Hearty et al., 2004).

While oxidative pre-treatments reduce [THAA] of foraminifera (**Fig. A.1.2Fig. A.1.3**), neither hydrogen peroxide nor bleach substantially affect the proportion of individual amino acids in a sample (**Fig. A.1.4Fig. A.1.5**), with the exception of *Ammonia* spp. For this benthic species, increasing the strength of the oxidizing agent causes the proportion of Asx, Glx, and Ala to increase and the proportion of Gly to decrease, most noticeably in the 12% NaOCI treatment. In contrast to *Ammonia* spp., the compositional differences between the pre-treatments for *H. germanica* and the planktic species are less pronounced. This has also been observed in naturally aged *N. pachyderma* (Wheeler et al., 2021), and suggests that in general, the inter- and intra-crystalline fractions of foraminifera have similar amino acid compositions. The different pattern seen in *Ammonia* spp. could be due to the sonication and weak oxidizing treatments being less effective at removing surface organic material for this species than the others investigated, although the variability of the composition data precludes a firm conclusion.

Effective removal of surface contaminants by bleach could also partly explain the overall reduction in the subsample variability in D/L values of bleach-treated samples with respect to those treated with peroxide only. Replicate analyses of the BBOR samples suggests that bleaching tends to reduce the variability within samples, albeit with differences in the extent depending on the amino acid. For D/L Asx, the reduction in CV is minimal overall, not very consistent, and not apparent in older samples. For D/L Glx, bleaching more effectively reduces the CV at all ages, although the difference in variability between bleached and peroxide-only samples is inconsistent. This slight reduction in D/L variability in bleached samples, especially younger samples, is consistent with bleaching experiments carried out on *Neogloboquadrina pachyderma* (sinistral) (Wheeler et al., 2021). Although the bleach pre-treatment appears to isolate the intra-crystalline fraction of

foraminiferal amino acids, the small reduction in subsample variability does not warrant the additional preparation time and larger sample size that the bleach pre-treatment requires. Instead, the hydrogen peroxide pre-treatment is sufficient at removing surface contaminants from foraminiferal tests, resulting in D/L values that are not statistically different between the pre-treatments.

Neither set of experiments demonstrates a consistent effect of oxidation on Asx and Glx D/L values that warrant extensive chemical pre-treatment. For the sub-modern benthic foraminifer species, there is no observable difference in D/L values between tests that were H₂O sonicated, peroxide-treated, or bleach-treated (Fig. A.1.6). Bleaching does cause statistically significant differences in the D/L values of mid Holocene-aged planktic foraminifera tests, although the differences are small and are inconsistent in their direction and magnitude (Table A.1.2; Fig. A.1.7Fig. A.1.8). In early Holocene through mid Pleistocene-aged samples, additional bleaching of peroxide-treated foraminifer tests does not consistently affect the overall D/L values. These irregularities suggest that most of the surface contaminants are removed before the oxidizing pre-treatments are applied; an interpretation that is supported by the observation that neither pre-treatment method consistently affects the D/L values of a sample.

Species-specific differences in D/L values are evident in several samples. By comparing down-core changes in D/L values for coeval species, we can see how the pre-treatments affect apparent species-specific racemization rates (**Fig. A.1.9**). The down-core changes in D/L values for *G. truncatulinoides* and *P. obliquiloculata* are similar, but not the same, suggesting small differences in racemization rates. The results show that D/L Asx in *G. truncatulinoides* has a higher racemization rate than in *P. obliquiloculata*, and pre-treatment has minimal effect on the rate (e.g., D/L Asx in *G. truncatulinoides* racemizes 5% and 9% faster than in *P. obliquiloculata* for H_2O_2 and NaOCI treated samples, respectively). Conversely, the bleach pre-treatment reduces the species differences for D/L Glx, where D/L Glx in *G. truncatulinoides* racemizes 13% and 6% faster than in *P. obliquiloculata* for H_2O_2 and bleach treated samples, respectively.

The bleach pre-treatment does not affect the overall trend of planktic foraminiferal D/L values over time (Fig. A.1.11), meaning D/L increases with age, reflecting the increased proportion of D-Asx and D-Glx due to the increased extent of racemization in older fossils. While the overall trend is consistent, the pre-treatments induce a relatively small effect on the D/L values of Glx in *G. truncatulinoides* (Fig. A.1.11a), but not in *P. obiquiloculata* (Fig. A.1.11b). Thus, in this study, bleaching of foraminifer tests does not improve the replicability of D/L values of planktic

foraminiferal species. While analyzing only the bleach-isolated intra-crystalline fraction of amino acids can reduce the variability of D/L values in some biominerals, this study suggests that this is not the case for foraminifera. This behavior is also seen in ostracod valves (Bright and Kaufman, 2011a) and some aragonitic mollusks (Orem and Kaufman, 2011; Demarchi et al., 2015; Ortiz et al., 2017).

The most likely explanation for why the older (mid Holocene through mid Pleistocene) foraminiferal tests do not show differences in D/L values between the pre-treatments could be because some of the more easily accessed free amino acids and matrix proteins from the intercrystalline fraction have already been removed over time, possibly due to leaching (diffusive loss) and/or microbial influences (Penkman et al., 2008; Demarchi and Collins, 2014; Ortiz et al., 2015, 2017). Therefore, the amino acids remaining in these older samples would be likely dominated by the intra-crystalline fraction, which is resistant to exposure to chemical oxidation (Stathoplos and Hare, 1993; Penkman et al., 2008; Wheeler et al., 2021). For peroxide treated mid Holocene samples (~5 ka), a larger proportion of inter-crystalline proteins would remain due to the younger age of these samples.

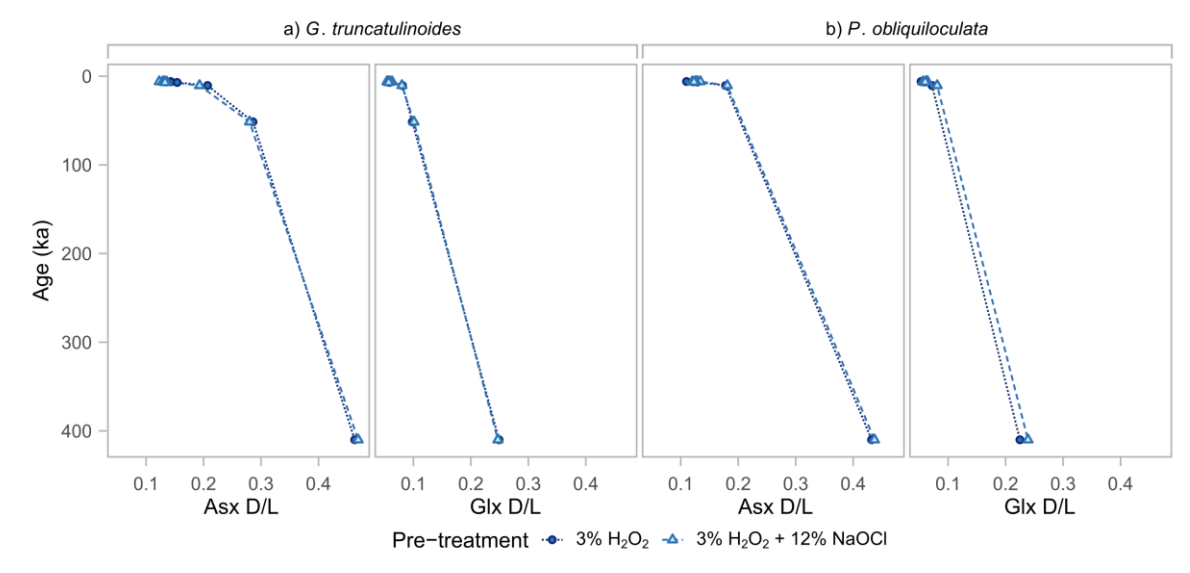


Fig. A.1.11 – Early Holocene through mid Pleistocene (10.5 – 410.0 ka) changes in a) *G. truncatulinoides* b) and *P. obliquiloculata* D/L Asx (and D/L Glx in c and d for the two species respectively) for peroxide treated (dark blue circles) and bleached (light blue triangles).

A1.5 Conclusions

If foraminifer tests contain a closed-system intra-crystalline protein fraction, bleaching should isolate this fraction and reduce post-depositional environmental influences on the preservation of amino acids (i.e., contamination by exogenous amino acids, microbial decomposition, and

leaching), thus improving the analytical variability (Penkman et al., 2008). We evaluate the effects of oxidative pre-treatments on benthic and planktic foraminiferal species through sequential oxidation experiments on sub-modern benthic foraminifer tests (0-5 cm sample depth) and through comparative oxidation experiments using peroxide and peroxide plus bleach on three species of planktic foraminiferal tests ($\sim 6.0-410.0$ ka). We investigate how bleach pre-treatment affects the variability in foraminiferal D/L values in three foraminiferal species of different ages. The results indicate that bleaching for 24 h reduces amino acid concentrations but does not completely remove amino acids within the foraminifer tests. This decrease in amino acid concentration reflects the removal of exogenous and/or easily accessed matrix proteins and the subsequent isolation of bleach resistant intra-crystalline amino acids.

The effective removal of surface contaminants and labile inter-crystalline matrix proteins by bleach can explain the overall reduction in subsample variability and change in some D/L values observed in our mid Holocene foraminifer tests. The older (i.e., early Holocene to mid Pleistocene) foraminiferal tests do not show differences in D/L values across the various pre-treatments and the reduction in subsample variability in D/L values is less apparent, especially for Asx. This could be due to the removal of easily accessed free amino acids and matrix proteins over time due to leaching and/or microbial influences, leaving behind a greater proportion of intra-crystalline amino acids.

In conclusion, due to the lack of consistent improvement in foraminiferal D/L variability between oxidation by hydrogen peroxide and bleach, the short oxidation procedure using hydrogen peroxide appears to be sufficient for AAR studies involving foraminifera. Analyzing the bleach-resistant fraction of amino acids requires a larger sample size and additional preparation time and does not yield results that are substantially better than results derived from the less time-intensive peroxide pre-treatment. This study shows that the inconsistent reduction in variability produced by the IcPD bleach pre-treatment does not outweigh the additional analyst time and larger sample size required, and therefore the short (2 h) 3% H₂O₂ oxidation protocol is recommended.

Acknowledgements

Funding: This work was supported by the Petroleum Research Fund (PRF #56964-ND), administered by the American Chemical Society (ACS) (KB).; the University of York Chemistry Department; the National Science Foundation (award #1855381); and the European Research Council (ERC) under the European Union's Horizon 2020 research and innovation program (grant

agreement #865222) as part of the EQuaTe study. This research used samples collected by the Ocean Drilling Program (ODP) and provided by the International Ocean Discovery Program (IODP). ODP and IODP are sponsored by the U.S. National Science Foundation (NSF) and participating countries.

We thank the editors and reviewers for their time. EM thanks Katherine Whitacre for running the instrument at Amino Acid Geochronology Lab, and John Wehmiller for insights and discussions regarding methods and application of AAR. LW would also like to thank Sheila Taylor and Maria Gehrels for technical support and Graham Rush for Humber estuary sample collection. Lastly, EM and LW thank Jordon Bright for insight with the manuscript.

Supplementary information

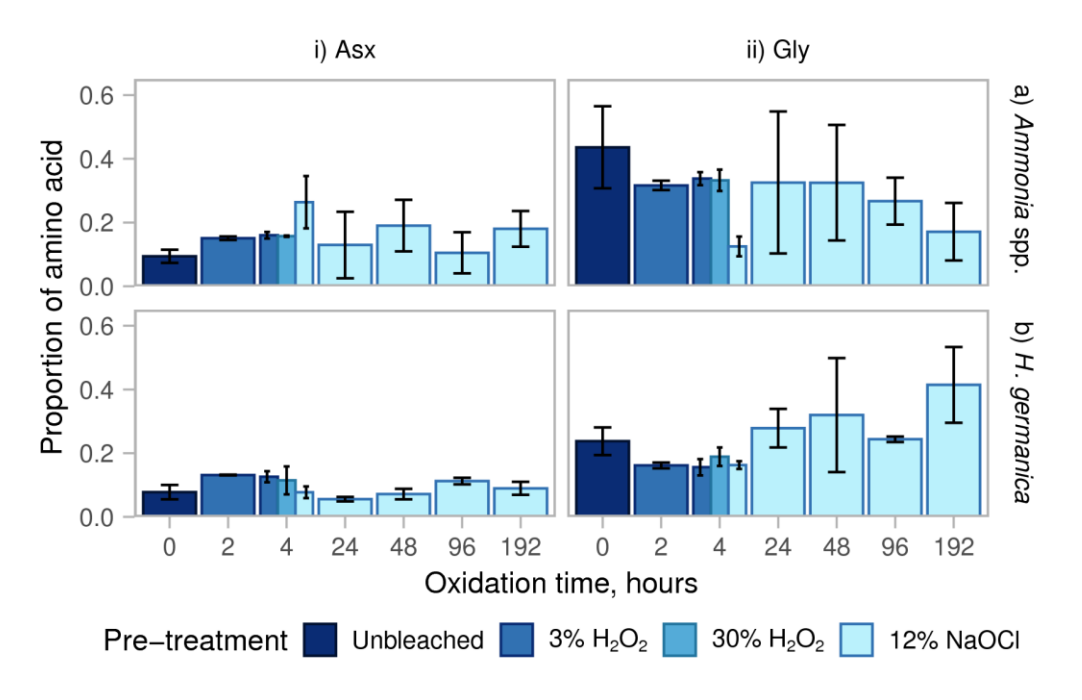


Fig. A.1.12 – Proportion of Asx and Glx in unbleached (i.e., H₂O sonication only) and oxidized (i.e., H₂O₂ or NaOCl) samples of modern benthic species a) *H. germanica* and b) *Ammonia* spp. from surface sediments of the Humber Estuary. Error bars represent the standard deviation.

Appendix 2 – Additional results of oxidative pretreatment experiments

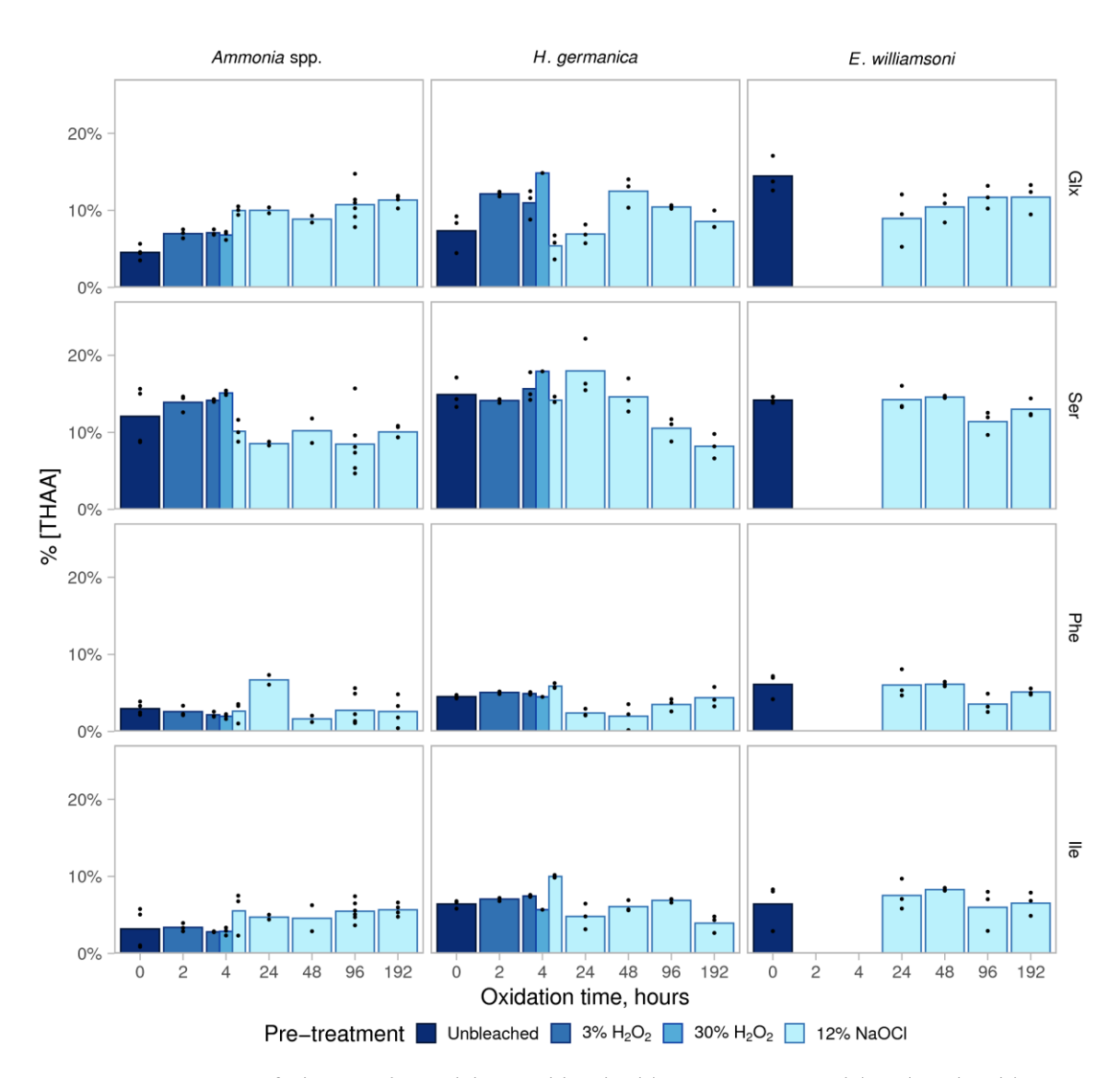


Fig. A2.1 – Proportion of Glx, Ser, Phe and Ile in unbleached (H_2O sonication only) and oxidized (H_2O_2 or NaOCl) samples of sub-modern *H. germanica*, *Ammonia* spp. and *E. williamsoni*. Dots show individual replicates; bars show means of all replicates.

Appendix 3 – Additional results of high-temperature decomposition experiments

This appendix relates to the high temperature decomposition experiments carried out on *Ammonia* spp. and *H. germanica* in **Chapter 5**.

A3.1 Patterns of leaching for Ser, Gly and all amino acids at 110°C

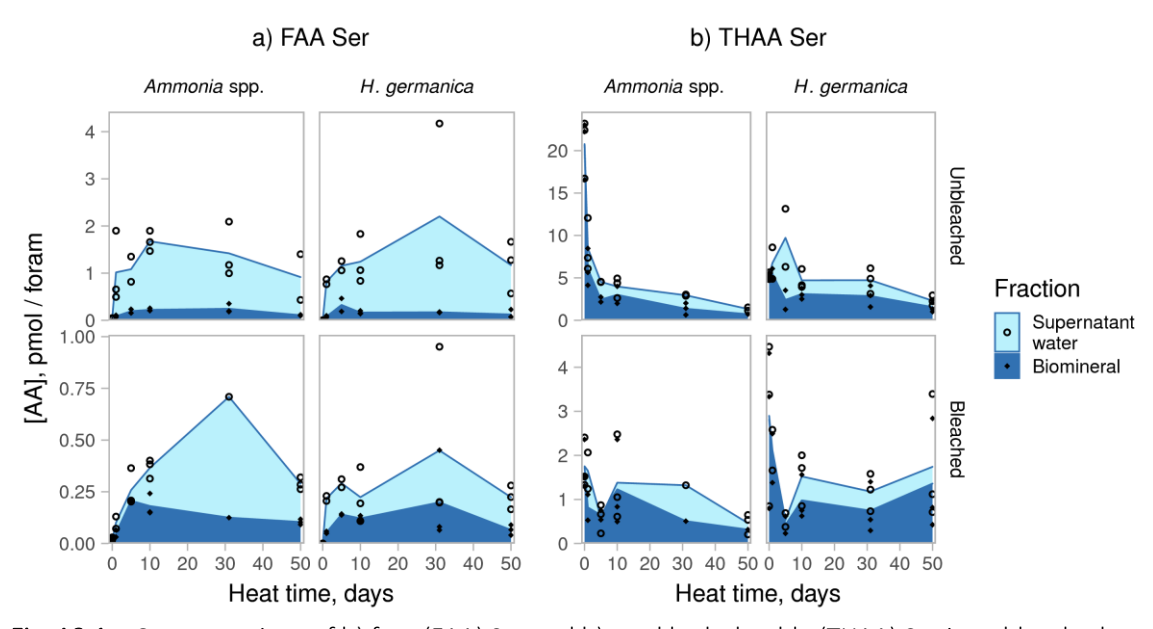


Fig. A3.1 – Concentrations of b) free (FAA) Ser and b) total hydrolysable (THAA) Ser in unbleached (whole-shell) and bleached (intra-crystalline) *Ammonia spp.* and *H. germanica* biomineral powders and the supernatant water in each vial during 110°C heating experiments. The shaded areas show the average concentration of each fraction over time; the points show individual replicates.

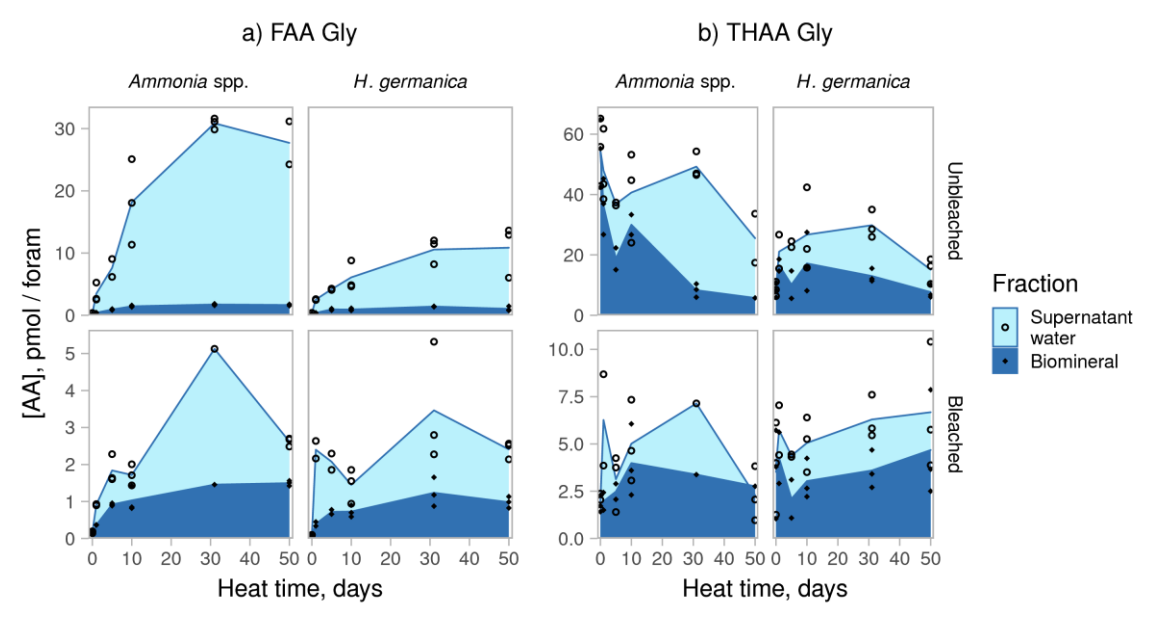


Fig. A3.2 – Concentrations of b) free (FAA) Gly and b) total hydrolysable (THAA) Gly in unbleached (whole-shell) and bleached (intra-crystalline) *Ammonia spp.* and *H. germanica* biomineral powders and the supernatant water in each vial during 110°C heating experiments. The shaded areas show the average concentration of each fraction over time; the points show individual replicates.

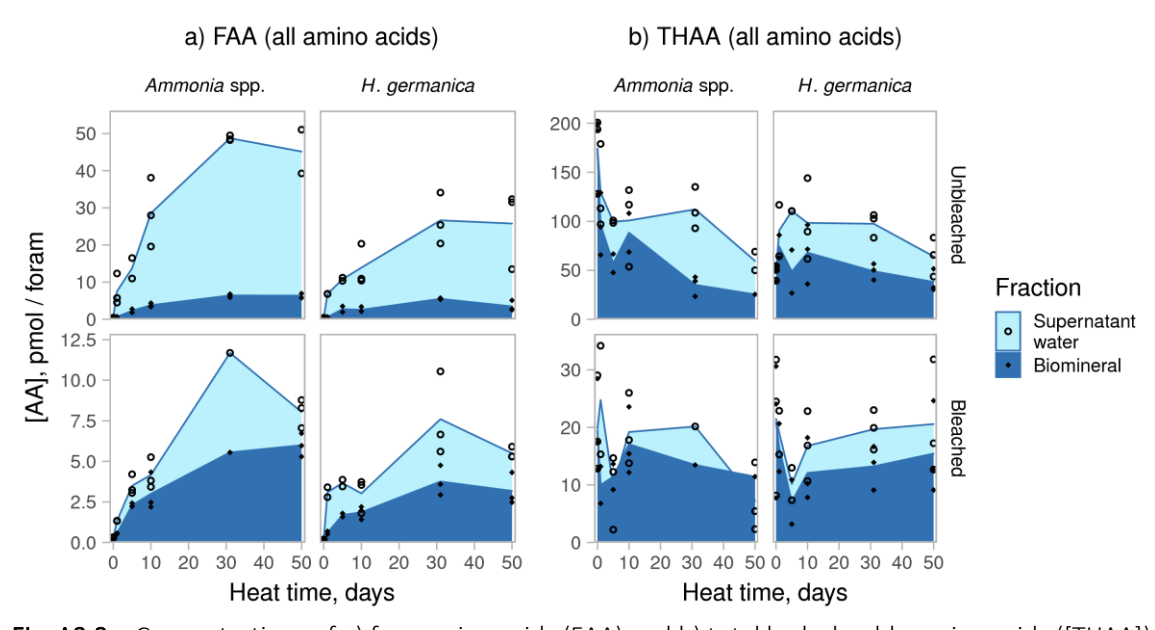


Fig. A3.3 – Concentrations of a) free amino acids (FAA) and b) total hydrolysable amino acids ([THAA]) in unbleached (whole-shell) and bleached (intra-crystalline) *Ammonia spp.* and *H. germanica* biomineral powders and the supernatant water in each vial during 110°C heating experiments. The shaded areas show the average concentration of each fraction over time; the points show individual replicates. Note the different y-axis scales used for the bleached and unbleached graphs.

A3.2 Composition trends of 140°C suite of experiments

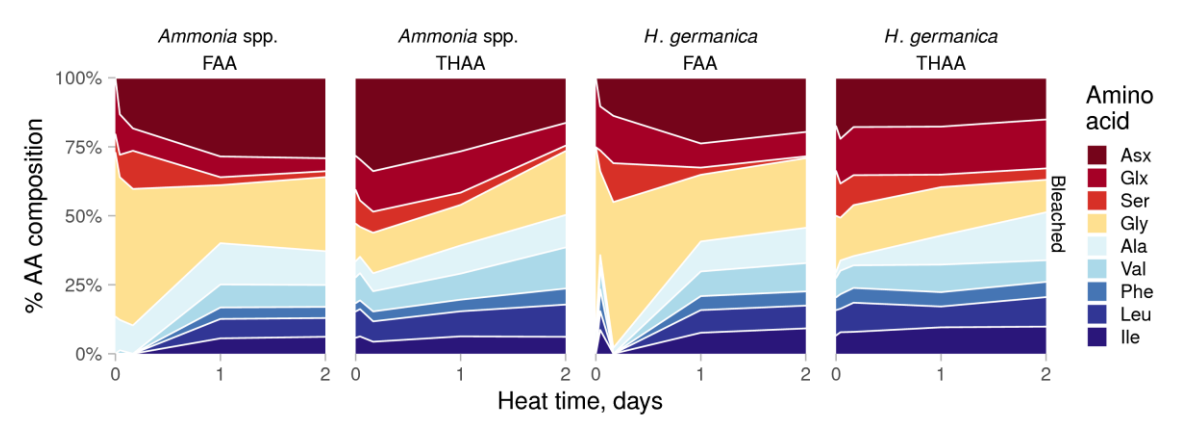


Fig. A3.4 – Change in composition of free (FAA) and total hydrolysable (THAA) amino acids in bleached (intra-crystalline) *Ammonia* spp. and *H. germanica* during 140°C heating experiment. X-axis labels show the time points for which data were collected. Arg, Tyr, Met, His and Thr are poorly resolved using RP-HPLC and have been excluded for comparison with the 110°C suite of experiments.

A3.3 Covariance trends and relative racemisation rates of 140°C suite of experiments

Ammonia spp. - 140°C

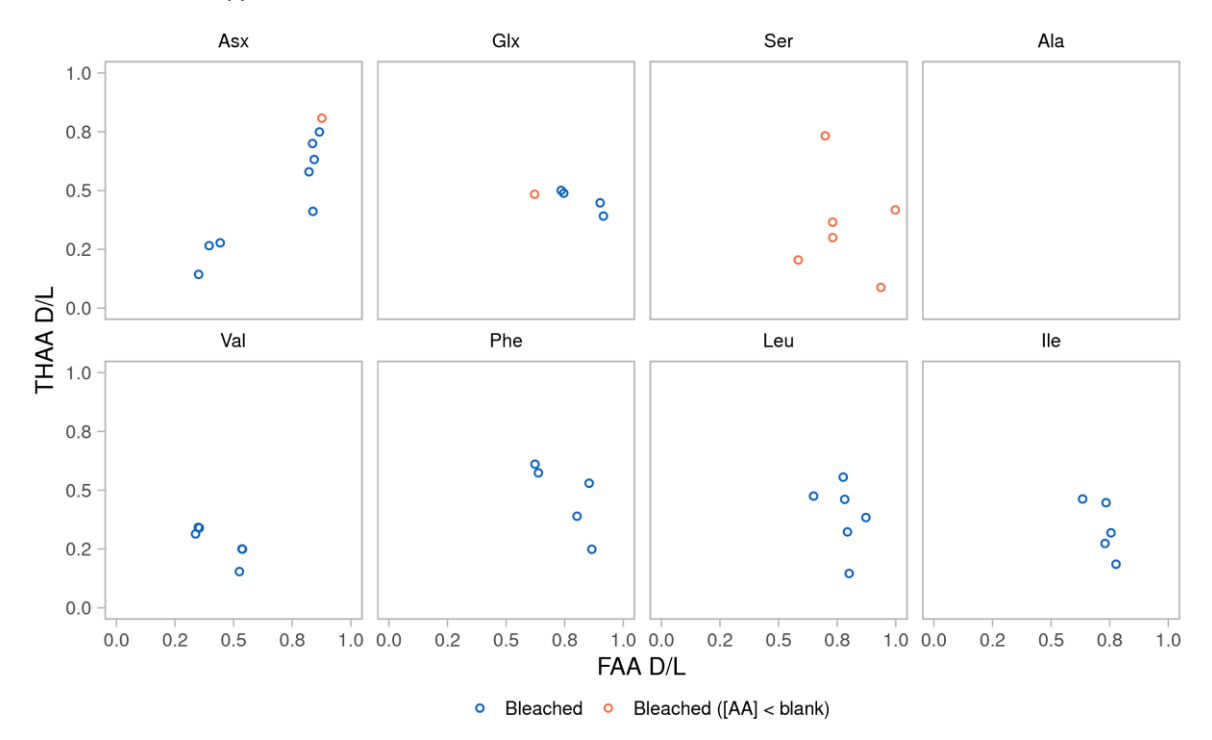


Fig. A3.5 – Covariance between D/L values in the free amino acid (FAA) and total hydrolysable amino acid (THAA) fractions for various amino acids in bleached (intra-crystalline) *Ammonia* spp., heated to 140°C. Samples with either an FAA or THAA concentration below the average + 1 σ of the blank are highlighted in orange.

H. germanica - 140°C

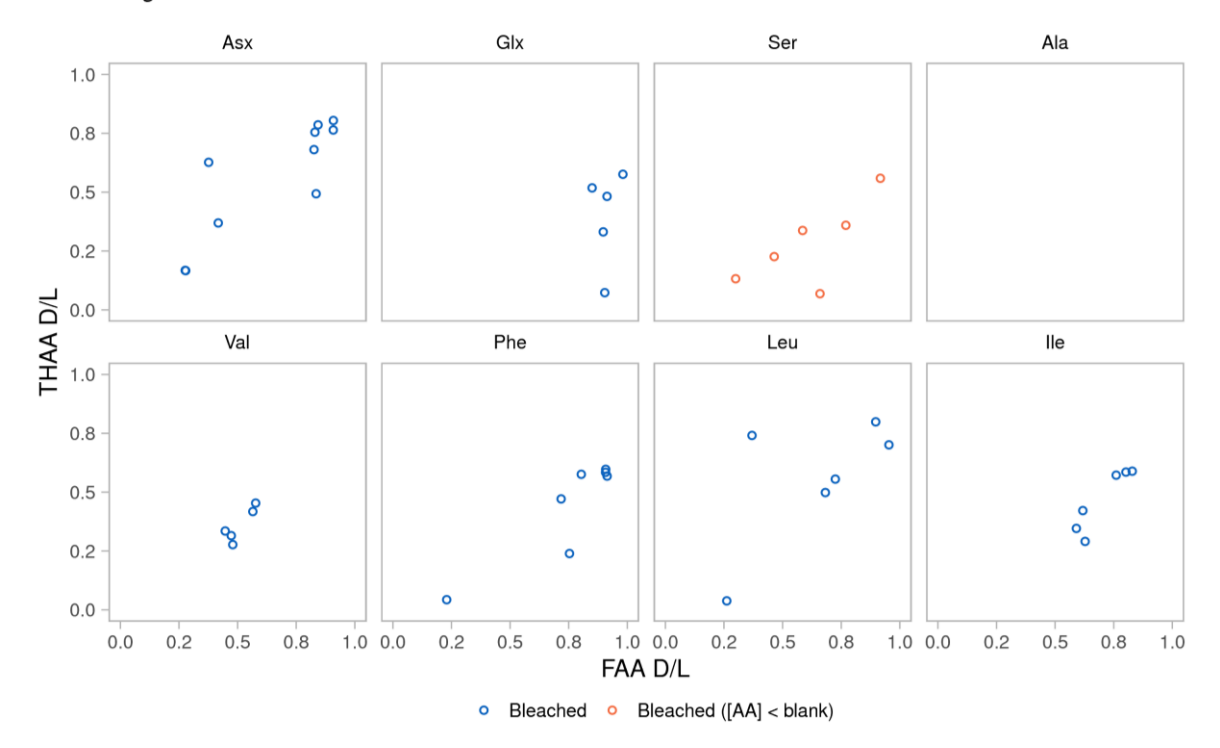


Fig. A3.6 – Covariance between D/L values in the free amino acid (FAA) and total hydrolysable amino acid (THAA) fractions for various amino acids in bleached (intra-crystalline) H. germanica, heated to 140°C. Samples with either an FAA or THAA concentration below the average + 1 σ of the blank are highlighted in orange.

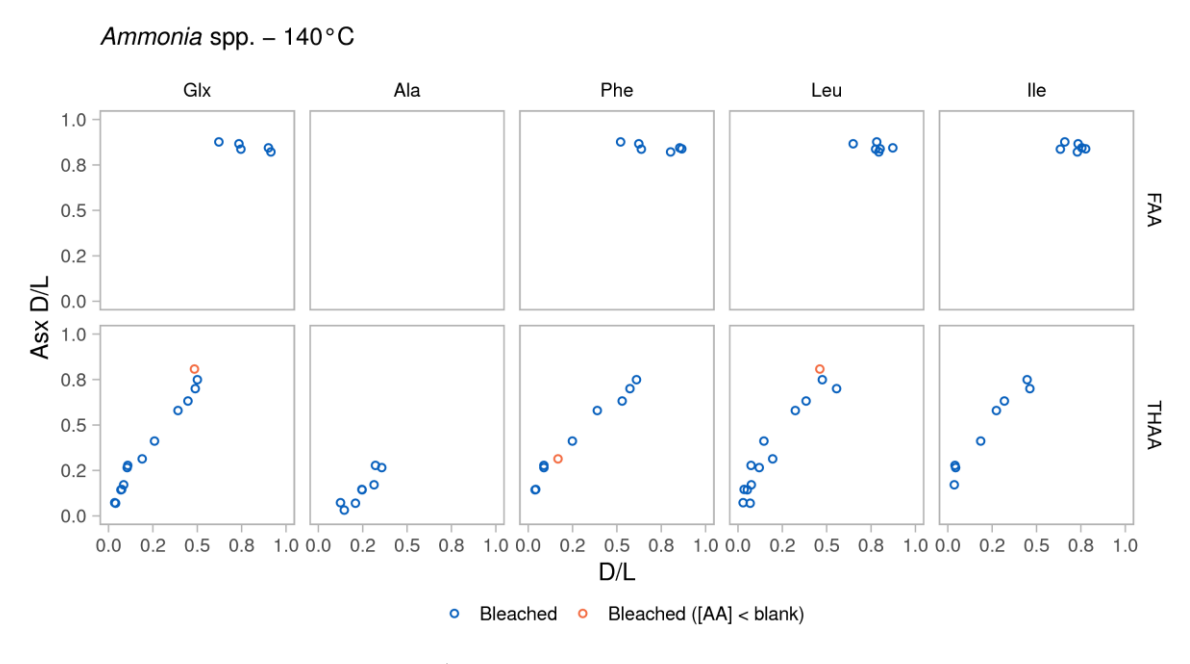


Fig. A3.7 – Covariance between Asx D/L and other amino acids in bleached (intra-crystalline) *Ammonia* spp., heated to 140°C. Samples with either Asx or another amino acid concentration below the average $+ 1 \sigma$ of the blank are highlighted in orange. Upper: free amino acids (FAA); lower: total hydrolysable amino acids (THAA).

H. germanica - 140°C

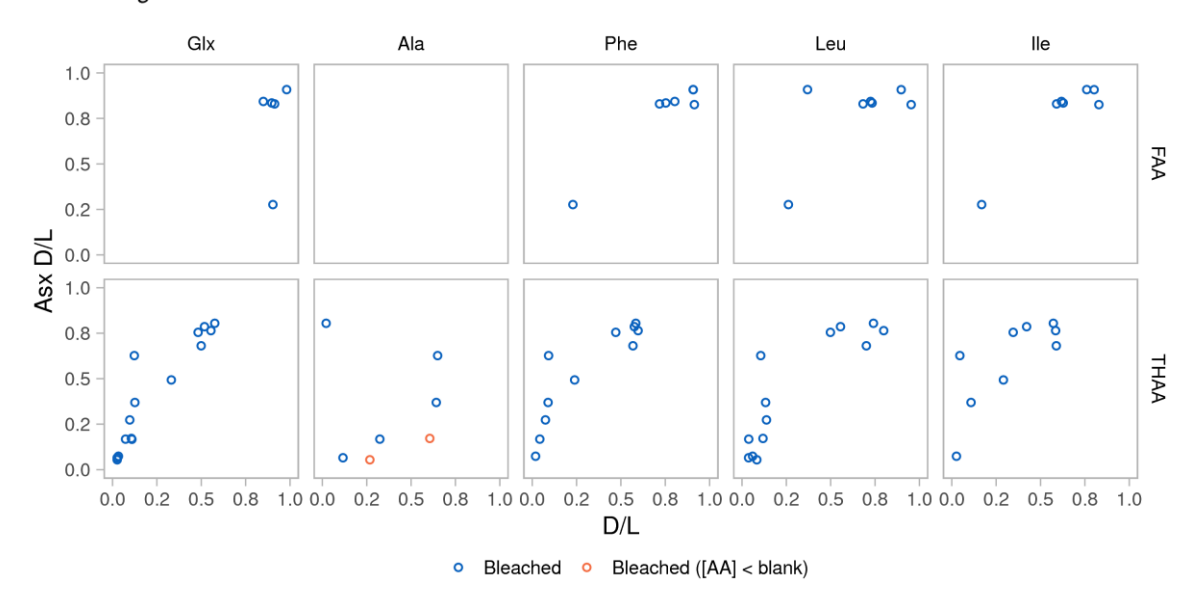


Fig. A3.8 – Covariance between Asx D/L and other amino acids in bleached (intra-crystalline) H. germanica, heated to 140°C. Samples with either Asx or another amino acid concentration below the average + 1 σ of the blank are highlighted in orange. Upper: free amino acids (FAA); lower: total hydrolysable amino acids (THAA).

Ammonia spp. and H. germanica - 140°C

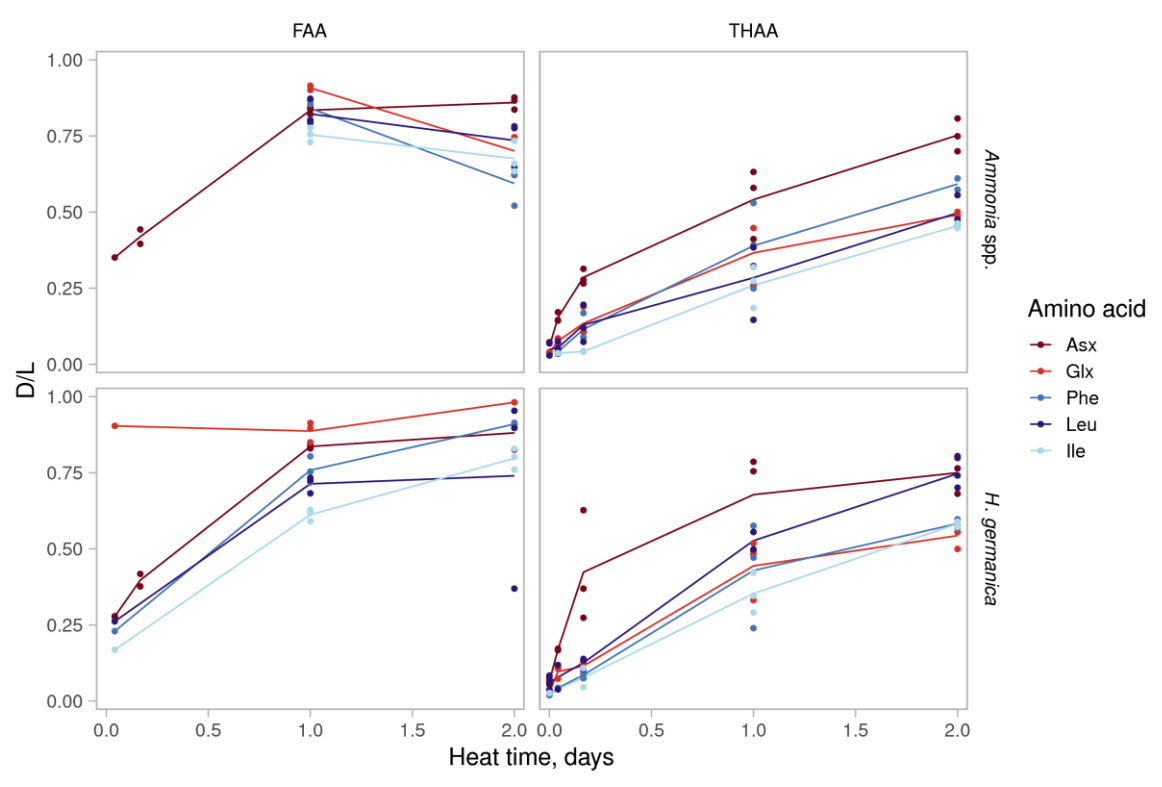


Fig. A3.9 - Comparison between racemisation of Asx, Glx, Phe and Ile in bleached (intra-crystalline) *Ammonia* spp. and *H. germanica*, heated to 140°C. The solid line shows the average D/L over time; the points are individual replicates. As this suite of experiments was analysed using UHPLC, Ala is poorly resolved and Ile is well resolved. Left: free amino acids (FAA); right: total hydrolysable amino acids (THAA).

A3.4 Results of SPK and CPK models for Glx, Ala, Phe and Leu

The results of the SPK and CPK models carried out on FAA and THAA Glx and Ala, and THAA Phe and Leu, are detailed in this appendix. FAA Phe and Leu have been excluded due to missing FAA D/L values at early time points (see **Section 5.3.4.2**).

Table A3.1 – Intercepts (c) of SPK and CPK linear models for Asx from unbleached (whole-shell) and bleached (intra-crystalline) *H. germanica* and *Ammonia* spp., heated to 110°C (see **Table 5.6** for other model parameters).

			Unbleached	Bleached
ø	SPK	FAA	-0.008 ± 0.006	-0.013 ± 0.007
Ammonia spp.	ß	THAA	0.	-0.001 ± 0.007
nm gs	CPK	FAA	4 ± 3	1 ± 2
▼	ט	THAA	40 ± 150	1.6 ± 0.3
ica	SPK	FAA	-0.005 ± 0.007	0.28 ± 0.06
nan	S	THAA	0.024 ± 0.017	0.18 ± 0.05
germanica	CPK	FAA	5 ± 6	1.16 ± 0.02
H.	ט	THAA	2.6 ± 0.7	1.06 ± 0.016

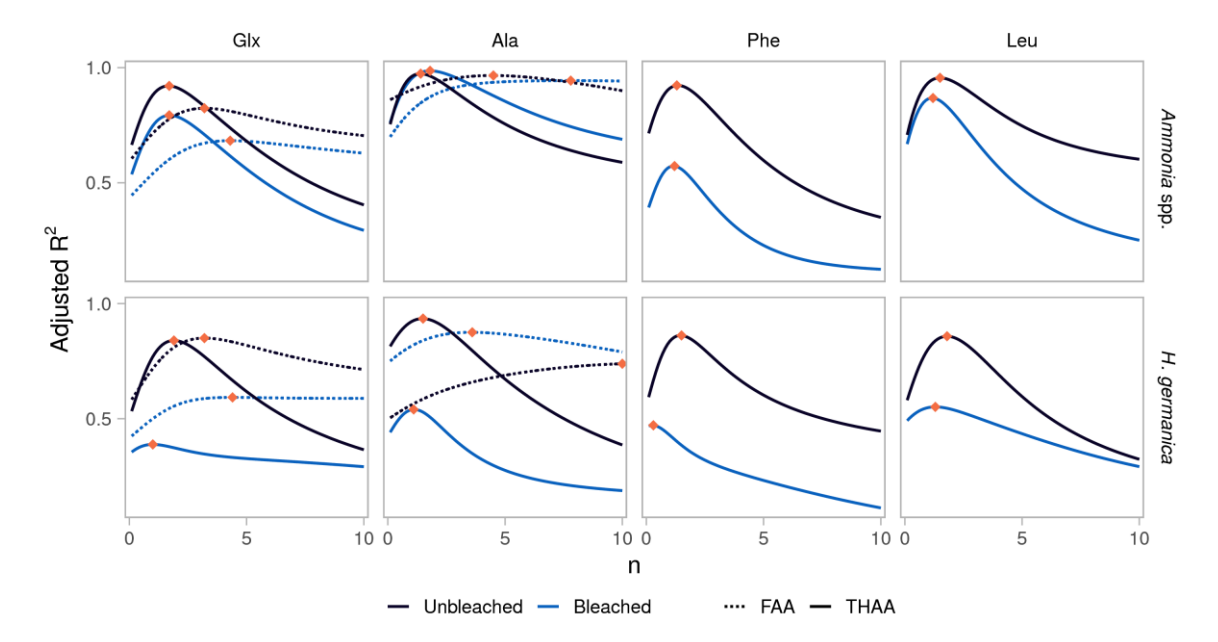


Fig. A3.10 – Optimisation of n for SPK model applied to Glx, Ala, Phe and Leu in unbleached (whole-shell) and bleached (intra-crystalline) *Ammonia* spp. and *H. germanica*, heated to 110°C. Orange diamonds show the value of n with the highest R^2 value. Optimisation was carried out using values of n between 0.1 and 10 in increments of 0.1.

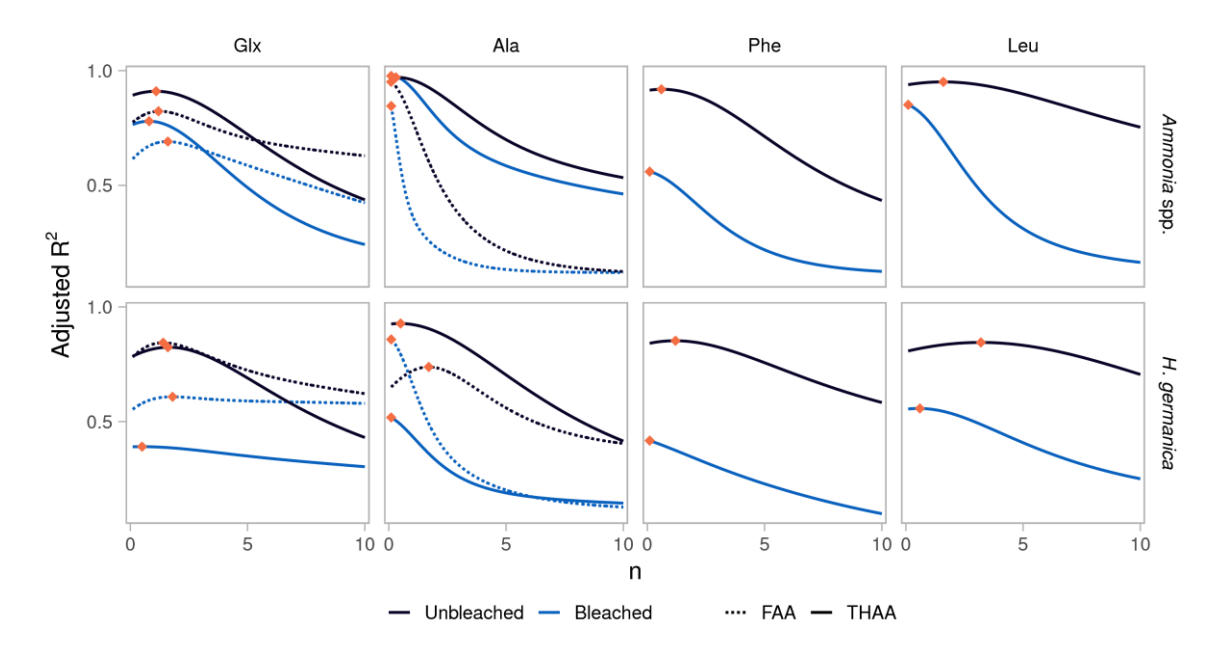


Fig. A3.11 – Optimisation of n for CPK model applied to Glx, Ala, Phe and Leu in unbleached (wholeshell) and bleached (intra-crystalline) Ammonia spp. and H. germanica, heated to 110°C. Orange diamonds show the value of n with the highest R^2 value. Optimisation was carried out using values of n between 0.1 and 10 in increments of 0.1.

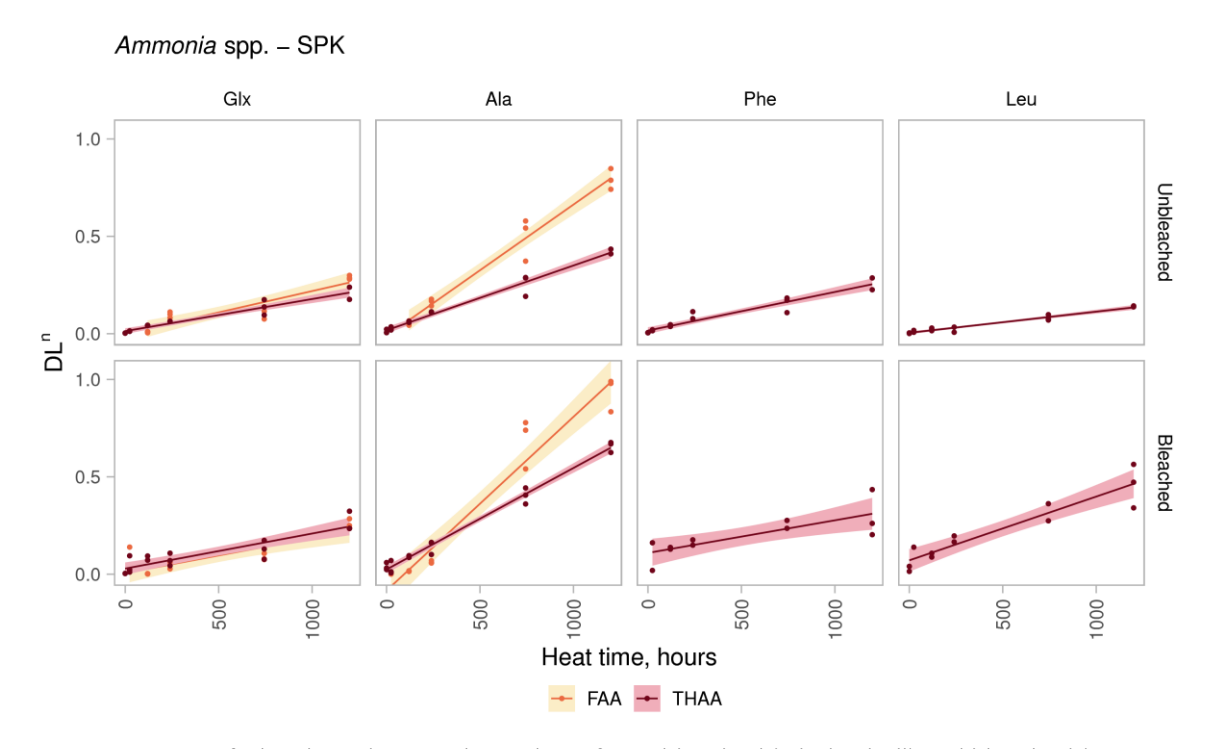


Fig. A3.12 – SPK of Glx, Ala and THAA Phe and Leu for unbleached (whole-shell) and bleached (intracrystalline) *Ammonia* spp., heated to 110°C. Line shows linear regression between time and D/Lⁿ, where the value of n is optimised to provide the highest value of R² (see Fig. A3.10). The shaded region shows \pm 1 σ around the linear regression.

H. germanica - SPK

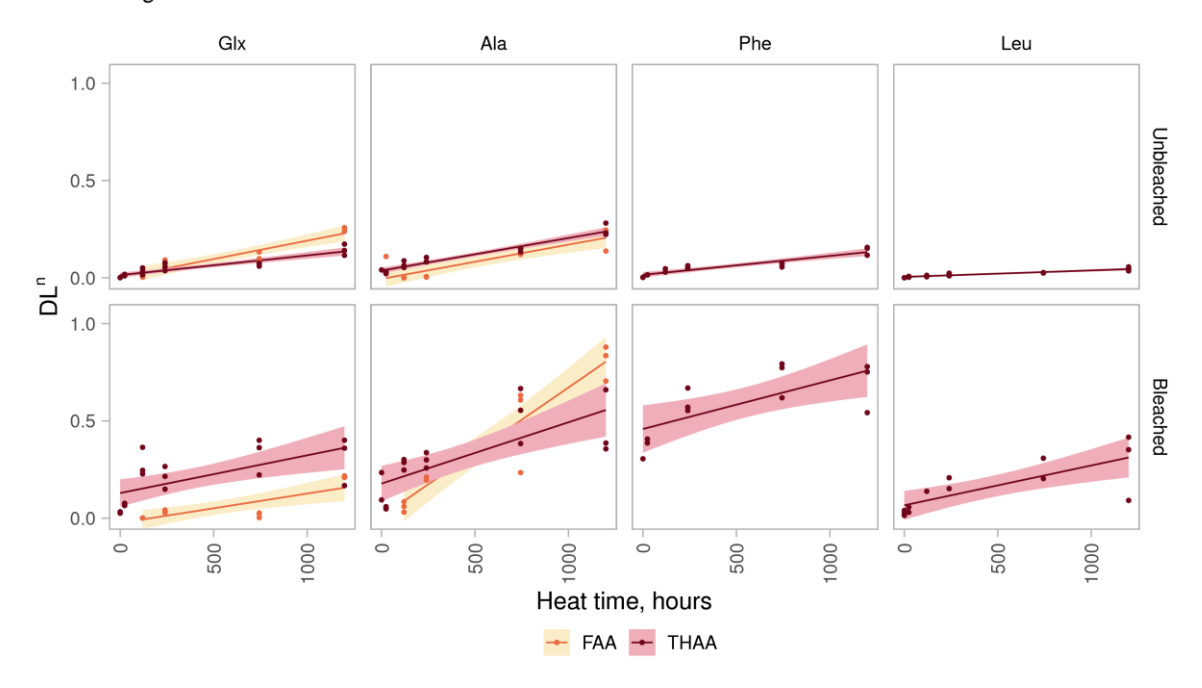


Fig. A.3.13 – SPK of Glx, Ala and THAA Phe and Leu for unbleached (whole-shell) and bleached (intracrystalline) *H. germanica*, heated to 110°C. Line shows linear regression between time and D/Lⁿ, where the value of n is optimised to provide the highest value of R² (see Fig. A3.10). The shaded region shows \pm 1 σ around the linear regression.

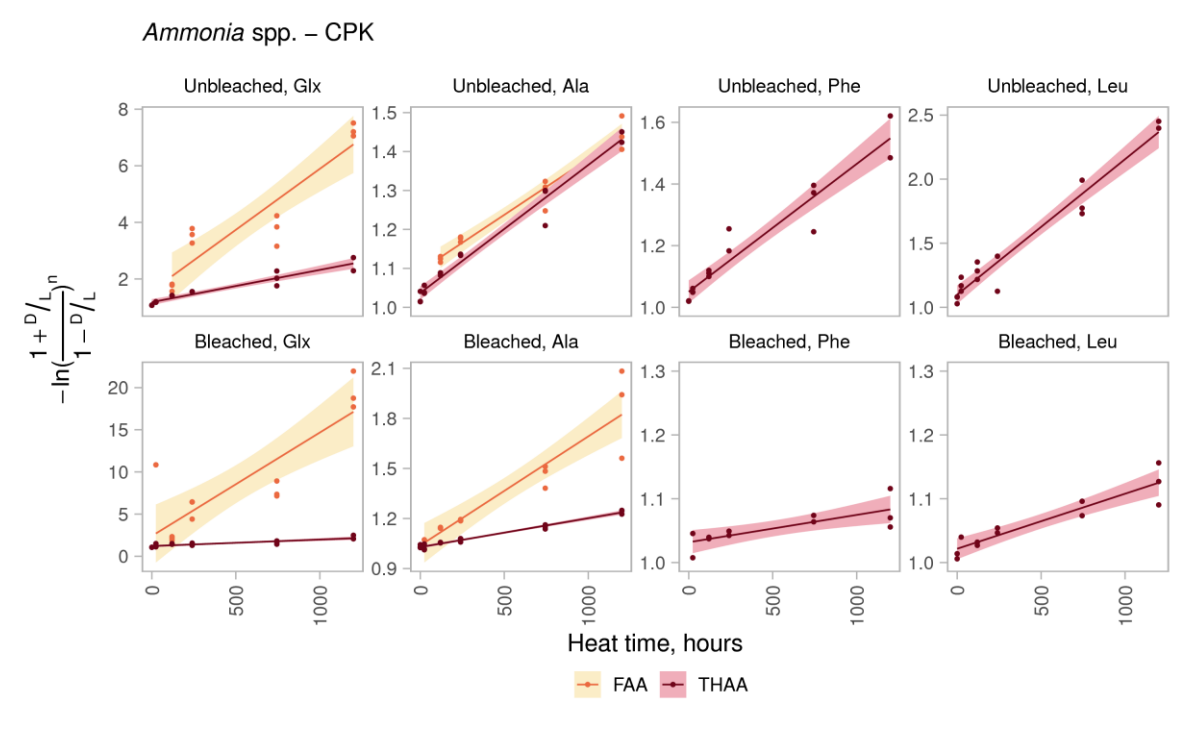


Fig. A3.14 – CPK of Glx, Ala and FAA Phe and Leu for unbleached (whole-shell) and bleached (intracrystalline) *Ammonia* spp., heated to 110°C. Line shows linear regression between time and - $\ln([1+D/L]/[1-D/L])^n$, where the value of n is optimised to provide the highest value of R^2 (see Fig. A3.11). The shaded region shows $\pm 1 \sigma$ around the linear regression. Note that each plot has its own y-axis scale, so the slope of each amino acid should not be directly compared.

H. germanica - CPK

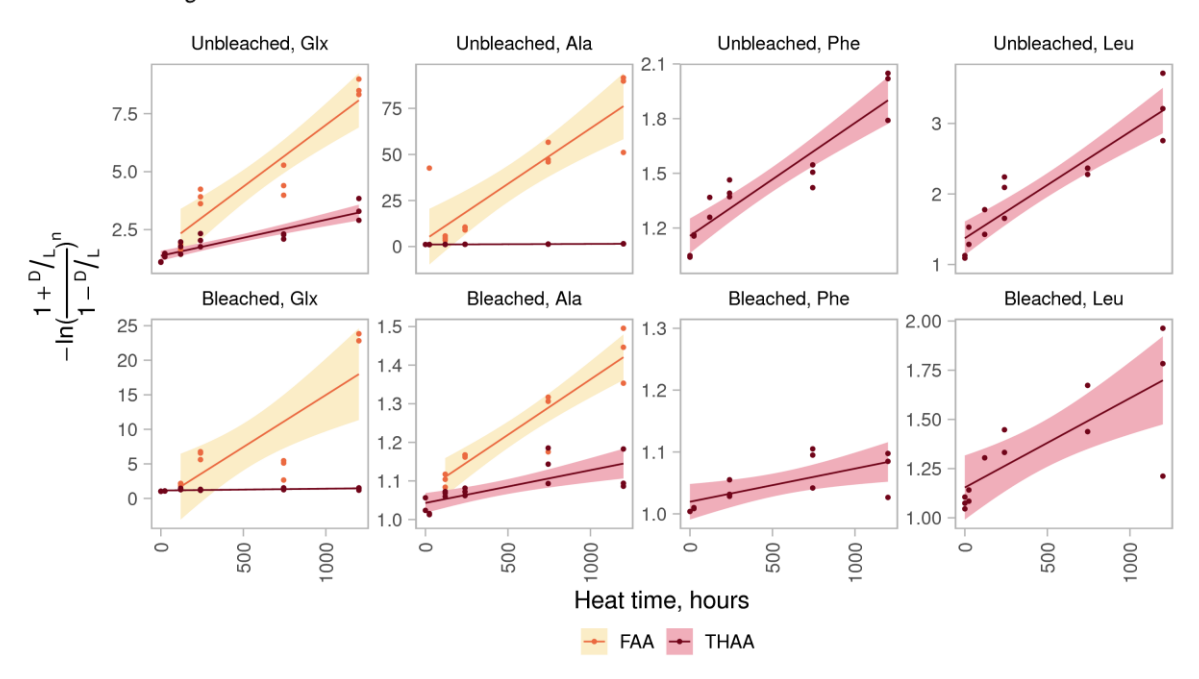


Fig. A.3.15 – CPK of Glx, Ala and FAA Phe and Leu for unbleached (whole-shell) and bleached (intracrystalline) H. germanica, heated to 110° C. Line shows linear regression between time and - $\ln([1+D/L]/[1-D/L])^n$, where the value of n is optimised to provide the highest value of R^2 (see Fig. A3.11). The shaded region shows $\pm 1 \sigma$ around the linear regression. Note that each plot has its own y-axis scale, so the slope of each amino acid should not be directly compared.

Table A.3.2 – Results of SPK linear models for Glx, Ala, Phe and Leu of unbleached (whole-shell) and bleached (intra-crystalline) *Ammonia* spp., heated to 110°C. Due to the small number of data available, FAA Phe and Leu have been excluded. k_1 is the rate of racemisation (slope / (1+K), where K = 1); c is the intercept; Adj. R^2 is the adjusted R^2 value. R^2 values R^2 value

uo	2 p		Unb	leached		Bleached				
Fraction	Fraction Amino acid	n	k ₁ (x10 ⁻⁴ h-1)	с	Adj. R ²	n	k ₁ (x10 ⁻⁴ h ⁻¹)	с	Adj. R ²	
₽¥	Glx	3.2	1.1 ± 0.15	0 ± 0.022	0.82	6.6	0.9 ± 0.17	0.006 ± 0.02	0.68	
₹.	Ala	4.5	3.37 ± 0.19	-0.01 ± 0.03	0.97	7.8	4.5 ± 0.3	-0.08 ± 0.04	0.94	
	Glx	1.7	0.82 ± 0.06	0.013 ± 0.007	0.92	1.8	0.9 ± 0.1	0.019 ± 0.013	0.80	
≨	Ala	1.4	1.66 ± 0.07	0.018 ± 0.008	0.97	1.9	2.59 ± 0.08	0.01 ± 0.01	0.98	
THAA	Phe	1.3	0.99 ± 0.07	0.016 ± 0.008	0.92	0.1	0.9 ± 0.2	0.08 ± 0.03	0.59	
	Leu	1.5	0.54 ± 0.03	0.004 ± 0.003	0.96	0.1	1.62 ± 0.19	0.05 ± 0.02	0.86	

Table A3.3 – Results of SPK linear models for Glx, Ala, Phe and Leu of unbleached (whole-shell) and bleached (intra-crystalline) H. germanica, heated to 110°C. Due to the small number of data available, FAA Phe and Leu have been excluded. k_1 is the rate of racemisation (slope / (1+K), where K = 1); c is the intercept; Adj. R^2 is the adjusted R^2 value. R^2 values R^2 values values R^2 values val

tion	rion no id		Unl	bleached	Bleached				
Fraction	Amino	n	k ₁ (x10 ⁻⁴ h ⁻¹)	С	Adj. R ²	n	k ₁ (x10 ⁻⁴ h ⁻¹)	С	Adj. R ²
4	Glx	3.2	0.94 ± 0.12	0.002 ± 0.019	0.85	3.9	0.76 ± 0.19	-0.03 ± 0.03	0.59
FAA	Ala	10	0.88 ± 0.15	-0.005 ± 0.02	0.74	3.6	3.3 ± 0.4	0.01 ± 0.05	0.88
	Glx	1.9	0.51 ± 0.05	0.014 ± 0.006	0.84	1	1.0 ± 0.3	0.13 ± 0.03	0.38
≨	Ala	1.5	0.84 ± 0.06	0.037 ± 0.007	0.94	0.1	1.6 ± 0.4	0.18 ± 0.04	0.54
THAA	Phe	1.5	0.49 ± 0.05	0.015 ± 0.007	0.86	0.3	1.3 ± 0.4	0.46 ± 0.05	0.47
	Leu	1.8	0.17 ± 0.02	0.005 ± 0.002	0.86	1.3	1.0 ± 0.3	0.07 ± 0.03	0.55

Table A.3.4 – Results of CPK linear models for Glx, Ala, Phe and Leu of unbleached (whole-shell) and bleached (intra-crystalline) *Ammonia* spp., heated to 110° C. Due to the small number of data available, FAA Phe and Leu have been excluded. k_1 is the rate of racemisation (slope / (1+K), where K = 1); c is the intercept; Adj. R^2 is the adjusted R^2 value. R^2 values ≤ 0.6 are highlighted in red.

uo	2 9		Unble	eached		Bleached			
Fraction	Fraction Amino acid	n	k ₁ (x10 ⁻⁴ h-1)	с	Adj. R ²	n	k ₁ (x10 ⁻⁴ h ⁻¹)	с	Adj. R ²
₽	Glx	1.2	22 ± 3	1.6 ± 0.4	0.82	1.6	61 ± 12	2.4 ± 1.6	0.69
¥	Ala	0.1	1.4 ± 0.1	1.094 ± 0.014	0.95	0.1	3.3 ± 0.4	1.04 ± 0.06	0.85
	Glx	1.1	5.7 ± 0.5	1.18 ± 0.05	0.91	0.9	4.7 ± 0.6	1.21 ± 0.08	0.78
≨	Ala	0.3	1.64 ± 0.07	1.037 ± 0.008	0.97	0.2	1.98 ± 0.08	1.05 ± 0.01	0.97
THAA	Phe	0.6	2.07 ± 0.16	1.051 ± 0.017	0.92	0.1	0.24 ± 0.06	1.027 ± 0.008	0.57
	Leu	1.6	5.3 ± 0.3	1.10 ± 0.03	0.95	0.1	0.45 ± 0.05	1.018 ± 0.007	0.85

Table A3.5 – Results of CPK linear models for Glx, Ala, Phe and Leu of unbleached (whole-shell) and bleached (intra-crystalline) H. germanica, heated to 110°C. Due to the small number of data available, FAA Phe and Leu have been excluded. k_1 is the rate of racemisation (slope / (1+K), where K = 1); c is the intercept; Adj. R^2 is the adjusted R^2 value. R^2 values ≤ 0.6 are highlighted in red.

6	0 p		Unble	eached		Bleached				
Fraction Amino acid	n	k ₁ (x10 ⁻⁴ h-1)	с	Adj. R ²	n	k ₁ (x10 ⁻⁴ h ⁻¹)	с	Adj. R ²		
₽	Glx	1.4	26.6 ± 3.6	1.7 ± 0.5	0.84	1.8	75 ± 19	0 ± 2	0.61	
7	Ala	1.7	300 ± 50	4 ± 7	0.74	0.1	1.44 ± 0.17	1.07 ± 0.02	0.86	
	Glx	1.6	7.8 ± 0.9	1.38 ± 0.10	0.82	0.5	1.3 ± 0.4	1.15 ± 0.04	0.39	
	Ala	0.5	1.59 ± 0.11	1.121 ± 0.014	0.93	0.1	0.4 ± 0.1	1.043 ± 0.012	0.59	
THAA	Phe	1.2	3.1 ± 0.3	1.16 ± 0.04	0.85	0.1	0.27 ± 0.09	1.02 ± 0.013	0.42	
₹	Leu	3.2	7.5 ± 0.9	1.37 ± 0.11	0.85	0.6	2.3 ± 0.6	1.15 ± 0.07	0.56	

Appendix 4 – Sampling locations at King's Dyke Quarry and West Face Quarry

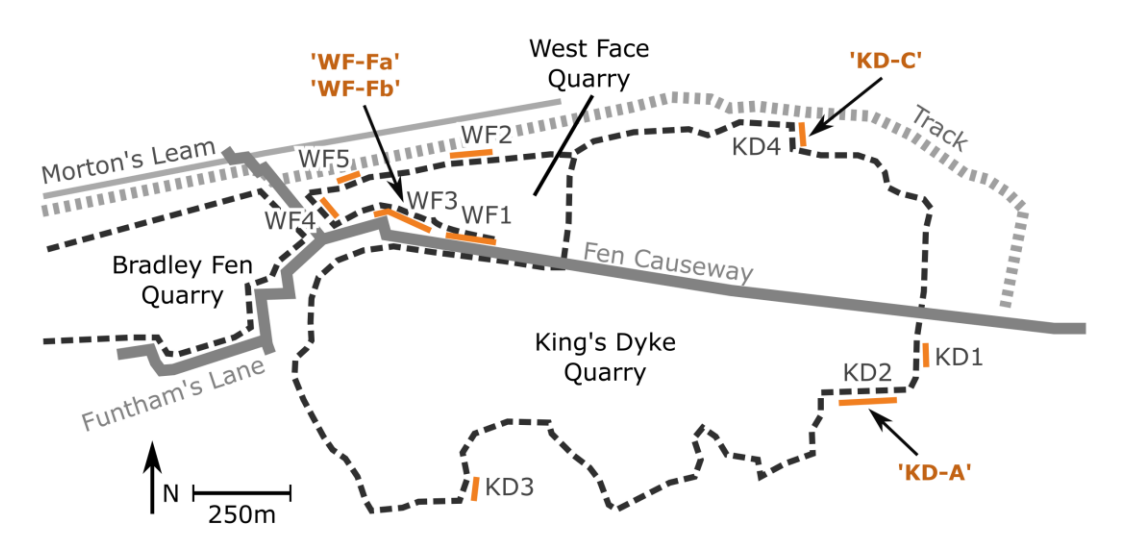


Fig. A4.1 – Map of section locations in King's Dyke Quarry and West Face Quarry, showing sampling locations of foraminifera in this study. Revised nomenclature taken from Langford (in preparation); for corresponding nomenclature from original publications, see **Table 6.6**.

Selected abbreviations

Abbreviation	Definition
AA	Amino acid
AAR	Amino acid racemisation dating (also known as amino acid geochronology)
AMS	Accelerator mass spectrometry
ВР	Before present (present defined as AD 1950 for 14 C dating)
СРК	Constrained power law kinetics
ESR	Electron spin resonance dating
FAA	Free amino acids
GC	Gas chromatography
GIA	Glacial isostatic adjustment
GMSL	Global mean sea level
HPLC, RP-HPLC	High performance liquid chromatography, reverse phase high performance liquid chromatography
IcPD	Intra-crystalline protein diagenesis or intra-crystalline protein decomposition
ICPMS	Inductively coupled plasma mass spectrometry
IEC	Ion exchange chromatography
LGM	Last Glacial Maximum (21 ka)
LIG	Last Interglacial (MIS 5e, ~128 - 116 ka)
MIS	Marine oxygen isotope stage
MS	Mass spectrometry
OSL	Optically stimulated luminescence dating
RFOK, RFOK₃	Reversible first order kinetics, apparent reversible first order kinetics
RSL	Relative sea level
SPK	Simple power law kinetics
THAA	Total hydrolysable amino acids (includes both free and bound amino acids)
TL	Thermoluminescence dating
UHPLC	Ultra high performance liquid chromatography
X	Denotes any amino acid in a peptide sequence

References

- Abelson, P.H., 1955. Organic Constituents in Fossils. Carnegie Inst. Washingt. Yearb. 54, 107–109.
- Abelson, P.H., 1954. Amino Acids in Fossils, in: National Academy of Sciences: Abstracts of Papers Presented at the Annual Meeting, 26-28 April 1954, Washington, D.C. American Association for the Advancement of Science, pp. 576–588.
- Adler, R.E., Polyak, L., Ortiz, J.D., Kaufman, D.S., Channell, J.E.T., Xuan, C., Grottoli, A.G., Sellén, E., Crawford, K.A., 2009. Sediment record from the western Arctic Ocean with an improved Late Quaternary age resolution: HOTRAX core HLY0503-8JPC, Mendeleev Ridge. Glob. Planet. Change 68, 18–29. https://doi.org/10.1016/j.gloplacha.2009.03.026
- Agassiz, L., 1840. Études sur les glaciers, Neuchâtel. ed.
- Aitken, M.J., Stokes, S., 1997. Climatostratigraphy, Chronometric Dating in Archaeology: Archaeological and Museum Science, Vol 2. Springer, Boston, MA.
- Albeck, S., Aizenberg, J., Addadi, L., Weiner, S., 1993. Interactions of Various Skeletal Intracrystalline Components with Calcite Crystals. J. Am. Chem. Soc. 115, 11691–11697. https://doi.org/10.1021/ja00078a005
- Allen, A.P., Kosnik, M.A., Kaufman, D.S., 2013. Characterizing the dynamics of amino acid racemization using time-dependent reaction kinetics: A Bayesian approach to fitting age-calibration models. Quat. Geochronol. 18, 63–77. https://doi.org/10.1016/j.quageo.2013.06.003
- Andersen, M.B., Stirling, C.H., Potter, E.K., Halliday, A.N., Blake, S.G., McCulloch, M.T., Ayling, B.F.,
 O'Leary, M.J., 2010. The timing of sea-level high-stands during Marine Isotope Stages 7.5 and
 9: Constraints from the uranium-series dating of fossil corals from Henderson Island.
 Geochim. Cosmochim. Acta 74, 3598–3620. https://doi.org/10.1016/j.gca.2010.03.020
- Andrews, J.T., Bowen, D.Q., Kidson, C., 1979. Amino acid ratios and the correlation of raised beach deposits in south-west England and Wales. Nature 281, 556–558. https://doi.org/doi.org/10.1038/281556a0
- Austermann, J., Mitrovica, J.X., Huybers, P., Rovere, A., 2017. Detection of a dynamic topography signal in last interglacial sea-level records. Sci. Adv. 3, 1–9. https://doi.org/10.1126/sciadv.1700457
- Bada, J.L., 1985. Amino-Acid Racemization Dating of Fossil Bones. Annu. Rev. Earth Planet. Sci. 13, 241–268.
- Bada, J.L., 1984. In Vivo Racemization in Mammalian Proteins. Methods Enzymol. 106, 98-115.
- Bada, J.L., 1982. Racemization of Amino Acids in Nature, in: Barrett, G.C. (Ed.), Interdisciplinary Science Reviews. Taylor & Francis, London, pp. 399–413. https://doi.org/10.1179/030801882789801304
- Bada, J.L., 1981. Racemization of amino acids in fossil bones and teeth from the Olduvai Gorge region, Tanzania, East Africa. Earth Planet. Sci. Lett. 55, 292–298. https://doi.org/10.1016/0012-821X(81)90108-4
- Bada, J.L., 1972a. The Dating of Fossil Bones using the Racemization of Isoleucine. Earth Planet. Sci.

- Bada, J.L., 1972b. Kinetics of racemization of amino acids as a function of pH. J. Am. Chem. Soc. 94, 1371–1373. https://doi.org/10.1021/ja00759a064
- Bada, J.L., 1970. Kinetics of the Nonbiological Decomposition and Racemization of Amino Acids in Natural Waters, in: Nonequilibrium Systems in Natural Water Chemistry, Advances in Chemistry. American Chemical Society, pp. 13–309. https://doi.org/doi:10.1021/ba-1971-0106.ch013
- Bada, J.L., Jolla, L., Man, E.H., 1973. Racemization of isoleucine in cores from Leg 15 Site 148. Initial Reports Deep Sea Drill. Proj. 947–951.
- Bada, J.L., Luyendyk, B.P., Maynard, J.B., 1970. Marine Sediments: Dating by the Racemisation of Amino Acids. Science (80-.). 170, 730–732. https://doi.org/10.1016/B978-0-12-384719-5.00008-3
- Bada, J.L., Man, E.H., 1980. Amino acid diagenesis in deep sea drilling project cores: Kinetics and mechanisms of some reactions and their applications in geochronology and in paleotemperature and heat flow determinations. Earth Sci. Rev. 16, 21–55. https://doi.org/10.1016/0012-8252(80)90003-3
- Bada, J.L., Miller, S.L., 1970. The Kinetics and Mechanism of the Reversible Nonenzymatic Deamination of Aspartic Acid. J. Am. Chem. Soc. 92, 2774–2782. https://doi.org/10.1021/ja00712a031
- Bada, J.L., Miller, S.L., Zhao, M., 1995. The stability of amino acids at submarine hydrothermal vent temperatures. Orig. Life Evol. Biosph. 25, 111–118. https://doi.org/10.1007/BF01581577
- Bada, J.L., Schroeder, R.A., 1975. Amino acid racemisation reactions and their geochemical implications. Naturwissenschaften 62, 71–79.
- Bada, J.L., Schroeder, R.A., 1972. Racemization of Isoleucine in Calcareous Marine Sediments: Kinetics and Mechanism. Earth Planet. Sci. Lett. 15, 1–11.
- Bada, J.L., Schroeder, R.A., Carter, G.F., 1974. New evidence for the antiquity of man in North America deduced from aspartic acid racemization. Science (80-.). 184, 791–793.
- Bada, J.L., Shou, M., 1980. Kinetics and Mechanism of Amino Acid Racemization in Aqueous Solution and in Bones, in: Hare, P.E., Hoering, T.C., King, K.J. (Eds.), Biogeochemistry of Amino Acids. John Wiley & Sons, Ltd., New York, pp. 235–255.
- Bada, J.L., Shou, M., Man, E.H., Schroeder, R.A., 1978. Decomposition of hydroxy amino acids in foraminiferal tests; kinetics, mechanism and geochronological implications. Earth Planet. Sci. Lett. 41, 67–76.
- Bada, J.L., Wang, X.S., Hamilton, H., 1999. Preservation of key biomolecules in the fossil record: current knowledge and future challenges. Philos. Trans. R. Soc. B Biol. Sci. 354, 77–87. https://doi.org/10.1098/rstb.1999.0361
- Barbieri, R., 2001. Taphonomic implications of foraminiferal composition and abundance in intertidal mud flats, Colorado River Delta (Mexico). Micropaleontology 47, 73–86. https://doi.org/10.2113/47.1.73

- Barbieri, R., 1996. Syndepositional taphonomic bias in foraminifera from fossil intertidal deposits, Colorado Delta (Baja California, Mexico). J. Foraminifer. Res. 26, 331–341. https://doi.org/10.2113/gsjfr.26.4.331
- Barlow, N.L.M., Long, A.J., Gehrels, W.R., Saher, M.H., Scaife, R., Davies, H.J., Penkman, K.E.H., Bridgland, D.R., Sparkes, A., Smart, C.W., Taylor, S., 2017. Relative sea-level variability during the late Middle Pleistocene: New evidence from eastern England. Quat. Sci. Rev. 173, 20–39. https://doi.org/10.1016/j.quascirev.2017.08.017
- Barlow, N.L.M., Shennan, I., Long, A.J., Gehrels, W.R., Saher, M.H., Woodroffe, S.A., Hillier, C., 2013. Salt marshes as late holocene tide gauges. Glob. Planet. Change 106, 90–110. https://doi.org/10.1016/j.gloplacha.2013.03.003
- Bateman, M.D., Briant, R.M., Langford, H.E., Wheeler, L.J., Whittaker, J.E., 2020. Quaternary Newsletter 151 (October 2020).
- Bates, M.R., Bates, R.C., Briant, R.M., 2007. Bridging the gap: a terrestrial view of shallow marine sequences and the importance of the transition zone. J. Archaeol. Sci. 34, 1537–1551. https://doi.org/10.1016/j.jas.2007.02.027
- Bates, M.R., Bates, R.C., Gibbard, P.L., Keen, D.H., Parfitt, S.A., Peglar, S.M., Schwenninger, J.-L., Wenban-Smith, F.F., Whittaker, J.E., 2009. Selsey West Street: Evaluation of Historical Material and Recent Field Investigations. Quat. Solent Basin West Sussex Rais. Beaches A F. Guid. 73–95.
- Bates, M.R., Bates, R.C., Gibbard, P.L., Macphail, R.I., Owen, F.J., Parfitt, S.A., Preece, R.C., Roberts, M.B., Robinson, J.E., Whittaker, J.E., Wilkinson, K.N., 2000. Late Middle Pleistocene deposits at Norton Farm on the West Sussex coastal plain, southern England. J. Quat. Sci. 15, 61–89. https://doi.org/10.1002/(SICI)1099-1417(200001)15:1<61::AID-JQS463>3.0.CO;2-K
- Bates, M.R., Briant, R.M., Rhodes, E.J., Schwenninger, J.-L., Whittaker, J.E., 2010. A new chronological framework for Middle and Upper Pleistocene landscape evolution in the Sussex/Hampshire Coastal Corridor, UK. Proc. Geol. Assoc. 121, 369–392. https://doi.org/10.1016/j.pgeola.2010.02.004
- Bates, M.R., Keen, D.H., Lautridou, J.P., 2003. Pleistocene marine and periglacial deposits of the English Channel. J. Quat. Sci. 18, 319–337. https://doi.org/10.1002/jqs.747
- Bates, Martin R., Briant, Rebecca M., 2009. Quaternary sediments of the Sussex/Hampsire Coastal Corridor: a brief overview, in: Briant, R. M., Bates, M.R., Hosfield, R.., Wenban-Smith, F.F. (Eds.), The Quaternary of the Solent Basin and West Sussex Raised Beaches: A Field Guide. pp. 21–41.
- Bauch, H.A., Erlenkeuser, H., Jung, J.A., Thiede, J., 2000. Surface and deep water changes in the subpolar North Atlantic during Termination II and the last interglaciation. Paleoceanography 15, 76–84.
- Bé, A.W.H., Hemleben, C.H., Anderson, O.R., Spindler, M., Be, A.W.H., 1979. Chamber Formation in Planktonic Foraminifera. Micropaleontology 25, 294. https://doi.org/10.2307/1485304
- Becker, L.W.M., Sejrup, H.P., Hjelstuen, B.O., Haflidason, H., Dokken, T.M., 2018. Ocean-ice sheet interaction along the SE Nordic Seas margin from 35 to 15 ka BP. Mar. Geol. 402, 99–117. https://doi.org/10.1016/j.margeo.2017.09.003

- Ben-Yaakov, S., Ruth, E., Kaplan, I.R., 1974. Carbonate Compensation Depth: Relation to Carbonate Solubility in Ocean Waters. Nature 184, 982–984.
- Berger, A., 1988. Milankovitch Theory and Climate. Rev. Geophys. 26, 624–657. https://doi.org/10.1029/RG026i004p00624
- Berkeley, A., Perry, C.T., Smithers, S.G., 2009. Taphonomic signatures and patterns of test degradation on tropical, intertidal benthic foraminifera. Mar. Micropaleontol. 73, 148–163. https://doi.org/10.1016/j.marmicro.2009.08.002
- Berkeley, A., Perry, C.T., Smithers, S.G., Horton, B.P., Taylor, K.G., 2007. A review of the ecological and taphonomic controls on foraminiferal assemblage development in intertidal environments. Earth-Science Rev. 83, 205–230. https://doi.org/10.1016/j.earscirev.2007.04.003
- Berman, A., Addadi, L., Kvick, Å., Leiserowitz, L., Nelson, M., Weiner, S., 1990. Intercalation of sea urchin proteins in calcite: Study of a crystalline composite material. Science (80-.). 250, 664–667. https://doi.org/10.1126/science.250.4981.664
- Berman, A., Addadi, L., Weiner, S., 1988. Interactions of Sea-Urchin Skeleton Macromolecules With Growing Calcite Crystals a Study of Intracrystalline Proteins. Nature 331, 546–548. https://doi.org/10.1038/331546a0
- Berstad, I.M., 2003. Quaternary climate variability in the eastern Nordic Sea region inferred from speleothems and deep-sea cores. University of Bergen, Norway.
- Bhattacharyya, S.K., Banerjee, A.B., 1974. D-amino acids in the cell pool of bacteria. Folia Microbiol. (Praha). 19, 43–50. https://doi.org/10.1007/BF02874501
- Billups, K., Chaisson, W.P., Worsnopp, M., Thunell, R., 2004. Millennial-scale fluctuations in subtropical northwestern Atlantic surface ocean hydrography during the mid-Pleistocene. Paleoceanography 19, n/a-n/a. https://doi.org/10.1029/2003PA000990
- Blaauw, M., Christeny, J.A., 2011. Flexible paleoclimate age-depth models using an autoregressive gamma process. Bayesian Anal. 6, 457–474. https://doi.org/10.1214/11-BA618
- Blakemore, A.G., 2014. Middle Pleistocene to Holocene sea-level changes and coastal evolution on the Mount Gambier coastal plain, southern Australia. University of Wollongong.
- Blakemore, A.G., Murray-Wallace, C. V., Westaway, K.E., Lachlan, T.J., 2015. Aminostratigraphy and sea-level history of the Pleistocene Bridgewater Formation, Mount Gambier region, southern Australia. Aust. J. Earth Sci. 62, 151–169. https://doi.org/10.1080/08120099.2015.1014523
- Bleil, U., Gard, G., 1989. Chronology and correlation of Quaternary magnetostratigraphy and nannofossil biostratigraphy in Norwegian-Greenland Sea sediments. Geol. Rundschau 78, 1173–1187. https://doi.org/10.1007/BF01829339
- Boudagher-Fadel, M., 2015a. An introduction to planktonic foraminifera, in: Biostratigraphic and Geological Significance of Planktonic Foraminifera. UCL Press, pp. 1–28.
- Boudagher-Fadel, M., 2015b. The biological and molecular characteristics of living planktonic foraminifera, in: Biostratigraphic and Geological Significance of Planktonic Foraminifera. UCL Press, pp. 29–38.

- Bowen, D.Q., Sykes, G.A., 1994. How old is 'Boxgrove man'? Nature 371, 751–751. https://doi.org/10.1038/371751a0
- Braconnot, P., Harrison, S.P., Kageyama, M., Bartlein, P.J., Masson-Delmotte, V., Abe-Ouchi, A., Otto-Bliesner, B.L., Zhao, Y., 2012. Evaluation of climate models using palaeoclimatic data. Nat. Clim. Chang. 2, 417–424. https://doi.org/10.1038/nclimate1456
- Bradley, R., 1999. Paleoclimatology: Reconstructing Climates of the Quaternary. Elsavier.
- Brasier, M.D., Armstrong, H., 1980. Microfossils. G. Allen & Unwin, London.
- Bravenec, A.D., Ward, K.D., Ward, T.J., 2018. Amino acid racemization and its relation to geochronology and archaeometry. J. Sep. Sci. 41, 1489–1506.
- Brendryen, J., 2011. A detailed chronological, sedimentological and tephrostratigraphical framework of a high resolution sediment core record from the Eastern Norwegian Sea spanning the two last glacial-interglacial cycles. University of Bergen.
- Brendryen, J., Haflidason, H., Sejrup, H.P., 2010. Norwegian Sea tephrostratigraphy of marine isotope stages 4 and 5: Prospects and problems for tephrochronology in the North Atlantic region. Quat. Sci. Rev. 29, 847–864. https://doi.org/10.1016/j.quascirev.2009.12.004
- Briant, R.M., Coope, G.R., Preece, R.C., Keen, D.H., Boreham, S., Griffiths, H.I., Seddon, M.B., Gibbard, P.L., 2004. Fluvial system response to Late Devensian (Weichselian) aridity, Baston, Lincolnshire, England. J. Quat. Sci. 19, 479–495. https://doi.org/10.1002/jqs.851
- Briant, R.M., Kilfeather, A.A., Parfitt, S.A., Penkman, K.E.H., Preece, R.C., Roe, H.M., Schwenninger, J.-L., Wenban-Smith, F.F., Whittaker, J.E., 2012. Integrated chronological control on an archaeologically significant Pleistocene river terrace sequence: The Thames-Medway, eastern Essex, England. Proc. Geol. Assoc. 123, 87–108. https://doi.org/10.1016/j.pgeola.2011.07.008
- Bright, J., Kaufman, D.S., 2011a. Amino acid racemization in lacustrine ostracodes, part I: Effect of oxidizing pre-treatments on amino acid composition. Quat. Geochronol. 6, 154–173. https://doi.org/10.1016/j.quageo.2010.11.006
- Bright, J., Kaufman, D.S., 2011b. Amino acids in lacustrine ostracodes, part III: Effects of pH and taxonomy on racemization and leaching. Quat. Geochronol. 6, 574–597. https://doi.org/10.1016/j.quageo.2011.08.002
- Bright, J., Kaufman, D.S., Forman, S.L., McIntosh, W.C., Mead, J.I., Baez, A., 2010. Comparative dating of a Bison-bearing late-Pleistocene deposit, Térapa, Sonora, Mexico. Quat. Geochronol. 5, 631–643. https://doi.org/10.1016/j.quageo.2010.05.002
- Brinton, K.L.F., Bada, J.L., 1995. Comment on "Aspartic acid racemization and protein diagenesis in corals over the last 350 years" by G. A. Goodfriend, P. E. Hare, and E. R. M. Druffel. Geochim. Cosmochim. Acta 59, 415–416. https://doi.org/10.1016/0016-7037(94)00324-F
- Brooks, A.S., Hare, P.E., Kokis, J.E., Miller, G.H., Ernst, R.D., Wendorf, F., 1990. Dating Pleistocene Archeological Sites by Protein Diagenesis in Ostrich Eggshell. Science (80-.). 248, 60–64.
- Brückner, H., Haasmann, S., Langer, M.R., Westhauser, T., Wittner, R., Godel, H., 1994. Liquid chromatographic determination of D- and L-amino acids by derivatization with ophthaldialdehyde and chiral thiols. J. Chromatogr. A 666, 259–273. https://doi.org/10.1016/0021-9673(94)80388-9

- Bryn, P., Berg, K., Forsberg, C.F., Solheim, A., Kvalstad, T.J., 2005. Explaining the Storegga Slide. Mar. Pet. Geol. 22, 11–19. https://doi.org/10.1016/j.marpetgeo.2004.12.003
- Buckley, M., Walker, A., Ho, S.Y.W., Yang, Y., Smith, C., Ashton, P., Thomas-Oates, J., Cappellini, E., Koon, H., Penkman, K.E.H., Elsworth, B., Ashford, D., Solazzo, C., Andrews, P., Strahler, J., Shapiro, B., Gandhi, H., Miller, W., Raney, B., Zylber, M.I., Thomas, M.P., Prigodich, R. V., Ryan, M., Rijsdijk, K.F., Janoo, A., Collins, M.J., 2008. Weighing the mass spectrometric evidence for authentic Tyrannosaurus rex collagen. Science (80-.). 319, 1–6. https://doi.org/10.1126/science.1147046.Weighing
- Buckley, M., Warwood, S., van Dongen, B., Kitchener, A.C., Manning, P.L., 2017. A fossil protein chimera; difficulties in discriminating dinosaur peptide sequences from modern cross-contamination. Proc. R. Soc. B Biol. Sci. 284. https://doi.org/10.1098/rspb.2017.0544
- Bush, S.L., Santos, G.M., Xu, X., Southon, J.R., Thiagarajan, N., Hines, S.K., Adkins, J.F., 2013. Simple, Rapid, and Cost Effective: A Screening Method for 14 C Analysis of Small Carbonate Samples. Radiocarbon 55, 631–640. https://doi.org/10.1017/S0033822200057787
- Butler, P.G., Wanamaker, A.D., Scourse, J.D., Richardson, C.A., Reynolds, D.J., 2013. Variability of marine climate on the North Icelandic Shelf in a 1357-year proxy archive based on growth increments in the bivalve Arctica islandica. Palaeogeogr. Palaeoclimatol. Palaeoecol. 373, 141–151. https://doi.org/10.1016/j.palaeo.2012.01.016
- Candy, I., Schreve, D.C., Sherriff, J., Tye, G.J., 2014. Marine Isotope Stage 11: Palaeoclimates, palaeoenvironments and its role as an analogue for the current interglacial. Earth-Science Rev. 128, 18–51. https://doi.org/10.1016/j.earscirev.2013.09.006
- Cann, J.H., Belperio, A.P., Gostin, V.A., Murray-Wallace, C. V., 1988. Sea-Level History, 45,000 to 30,000 yr B.P., Inferred from Benthic Foraminifera, Gulf St. Vincent, South Australia. Quat. Res. 29, 153–175.
- Cann, J.H., Murray-Wallace, C. V., 1986. Holocene distribution and amino acid racemisation of the benthic foraminifer Massilina Milletti, northern Spencer Gulf, South Australia. Alcheringa 10, 45–54. https://doi.org/10.1080/03115518608619041
- Child, A.M., Gillard, R.D., Pollard, A.M., 1993. Microbially-Induced Promotion of Amino Acid Racemization in Bone: Isolation of the Microorganisms and the Detection of Their Enzymes. J. Archaeol. Sci. 20, 159–168. https://doi.org/10.1006/jasc.1993.1011
- Cho, K.R., Kim, Y.-Y., Yang, P., Cai, W., Pan, H., Kulak, A.N., Lau, J.L., Kulshreshtha, P., Armes, S.P., Meldrum, F.C., De Yoreo, J.J., 2016. Direct observation of mineral-organic composite formation reveals occlusion mechanism. Nat. Commun. 7, 1–7. https://doi.org/10.1038/ncomms10187
- Chutcharavan, P.M., Dutton, A., 2021. A Global Compilation of U-series Dated Fossil Coral Sea-level Indicators for the Last Interglacial Period (MIS 5e). Earth Syst. Sci. Data 1–41. https://doi.org/10.5194/essd-2020-381
- Clark, P.U., Mix, A.C., 2002. Ice sheets and sea level of the Last Glacial Maximum. Quat. Sci. Rev. 21, 1–7. https://doi.org/10.1016/S0277-3791(01)00118-4
- Clarke, S.J., Murray-Wallace, C. V., 2006. Mathematical expressions used in amino acid racemisation geochronology-A review. Quat. Geochronol. 1, 261–278.

- Cohen, K.M., Finney, S.C., Gibbard, P.L., Fan, J.-X., 2013. The ICS International Chronostratigraphic Chart. Episodes 36, 199–204. https://doi.org/10.18814/epiiugs/2013/v36i3/002
- Collins, M.J., Riley, M.S., 2000. Amino acid racemization in biominerals: the impact of protein degradation and loss, in: Goodfriend, G. a, Collins, M.J., Fogel, M.A., Macko, S.A., Wehmiller, J.F. (Eds.), Perspectives in Amino Acid and Protein Geochemistry. Oxford University Press, New York.
- Collins, M.J., Waite, E.R., van Duin, A.C.T., 1999. Predicting protein decomposition: the case of aspartic-acid racemization kinetics. Philos. Trans. R. Soc. B, Biol. Sci. 354, 51–64. https://doi.org/10.1098/rstb.1999.0359
- Conrad, U., Fahr, A., Scriba, G.K.E., 2010. Kinetics of Aspartic Acid Isomerization and Enantiomerization in Model Aspartyl Tripeptides under Forced Conditions. J. Pharm. Sci. 99, 4162–4173. https://doi.org/10.1002/jps
- Creveling, J.R., Mitrovica, J.X., Clark, P.U., Waelbroeck, C., Pico, T., 2017. Predicted bounds on peak global mean sea level during marine isotope stages 5a and 5c. Quat. Sci. Rev. 163, 193–208. https://doi.org/10.1016/j.quascirev.2017.03.003
- Crisp, M.K., 2013. Amino acid racemization dating: Method development using African ostrich (Struthio camelus) eggshell. University of York.
- Crisp, M.K., Demarchi, B., Collins, M.J., Morgan-Williams, M., Pilgrim, E., Penkman, K.E.H., 2013. Isolation of the intra-crystalline proteins and kinetic studies in Struthio camelus (ostrich) eggshell for amino acid geochronology. Quat. Geochronol. 16, 110–128. https://doi.org/10.1016/j.quageo.2012.09.002
- Dahlgren, K.I.T., Vorren, T.O., 2003. Sedimentary environment and glacial history during the last 40 ka of the Vøring continental margin, mid-Norway. Mar. Geol. 193, 93–127. https://doi.org/10.1016/S0025-3227(02)00617-5
- De Nooijer, L.J., Spero, H.J., Erez, J., Bijma, J., Reichart, G.J., 2014. Biomineralization in perforate foraminifera. Earth-Science Rev. 135, 48–58. https://doi.org/10.1016/j.earscirev.2014.03.013
- Debenay, J.-P., Guillou, J.-J., Geslin, E., Lesourd, M., 2000. Crystallization of Calcite in Foraminiferal Tests. Micropaleontology 46, 87–94.
- Demarchi, B., 2009. Geochronology of coastal prehistoric environments: a new closed system approach using amino acid racemisation. University of York.
- Demarchi, B., Clements, E., Coltorti, M., van de Locht, R., Kröger, R., Penkman, K.E.H., Rose, J., 2015. Testing the effect of bleaching on the bivalve Glycymeris: A case study of amino acid geochronology on key Mediterranean raised beach deposits. Quat. Geochronol. 25, 49–65. https://doi.org/10.1016/j.quageo.2014.09.003
- Demarchi, B., Collins, M.J., 2014. Amino Acid Racemization Dating, in: Encyclopedia of Scientific Dating Methods. Springer Netherlands, Dordrecht, pp. 1–22. https://doi.org/10.1007/978-94-007-6326-5_73-1
- Demarchi, B., Collins, M.J., Bergström, E., Dowle, A., Penkman, K.E.H., Thomas-Oates, J., Wilson, J., 2013a. New Experimental Evidence for In-Chain Amino Acid Racemization of Serine in a

- Model Peptide. Anal. Chem. 85, 5835-5842. https://doi.org/10.1021/ac4005869
- Demarchi, B., Collins, M.J., Tomiak, P.J., Davies, B.J., Penkman, K.E.H., 2013b. Intra-crystalline protein diagenesis (IcPD) in Patella vulgata. Part II: Breakdown and temperature sensitivity. Quat. Geochronol. 16, 158–172. https://doi.org/10.1016/J.QUAGEO.2012.08.001
- Demarchi, B., Hall, S., Roncal-Herrero, T., Freeman, C.L., Woolley, J., Crisp, M.K., Wilson, J., Fotakis, A., Fischer, R., Kessler, B.M., Rakownikow Jersie-Christensen, R., Olsen, J. V., Haile, J., Thomas, J., Marean, C.W., Parkington, J., Presslee, S., Lee-Thorp, J., Ditchfield, P., Hamilton, J.F., Ward, M.W., Wang, C.M., Shaw, M.D., Harrison, T., Domínguez-Rodrigo, M., MacPhee, R.D.E., Kwekason, A., Ecker, M., Kolska Horwitz, L., Chazan, M., Kröger, R., Thomas-Oates, J., Harding, J.H., Cappellini, E., Penkman, K.E.H., Collins, M.J., 2016. Protein sequences bound to mineral surfaces persist into deep time. Elife 5. https://doi.org/10.7554/eLife.17092
- Demarchi, B., Rogers, K., Fa, D.A., Finlayson, C.J., Milner, N., Penkman, K.E.H., 2013c. Intracrystalline protein diagenesis (IcPD) in Patella vulgata. Part I: Isolation and testing of the closed system. Quat. Geochronol. 16, 144–157. https://doi.org/10.1016/j.quageo.2012.08.001
- Demarchi, B., Williams, M.G., Milner, N., Russell, N., Bailey, G., Penkman, K.E.H., 2011. Amino acid racemization dating of marine shells: A mound of possibilities. Quat. Int. 239, 114–124. https://doi.org/10.1016/j.quaint.2010.05.029
- Dickinson, M.R., 2018. Enamel Amino Acid Racemisation Dating and its Application to Building Proboscidean Geochronologies. University of York.
- Dickinson, M.R., Lister, A.M., Penkman, K.E.H., 2019. A new method for enamel amino acid racemization dating: A closed system approach. Quat. Geochronol. 50, 29–46. https://doi.org/10.1016/j.quageo.2018.11.005
- Dowling, L.A., Sejrup, H.P., Coxon, P., Heijnis, H., 1998. Palynology, aminostratigraphy and U-series dating of marine Gortian interglacial sediments in Cork Harbour, Southern Ireland. Quat. Sci. Rev. 17, 945–962. https://doi.org/10.1016/S0277-3791(98)00027-4
- Dowsett, A., 2017. Reconstructing palaeoenvironments in archaeology: the foraminifera and ostracods of the Burtle Beds, during MIS 5e. University College London.
- Duller, G.A.T., 2008. Luminescence Dating: guidelines on using luminescence dating in archaeology. Swindon.
- Dungworth, G., 1976. Optical configuration and the racemisation of amino acids in sediments and in fossils A review. Chem. Geol. 17, 135–153. https://doi.org/10.1016/0009-2541(76)90027-9
- Dungworth, G., Schwartz, A.W., van de Leemput, L., 1976. Composition and racemization of amino acids in mammoth collagen determined by gas and liquid chromatography. Comp. Biochem. Physiol. -- Part B Biochem. 53, 473–480. https://doi.org/10.1016/0305-0491(76)90202-9
- Dutton, A., Bard, E., Antonioli, F., Esat, T.M., Lambeck, K., McCulloch, M.T., 2009. Phasing and amplitude of sea-level and climate change during the penultimate interglacial. Nat. Geosci. 2, 355–359. https://doi.org/10.1038/ngeo470
- Dutton, A., Carlson, A.E., Long, A.J., Milne, G.A., Clark, P.U., DeConto, R.M., Horton, B.P., Rahmstorf, S., Raymo, M.E., 2015. Sea-level rise due to polar ice-sheet mass loss during past warm

- periods. Science (80-.). 349, 153-164. https://doi.org/10.1126/science.aaa4019
- Dwyer, G.S., Cronin, T.M., Baker, P.A., Rodriguez-Lazaro, J., 2000. Changes in North Atlantic deep-sea temperature during climatic fluctuations of the last 25,000 years based on ostracode Mg/Ca ratios. Geochemistry, Geophys. Geosystems 1. https://doi.org/10.1029/2000GC000046
- Edgar, K.M., Palike, H., Wilson, P.A., 2013. Testing the impact of diagenesis on the d18O and d13C of benthic foraminiferal calcite from a sediment burial depth transect in the equatorial Pacific. Palaeoceanography 28, 468–480.
- Farrell, W.E., Clark, J.A., 1976. On Postglacial Sea Level. Geophys. J. R. Astron. Soc. 46, 647–667. https://doi.org/10.1111/j.1365-246X.1976.tb01252.x
- Figueira, B., Hayward, B.W., 2014. Impact of reworked foraminifera from an eroding salt marsh on sea-level studies, New Zealand. New Zeal. J. Geol. Geophys. 57, 378–389. https://doi.org/10.1080/00288306.2014.924971
- Fox-Kemper, B., Hewitt, H.T., Xiao, C., Aðalgeirsdóttir, G., Drijfhout, S.S., Edwards, T.L., Golledge, N.R., Hemer, M., Kopp, R.E., Krinner, G., Mix, A., Notz, D., Nowicki, S., Nurhati, I.S., Ruiz, L., Sallée, J.-B., Slangen, A.B.A., Yu, Y., 2021. Ocean, Cryosphere and Sea Level Change, in: Masson-Delmotte, V., Zhai, P., Pirani, A., Connors, S.L., Péan, C., Berger, S., Caud, N., Chen, Y., Goldfarb, L., Gomis, M.I., Huang, M., Leitzell, K., Lonnoy, E., Matthews, J.B.R., Maycock, T.K., Waterfield, T., Yelekçi, O., Yu, R., Zhou, B. (Eds.), Climate Change 2021: The Physical 12 Science Basis. Contribution of Working Group I to the Sixth Assessment Report of the Intergovernmental 13 Panel on Climate Change. Cambridge University Press.
- Frank, N., Turpin, L., Cabioch, G., Blamart, D., Tressens-Fedou, M., Colin, C., Jean-Baptiste, P., 2006. Open system U-series ages of corals from a subsiding reef in New Caledonia: Implications for sea level changes, and subsidence rate. Earth Planet. Sci. Lett. 249, 274–289. https://doi.org/10.1016/j.epsl.2006.07.029
- Fuchs, M., Owen, L.A., 2008. Luminescence dating of glacial and associated sediments: review, recommendations and future directions. Boreas 37, 636–659. https://doi.org/10.1111/j.1502-3885.2008.00052.x
- Gaines, S.M., Jeffrey, L.B., 1988. Aspartame Decomposition and Epimerization in the Diketopiperazine and Dipeptide Products as a Function of pH and Temperature. J. Org. Chem. 53, 2757–2764. https://doi.org/10.1021/jo00247a018
- Gallup, C.D., Edwards, R.L., Johnson, R.G., 1994. The timing of high sea levels over the past 200,000 years. Science (80-.). 263, 796–800. https://doi.org/10.1126/science.263.5148.796
- Gehrels, W.R., 1994. Determining Relative Sea-Level Change from Salt-Marsh Foraminifera and Plant Zones on the Coast of Maine, U.S.A. J. Coast. Res. 10, 990–1009.
- Geiger, T., Clarke, S.J., 1987. Deamidation, isomerization, and racemization at asparaginyl and aspartyl residues in peptides. Succinimide-linked reactions that contribute to protein degradation. J. Biol. Chem. 262, 785–794. https://doi.org/papers3://publication/uuid/6A809B4D-DF92-42E8-A3F0-3B5AD39836F6
- Geophysics Study Committee, National Research Council, 1991. Sea-Level Change. National Academies Press.

- Gibbard, P.L., Head, M.J., Walker, M.J.C., The Subcomission on Quaternary Stratigraphy, 2010. Formal ratification of the Quaternary System/Period and the Pleistocene Series/Epoch with a base at 2.58 Ma. J. Quat. Sci. 25, 96–102. https://doi.org/10.1002/jqs
- Gibbard, P.L., Hughes, P.D., 2020. Terrestrial stratigraphical division in the quaternary and its correlation. J. Geol. Soc. London. 178. https://doi.org/10.1144/jgs2020-134
- Gibbard, P.L., West, R.G., Andrew, R., Pettit, M.E., 1992. The margin of a Middle Pleistocene ice advance at Tottenhill, Norfolk, England. Geol. Mag. 129, 59–76. https://doi.org/10.1017/S0016756800008128
- Gilford, D.M., Ashe, E.L., DeConto, R.M., Kopp, R.E., Pollard, D., Rovere, A., 2020. Could the Last Interglacial Constrain Projections of Future Antarctic Ice Mass Loss and Sea-Level Rise? J. Geophys. Res. Earth Surf. 125. https://doi.org/10.1029/2019JF005418
- Gillard, R.D., Phipps, D.A., 1970. The selective activation of amino-acids and peptides. J. Chem. Soc. D Chem. Commun. 800–801. https://doi.org/10.1039/C29700000800
- Godwin, H., 1962. Half-life of radiocarbon. Nature 195, 984. https://doi.org/10.1038/195984a0
- Goelzer, H., Huybrechts, P., Marie-France, L., Fichefet, T., 2016. Last Interglacial climate and sealevel evolution from a coupled ice sheet-climate model. Clim. Past 12, 2195–2213. https://doi.org/10.5194/cp-12-2195-2016
- Gold, V. (Ed.), 2019. The IUPAC Compendium of Chemical Terminology, 2nd ed. (t. ed. International Union of Pure and Applied Chemistry (IUPAC), Research Triangle Park, NC. https://doi.org/10.1351/goldbook
- Goodfriend, G.A., 1989. Complementary Use of Amino-Acid Epimerization and Radiocarbon Analysis for Dating of Mixed-Age Fossil Assemblages. Radiocarbon 31, 1041–1047. https://doi.org/10.1017/S0033822200012698
- Goodfriend, G.A., Brigham-Grette, J., Miller, G.H., 1996. Enhanced Age Resolution of the Marine Quaternary Record in the Arctic Using Aspartic Acid Racemization Dating of Bivalve Shells. Quat. Res. 45, 176–187. https://doi.org/10.1006/qres.1996.0018
- Goodfriend, G.A., Hare, P.E., 1995. Reply to the Comment by K. L. F. Brinton and J. L. Bada on "Aspartic acid racemization and protein diagenesis in corals over the last 350 years." Geochim. Cosmochim. Acta 59, 417–418. https://doi.org/10.1016/0016-7037(94)00331-F
- Goodfriend, G.A., Hare, P.E., Druffel, E.R.M., 1992. Aspartic acid racemization and protein diagenesis in corals over the last 350 years. Geochim. Cosmochim. Acta 56, 3847–3850. https://doi.org/10.1016/0016-7037(92)90176-J
- Goodfriend, G.A., Kashgarian, M., Harasewych, M.G., 1995. Use of aspartic acid racemisation and post-bomb 14C to reconstruct growth rate and longevity of the deep-water slit shell Entemnotrochus adansonianus. Geochim. Cosmochim. Acta 59, 1125–1129.
- Goodfriend, G.A., Meyer, V.R., 1991. A Comparative-Study Of the Kinetics Of Amino-Acid Racemization Epimerization In Fossil and Modern Mollusk Shells. Geochim. Cosmochim. Acta 55, 3355–3367.
- Gotliv, B.A., Addadi, L., Weiner, S., 2003. Mollusk shell acidic proteins: In search of individual functions. ChemBioChem 4, 522–529. https://doi.org/10.1002/cbic.200200548

- Gregory, J.M., Griffies, S.M., Hughes, C.W., Lowe, J.A., Church, J.A., Fukimori, I., Gomez, N., Kopp, R.E., Landerer, F., Cozannet, G. Le, Ponte, R.M., Stammer, D., Tamisiea, M.E., van de Wal, R.S.W., 2019. Concepts and Terminology for Sea Level: Mean, Variability and Change, Both Local and Global, Surveys in Geophysics. https://doi.org/10.1007/s10712-019-09525-z
- Gries, K.I., Heinemann, F., Rosenauer, A., Fritz, M., 2012. In vitro growth of flat aragonite crystals between the layers of the insoluble organic matrix of the abalone Haliotis laevigata. J. Cryst. Growth 358, 75–80. https://doi.org/10.1016/j.jcrysgro.2012.08.005
- Gries, K.I., Kröger, R., Kübel, C., Fritz, M., Rosenauer, A., 2009. Investigations of voids in the aragonite platelets of nacre. Acta Biomater. 5, 3038–3044. https://doi.org/10.1016/j.actbio.2009.04.017
- Griffin, R.C., 2006. Application of amino acid racemization in enamel to the estimation of age at death of archaeological remains. University of York.
- Grimley, D.A., Oches, E.A., 2015. Amino acid geochronology of gastropod-bearing Pleistocene units in Illinois, central USA. Quat. Geochronol. 25, 10–25. https://doi.org/10.1016/j.quageo.2014.08.003
- Grützner, J., Giosan, L., Franz, S.O., Tiedemann, R., Cortijo, E., Chaisson, W.P., Flood, R.D., Hagen, S., Keigwin, L.D., Poli, S., Rio, D., Williams, T., 2002. Astronomical age models for Pleistocene drift sediments from the western North Atlantic (ODP Sites 1055–1063). Mar. Geol. 189, 5–23. https://doi.org/10.1016/S0025-3227(02)00320-1
- Gualtieri, L., Vartanyan, S., Brigham-Grette, J., Anderson, P.M., 2003. Pleistocene raised marine deposits on Wrangel Island, northeast Siberia and implications for the presence of an East Siberian ice sheet. Quat. Res. 59, 399–410. https://doi.org/10.1016/S0033-5894(03)00057-7
- Hagen, S., Keigwin, L.D., 2002. Sea-surface temperature variability and deep water reorganisation in the subtropical North Atlantic during Isotope Stage 2–4. Mar. Geol. 189, 145–162. https://doi.org/10.1016/S0025-3227(02)00327-4
- Hamblin, R.J.O., Moorlock, B.S.P., Booth, S.J., Jeffery, D.H., Morigi, A.N., 1997. The Red Crag and Norwich Crag formations in eastern Suffolk. Proc. Geol. Assoc. 108, 11–23. https://doi.org/10.1016/S0016-7878(97)80002-8
- Harada, N., Handa, N., 1995. Amino acid chronology in the fossil planktonic foraminifera, Pulleniatina obliquiloculata from Pacific Ocean. Geophys. Resarch Lett. 22, 2353–2356.
- Harada, N., Handa, N., Ito, M., Oba, T., Matsumoto, E., 1996. Chronology of marine sediments by the racemisation reaction of aspartic acid in planktonic foraminifera. Org. Geochem. 24, 921–930.
- Harada, N., Handa, N., Oba, T., Matsuoka, H., Kimoto, K., Kusakabe, M., 1997. Age Determination of Marine Sediments in the Western North Pacific by Aspartic Acid Chronology. J. Oceanogr. 53, 1–7.
- Hare, P.E., 1976. Relative reaction rates and activation energies for some amino acid reactions. Carnegie Inst. Washingt. Yearb. 75, 801–806.
- Hare, P.E., Abelson, P.H., 1967. Racemisation of amino acids in fossil shells. Carnegie Inst. Geophys. Lab. 66, 526.

- Hare, P.E., Mitterer, R.M., 1968. Laboratory simulation of amino acid diagenesis in fossils. Carnegie Inst. Washingt. Yearb. 67, 205–208.
- Hayward, B.W., Holzmann, M., Grenfell, H.R., Pawlowski, J., Triggs, C.M., 2004. Morphological distinction of molecular types in Ammonia Towards a taxonomic revision of the world's most commonly misidentified foraminifera. Mar. Micropaleontol. 50, 237–271. https://doi.org/10.1016/S0377-8398(03)00074-4
- Head, M.J., Gibbard, P.L., Salvador, A., 2008. The Quaternary: Its character and definition. Episodes 31, 234–238. https://doi.org/10.18814/epiiugs/2008/v31i2/009
- Hearty, P.J., O'Leary, M.J., Kaufman, D.S., Page, M.C., Bright, J., 2004. Amino acid geochronology of individual foraminifer (Pulleniatina obliquiloculata) tests, north Queensland margin, Australia: A new approach to correlating and dating Quaternary tropical marine sediment cores. Paleoceanography 19, 1–14. https://doi.org/10.1029/2004PA001059
- Hearty, P.J., Webster, J.M., Clague, D.A., Kaufman, D.S., Bright, J., Southon, J.R., Renema, W., 2010. A pulse of ooid formation in Maui Nui (Hawaiian Islands) during Termination I. Mar. Geol. 268, 152–162. https://doi.org/10.1016/j.margeo.2009.11.007
- Hemleben, C.H., Spindler, M., Anderson, O.R., 1989. Modern Planktonic Foraminifera. Springer Verlag.
- Hendy, E.J., Tomiak, P.J., Collins, M.J., Hellstrom, J., Tudhope, A.W., Lough, J.M., Penkman, K.E.H., 2012. Assessing amino acid racemization variability in coral intra-crystalline protein for geochronological applications. Geochim. Cosmochim. Acta 86, 338–353. https://doi.org/10.1016/j.gca.2012.02.020
- Hibbert, F.D., Rohling, E.J., Dutton, A., Williams, F.H., Chutcharavan, P.M., Zhao, C., Tamisiea, M.E., 2016. Coral indicators of past sea-level change: A global repository of U-series dated benchmarks. Quat. Sci. Rev. 145, 1–56. https://doi.org/10.1016/j.quascirev.2016.04.019
- Hibbert, F.D., Williams, F.H., Fallon, S.J., Rohling, E.J., 2018. A database of biological and geomorphological sea-level markers from the Last Glacial Maximum to present. Sci. Data 5, 1–25. https://doi.org/10.1038/sdata.2018.88
- Hill, R.L., 1965. Hydrolysis of Proteins. Adv. Protein Chem. 20, 37–107. https://doi.org/10.1016/S0065-3233(08)60388-5
- Hjelstuen, B.O., Haflidason, H., Sejrup, H.P., Nygård, A., 2010. Sedimentary and structural control on pockmark development-evidence from the Nyegga pockmark field, NW European margin. Geo-Marine Lett. 30, 221–230. https://doi.org/10.1007/s00367-009-0172-4
- Horton, B.P., Kopp, R.E., Garner, A.J., Hay, C.C., Khan, N.S., Roy, K., Shaw, T.A., 2018. Mapping sealevel change in time, space, and probability. Annu. Rev. Environ. Resour. 43, 481–521. https://doi.org/10.1146/annurev-environ-102017-025826
- Hovland, M., Svensen, H., Forsberg, C.F., Johansen, H., Fichler, C., Fosså, J.H., Jonsson, R., Rueslåtten, H., 2005. Complex pockmarks with carbonate-ridges off mid-Norway: Products of sediment degassing. Mar. Geol. 218, 191–206. https://doi.org/10.1016/j.margeo.2005.04.005
- Howard, W.R., 1997. A warm future in the past. Nature 388, 418–419. https://doi.org/10.1038/41201

- Hunt, C.O., Gilbertson, D.D., Thew, N.M., 1984. The Pleistocene Chadbrick Gravels of the Cary Valley, Somerset: Amino-acid racemisation and molluscan studies. Proc. Ussher Soc. 6, 129–135.
- Imbrie, J., 1982. Astronomical theory of the Pleistocene ice ages: A brief historical review. Icarus 50, 408–422. https://doi.org/10.1016/0019-1035(82)90132-4
- Ingalls, A.E., Lee, C., Druffel, E.R.M., 2003. Preservation of organic matter in mound-forming coral skeletons. Geochim. Cosmochim. Acta 67, 2827–2841. https://doi.org/10.1016/S0016-7037(03)00079-6
- Jevrejeva, S., Grinsted, A., Moore, J.C., Holgate, S., 2006. Nonlinear trends and multiyear cycles in sea level records. J. Geophys. Res. Ocean. 111, 1–11. https://doi.org/10.1029/2005JC003229
- Kaufman, D.S., 2006. Temperature sensitivity of aspartic and glutamic acid racemization in the foraminifera Pulleniatina. Quat. Geochronol. 1, 188–207. https://doi.org/10.1016/j.quageo.2006.06.008
- Kaufman, D.S., 2003a. Dating deep-lake sediments by using amino acid racemization in fossil ostracodes. Geology 31, 1049–1052. https://doi.org/10.1130/G20004.1
- Kaufman, D.S., 2003b. Amino acid paleothermometry of Quaternary ostracodes from the Bonneville Basin, Utah. Quat. Sci. Rev. 22, 899–914. https://doi.org/10.1016/S0277-3791(03)00006-4
- Kaufman, D.S., 2000. Amino acid racemization in ostracodes, in: Goodfriend, G. a, Collins, M.J., Fogel, M.L., Macko, S.A., Wehmiller, J.F. (Eds.), Perspectives in Amino Acid and Protein Geochemistry. Oxford University Press, New York, pp. 145–160.
- Kaufman, D.S., Cooper, K., Behl, R., Billups, K., Bright, J., Gardner, K., Hearty, P.J., Jakobsson, M., Mendes, I., O'Leary, M.J., Polyak, L., Rasmussen, T.L., Rosa, F., Schmidt, M., 2013. Amino acid racemization in mono-specific foraminifera from Quaternary deep-sea sediments. Quat. Geochronol. 16, 50–61. https://doi.org/10.1016/j.quageo.2012.07.006
- Kaufman, D.S., Manley, W.F., 1998. A new procedure for determining DL amino acid ratios in fossils using reverse phase liquid chromatography. Quat. Sci. Rev. 17, 987–1000. https://doi.org/10.1016/S0277-3791(97)00086-3
- Kaufman, D.S., Miller, G.H., 1992. Overview of amino acid geochronology. Comp. Biochem. Physiol. Part B Comp. Biochem. 102, 199–204. https://doi.org/10.1016/0305-0491(92)90110-D
- Kaufman, D.S., Polyak, L., Adler, R.E., Channell, J.E.T., Xuan, C., 2008. Dating late Quaternary planktonic foraminifer Neogloboquadrina pachyderma from the Arctic Ocean using amino acid racemization. Paleoceanography 23, 1–11. https://doi.org/10.1029/2008PA001618
- Kaufman, D.S., Sejrup, H.P., 1995. Isoleucine Epimerization in the High-Molecular-Weight Fraction of Pleistocene Arctica. Quat. Sci. Rev. 14, 337–350.
- Keen, D.H., Robinson, J.E., West, R.G., Lowry, F., Bridgland, D.R., Davey, N.D.W., 1990. The fauna and flora of the March Gravels at Northam Pit, Eye, Cambridgeshire, England. Geol. Mag. 127, 453–465. https://doi.org/10.1017/S001675680001520X
- Khan, N.S., Horton, B.P., Engelhart, S., Rovere, A., Vacchi, M., Ashe, E.L., Törnqvist, T.E., Dutton, A., Hijma, M.P., Shennan, I., 2019. Inception of a global atlas of sea levels since the Last Glacial

- Kidson, C., Gilbertson, D.D., Haynes, J.R., Heyworth, A., Hughes, C.E., Whatley, R.C., 1978. Interglacial marine deposits of the Somerset Levels, South West England. Boreas 7, 215–228. https://doi.org/10.1111/j.1502-3885.1978.tb00280.x
- Kimber, R.W.L., Griffin, C. V., 1987. Further evidence of the complexity of the racemization process in fossil shells with implications for amino acid racemization dating. Geochim. Cosmochim. Acta 51, 839–846. https://doi.org/10.1016/0016-7037(87)90097-4
- King, K.J., Hare, P.E., 1972a. Species effects in the epimerization of L-isoleucine in fossil planktonic foraminifera. Carnegie Inst. Washingt. Yearb. 71, 596–598.
- King, K.J., Hare, P.E., 1972b. Amino acid composition of the test as a taxonomic character for living and fossil planktonic foraminifera. Micropaleontology 18, 285–293. https://doi.org/10.2307/1485009
- King, K.J., Neville, C., 1977. Isoleucine epimerization for dating marine sediments: importance of analyzing monospecific foraminiferal samples. Science (80-.). 195, 1333–1335. https://doi.org/10.1126/science.195.4284.1333
- Kobayashi, I., Samata, T., 2006. Bivalve shell structure and organic matrix. Mater. Sci. Eng. C 26, 692–698. https://doi.org/10.1016/j.msec.2005.09.101
- Kosnik, M.A., Hua, Q., Kaufman, D.S., Kowalewski, M., Whitacre, K.E., 2017. Radiocarbon-calibrated amino acid racemization ages from Holocene sand dollars (Peronella peronii). Quat. Geochronol. 39, 174–188. https://doi.org/10.1016/j.quageo.2016.12.001
- Kosnik, M.A., Kaufman, D.S., 2008. Identifying outliers and assessing the accuracy of amino acid racemization measurements for geochronology: II. Data screening. Quat. Geochronol. 3, 328–341. https://doi.org/10.1016/j.quageo.2008.04.001
- Kosnik, M.A., Kaufman, D.S., Hua, Q., 2013. Radiocarbon-calibrated multiple amino acid geochronology of Holocene molluscs from Bramble and Rib Reefs (Great Barrier Reef, Australia). Quat. Geochronol. 16, 73–86. https://doi.org/10.1016/j.quageo.2012.04.024
- Kosnik, M.A., Kaufman, D.S., Hua, Q., 2008. Identifying outliers and assessing the accuracy of amino acid racemization measurements for geochronology: I. Age calibration curves. Quat. Geochronol. 3, 308–327. https://doi.org/10.1016/j.quageo.2008.04.002
- Kotler, E., Martin, R.E., Liddell, W.D., 1992. Experimental analysis of abrasion and dissolution resistance of modern reef-dwelling foraminifera: implications for the preservation of biogenic carbonate. Palaios 7, 244–276. https://doi.org/10.2307/3514972
- Kriausakul, N., Mitterer, R.M., 1978. Isoleucine epimerization in peptides and proteins: kinetic factors and application to fossil proteins. Science (80-.). 201, 1011–1014. https://doi.org/10.1126/science.201.4360.1011
- Kristensen, P., Knudsen, K.L., Lykke-Andersen, H., Nørmark, E., Peacock, J.D., Sinnott, A., 1998. Interglacial and glacial climate oscillations in a marine shelf sequence from northern Denmark a multidisciplinary study. Quat. Sci. Rev. 17, 813–837. https://doi.org/10.1016/S0277-3791(98)00020-1
- Kuge, K., Fujii, N., Miura, Y., Tajima, S., Saitta, E.T., 2004. Kinetic study of racemization of aspartyl

- residues in synthetic elastin peptides. Amino Acids 27, 193–197. https://doi.org/10.1007/s00726-004-0107-3
- Lajoie, K.R., Wehmiller, J.F., Kennedy, G.L., 1980. Inter- and intrageneric trends in apparent racemization kinetics of amino acids in Quaternary mollusks. Biogeochem. Amin. Acids 305–340.
- Langford, H.E., Bateman, M.D., Boreham, S., Knudsen, K.L., Merry, J., Penney, D.N., 2004. King's Dyke, in: Langford, H.E., Briant, R.M. (Eds.), Nar Valley Field Guide. Quaternary Research Association, Cambridge, pp. 174–194.
- Langford, H.E., Bateman, M.D., Penkman, K.E.H., Boreham, S., Briant, R.M., Coope, G.R., Keen, D.H., 2007. Age-estimate evidence for Middle-Late Pleistocene aggradation of River Nene 1st Terrace deposits at Whittlesey, eastern England. Proc. Geol. Assoc. 118, 283–300. https://doi.org/10.1016/S0016-7878(07)80029-0
- Langford, H.E., Boreham, S., Coope, G.R., Fletcher, W., Horne, D.J., Keen, D.H., Mighall, T., Penkman, K.E.H., Schreve, D.C., Whittaker, J.E., 2014. Palaeoecology of a late MIS 7 interglacial deposit from eastern England. Quat. Int. 341, 27–45. https://doi.org/10.1016/j.quaint.2013.05.046
- Langford, H.E., Briant, Rebecca M., 2004. Post-Anglian deposits in the Peterborough area and the Pleistocene history of the Fen Basin, in: Langford, H.E., Briant, R. M. (Eds.), Nene Valley Field Guide. Quaternary Research Association, Cambridge, pp. 22–35.
- Lee, C., Bada, J.L., Peterson, E., 1976. Amino acids in fossil woods. Nature 259, 183–186. https://doi.org/10.1038/267468a0
- Lee, J.R., Candy, I., Haslam, R., 2018. The Neogene and Quaternary of England: landscape evolution, tectonics, climate change and their expression in the geological record. Proc. Geol. Assoc. 129, 452–481. https://doi.org/10.1016/j.pgeola.2017.10.003
- Li, H., Xin, H.L., Kunitake, M.E., Keene, E.C., Muller, D.A., Estroff, L.A., 2011. Calcite prisms from mollusk shells (Atrina rigida): Swiss-cheese-like organic-inorganic single-crystal composites. Adv. Funct. Mater. 21, 2028–2034. https://doi.org/10.1002/adfm.201002709
- Li, H., Xin, H.L., Muller, D.A., Estroff, L.A., 2009. Visualizing the 3D Internal Structure of Calcite Single Crystals Grown in Agarose Hydrogels. Science (80-.). 326, 1244–1247. https://doi.org/10.1126/science.1178583
- Liang, R., Lau, M.C.Y., Saitta, E.T., Garvin, Z.K., Onstott, T.C., 2020. Genome-centric resolution of novel microbial lineages in an excavated Centrosaurus dinosaur fossil bone from the Late Cretaceous of North America. Environ. Microbiomes 15, 1–18. https://doi.org/10.1186/s40793-020-00355-w
- Lisiecki, L.E., Raymo, M.E., 2005. A Pliocene-Pleistocene stack of 57 globally distributed benthic δ 180 records. Paleoceanography 20, 1–17. https://doi.org/10.1029/2004PA001071
- Long, A.J., Innes, J.B., Kirby, J.R., Lloyd, J.M., Rutherford, M.M., Shennan, I., Tooley, M.J., 1998. Holocene sea-level change and coastal evolution in the Humber estuary, eastern England: An assessment of rapid coastal change. Holocene 8, 229–247. https://doi.org/10.1191/095968398677984183
- Loutre, M.F., Berger, A., 2000. Future climatic changes: Are we entering an exceptionally long

- interglacial? Clim. Change 46, 61–90. https://doi.org/10.1023/a:1005559827189
- Lowe, J., Walker, M.J.C., 2014. Reconstructing Quaternary Environments. Routledge, London.
- Macko, S.A., Aksu, A.E., 1986. Amino acid epimerization in plantonic foraminifera suggests slow sedimentation rates for Alpha Ridge, Arctic Ocean. Nature 322, 730–732. https://doi.org/10.1038/324227a0
- Manley, W.F., Miller, G.H., Czywczynski, J., 2000. Kinetics of aspartic acid racemisation in Mya and Hiatella: modeling age and palaeotemperature of high-latitude quaternary mollusks, in: Goodfriend, G. a, Collins, M.J., Fogel, M.L., Macko, S.A., Wehmiller, J.F. (Eds.), Perspectives in Amino Acid and Protein Geochemistry. Oxford University Press, New York, pp. 202–218.
- Marino, G., Rohling, E.J., Rodríguez-Sanz, L., Grant, K.M., Heslop, D., Roberts, A.P., Stanford, J.D., Yu, J., 2015. Bipolar seesaw control on last interglacial sea level. Nature 522, 197–201. https://doi.org/10.1038/nature14499
- Marks, L., Gałaogonekzka, D., Krzymińska, J., Nita, M., Stachowicz-Rybka, R., Witkowski, A., Woronko, B., Dobosz, S., 2014. Marine transgressions during Eemian in northern Poland: A high resolution record from the type section at Cierpieogonekta. Quat. Int. 328–329, 45–49. https://doi.org/10.1016/j.quaint.2013.12.007
- McCarroll, D., 2002. Amino-acid geochronology and the British Pleistocene: Secure statigraphical framework or a case of circular reasoning? J. Quat. Sci. 17, 647–651. https://doi.org/10.1002/jqs.690
- McCoy, V.E., Gabbott, S.E., Penkman, K.E.H., Collins, M.J., Presslee, S., Holt, J., Grossman, H., Wang, B., Solórzano-Kraemer, M.M., Delclòs, X., Peñalver, E., 2019. Ancient amino acids from fossil feathers in amber. Sci. Rep. 9, 6420. https://doi.org/10.1038/s41598-019-42938-9
- McCoy, W.D., 1987. The precision of amino acid geochronology and paleothermometry. Quat. Sci. Rev. 6, 43–54. https://doi.org/10.1016/0277-3791(87)90016-3
- McGranahan, G., Balk, D., Anderson, B., 2007. The rising tide: Assessing the risks of climate change and human settlements in low elevation coastal zones. Environ. Urban. 19, 17–37. https://doi.org/10.1177/0956247807076960
- Met Office, 2022. UK Climate Averages [WWW Document]. URL https://www.metoffice.gov.uk/research/climate/maps-and-data/uk-climate-averages
- Miller, G.H., Beaumont, P.B., Jull, A.J.T., Johnson, B.J., 1992. Pleistocene geochronology and palaeothermometry from protein diagenesis in ostrich eggshells: implications for the evolution of modern humans. Philos. Trans. R. Soc. B, Biol. Sci. 337, 149–157.
- Miller, G.H., Brigham-Grette, J., 1989. Amino acid geochronology: Resolution and precision in carbonate fossils. Quat. Int. 1, 111–128. https://doi.org/10.1016/1040-6182(89)90011-6
- Miller, G.H., Hare, P.E., 1980. Amino acid geochronology: integrity of the carbonate matrix and potential of molluscan fossils, in: Hare, P.E., Hoering, T.C., King, Jr., K. (Eds.), Biogeochemistry of Amino Acids. Wiley, New York, pp. 415–443.
- Miller, G.H., Hare, P.E., 1975. Use of amino acid reactions in some Arctic mariine fossils as stratigraphic and geochronologic indicators. Carnegie Inst. Washingt. Yearb. 74, 612–617.

- Miller, G.H., Hart, C.P., Roark, E.B., Johnson, B.J., 2000. Isoleucine epimerization in eggshells of the flightless Australian birds Genyornis and Dromaius, in: Goodfriend, G. a., Collins, M.J., Fogel, M.L., Macko, S.A., Wehmiller, J.F. (Eds.), Perspectives in Amino Acid and Protein Geochemistry. Oxford University Press, Oxford, pp. 161–181.
- Miller, G.H., Hollin, J.T., Andrews, J.T., 1979. Aminostratigraphy of UK Pleistocene deposits. Nature 281, 539–543.
- Miller, G.H., Kaufman, D.S., Clarke, S.J., 2013. Amino Acid Dating, 2nd ed, Encyclopedia of Quaternary Science: Second Edition. Elsevier B.V. https://doi.org/10.1016/B978-0-444-53643-3.00054-6
- Miller, G.H., Magee, J.W., Jull, A.J.T., 1997. Low-latitude glacial cooling in the Southern Hemisphere from amino-acid racemization in emu eggshells. Lett. to Nat. 385, 241–244. https://doi.org/10.1038/255243a0
- Miller, G.H., Mangerud, J., 1985. Aminostratigraphy of European marine interglacial deposits. Quat. Sci. Rev. 4, 215–278.
- Miller, G.H., Sejrup, H.P., Mangerud, J., Andersen, B.G., 1983. Amino acid ratios in Quaternary molluscs and foraminifera from western Norway: correlation, geochronology and paleotemperature estimates. Boreas 12, 107–124. https://doi.org/10.1111/j.1502-3885.1983.tb00442.x
- Millman, E., Wheeler, L. J., Billups, K., Kaufman. D., Penkman, K. E. H. (2022). Testing the effect of oxidizing pre-treatments on amino acids in benthic and planktic foraminifera tests.

 Quaternary Geochronology, 73, 101401. https://doi.org/10.1016/j.quageo.2022.101401
- Milne, G.A., 2014. Sea Level, in: Masselink, G., Gehrels, R. (Eds.), Coastal Environments and Global Change. John Wiley & Sons, Ltd., pp. 28–51.
- Milne, G.A., Mitrovica, J.X., Schrag, D.P., 2002. Estimating past continental ice volume from sealevel data. Quat. Sci. Rev. 21, 361–376. https://doi.org/10.1016/S0277-3791(01)00108-1
- Mitrovica, J.X., Milne, G.A., 2003. On post-glacial sea level: I. General theory. Geophys. J. Int. 154, 253–267. https://doi.org/10.1046/j.1365-246X.2003.01942.x
- Mitterer, R.M., Kriausakul, N., 1989. Calculation of amino acid racemization ages based on apparent parabolic kinetics. Quat. Sci. Rev. 8, 353–357. https://doi.org/10.1016/0277-3791(89)90035-8
- Mitterer, R.M., Kriausakul, N., 1984. Comparison of rates and degrees of isoleucine epimerization in dipeptides and tripeptides. Org. Geochem. 7, 91–98. https://doi.org/10.1016/0146-6380(84)90140-2
- Miyamoto, T., Homma, H., 2018. Detection and quantification of D-amino acid residues in peptides and proteins using acid hydrolysis. Biochim. Biophys. Acta Proteins Proteomics 1866, 775–782. https://doi.org/10.1016/j.bbapap.2017.12.010
- Moir, M.E., Crawford, R.J., 1988. Model studies of competing hydrolysis and epimerization of some tetrapeptides of interest in amino acid racemization studies in geochronology. Can. J. Chem. 66, 2903–2913. https://doi.org/10.1139/v88-449
- Murray-Wallace, C. V., 1995. Aminostratigraphy of Quaternary coastal sequences in southern

- Australia an overview. Quat. Int. 26, 69-86.
- Murray-Wallace, C. V., Belperio, A.P., 1994. Identification of remanié fossils using amino acid racemisation. Alcheringa An Australas. J. Palaeontol. 18, 219–227. https://doi.org/10.1080/03115519408619496
- Murray-Wallace, C. V., Bourman, R.P., Prescott, J.R., Williams, F., Price, D.M., Belperio, A.P., 2010. Aminostratigraphy and thermoluminescence dating of coastal aeolianites and the later Quaternary history of a failed delta: The River Murray mouth region, South Australia. Quat. Geochronol. 5, 28–49. https://doi.org/10.1016/j.quageo.2009.09.011
- Murray-Wallace, C. V., Kimber, R.W.L., Belperio, A.P., 1988. Geological note: Holocene palaeotemperature studies using amino acid racemization reactions. Aust. J. Earth Sci. 35, 575–577. https://doi.org/10.1080/08120098808729472
- Murray, J.W., 1979. British Nearshore Foraminiferids, in: Synopses of the British Fauna (New Series). The Linnean Sorciety of London and the Estuarine and Brackish-water Sciences Association.
- Murray, J.W., Alve, E., 1999. Taphonomic experiments on marginal marine foraminiferal assemblages: How much ecological information is preserved? Palaeogeogr. Palaeoclimatol. Palaeoecol. 149, 183–197. https://doi.org/10.1016/S0031-0182(98)00200-4
- Nakayoshi, T., Kato, K., Fukuyoshi, S., Takahashi, H., Takahashi, O., Kurimoto, E., Oda, A., 2020. Computational studies on nonenzymatic succinimide-formation mechanisms of the aspartic acid residues catalyzed by two water molecules. Biochim. Biophys. Acta Proteins Proteomics 1868. https://doi.org/10.1016/j.bbapap.2020.140459
- Nash, G.J., De Deckker, P., Mitchell, C., Murray-Wallace, C. V., Hua, Q., 2018. Micropalaeontological evidence for deglacial marine flooding of the ancient courses of the River Murray across the Lacepede Shelf, southern Australia. Mar. Micropaleontol. 141, 55–72. https://doi.org/10.1016/j.marmicro.2018.04.002
- Neuberger, A., 1948. Stereochemistry of Amino Acids. Adv. Protein Chem. 4, 297–383. https://doi.org/10.1016/S0065-3233(08)60009-1
- Nicholas, W.A., 2012. Aminostratigraphy of semi-enclosed basins. University of Wollongong.
- Nicholas, W.A., Lachlan, T.J., Murray-Wallace, C. V., Price, G.J., 2019. Amino acid racemisation and uranium-series dating of a last interglacial raised beach, Kingscote, Kangaroo Island, southern Australia. Trans. R. Soc. South Aust. 143, 1–26. https://doi.org/10.1080/03721426.2018.1532269
- Nicholls, R.J., Cazenave, A., 2010. Sea-Level Rise and Its Impact on Coastal Zones. Science (80-.). 328, 1517–1520. https://doi.org/10.1126/science.1185782
- Nilsen, T.E., 2014. Kronologi, askestratigrafi og utbredelse av store askeutbrudd fra de siste 40 ka i kjerne MD99-2289 fra Norskehavet. University of Bergen.
- Onac, Bogdan P., Ginés, Angel, Ginés, Joaquín, Fornós, Joan J., Dorale, J.A., 2012. Late quaternary sea-level history: A Speleothem perspective, in: Ginés, A., Ginés, J., Gómez-Pujol, L., Onac, B.P., Fornós, J.J. (Eds.), Mallorca: A Mediterranean Benchmark for Quaternary Studies. Monografies de la Societat d'Historia Natural de les Balears, pp. 147–162.

- Oppenheimer, M., Glavovic, B.C., Hinkel, J., van de Wal, R.S.W., Magnan, A.K., Abd-Elgawad, A., Cai, R., Cifuentes-Jara, M., DeConto, R.M., Ghosh, T., Hay, J., Isla, F., Marzeion, B., Meyssignac, B., Sebesvar, Z., 2019. Sea Level Rise and Implications for Low-Lying Islands, Coasts and Communities, in: Pörtner, H.-O., Roberts, D.C., Masson-Delmotte, V., Zhai, P., Tignor, M., Poloczanska, E., Mintenbeck, K., Alegría, A., Nicolai, M., Okem, A., Petzold, J., Rama, B., Weyer, N.M. (Eds.), IPCC Special Report on the Ocean and Cryosphere in a Changing Climate.
- Orem, C.A., Kaufman, D.S., 2011. Effects of basic pH on amino acid racemization and leaching in freshwater mollusk shell. Quat. Geochronol. 6, 233–245. https://doi.org/10.1016/j.quageo.2010.11.005
- Ortiz, J.E., Gutiérrez-Zugasti, I., Sánchez-Palencia, Y., Torres, T., González-Morales, M., 2019.

 Quaternary Geochronology Protein diagenesis in archaeological shells of Littorina littorea
 (Linnaeus, 1758) and the suitability of this material for amino acid racemisation dating. Quat.
 Geochronol. 54, 11. https://doi.org/10.1016/j.quageo.2019.101017
- Ortiz, J.E., Gutiérrez-Zugasti, I., Torres, T., González-Morales, M., Sánchez-Palencia, Y., 2015.

 Protein diagenesis in Patella shells: Implications for amino acid racemisation dating. Quat. Geochronol. 27, 105–118. https://doi.org/10.1016/j.quageo.2015.02.008
- Ortiz, J.E., Sánchez-Palencia, Y., Gutiérrez-Zugasti, I., Torres, T., González-Morales, M., 2020. Mimicking the effects of anthropogenic heating on amino acid racemisation dating of gastropod shells. Quat. Geochronol. 59. https://doi.org/10.1016/j.quageo.2020.101084
- Ortiz, J.E., Sánchez-Palencia, Y., Gutiérrez-Zugasti, I., Torres, T., González-Morales, M., 2018.

 Protein diagenesis in archaeological gastropod shells and the suitability of this material for amino acid racemisation dating: Phorcus lineatus (da Costa, 1778). Quat. Geochronol. 46, 16–27. https://doi.org/10.1016/j.quageo.2018.02.002
- Ortiz, J.E., Torres, T., Pérez-González, A., 2013. Amino acid racemization in four species of ostracodes: Taxonomic, environmental, and microstructural controls. Quat. Geochronol. 16, 129–143. https://doi.org/10.1016/j.quageo.2012.11.004
- Ortiz, J.E., Torres, T., Sánchez-Palencia, Y., Ferrer, M., 2017. Inter- and intra-crystalline protein diagenesis in Glycymeris shells: Implications for amino acid geochronology. Quat. Geochronol. 41, 37–50. https://doi.org/10.1016/j.quageo.2017.05.007
- Otto-Bliesner, B.L., Brady, E.C., Zhao, A., Brierley, C.M., Axford, Y., Capron, E., Govin, A., Hoffman, J.S., Isaacs, E., Kageyama, M., Scussolini, P., Tzedakis, P.C., Williams, C.J.R., Wolff, E.W., Abe-Ouchi, A., Braconnot, P., Ramos Buarque, S., Cao, J., De Vernal, A., Vittoria Guarino, M., Guo, C., Legrande, A.N., Lohmann, G., Meissner, K.J., Menviel, L., Morozova, P.A., Nisancioglu, K.H., O'Ishi, R., Mélia, D.S.Y., Shi, X., Sicard, M., Sime, L.C., Stepanek, C., Tomas, R., Volodin, E., Yeung, N.K.H., Zhang, Q., Zhang, Z., Zheng, W., 2021. Large-scale features of Last Interglacial climate: Results from evaluating the lig127k simulations for the Coupled Model Intercomparison Project (CMIP6)-Paleoclimate Modeling Intercomparison Project (PMIP4). Clim. Past 17, 63–94. https://doi.org/10.5194/cp-17-63-2021
- Owen, L.A., Bright, J., Finkel, R.C., Jaiswal, M.K., Kaufman, D.S., Mahan, S., Radtke, U., Schneider, J.S., Sharp, W., Singhvi, A.K., Warren, C.N., 2007. Numerical dating of a Late Quaternary spit-shoreline complex at the northern end of Silver Lake playa, Mojave Desert, California: A comparison of the applicability of radiocarbon, luminescence, terrestrial cosmogenic nuclide, electron spin resonance, U-se. Quat. Int. 166, 87–110. https://doi.org/10.1016/j.quaint.2007.01.001

- Past Interglacials Working Group of PAGES, 2016. Interglacials of the last 800,000 years. Rev. Geophys. 54, 162–219. https://doi.org/10.1002/2015RG000482
- Pawlowski, J., Holzmann, M., Berney, C., Fahrni, J., Gooday, A.J., Cedhagen, T., Habura, A., Bowser, S.S., 2003. The evolution of early Foraminifera. Proc. Natl. Acad. Sci. U. S. A. 100, 11494–11498. https://doi.org/10.1073/pnas.2035132100
- Pearson, P.N., Burgess, C.E., 2008. Foraminifer test preservation and diagenesis: comparison of high latitude Eocene sites. Geol. Soc. London, Spec. Publ. 303, 59–72. https://doi.org/10.1144/SP303.5
- Pedoja, K., Husson, L., Johnson, M.E., Melnick, D., Witt, C., Pochat, S., Nexer, M., Delcaillau, B., Pinegina, T., Poprawski, Y., Authemayou, C., Elliot, M., Regard, V., Garestier, F., 2014. Coastal staircase sequences reflecting sea-level oscillations and tectonic uplift during the Quaternary and Neogene. Earth-Science Rev. 132, 13–38. https://doi.org/10.1016/j.earscirev.2014.01.007
- Penkman, K.E.H., 2017. Amino Acid Racemization, in: Gilbert, A.S. (Ed.), Encyclopedia of Geoarchaeology. Springer, Dordrecht, pp. 14–15. https://doi.org/10.1007/978-1-4020-4409-0_38
- Penkman, K.E.H., 2005. Amino acid geochronology: a closed system approach to test and refine the UK model. University of Newcastle-upon-Tyne.
- Penkman, K.E.H., Kaufman, D.S., Maddy, D., Collins, M.J., 2008. Closed-system behaviour of the intra-crystalline fraction of amino acids in mollusc shells. Quat. Geochronol. 3, 2–25. https://doi.org/10.1016/j.quageo.2007.07.001
- Penkman, K.E.H., Preece, R.C., Bridgland, D.R., Keen, D.H., Meijer, T., Parfitt, S.A., White, T.S., Collins, M.J., 2013. An aminostratigraphy for the British Quaternary based on Bithynia opercula. Quat. Sci. Rev. 61, 111–134. https://doi.org/10.1016/j.quascirev.2012.10.046
- Penkman, K.E.H., Preece, R.C., Bridgland, D.R., Keen, D.H., Meijer, T., Parfitt, S.A., White, T.S., Collins, M.J., 2011. A chronological framework for the British Quaternary based on Bithynia opercula. Nature 476, 446–449. https://doi.org/10.1016/j.quascirev.2012.10.046
- Pereira-Mouriès, L., Almeida, M.J., Riberio, C., Peduzzi, J., Barthélemy, M., Milet, C., Lopez, E., 2002. Soluble silk-like organic matrix in the nacreous layer of the bivalve Pinctada maxima. Eur. J. Biochem. 269, 4994–5003.
- Pierini, F., Demarchi, B., Turner, J., Penkman, K.E.H., 2016. Pecten as a new substrate for IcPD dating: The quaternary raised beaches in the Gulf of Corinth, Greece. Quat. Geochronol. 31, 40–52. https://doi.org/10.1016/j.quageo.2015.10.006
- Pillans, B., Chappell, J., Naish, T.R., 1998. A review of the Milankovitch climatic beat: Template for Plio-Pleistocene sea-level changes and sequence stratigraphy. Sediment. Geol. 122, 5–21. https://doi.org/10.1016/S0037-0738(98)00095-5
- Povinec, P.P., 2018. Developments in radioanalytics: from Geiger counters to single atom counting. J. Radioanal. Nucl. Chem. 318, 1573–1585. https://doi.org/10.1007/s10967-018-6248-8
- Powell, J., 2012. Evaluating measurement uncertainty in amino acid racemisation analysis: towards a new chronology. University of York.

- Powell, J., Collins, M.J., Cussens, J., MacLeod, N., Penkman, K.E.H., 2013. Results from an amino acid racemization inter-laboratory proficiency study; design and performance evaluation. Quat. Geochronol. 16, 183–197. https://doi.org/10.1016/j.quageo.2012.11.001
- Preece, R.C., Meijer, T., Penkman, K.E.H., Demarchi, B., Mayhew, D.F., Parfitt, S.A., 2020. The palaeontology and dating of the 'Weybourne Crag', an important marker horizon in the Early Pleistocene of the southern North Sea basin. Quat. Sci. Rev. 236. https://doi.org/10.1016/j.quascirev.2020.106177
- Preece, R.C., Penkman, K.E.H., 2005. New faunal analyses and amino acid dating of the Lower Palaeolithic site at East Farm, Barnham, Suffolk. Proc. Geol. Assoc. 116, 363–377. https://doi.org/10.1016/S0016-7878(05)80053-7
- Preece, R.C., Scourse, J.D., Houghton, S.D., Knudsen, K.L., Penney, D.N., 1990. The Pleistocene sealevel and neotectonic history of the eastern Solent, southern England. Philos. Trans. R. Soc. B, Biol. Sci. 328, 425–477.
- Preusser, F., Degering, D., Fuchs, M., Hilgers, A., Kadereit, A., Klasen, N., Krbetschek, M., Richter, D., Spencer, J.Q.G., 2008. Luminescence dating: basics, methods and applications. E&G Quat. Sci. J. 57, 95–149. https://doi.org/10.3285/eg.57.1-2.5
- Radkiewicz, J.L., Zipse, H., Clarke, S.J., Houk, K.N., 1996. Accelerated racemization of aspartic acid and asparagine residues via succinimide intermediates: An ab initio theoretical exploration of mechanism. J. Am. Chem. Soc. 118, 9148–9155. https://doi.org/10.1021/ja953505b
- Rafalska, J.K., Engel, M.H., Lanier, W.P., 1991. Retardation of racemization rates of amino acids incorporated into melanoidins. Geochim. Cosmochim. Acta 55, 3669–3675. https://doi.org/10.1016/0016-7037(91)90065-D
- Rasbury, E.T., Cole, J.M., 2009. Directly dating geologic events: U-Pb dating of carbonates. Rev. Geophys. 47, 1–27. https://doi.org/10.1029/2007RG000246
- Raymo, M.E., Kozdon, R., Evans, D., Lisiecki, L.E., Ford, H.L., 2018. The accuracy of mid-Pliocene δ18O-based ice volume and sea level reconstructions. Earth-Science Rev. 177, 291–302. https://doi.org/10.1016/j.earscirev.2017.11.022
- Read, A., Godwin, M., Mills, C.A., Juby, C., Lee, J.R., Palmer, A.P., Candy, I., Rose, J., 2007. Evidence for Middle Pleistocene temperate-climate high sea-level and lowland-scale glaciation, Chapel Hill, Norwich, UK. Proc. Geol. Assoc. 118, 143–156. https://doi.org/10.1016/S0016-7878(07)80032-0
- Reimer, P.J., Austin, W.E.N., Bard, E., Bayliss, A., Blackwell, P.G., Bronk Ramsey, C., Butzin, M., Cheng, H., Edwards, R.L., Friedrich, M., Grootes, P.M., Guilderson, T.P., Hajdas, I., Heaton, T.J., Hogg, A.G., Hughen, K.A., Kromer, B., Manning, S.W., Muscheler, R., Palmer, J.G., Pearson, C., Van Der Plicht, J., Reimer, R.W., Richards, D.A., Scott, E.M., Southon, J.R., Turney, C.S.M., Wacker, L., Adolphi, F., Büntgen, U., Capano, M., Fahrni, S.M., Fogtmann-Schulz, A., Friedrich, R., Köhler, P., Kudsk, S., Miyake, F., Olsen, J. V., Reinig, F., Sakamoto, M., Sookdeo, A., Talamo, S., 2020. The IntCal20 Northern Hemisphere Radiocarbon Age Calibration Curve (0-55 cal kBP). Radiocarbon 62, 725–757. https://doi.org/10.1017/RDC.2020.41
- Reimer, P.J., Bard, E., Bayliss, A., Beck, J.W., Blackwell, P.G., Ramsey, C.B., Buck, C.E., Cheng, H., Edwards, R.L., Friedrich, M., Grootes, P.M., Guilderson, T.P., Haflidason, H., Hajdas, I., Hatte, C., Heaton, T.J., Hoffman, D.L., Hogg, A.G., Hughen, K.A., Kaiser, K.F., Kromer, B., Manning,

- S.W., Niu, M., Reimer, R.W., Richards, D.A., Scott, E.M., Southon, J.R., Staff, R.A., Turney, C.S.M., Van Der Plicht, J., 2013. Intcal13 and Marine13 Radiocarbon Age Calibration Curves 0–50,000 Years Cal Bp. Radiocarbon 55, 1869–1887. https://doi.org/10.2458/azu_js_rc.46.4183
- Reimer, P.J., Reimer, R.W., 2001. A marine reservoir correction database and on-line interface. Radiocarbon 43, 461–463. https://doi.org/10.1017/s0033822200038339
- Reinardy, B.T.I., Hjelstuen, B.O., Sejrup, H.P., Augedal, H., Jørstad, A., 2017. Late Pliocene-Pleistocene environments and glacial history of the northern North Sea. Quat. Sci. Rev. 158, 107–126. https://doi.org/10.1016/j.quascirev.2016.12.022
- Rhodes, E.J., 2011. Optically stimulated luminescence dating of sediments over the past 200,000 years. Annu. Rev. Earth Planet. Sci. 39, 461–488. https://doi.org/10.1146/annurev-earth-040610-133425
- Robbins, L.L., Brew, K., 1990. Proteins from the organic matrix of core-top and fossil planktonic foraminifera. Geochim. Cosmochim. Acta 54, 2285–2292. https://doi.org/10.1016/0016-7037(90)90052-M
- Roberts, M.B., Pope, M.I., 2009. The archaeological and sedimentary records from Boxgrove and Slindon, in: Briant, R.M., Bates, M.R., Hosfield, R.T., Wenban-Smith, F.F. (Eds.), The Quaternary of the Solent Basin and West Sussex Raised Beaches. Quaternary Research Association, London, pp. 96–122.
- Roe, H.M., Preece, R.C., 2011. Incised palaeo-channels of the late Middle Pleistocene Thames: Age, origins and implications for fluvial palaeogeography and sea-level reconstruction in the southern North Sea basin. Quat. Sci. Rev. 30, 2498–2519. https://doi.org/10.1016/j.quascirev.2011.04.007
- Rohling, E.J., Braun, K., Grant, K.M., Kucera, M., Roberts, A.P., Siddall, M., Trommer, G., 2010. Comparison between Holocene and Marine Isotope Stage-11 sea-level histories. Earth Planet. Sci. Lett. 291, 97–105. https://doi.org/10.1016/j.epsl.2009.12.054
- Rohling, E.J., Foster, G.L., Grant, K.M., Marino, G., Roberts, A.P., Tamisiea, M.E., Williams, F., 2014. Sea-level and deep-sea-temperature variability over the past 5.3 million years. Nature 508, 477–482. https://doi.org/10.1038/nature13230
- Rohling, E.J., Grant, K.M., Hemleben, C., Siddall, M., Hoogakker, B.A.A., Bolshaw, M., Kucera, M., 2008. High rates of sea-level rise during the last interglacial period. Nat. Geosci. 1, 38–42. https://doi.org/10.1038/ngeo.2007.28
- Rose, J., Moorlock, B.S.P., Hamblin, R.J.O., 2001. Pre-Anglian fluvial and coastal deposits in Eastern England: Lithostratigraphy and palaeoenvironments. Quat. Int. 79, 5–22. https://doi.org/10.1016/S1040-6182(00)00119-1
- Rovere, A., Raymo, M.E., Vacchi, M., Lorscheid, T., Stocchi, P., Gómez-Pujol, L., Harris, D.L., Casella, E., O'Leary, M.J., Hearty, P.J., 2016. The analysis of Last Interglacial (MIS 5e) relative sea-level indicators: Reconstructing sea-level in a warmer world. Earth-Science Rev. 159, 404–427. https://doi.org/10.1016/j.earscirev.2016.06.006
- Rowe, P.J., Richards, D.A., Atkinson, T.C., Bottrell, S.H., Cliff, R.A., 1997. Geochemistry and radiometric dating of a Middle Pleistocene peat. Geochim. Cosmochim. Acta 61, 4201–4211. https://doi.org/10.1016/S0016-7037(97)00213-5

- Ryan, D.D., Lachlan, T.J., Murray-Wallace, C. V., Price, D.M., 2020. The utility of single foraminifera amino acid racemization analysis for the relative dating of Quaternary beach barriers and identification of reworked sediment. Quat. Geochronol. 60, 101103. https://doi.org/10.1016/j.quageo.2020.101103
- Sabbatini, A., Bédouet, L., Marie, A., Bartolini, A., Landemarre, L., Weber, M.X., Gusti Ngurah Kade Mahardika, I., Berland, S., Zito, F., Vénec-Peyré, M.T., 2014. Biomineralization of Schlumbergerella floresiana, a significant carbonate-producing benthic foraminifer. Geobiology 12, 289–307. https://doi.org/10.1111/gbi.12085
- Saitta, E.T., Liang, R., Lau, M.C.Y., Brown, C.M., Longrich, N.R., Kaye, T.G., Novak, B.J., Salzberg, S.L., Norell, M.A., Abbott, G.D., Dickinson, M.R., Vinther, J., Bull, I.D., Brooker, R.A., Martin, P., Donohoe, P., Knowles, T.D.J., Penkman, K.E.H., Onstott, T.C., 2019. Cretaceous dinosaur bone contains recent organic material and provides an environment conducive to microbial communities. Elife 8. https://doi.org/10.7554/eLife.46205.001
- Saitta, E.T., Vinther, J., Crisp, M.K., Abbott, G.D., Kaye, T.G., Pittman, M., Bull, I.D., Fletcher, I., Chen, X., Collins, M.J., Sakalauskaite, J., Mackie, M., Dal Bello, F., Dickinson, M.R., Stevenson, M.A., Donohoe, P., Heck, P.R., Demarchi, B., Penkman, K.E.H., 2020. Non-avian dinosaur eggshell calcite contains ancient, endogenous amino acids. 1. bioRxiv 2020.06.02.129999. https://doi.org/10.1101/2020.06.02.129999
- Sarnthein, M., Altenbach, A. V., 1995. Late Quaternary changes in surface water and deep water masses of the Nordic Seas and north-eastern North Atlantic: a review. Geol. Rundschau 84, 89–107. https://doi.org/10.1007/BF00192244
- Sato, M., Tatsuno, T., Matsuo, H., 1970. Studies on the Racemization of Amino Acids and Their Derivatives III The Effect of Alkyl, Arakyl and Aryl-Side Chain at the alpha-Position of Amino Acids on Their Base-Catalyzed Racemization. Chem. Pharm. Bull. 18, 1794–1798. https://doi.org/10.1248/cpb.37.3229
- Sato, N., Quitain, A.T., Kang, K., Daimon, H., Fujie, K., 2004. Reaction Kinetics of Amino Acid Decomposition in High-Temperature and High-Pressure Water. Ind. Eng. Chem. Res. 43, 3217–3222. https://doi.org/10.1021/ie020733n
- Schmidt, G.A., Annan, J.D., Bartlein, P.J., Cook, B.I., Guilyardi, E., Hargreaves, J.C., Harrison, S.P., Kageyama, M., Legrande, A.N., Konecky, B., Lovejoy, S., Mann, M.E., Masson-Delmotte, V., Risi, C., Thompson, D., Timmermann, A., Yiou, P., 2014. Using palaeo-climate comparisons to constrain future projections in CMIP5. Clim. Past 10, 221–250. https://doi.org/10.5194/cp-10-221-2014
- Schreve, D.C., Thomas, G.N., 2001. Critical issues in European Quaternary Biostratigraphy. Quat. Sci. Rev. 20, 1577–1582. https://doi.org/10.1016/S0277-3791(01)00024-5
- Schroeder, R.A., Bada, J.L., 1977. Kinetics and mechanism of the epimerization and decomposition of threonine in fossil foraminifera. Geochim. Cosmochim. Acta 41, 1087–1095. https://doi.org/10.1016/0016-7037(77)90103-X
- Schroeder, R.A., Bada, J.L., 1976. A review of the geochemical applications of the amino acid racemization reaction. Earth Sci. Rev. 12, 347–391. https://doi.org/10.1016/0012-8252(76)90011-8
- Scott, D.S., Medioli, F.S., 1978. Vertical zonations of marsh foraminifera as accurate indicators of

- former sea-levels. Nature 272, 528-531. https://doi.org/10.1038/272528a0
- Scourse, J.D., Austin, W.E.N., Sejrup, H.P., Ansari, M.H., 1999. Foraminiferal isoleucine epimerization determinations from the Nar Valley Clay, Norfolk, UK: implications for Quaternary correlations in the southern North Sea basin. Geol. Mag. 136, 543–560. https://doi.org/10.1017/S0016756899002812
- Sejrup, H.P., Aarseth, I., Haflidason, H., 1991. The Quaternary succession in the central North Sea. Mar. Geol. 101, 103–111.
- Sejrup, H.P., Haugen, J.E., 1992. Foraminiferal amino acid stratigraphy of the Nordic Seas: geological data and pyrolysis experiments. Deep Sea Res. Part A, Oceanogr. Res. Pap. 39. https://doi.org/10.1016/S0198-0149(06)80022-1
- Sejrup, H.P., Miller, G.H., Brigham-Grette, J., Lovlie, R., Hopkins, D.M., 1984a. Amino acid epimerisation implies rapid sedimentation rates in Arctic Ocean cores. Nature 311, 276–279.
- Sejrup, H.P., Rokoengen, K., Miller, G.H., 1984b. Isoleucine epimerisation in Quaternary benthonic foraminifera from the Norwegian continental shelf: a pilot study. Mar. Geol. 56, 227–239.
- Sexton, P.F., Wilson, P.A., Pearson, P.N., 2006. Microstructural and geochemical perspectives on planktic foraminiferal preservation: "glassy" versus "frosty." Geochemistry, Geophys. Geosystems 7. https://doi.org/10.1029/2006GC001291
- Shackleton, N.J., Opdyke, N.D., 1977. Oxygen isotope and palaeomagnetic evidence for early Northern Hemisphere glaciation. Nature 270, 216–219. https://doi.org/10.1038/270216a0
- Shennan, I., Long, A.J., Horton, B.P., 2015. Handbook of Sea-Level Research. John Wiley & Sons, Ltd.
- Shennan, I., Milne, G.A., Bradley, S., 2012. Late Holocene vertical land motion and relative sea-level changes: Lessons from the British Isles. J. Quat. Sci. 27, 64–70. https://doi.org/10.1002/jqs.1532
- Simonson, A.E., Lockwood, R., Wehmiller, J.F., 2013. Three approaches to radiocarbon calibration of amino acid racemization in Mulinia lateralis from the Holocene of the Chesapeake Bay, USA. Quat. Geochronol. 16, 62–72. https://doi.org/10.1016/j.quageo.2012.06.005
- Smart, P.L., Frances, P.D., 1991. Quaternary Dating Methods A User's Guide. Quaternary Research Association, Cambridge.
- Smith, D.E., Firth, C.R., Brooks, C.L., Robinson, M., Collins, P.E.F., 1999. Relative sea-level rise during the Main Postglacial Transgression in NE Scotland, U.K. Trans. R. Soc. Edinburgh, Earth Sci. 90, 1–27. https://doi.org/10.1017/S0263593300002480
- Smith, G.G., Evans, R.C., 1980. The Effect of Structure and Conditions on the Rate of Racemisation of Free and Bound Amino Acids, in: Hare, P.E., Hoering, T.C., King, K. (Eds.), Biogeochemistry of Amino Acids. John Wiley & Sons, Ltd., New York, pp. 257–282.
- Smith, G.G., Reddy, G.V., 1989. Effect of the Side Chain on the Racemization of Amino Acids in Aqueous Solution. J. Org. Chem. 54, 4529–4535. https://doi.org/10.1021/jo00280a017
- Smith, G.G., Williams, K.M., Wonnacott, D.M., 1978. Factors Affecting the Rate of Racemization of Amino Acids and Their Significance to Geochronology. J. Org. Chem. 43, 1–5. https://doi.org/10.1021/jo00395a001

- Spindler, M., 1996. On the salinity tolerance of the planktonic foraminifer Neogloboquadrina pachygerma from Antarctic sea ice. Proc. NIPR Symp. Polar Biol. 9, 85–91.
- Stathoplos, L., Hare, P.E., 1993. Bleach removes labile amino acids from deep sea planktonic foraminiferal shells. J. Foraminifer. Res. 23, 102–107.
- Steinberg, S.M., Bada, J.L., 1983. Peptide Decomposition in the Neutral pH Region via the Formation of Diketopiperazines. J. Org. Chem. 48, 2295–2298. https://doi.org/10.1021/jo00161a036
- Steinberg, S.M., Bada, J.L., 1981. Diketopiperazine Formation During Investigations of Amino Acid Racemization in Dipeptides. Science (80-.). 213, 544–545. https://doi.org/10.1126/science.213.4507.544
- Steiner, R.F., 1968. Life Chemistry: an introduction to biochemistry. D. Van Nostrand Company, Inc, Princeton.
- Stevens, L.A., 1959. The interglacial of the Nar Valley, Norfolk. Q. J. Geol. Soc. 115, 291–316. https://doi.org/10.1144/GSL.JGS.1959.115.01.14
- Stirling, C.H., Andersen, M.B., 2009. Uranium-series dating of fossil coral reefs: Extending the sealevel record beyond the last glacial cycle. Earth Planet. Sci. Lett. 284, 269–283. https://doi.org/10.1016/j.epsl.2009.04.045
- Stirling, C.H., Esat, T.M., Lambeck, K., McCulloch, M.T., 1998. Timing and duration of the Last Interglacial: Evidence for a restricted interval of widespread coral reef growth. Earth Planet. Sci. Lett. 160, 745–762. https://doi.org/10.1016/S0012-821X(98)00125-3
- Stuiver, M., Polach, H.A., 1977. Discussion Reporting of 14 C Data. Radiocarbon 19, 355–363. https://doi.org/10.1017/S0033822200003672
- Svensson, A., Andersen, K.K., Bigler, M., Clausen, H.B., Dahl-Jensen, D., Davies, S.M., Johnsen, S.J., Muscheler, R., Parrenin, F., Rasmussen, S.O., Röthlisberger, R., Seierstad, I., Steffensen, J.-P., Vinther, B.M., 2008. A 60 000 year Greenland stratigraphic ice core chronology. Clim. Past 4, 47–57. https://doi.org/10.5194/cp-4-47-2008
- Sykes, G.A., Collins, M.J., Walton, D.I., 1995. The significance of a geochemically isolated intracrystalline organic fraction within biominerals. Org. Geochem. 23, 1059–1065. https://doi.org/10.1016/0146-6380(95)00086-0
- Takahashi, O., Kobayashi, K., Oda, A., 2010. Computational insight into the mechanism of serine residue racemization. Chem. Biodivers. 7, 1625–1629. https://doi.org/10.1002/cbdv.200900297
- Thomas, G.N., 2001. Late Middle Pleistocene pollen biostratigraphy in Britain: Pitfalls and possibilities in the separation of interglacial sequences. Quat. Sci. Rev. 20, 1621–1630. https://doi.org/10.1016/S0277-3791(01)00026-9
- Thompson, W.G., Spiegelman, M.W., Goldstein, S.L., Speed, R.C., 2003. An open-system model for U-series age determinations of fossil corals. Earth Planet. Sci. Lett. 210, 365–381. https://doi.org/10.1016/S0012-821X(03)00121-3
- Tomiak, P.J., Penkman, K.E.H., Hendy, E.J., Demarchi, B., Murrells, S., Davis, S.A., McCullagh, P., Collins, M.J., 2013. Testing the limitations of artificial protein degradation kinetics using

- known-age massive Porites coral skeletons. Quat. Geochronol. 16, 87–109. https://doi.org/10.1016/j.quageo.2012.07.001
- Torres, T., Ortiz, J.E., Sánchez-Palencia, Y., 2016. Amino acid epimerization dating of Quaternary coastal deformation in SE Iberian Peninsula: The region between Aguas and Antas Rivers' mouths. Comptes Rendus Geosci. 348, 398–407. https://doi.org/10.1016/j.crte.2015.12.004
- Towe, K.M., 1980. Preserved Organic Ultrastructure: An Unreliable Indicator for Palaeozoic Amino Acid Biogeochemistry, in: Hare, P.E., Hoering, T.C., King, K.J. (Eds.), Biogeochemistry of Amino Acids. John Wiley & Sons, Ltd., New York, pp. 65–74.
- Towe, K.M., Thompson, G.R., 1972. The structure of some bivalve shell carbonates prepared by ion-beam thinning A Comparison Study. Calcif. Tissue Res. 10, 38–48. https://doi.org/10.1007/BF02012534
- Tyszka, J., Bickmeyer, U., Raitzsch, M., Bijma, J., Kaczmarek, K., Mewes, A., Topa, P., Janse, M., 2019. Form and function of F-actin during biomineralization revealed from live experiments on foraminifera. Proc. Natl. Acad. Sci. U. S. A. 116, 4111–4116. https://doi.org/10.1073/pnas.1810394116
- Tzedakis, P.C., Andrieu, V., de Beaulieu, J.L., Birks, H.J.B., Crowhurst, S., Follieri, M., Hooghiemstra, H., Magri, D., Reille, M., Sadori, L., Shackleton, N.J., Wijmstra, T.A., 2001. Establishing a terrestrial chronological framework as a basis for biostratigraphical comparisons. Quat. Sci. Rev. 20, 1583–1592. https://doi.org/10.1016/S0277-3791(01)00025-7
- Tzedakis, P.C., Channell, J.E.T., Hodell, D.A., Kleiven, H.F., Skinner, L.C., 2012. Determining the natural length of the current interglacial. Nat. Geosci. 5, 138–142. https://doi.org/10.1038/ngeo1358
- Vallentyne, J.R., 1964. Biogeochemistry of organic matter—II Thermal reaction kinetics and transformation products of amino compounds. Geochim. Cosmochim. Acta 28, 157–188. https://doi.org/10.1016/0016-7037(64)90147-4
- Van De Berg, W.J., Van Den Broeke, M., Ettema, J., Van Meijgaard, E., Kaspar, F., 2011. Significant contribution of insolation to Eemian melting of the Greenland ice sheet. Nat. Geosci. 4, 679–683. https://doi.org/10.1038/ngeo1245
- Ventris, P., 1996. Hoxnian interglacial freshwater and marine deposits in northwest Norfolk, England and their implications for sea-level reconstruction. Quat. Sci. Rev. 15, 437–442. https://doi.org/10.1016/0277-3791(96)00020-0
- Villemant, B., Feuillet, N., 2003. Dating open systems by the 238U-234U-230Th method: Application to Quaternary reef terraces. Earth Planet. Sci. Lett. 210, 105–118. https://doi.org/10.1016/S0012-821X(03)00100-6
- Walker, M.J.C., 2005. Quaternary Dating Methods. John Wiley & Sons, Ltd.
- Walker, M.J.C., Lowe, J., 2007. Quaternary science 2007: a 50-year retrospective. J. Geol. Soc. London. 164, 1073–1092. https://doi.org/10.1144/0016-76492006-195
- Wallinga, J., 2002. Optically stimulated luminescence dating of fluvial deposits: A review. Boreas 31, 303–322. https://doi.org/10.1080/030094802320942536
- Walton, D.I., 1998. Degradation of intracrystalline proteins and amino acids in fossil brachiopods.

- Org. Geochem. 28, 389-410. https://doi.org/10.1016/S0146-6380(97)90126-1
- Wang, P., Chappell, J., 2001. Foraminifera as Holocene environmental indicators in the South Alligator River, Northern Australia. Quat. Int. 82, 47–62. https://doi.org/10.1016/S1040-6182(01)00030-1
- Watson, E., 2019. Amino acid racemization of planktonic foraminifera: Pretreatment effects and temperature reconstructions. University of Delaware.
- Wehmiller, J.F., 2013a. Interlaboratory comparison of amino acid enantiomeric ratios in Pleistocene fossils. Quat. Geochronol. 16, 173–182. https://doi.org/10.1016/j.quageo.2012.05.008
- Wehmiller, J.F., 2013b. United States Quaternary coastal sequences and molluscan racemization geochronology What have they meant for each other over the past 45 years? Quat. Geochronol. 16, 3–20. https://doi.org/10.1016/j.quageo.2012.05.008
- Wehmiller, J.F., 1980. Intergeneric Differences in Apparent Racemisation Kinetics in Mollusks and Foraminifera: Implications for Models of Diagenetic Racemisation, in: Hare, P.E., Hoering, T.C., King, K. (Eds.), Biogeochemistry of Amino Acids. John Wiley & Sons, Ltd., New York, pp. 341–356.
- Wehmiller, J.F., 1977. Amino acid studies of the Del Mar, California, midden site: Apparent rate constants, ground temperature models, and chronological implications. Earth Planet. Sci. Lett. 37, 184–196. https://doi.org/10.1016/0012-821X(77)90163-7
- Wehmiller, J.F., Hall, F.R., 1997. Data Report: Amino acid racemisation geochronological studies of selected Leg 155 samples. Proc. Ocean Drill. Program, Sci. Results 155, 375–378.
- Wehmiller, J.F., Hare, P.E., 1971. Racemisation of Amino Acids in Marine Sediments. Science (80-.). 173, 907–911. https://doi.org/10.1126/science.124.3230.1026
- Wehmiller, J.F., Hare, P.E., Kujala, G.A., 1976. Amino acids in fossil corals: racemization (epimerization) reactions and their implications for diagenetic models and geochronological studies. Geochim. Cosmochim. Acta 40, 763–776. https://doi.org/10.1016/0016-7037(76)90029-6
- Wehmiller, J.F., Miller, G.H., 2000. Aminostratigraphic dating methods in Quaternary geology. Quat. Geochronol. methods Appl. 187–222.
- Wehmiller, J.F., Thieler, E.R., Miller, D., Pellerito, V., Bakeman Keeney, V., Riggs, S.R., Culver, S.J., Mallinson, D., Farrell, K.M., York, L.L., Pierson, J., Parham, P.R., 2010. Aminostratigraphy of surface and subsurface Quaternary sediments, North Carolina coastal plain, USA. Quat. Geochronol. 5, 459–492. https://doi.org/10.1016/j.quageo.2009.10.005
- Weiner, S., 1979. Aspartic acid-rich proteins: Major components of the soluble organic matrix of mollusk shells. Calcif. Tissue Int. 29, 163–167. https://doi.org/10.1007/BF02408072
- Weiner, S., Erez, J., 1984. Organic matrix of the shell of the foraminifer, Heterostegina depressa. J. Foraminifer. Res. 14, 206–212. https://doi.org/10.2113/gsjfr.14.3.206
- West, G., Kaufman, D.S., Muschitiello, F., Forwick, M., Wollenburg, J., Regan, M.O., 2019. Amino acid racemization in Quaternary foraminifera from the Yermak Plateau. Geochronology 1, 53–67.

- West, R.G., Andrew, R., Catt, J.A., Hart, C.P., Hollin, J.T., Knudsen, K.L., Miller, G.F., Penney, D.N., Pettit, M.E., Preece, R.C., Switsur, V.R., Whiteman, C.A., Zhou, L.P., 1999. Late and Middle Pleistocene deposits at Somersham, Cambridgeshire, U.K.: A model for reconstructing fluvial/estuarine depositional environments. Quat. Sci. Rev. 18, 1247–1314. https://doi.org/10.1016/S0277-3791(98)00067-5
- West, R.G., Devoy, R.J.N., Funnell, B.M., Robinson, J.E., 1984. Pleistocene Deposits at Earnley, Bracklesham Bay, Sussex. Philos. Trans. R. Soc. B, Biol. Sci. 306, 137–157.
- West, R.G., Knudsen, K.L., Penney, D.N., Preece, R.C., Robinson, J.E., 1994. Palaeontology and taphonomy of Late Quaternary fossil assemblages at Somersham, Cambridgeshire, England, and the problem of reworking. J. Quat. Sci. 9, 357–366. https://doi.org/10.1002/jqs.3390090406
- Westaway, R., 2009. Calibration of decomposition of serine to alanine in Bithynia opercula as a quantitative dating technique for Middle and Late Pleistocene sites in Britain. Quat. Geochronol. 4, 241–259. https://doi.org/10.1016/j.quageo.2009.01.007
- Westaway, R., Bridgland, D.R., White, M.J., 2006. The Quaternary uplift history of central southern England: evidence from the terraces of the Solent River system and nearby raised beaches. Quat. Sci. Rev. 25, 2212–2250. https://doi.org/10.1016/j.quascirev.2005.06.005
- Wheeler, L.J., Penkman, K.E.H., Sejrup, H.P., 2021. Assessing the intra-crystalline approach to amino acid geochronology of Neogloboquadrina pachyderma (sinistral). Quat. Geochronol. 61, 101131. https://doi.org/10.1016/j.quageo.2020.101131
- Whitacre, K.E., Kaufman, D.S., Kosnik, M.A., Hearty, P.J., 2017. Converting A/I values (ion exchange) to D/L values (reverse phase) for amino acid geochronology. Quat. Geochronol. 37, 1–6. https://doi.org/10.1016/j.quageo.2016.10.004
- Williams, K.M., Smith, G.G., 1977. A critical evaluation of the application of amino acid racemization to geochronology and geothermometry. Orig. Life Evol. Biosph. 8, 91–144. https://doi.org/10.1007/BF00927978
- Yin, Q.Z., Berger, A., 2012. Individual contribution of insolation and CO2 to the interglacial climates of the past 800,000 years. Clim. Dyn. 38, 709–724. https://doi.org/10.1007/s00382-011-1013-5